THE HERPES SIMPLEX VIRUS VIRION HOST SHUTOFF PROTEIN IS TARGETED TO mRNA CLEAVAGE SITES THROUGH INTERACTIONS WITH COMPONENTS OF THE HOST TRANSLATIONAL APPARATUS

A DISSERTATION IN
Cell Biology and Biophysics
and
Molecular Biology and Biochemistry

Presented to the Faculty of the University
of Missouri-Kansas City in partial fulfillment of
the requirements for the degree

DOCTOR OF PHILOSOPHY

by
LORA ANN SHIFLETT

M.S., University of Missouri-Kansas City, Kansas City, MO 2007
B.S., Iowa State University, Ames, Iowa, 2005

Kansas City, MO
2010

THE HERPES SIMPLEX VIRUS VIRION HOST SHUTOFF PROTEIN IS TARGETED TO mRNA CLEAVAGE SITES THROUGH INTERACTIONS WITH COMPONENTS OF THE HOST TRANSLATIONAL APPARATUS

Lora Ann Shiflett, Candidate for the Doctor of Philosophy Degree

University of Missouri-Kansas City, 2010

ABSTRACT

The virion host shutoff protein (Vhs) is a herpes simplex virus (HSV) protein involved in early shutoff of the host cell. It is a component of the infecting virion, located in the tegument region, that works by rapidly degrading both viral and cellular messenger RNA (mRNA). *in vivo* and within infected cells, Vhs is selective for degrading messenger RNA opposed to non-messenger RNA. This dissertation sought to examine Vhs cleavage of an mRNA that utilizes the cap-dependent scanning mechanism for translation initiation and to see if cleavage was connected to early events of translation initiation. mRNA encoding HSV-1 thymidine kinase (pBK2) was used for the majority of the experiments, and studies were designed to map the cut sites produced by Vhs in a rabbit reticulocyte lysate (RRL) system. Additional experiments investigated whether Vhs was selective for degrading certain types of mRNAs over others, particularly IRES-containing mRNAs.

Studies revealed that Vhs specifically cleaves pBK2 mRNA within the first 300 bases from the 5′ cap, and these cut sites are close to and slightly upstream from the first three AUG codons of the sequence. The proximity of the cutting to the AUG codons led to speculations that early events of translation initiation might be involved in Vhs degradation of mRNA. This was found to be true, where data revealed that blocking early stages such as (1) recruitment of

translation initiation factors to the 5′ cap and/or (2) ATP hydrolysis RNA helicase activity important for unwinding RNA secondary structure and the scanning process hinder Vhs cleavage. However, blocking later stages of translation initiation only had a modest effect on RNase activity. Results also found that a 5′ cap analog inhibits Vhs site-specific cleavage of mRNA at regions near the 5′ cap. Interestingly, a cap appears to be required for Vhs production of specific cleavage sites within the first 300 bases of the transcript.

Work went on to study whether there was a difference between Vhs cleavage of circularized RNA that normally experiences cap-dependent scanning and circularized RNA that initiates translation in a cap-independent manner. Results indicated that Vhs requires a free 5′ end for specific cleavage of mRNA that undergoes cap-dependent scanning. However, Vhs does not require a free 5′ end to specifically cleave a circular RNA that utilizes cap-independent methods for translation initiation. Mutational work, with pBK2 mutants which contained mutations in or surrounding the AUG codon, further supported a mechanism for Vhs cleavage that involved Vhs association with the scanning complex to reach some of its preferred cut sites. Mutating the first AUG to a non-AUG inhibited Vhs specific cleavage of pBK2 mRNA at a region just upstream from the AUG codon. Additionally, mutating bases surrounding the AUG codon to put it in an optimal context enhanced cleavage at regions near the start codon. Inserting a stable hairpin near the 5′ cap to block scanning also reduced Vhs cleavage at prominent sites within the first 300 bases of the transcript. To conclude, this work provides several indications that Vhs associates with components of the translational apparatus to access at least some of its cut sites.

APPROVAL PAGE

The faculty listed below, appointed by the Dean of the School of Graduate Studies, have examined a dissertation titled "The Herpes Simplex Virus Virion Host Shutoff Protein is Targeted to mRNA Cleavage Sites through Interactions with Components of the Host Translational Apparatus," presented by Lora Ann Shiflett, candidate for the Doctor of Philosophy degree, and certify that in their opinion it is worthy of acceptance.

SUPERVISORY COMMITTEE

G. Sullivan Read, Ph.D., Committee Chair
Cell Biology and Biophysics

Thomas Menees, Ph.D.
Cell Biology and Biophysics

Michael Plamann, Ph.D.
Cell Biology and Biophysics

Stephen King, Ph.D.
Molecular Biology and Biochemistry

Michael O'Connor, Ph.D.
Molecular Biology and Biochemistry

CONTENTS

ILLUSTRATIONS

TABLES

AKNOWLEDGEMENTS

I would like to thank my advisor, Dr. G. Sullivan Read, for his creativity in designing experiments, his mentorship along the way, his patience through my years of development, and his constant positivity during complicated times. I will especially remember him walking in the lab to tell a funny story and his recitation of poetry. I am grateful toward my supervisory committee who spent numerous hours attending my presentations and addressing key questions that needed to be answered for this work to develop and help shape me as an investigator. I would like to thank my classmates and peers in the lab, especially Deepali Agarwal and Jouliana Sadek, who provided helpful insight, were involved in many group discussions, and assisted with various phases of this work. I'm also appreciative of the time we spent away from the lab getting to know one another.

I would like to thank my family for their continuous support and unending faith in my abilities. I would like to thank my mom for spending so much time with my sisters and me in the summertime encouraging learning through stimulating activities. I would like to thank my dad for wanting the best for each of us, his adamant confidence in my future grew on me and helped me overcome many barriers. I'd like to thank my sisters, Jessi and Teresa. Jessi, you have taught me responsibility and how to cherish those closest to your heart. Teresa, you have taught me that you have only one life, it is an adventure, and you need to live it to its fullest. I cannot express how important all of these people have been in my life, and without them this work would not be possible.

CHAPTER 1

INTRODUCTION

Lytic infection with herpes simplex virus (HSV) causes a global reduction in protein synthesis and mRNA abundance in the cell. One of the key players in shutoff is the virion host shutoff protein (Vhs), a component of the infecting virion that is active immediately upon infection at degrading both viral and cellular mRNA. The mechanism for how Vhs recognizes mRNA opposed to non messenger RNA remains uncertain, however many lines of evidence suggest that Vhs may associate with cellular factors when targeting mRNA. These proposed factors are involved in early stages of protein synthesis.

Prior to this dissertation, no connections had been made between translation initiation and Vhs degradation of mRNA. Specifically, no previous studies investigated the importance of cap-dependent scanning and recruitment of translation initiation factors to the 5′ cap for Vhs activity. Additionally, the two defining features of mRNA, a 5′ cap and a poly(A) tail, had never been shown to be vital for Vhs site-specific cleavage. Many studies were focused on determining the sequences that were preferable for Vhs cutting, but they lacked an explanation about how Vhs cleavage might be affected by mRNA secondary structure.

This dissertation investigates the importance of early events of translation initiation on Vhs function. mRNA was analyzed in an *in vitro* Vhs degradation system where specific cut sites were mapped and then further studied in the presence of several translation inhibitors. mRNA was analyzed using many different methods for radiolabeling. The results from these experiments indicate that early stages of translation initiation are required for Vhs site-specific cleavage. The assay was then studied to test whether mutating the AUG codon or bases surrounding the codon affected Vhs cleavage in an attempt to determine whether Vhs utilized

the scanning complex to achieve cutting. RNA was further manipulated to block the cap-dependent scanning process through circularization experiments and studies with hairpin inserts to further tie together the role of early translation events in Vhs cleavage.

Herpesviridae

The three subfamilies of the family *Herpesviridae* are alphaherpesvirinae, betaherpesvirinae, and gammaherpesvirinae. The members of this group are characterized within *Herpesviridae* because they have a similar genome and commonalities in their virion structure (83). They infect a plethora of vertebrate hosts and perform DNA replication and capsid assembly in the nucleus. Productive infection with members of the family *Herpesviridae* leads to destruction of the host cell (83). They are known for synthesizing a wide variety of proteins important for DNA synthesis, nucleic acid metabolism, and protein processing (83). These viruses have the ability to establish latency and maintain regulation of their genome in the nucleus under the expression of few viral genes (83). Only eight herpesviruses have the ability to regularly infect humans. They are herpes simplex virus 1 (HSV-1), herpes simplex virus 2 (HSV-2), human cytomegalovirus (HCMV), varicella-zoster virus (VZV), Epstein-Barr virus (EBV), human herpes virus 6A/B (HHV6A, HHV6B), human herpesvirus 7 (HHV7), and human herpes virus 8 (Kaposi's sarcoma-associated herpesvirus (KSHV)) (83).

There are many general differences between the three viral subfamilies. Alphaherpesviruses have a short reproductive cycle of around 18 hrs. and establish infection in neuronal cells (83). They have a wide host range and destroy the productively infected cell (83). Examples of alphaherpesviruses are HSV-1, HSV-2, and VZV. HSV-1 causes labial, ocular, and facial lesions and HSV-2 infection causes genital lesions. VZV leads to chicken pox, and

reactivation of virus results in shingles. Betaherpesviruses have a limited host range and a much longer reproductive cycle (83). They are lymphotropic and characterized by causing enlargement of the infected cell (83). HCMV belongs to this class, and it is an important infectious cause of birth defects. Gammaherpesviruses are also lymphotropic, but their latency is restricted to T and B lymphocytes (83). Members of this family include the EBV and KSHV. EBV and KSHV are cofactors to human cancers.

The herpes simplex virus infects 40-80% of the population (83). HSV-1 infection is performed in 80% of Americans by the age of 50 (109). Although most genital infections (HSV-1 or HSV-2) are mild and leave the patient unharmed, infection can be severely detrimental to individuals in developing countries who are later infected with the human immunodeficiency virus (HIV). Infection with both viruses causes a 2-4 fold rise in the transmission of HIV (82). HSV is generally a mild virus, however infection of newborns or immunocompromised individuals can lead to serious problems such as encephalitis or hepatitis.

HSV Virion

Herpes simplex virus is the prototypical member of the neurotropic alphaherpesviruses. The HSV virion is composed of 4 main components; the core, icosadeltahedral capsid, tegument, and viral envelope (83). The core contains the viral linear, double stranded DNA genome which consists of around 152,000 bases, and it is surrounded by the icosadelthedral capsid (Fig. 1) (83). The capsid contains 162 capsomeres and is predicted to be 100-110 nm in diameter (83). The tegument is a flexible region located between the viral capsid and outer envelope which contains around 20 proteins that are components of the infecting viral particle (83). The outer envelope contains several glycoproteins important for viral attachment to cell surface receptors, and they

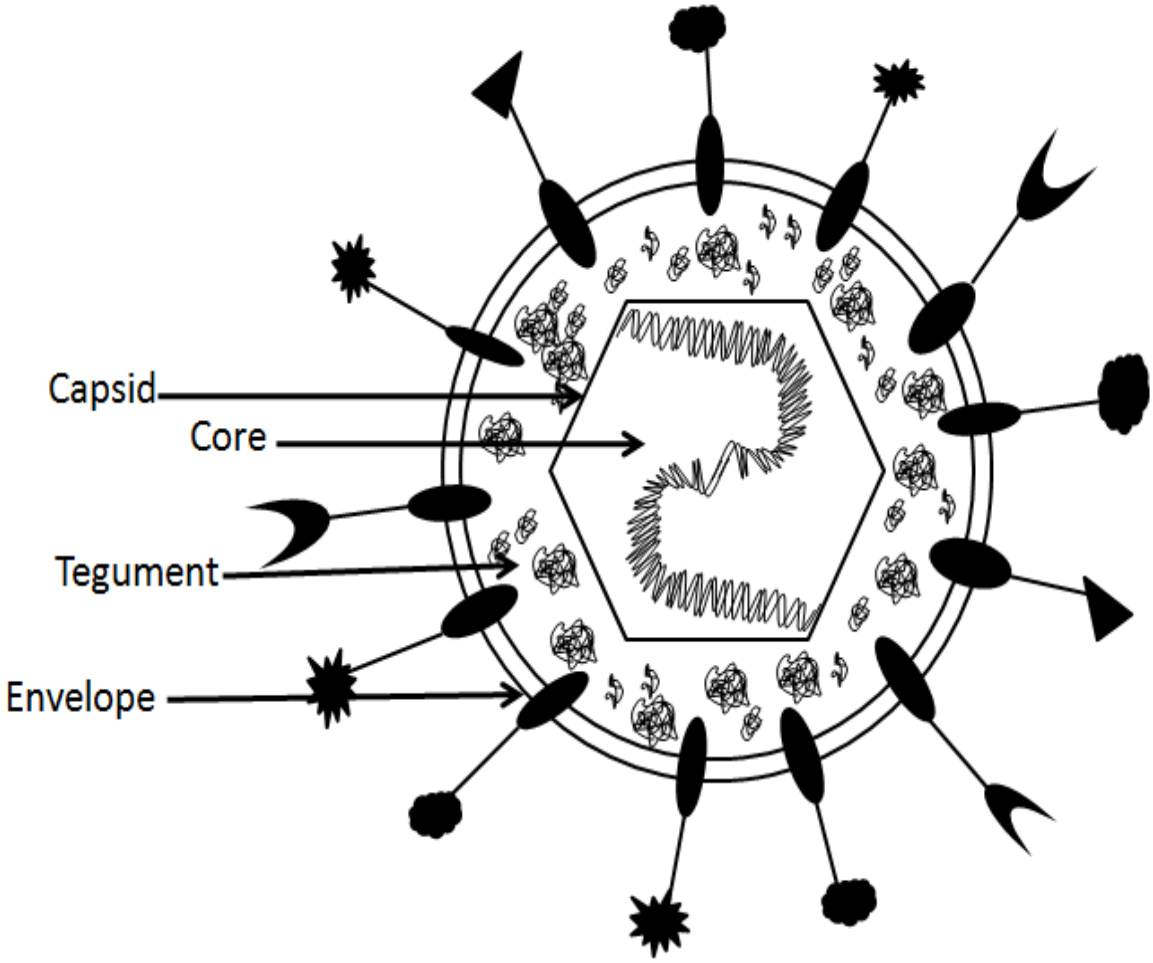

Figure 1.HSV Virion Components

The four main components of the HSV virion are listed in Figure 1. The core contains the double stranded DNA genome. The capsid is an icosadeltahedral structure which surrounds the core. The tegument is an amorphous region between the capsid and the viral envelope which contains several proteins that are packaged into the virus during assembly. The outer envelope contains glycoproteins which project out of the virion and make contacts with the host that are important for viral entry.

TABLE 1

PROTEINS WITHIN THE HSV VIRION

Capsid	Tegument	Envelope
pUL6	pUL4	pUL1 (gL)
pUL18(VP23)	pUL11	pUL10 (gM)
pUL19 (VP5)	pUL13	pUL20
pUL25	pUL14	pUL22 (gH)
pUL35 (VP26)	pUL16	pUL27(gB)
pUL38 (VP19C)	pUL17	pUL43
	pUL21	pUL44 (gC)
	pUL36 (VP1/2)	pUL45
	pUL37	pUL49.5(gN)
	pUL41(Vhs)	pUL53 (g)K
	pUL46 (VP11/12)	pUS4 (gG)
	pUL47 (VP13/14)	pUS5(gJ)
	pUL48 (VP16)	pUS6(gD)
	pUL49 (VP22)	pUS7(gI)
	pUL51	pUS8(gE)
	pUL56	pUS9
	pUS2	
	pUS3	
	pUS10	
	pUS11	
	ICP0	
	ICP4	

are also vital for fusion with the host plasma membrane (83). There are 33 known proteins within the virion structure (Table 1, derived from ref. 95). The outer envelope contains 16 membrane proteins, and 12 of them are glycoproteins (96). 22 proteins are located in the tegument and six are present on the capsid surface (96). HSV stands out from most nuclear-replicating DNA viruses because it brings regulatory proteins into the cell and does not have to wait for gene expression.

HSV Entry

HSV has been demonstrated to enter the cell through two different mechanisms. In the primary pathway, HSV enters by binding the cell membrane and fusing its viral envelope with the plasma membrane (84). An alternative mechanism for entry involves endocytosis of the virion followed by fusion of the viral envelope with endocytic vesicular membranes (105, 109). Since this pathway has only recently been brought to attention, it is still unknown how important it is in a natural infection. Therefore, background information will focus on the prominent pathway. Several lines of evidence indicate that attachment of the viral envelope to the cellular membrane is first achieved by virion binding to cell surface proteoglycan glycosaminoglycan (GAG) chains (97, 107, 108). Heparan sulfate is the prevalent GAG receptor used for binding, but it is not a receptor utilized for entry. Glycoprotein B (gB) and/or glycoprotein C (gC) binding to heparan sulfate greatly enhances infectivity, however binding is not required for productive infection (97, 99,100). Filopodia protrusions contain heparan sulfate proteoglycan (HSPG)-rich sites and may be involved in assisting this binding (98). Glycoprotein H (gH), L (gL), B (gB), D (gD), and C (gC) are all involved in the entry process, but gC is the only nonessential protein (97, 102). However, absence of gC can have as much as a 10 fold reduction

in viral infectivity, but results vary depending on the serotype of HSV studied (101).

Upon virion binding, gD associates with various receptors on the cell surface to trigger fusion with the host cell in a process that is mediated by gB and the heterodimer gH/gL (reviewed in 103, 104). gD itself is not a fusogen, however gB and gH display properties common to many fusion proteins and are speculated to be important for this function (102, 106). HSV associates with 3 types of cellular receptors for viral entry. These include the herpes virus entry mediator (HVEM), which belongs to the tumor necrosis factor (TNF) receptor family; components of the immunoglobulin superfamily, nectin 1 and 2; and 3-0-sulfotransferase sites within heparan sulfate (104). HVEM and nectin-1 appear to be the prominent receptors for entry (104). Following fusion, the nucleocapsid and tegument components enter the cytoplasm (87, 88). All herpesviruses have structural conservation in gB, gH, and gL; but structural conservation in gD and gC is only maintained in alphaherpesviruses.

Capsid Translocation to the Nucleus

After fusion, viral capsid and tegument proteins enter the cytoplasm. Tegument proteins have one of three fates; they remain in a complex with the capsid, stay in the cytoplasm, or travel to the nucleus (109). The capsid, along with associating tegument proteins, is transported to the nuclear perimeter and DNA is inserted through nuclear pores in a process that is heavily dependent on *UL36* VP1-2 (110, 111). DNA replication, viral transcription, and capsid assembly all occur in the nucleus (109). The virus utilizes host RNA polymerase II for RNA synthesis, however the process is regulated by several viral proteins (109).

Once viral DNA enters the nucleus it quickly circularizes, and several nuclear remodeling events occur. Replication takes place near cellular nuclear domain 10 (ND-10)

structures (112, 113). It is unclear whether the DNA travels to ND-10 sites or if ND-10 structures target viral DNA. It is also unknown if association of viral DNA with ND-10 bodies requires expression of viral proteins and whether transcription occurs at these sites (109). Infectious cell protein 0 (ICP0) has been shown to breakdown ND-10 structures (109,118). During DNA synthesis, replication compartments expand and overwhelm the nucleus which causes cellular chromatin condensation at the nuclear border (109, 114, 115, 116, 117). This condensation may play a role in inhibiting cellular transcription. Eventually, the chromatin disperses which improves viral egress.

Gene Expression

Transcription of the HSV genome occurs in the nucleus, and protein synthesis takes place in the cytoplasm. All viral DNA is transcribed by cellular RNA pol II, yet viral proteins can regulate RNA pol II activity and configuration (119, 120). Transcription undergoes a temporal regulation of gene expression, featuring three different classes of viral genes. HSV α (immediate early) genes are expressed 2-4 hours post infection when cells are infected with a multiplicity of infection (MOI) of 10-20 plaque forming units per cell (PFU) (83). Alpha gene expression is stimulated by VP16, however, no *de novo* protein synthesis is required for immediate early gene expression. Viral α promoters have been shown to contain key sequences for cellular transcriptonal factor binding (135, 136). Six immediate early proteins are produced from alpha gene expression, and five of them are involved in regulating β (early) gene expression. β genes are expressed 4-8 hours postinfection and require functional immediate early protein ICP4 (83). Early proteins regulate DNA replication and expression of late (γ) genes. β proteins are also involved in turning down α gene expression. Once DNA replication begins, γ genes are

increasingly expressed which encode structural proteins (121). Products of late gene expression will turn off α and β gene expression. During lytic infection over 80 viral proteins are synthesized.

RNA Export

In the cellular system, mRNA export and splicing are tied together in a sequential process. It appears that HSV infection stimulates a new mRNA export system since splicing is inhibited. The immediate early protein ICP27, the product of the *α27* gene, has the ability to travel to and from the nucleus, and several lines of evidence indicate that it promotes RNA export (137-142).

HSV Latency and Reactivation

When skin or mucous membrane is infected with virus, most of the virus will first take part in replicating DNA at the site of infection before traveling to the dorsal root ganglion sensory neurons (83, 85, 86). The virus then travels to the cell body by retrograde transport along axons and latency is established (83, 85, 86). Upon reactivation, the virus will travel in the opposite direction toward the axon perimeter to cause lytic infection or unnoticeable shedding at the site of original infection (83). Dynein and kinesin host molecular motors are believed to be involved in HSV neuronal transport (90, 91, 92, 93, 94).

Key Factors for Host Invasion

HSV has mastered the ability of settling into a host to cause destruction of the infected cell. Yet, it cleverly works to maintain forever establishment in the body by recruiting progeny

virus to sensory neurons to establish latency. The virus achieves this by using several key strategies. The earliest strategy is how the virus quickly shuts off protein synthesis and delivers its DNA to the nucleus for immediate transcription and replication (109). A second strategy involves inhibition of the host's advances at removing virus by interfering with mRNA splicing and apoptosis (109). A third strategy is the virus's ability to keep its genome safe from destruction in the central nervous system during latency and then carefully direct virus to the sites of initial infection during reactivation (109).

One key protein involved in shutting down cellular protein synthesis is the *UL41* virion host shutoff protein (Vhs). Vhs is located in the virion tegument, so it's immediately active at downregulating cellular protein synthesis, degrading mRNA, and destroying pre-existing polyribosomes upon viral fusion with the host cell (reviewed in 1).

A second important viral protein is the VP16 tegument protein. VP16 is involved in rapid gene expression once viral DNA enters the nucleus, because it directs cellular RNA pol II to viral genes (109). VP16 has been found to assist in the binding of chromatin-modifying proteins to α gene promoters, and it also decreases levels of histone H3 to promote active chromatin formation (133, 134). The immediate early protein, ICP27, is believed to inhibit splicing by interacting with SRPK1 to regulate SR protein phosphorylation levels. However, ICP27 still permits viral unspliced mRNA export into the cytoplasm (143, 144, 145). Hindering mRNA splicing leads to reduction of cellular mRNA, but most viral mRNA is unaffected because few transcripts are spliced (109).

Vhs Characteristics

The defining characteristics attributed to virion host shutoff activity are the rapid inhibition of cellular protein synthesis, degradation of mRNA, and disruption of pre-existing polyribosomes (54, 122, 131, 132, 146). Inhibition of cellular protein synthesis, degradation of mRNA, and polyribosome disassembly are still achieved when cells are infected with UV-light irradiated virus or in the presence of Actinomycin D (a drug that blocks transcription), indicating that the shutoff function is caused by a component of the infecting virion (123, 124-132). The viral function causes degradation of both viral and cellular RNAs (14). Studies testing mutants deficient in protein shutoff and mRNA degradation mapped shutoff activity to the HSV open reading frame (ORF) *UL41* which encodes the 58-kDa phosphoprotein Vhs (129, 130, 147, 148). Interestingly, Vhs mutants cause an increase in viral mRNA half lives, indicating that the virion host shutoff function is important for temporal regulation of HSV gene expression (14, 129). Vhs has been shown to be a nonessential protein for viral propagation in cell culture, however Vhs mutants are significantly reduced in viral growth (129, 151). Importantly, several lines of evidence in mice indicate that Vhs is critical for pathogenesis (152-157).

Work testing solubilized virions has shown that, in the absence of cellular factors, Vhs is not restricted to mRNAs and will cleave target RNAs at many locations (4). However; *in vivo*, in cytoplasmic extracts, and in the RRL system Vhs preferentially cleaves mRNA, as opposed to non-messenger RNA (4, 9, 52, 53, 55). For some of these mRNAs, cleavage is preferred near regions at the 5′ cap (5, 8). Northern blot analysis of viral thymidine kinase mRNA revealed that the 5′ end was degraded before the 3′ end *in vivo* (8). *in vitro* work in a rabbit reticulocyte lysate (RRL) system found that Vhs degraded SRPα (the signal recognition particle receptor alpha) mRNA at specific sites within the 5′ quadrant of the mRNA from bases 200-700 (5).

However, Vhs has been reported to not cleave all mRNAs at the 5′ end (4). According to Zelus et al., Vhs cleaves globin γ mRNA at regions near the 3′ UTR, and in these studies Vhs appeared to cleave preferentially at AC and CU dinucleotides (4). It has been suggested that Vhs cleavage near regions at the 5′ cap is dependent on the type of mRNA studied (45-47). While it was previously believed that all mRNAs had similar sensitivities to Vhs cleavage, more recent reports have suggested that Vhs degrades certain mRNAs with different efficiencies (9, 14, 45-47, 49, 50, 52-54). Roizman has shown that certain mRNAs such as IEX-1, COX-2, IkB, and c-Fos (which contain an AU-rich element (ARE) in their 3′ UTR and have very short half lives) appear to be regulated differently upon infection (45-47). During infection, these mRNAs are deadenylated and then cleaved just upstream of the AREs, leaving a stable 5′ product that remains in the cell for an extended time prior to degradation (45-47). Since the ARE is located in the 3′ UTR, these data support a model where Vhs is targeted to the 3′ end of the transcript. Vhs has been suggested to target the 3′ UTR of mRNAs containing AREs by binding the protein tristetraprolin (TPP) (45, 50). This has been built around the findings that TPP protein levels are increased after infection with HSV-1, and TPP has been found to associate with Vhs in coimmunoprecipitation assays (45, 50). Tristetraprolin is a protein that has an important role in the degradation of some AU-rich mRNAs by facilitating their recruitment to the exosome (51, 56, 57).

At present, whether or not Vhs cleaves cellular stress-inducible IEX-1 mRNA at its 3′ UTR is controversial. Initial studies on HSV-1 regulation of ARE mRNAs suggested that these mRNAs were spared from cutting due to ICP27 binding at the ARE (58). Additional studies have implicated that the increase in intermediate IEX-1 mRNA products is not due to Vhs cleavage

but is instead due to HSV-1 infection having an inhibitory effect on the normal turnover of ARE mRNAs (5).

Vhs Sequence Preference

A purified GST-Vhs fusion protein has been shown to have substrate specificity similar to RNase A, where it prefers cleaving mRNA after C and U bases (10,11). However, Zelus et al. have reported a preference for cleavage between AC and CU dinucleotides, and work by Smiley has indicated that Vhs has a slight preference for cleaving between purines but an overall lax sequence specificity (4, 5). Additional studies by Smiley showed that secondary cleavage of the 3′ cleavage product that results from cutting of an EMCV IRES proceeds in a 5′ to 3′ direction (48). The endoribonucleolytic activity was concluded to be sequence nonspecific with a slight preference for cleaving between purines (5).

Vhs Effect on Immune Response

Although Vhs is not essential for viral growth in cell culture, it appears to play a vital role in virulence, replication, and pathogenesis *in vivo* (152-157). In continuous cell lines, Vhs null viruses display similar growth kinetics to wild type and feature single and multi-step curves. Yet in primary cells, the growth pattern switches to a novel multi-step curve. Vhs has an effect on innate and adaptive immune response (238). Cell culture studies have shown that Vhs is important for decreasing interferon recognition, hindering dendritic cell response, and turning down regulation by major histocompatibility factor I (MHCI) (235, 236, 237). It is believed to have a more prominent role in interfering with the innate immune response, because Vhs null virus is significantly hindered in its ability to replicate in the mouse cornea and vaginal

epithelium just 24 hours postinfection (239, 156). HSV-2 Vhs has been shown to hinder the interferon (IFN)-mediated cellular response to virus (240). Animal models using Vhs null viruses as live attenuated vaccines have been successful in preventing or ameliorating HSV infection (241-244).

Vhs Association with Viral Factors

Current data indicate that Vhs exists in three different states throughout the viral lifecycle. In the first state, Vhs exists as a component of the virion that is located in the tegument region. The mRNA in the tegument region is either inaccessible, or Vhs is inactive in this state because it does not lead to mRNA decay in the complex (227). Upon infection, Vhs enters the cytoplasm and exists in its second state where it is active at degrading mRNA and in additional shutoff functions. Several hours after infection, at the commencement of late protein synthesis, Vhs exists in its third state where it no longer shows RNase activity. Vhs association with VP16 leads to inhibition of *de novo* synthesized Vhs in a process that is believed to require further association with VP22 (228, 229, 230, 231). Vhs can interact with VP16 and VP22, however, it is unable to associate with VP22 in the absence of VP16 (231). VP22 is a tegument protein that is able to travel from infected to uninfected cells (232, 233). *in vitro* studies have revealed that it can bind mRNA, and it has been speculated to be important for transporting mRNA into virions during virus assembly (234).

Vhs Homologues

HSV-1 and HSV-2 both encode Vhs, and the sequence is 87% identical (249). Additional alphaherpesviruses which contain a *UL41* homolog include the varicella-zoster virus, bovine

herpesvirus, gallid herpesvirus, equine herpesvirus, and pseudorabies virus (245, 246, 247, 248). All viral *UL41* open reading frames (ORFs) have sequence homology in their amino, internal, and C-terminal domains (246, 31, 250). There are around 100 conserved amino acids in the N and C terminus, and mutations that lead to a loss of Vhs activity are often mapped to one of the three regions of homology (13, 31, 32, 250, 72).

Vhs also shows sequence homology to a family of nucleases important in DNA synthesis and repair (13, 31, 149). This family contains members from bacteria, yeast, mammals, and phage (13). These members have sequence homology in their amino and internal domains (251, 252, 253, 150). Vhs shares this sequence homology, but it varies in the length of amino acids that separate the conserved domains (13). However, the C-terminal domain of Vhs has no sequence homology to the nonviral nucleases (13).

There are 8 conserved amino acids in all cellular and viral members. They include 3 charged residues in the amino terminal domain, 3 charged residues in the internal region, and 1 uncharged residue in the internal domain (13). Key members of the nuclease family include the flap 1 endonucleases (FEN-1), XPG proteins, DNA polymerases, and the RAD2 nucleases involved in DNA repair (13). FEN-1 nucleases have also been shown to cleave RNA by working during DNA synthesis to remove Okazaki fragment RNA primers (150). Crystal structures have been obtained for some of the nonviral nucleases, and further analysis has found that the active site contains many residues that were previously found to be vital for nuclease activity. At least two divalent metal ions bind each active site, and the conserved residues are vital for this binding (251, 13). These conserved residues were altered in HSV-1 Vhs, and every mutant strongly reduced or eliminated Vhs cleavage of mRNA (13).

Vhs Association with Translation Initiation Factors

The mechanism for how Vhs targets mRNA, as opposed to non-messenger RNA, remained a mystery until yeast-2-hybrid studies revealed that Vhs could associate with eukaryotic translation initiation factor eIF4H (6). This finding was also confirmed through GST pull-down and coimmunoprecipitation studies. Additionally, mutations in Vhs that abrogated association with eIF4H led to Vhs loss of function (6, 13). Vhs was later found to associate with eIF4A in GST pull-down and coimmunoprecipitations and eIF4B through Far Western analysis (7,27). Vhs was recently shown to associate with the eIF4F cap binding through experiments using 7-methyl cellulose beads to pull out eIF4E from infected cells (59). Furthermore, siRNA-mediated knockdown against eIF4H, eIF4B, or eIF4AI/II has indicated that eIF4H and eIF4AI/II are essential for Vhs degradation of GAPDH mRNA while eIF4B is not required (28, Agarwal et al. unpublished).

Cap-mediated Translation Initiation

Cap-dependent scanning is the canonical mode for protein synthesis in eukaryotes. Currently, nine initiation factors have been determined to be required for this process. The ribosomal subunits involved in translation are constantly recycled and further recruited to mRNA transcripts for additional rounds of scanning and polypeptide production. The first step involves assembly of the 43S pre-initiation complex. During the recycling process, eukaryotic translation initiation factors eIF3, eIF1, and eIF1A associate with the 40S small ribosomal subunit (Fig. 2). Another complex, known as the ternary complex, is also assembled. The ternary complex is composed of eIF2-GTP-Met-tRNA$^{Met}_{i}$, and it is recruited to the 40S subunit that has pre-bound eIF3, eIF1, and eIF1A to form the 43S pre-initiation complex (reviewed in reference

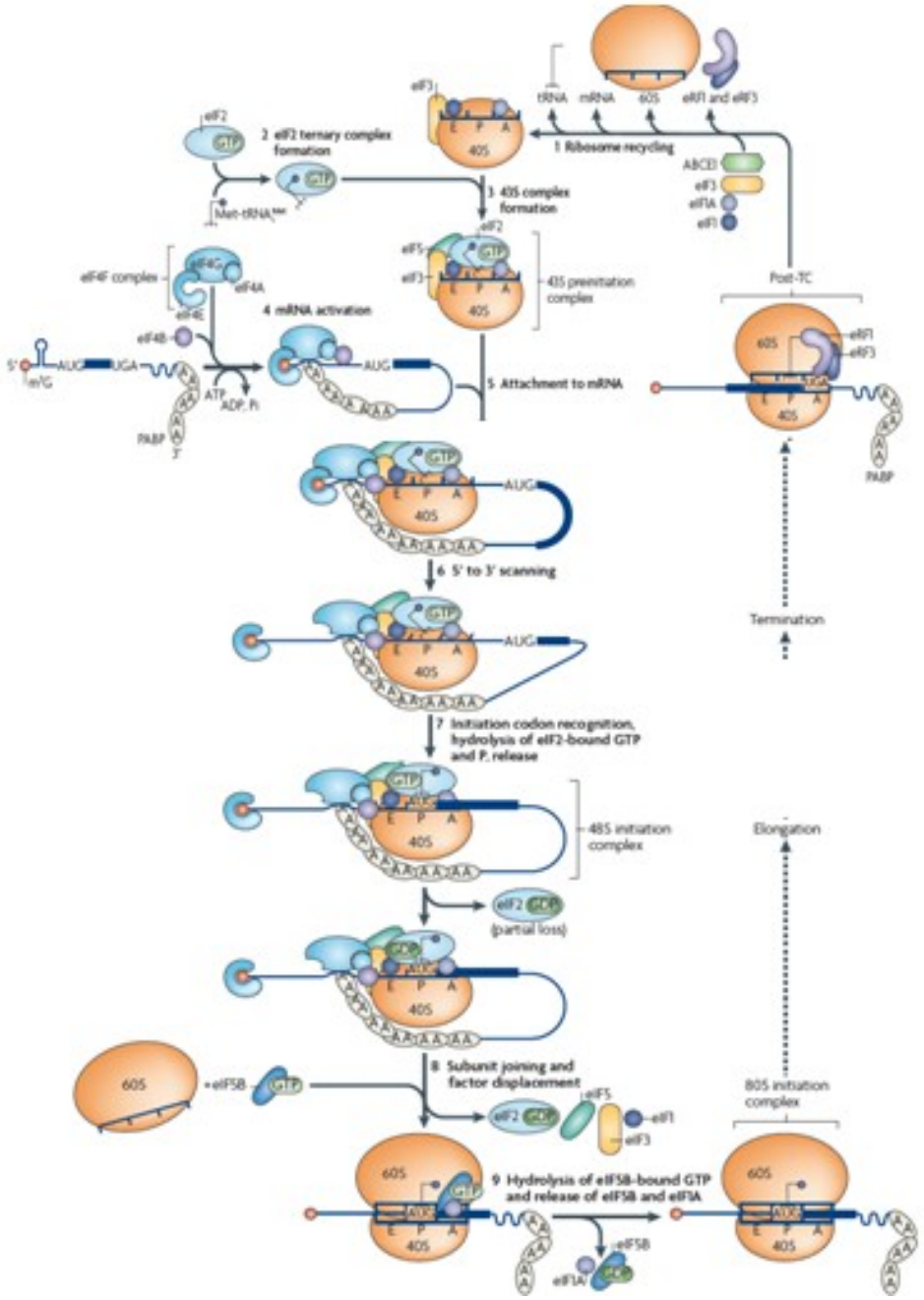

Figure 2.Cap-mediated Translation Initiation

Figure 2 shows a summary of the key events involved in cap-dependent translation initiation. Beginning at the top right, the ribosomal subunits are recruited from post translation complexes (pTCs) for additional rounds of translation. The small ribosomal subunit associates with various initiation factors to form the 43S complex. This complex is then recruited to the 5' cap to bind the eIF4F cap-binding complex. The complex scans to the start codon, and the Met-tRNA$^{Met}_i$ anticodon binds the AUG codon. The large ribosomal subunit is then recruited and polypeptide synthesis begins. Figure derived from reference 73.

73). The high degree of secondary structure in a natural 5′ UTR hinders direct binding of the 43S complex to mRNA (64, 73). Yet, the eIF4F cap-binding complex, along with eIF4H and/or eIF4B, works in a cooperative manner to facilitate binding of 43S to the 5′ end (161-164, 168, 73).

The eIF4F cap-binding complex consists of three proteins; eIF4E, eIF4G, and eIF4A. eIF4E is the cap binding protein that ties eIF4F to the 5′ end (165). eIF4G serves as a scaffolding protein whose binding to several initiation factors is vital for assembly of the 48S complex at the 5′ end (73). A region of eIF4G wraps around the amino terminal region of eIF4E which enhances binding of eIF4E at the 5′ cap (166, 167). eIF4G also binds eIF3 of the 43S complex and the poly(A)-binding protein (PABP). eIF4A has intrinsic RNA helicase/ATPase activity, due to its DEAD-box motif, which facilitates unwinding of the 5′ UTR secondary structure (159, 160, reviewed in ref. 73). eIF4A alone has low helicase activity, however it is greatly enhanced by eIF4G and eIF4B/H (168). Unwinding creates a favorable environment for binding of (1) the 43S complex to the 5′ end and (2) scanning (73).

Although a substantial amount of data have revealed how many initiation factors are configured at the 5′ cap, much remains unknown about how mRNA is transported through the mRNA binding channel of the 40S ribosomal subunit. Once the 43S complex is assembled at the 5′ cap, the complex travels along the mRNA transcript in a downstream direction until it reaches the AUG start codon. eIF1 and eIF1A are crucial for scanning, and are believed to facilitate an optimal complex conformation for movement (64, 65). ATP, eIF4A, and eIF4G are also required for scanning, even when the 5′ UTR contains a low degree of secondary structure (64).

Currently, varying opinions exist about whether eIF4G, 4A, and 4H are located behind or in front of the 40S ribosomal subunit (reviewed in 73). Modeling by cryoelectron microscopy predicts that eIF4G is positioned behind the ribosome so that the ribosome unwinds mRNA

secondary structure and eIF4G, eIF4A, and eIF4B/H serve to 'ratchet' mRNA through the binding channel using their helicase activity (74). However, an alternative model proposes that eIF4G, 4A, and 4H are positioned in front of the 40S ribosomal subunit and are involved in unwinding mRNA secondary structure before it enters the mRNA binding channel (75). Even though much data have been obtained to understand how the 43S complex is assembled at the 5' end, it is still unclear how the complex is oriented after leaving the 5' end during the initial events of scanning. Futhermore, it remains uncertain what conformational changes take place during the processive scanning process.

The complex scans along the transcript until it reaches the start codon. This is usually the first AUG codon of the mRNA sequence with optimal bases of a -3 purine and a +4 guanine surrounding the codon, with the first A in the AUG sequence located at +1 (170). eIF1 has a vital function in recognition of AUG vs. non-AUG sequences, and it is also important in finding AUGs that are in an optimal context and are not located too close to the 5' end (64, 171, 172). Once the complex locates an optimal AUG codon, ribosomal conformational changes occur that are mediated by eIF1 (171, 172). This allows binding of the Met-tRNA$^{Met}_i$ anticodon to the AUG codon and leads to tighter binding of eIF4AI to 40S. eIF1 is then displaced from the 40S P site and the complex transitions to a 'locked' conformation around the mRNA (65, 173, 174). At this step the 48S complex is formed. Displacement of eIF1 permits eIF5 GTP hydrolysis of eIF2-GTP-Met-tRNA$^{Met}_i$ (173, 175). eIF1A is required for proper ribosomal subunit joining by taking part in an event involving interaction of its C-terminal domain with eIF5B (176, 177). This interaction recruits the large 60S ribosomal subunit to 40S and permits eIF5B-stimulated hydrolysis of GTP (176,177). eIF1A is most likely displaced with eIF5B after subunit joining (178, 179). eIF3, and eIF2-GDP are displaced at some time in this process, but it remains uncertain whether it occurs

before, during, or after ribosomal subunit binding. Polypeptide synthesis then commences upon 40S and 60S subunit joining to form the 80S ribosomal complex.

Cap-independent Translation Initiation

Some mRNAs use cap-independent mechanisms for ribosomal recruitment during translation initiation. One method involves binding of the 40S subunit to an internal ribosome entry site (IRES) at or near the AUG start codon. IRESs have been identified in cellular and viral mRNA transcripts, but they have been best characterized in viral transcripts. Studies were first performed in poliovirus to understand how a virus that used protease 2A to cleave eIF4G and shut down cellular translation was still able to synthesize viral protein. A viral IRES was identified which recruited the ribosomal subunit to an internal site in a process that was not dependent on containing a cap.

Viral IRESs contain a large amount of secondary structure and are located at regions within the 5′ UTR. Currently, there are four classifications of viral IRES; Type 1, Type 2, Type 3, and Type 4 (Fig. 3) (reviewed in Ref. 73). In Type 1 and 2 IRESs, eIF4G and eIF4A bind the IRES structure through interaction of eIF4G's p50 domain with the IRES which is enhanced by eIF4A (Fig. 3) (70, 23, 180). The 43S complex then associates with this region, however, cap-binding protein eIF4E is not recruited. The poliovirus is a member of Type 1 IRESs and encephalomyocarditis virus (EMCV) contains a Type 2 IRES. The eIF4F cap-binding complex, eIF4B, eIF1A, and eIF1 are not involved in translation initiation on Type 3 IRESs (Fig. 3). Instead, the 43S complex binds directly to the AUG codon through IRES interactions with eIF3 and the small 40S ribosomal subunit (74, 181). Hepatitis C virus contains a Type 3 IRES. Translation

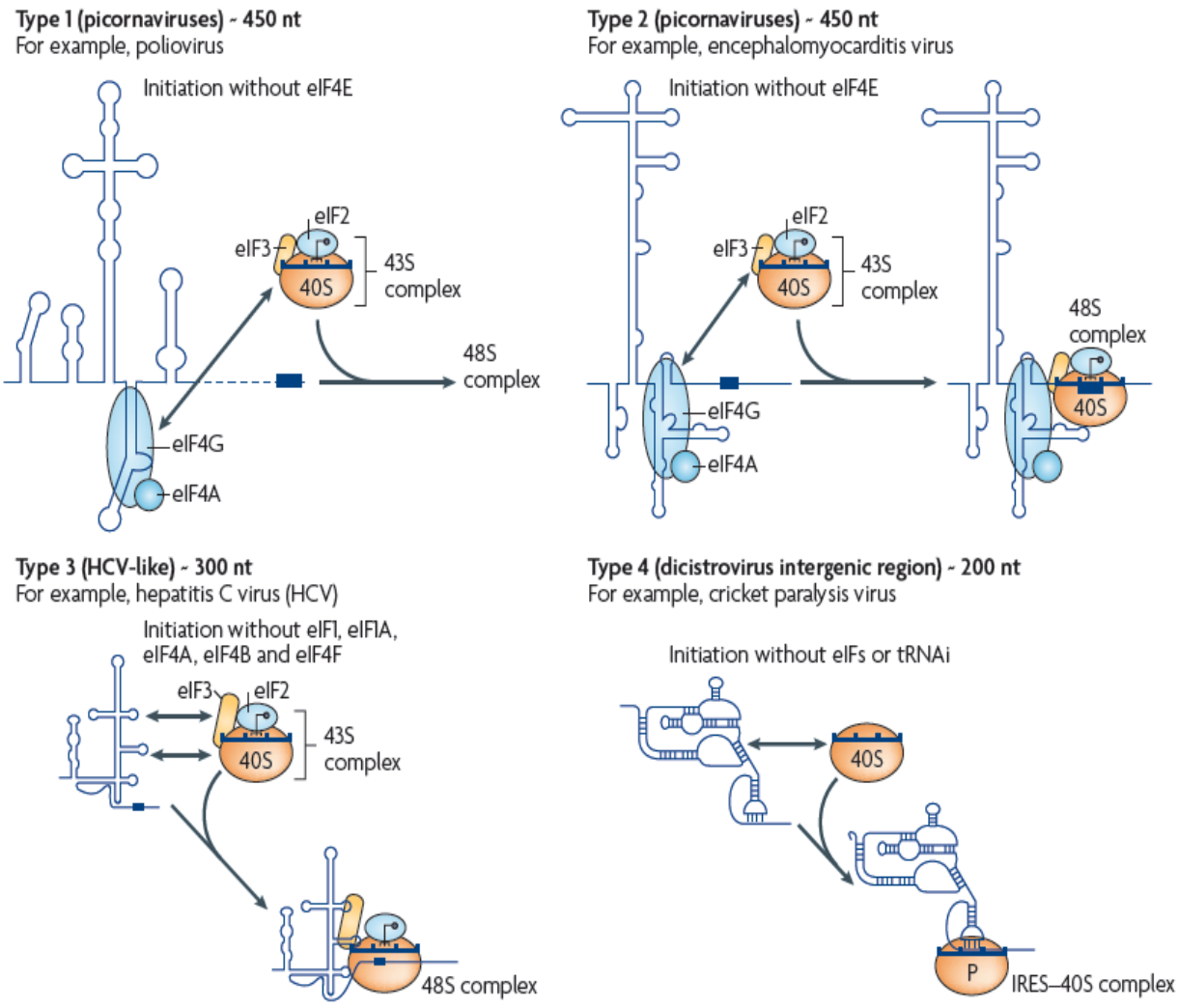

Figure 3. Viral Internal Ribosome Entry Sites

Figure 3 shows the four classifications of viral IRESs. Type 1 and 2 IRESs do not require cap-binding protein eIF4E, but they still require the remaining canonical translation initiation factors. Type 3 IRESs do not require any proteins of the eIF4F complex, but they still recruit the 40S ribosomal subunit through association with eIF3 and additional translation initiation factors. The Type 4 IRES does not utilize any of the common translation initiation factors or $tRNA_i^{Met}$ for recruitment of the 40S ribosomal subunit, and it instead has an IRES structure that forms a pseudo-tRNA-like structure. Figure derived from reference 73.

initiation of Type 4 IRESs is rather intriguing because it does not require any of the canonical translation initiation factors nor Met-tRNA$^{Met}_{i}$. Instead, the mRNA transcript forms a pseudo-tRNA structure, and the small ribosomal subunit is directly recruited to bind the IRES in its P-site (71, 182). The cricket paralysis virus (CrPV) contains a Type 4 IRES.

RNA Regulation

RNA is important for several biological processes. As mentioned previously, it carries the code for protein synthesis, and it recruits initiation factors and the 40S and 60S ribosomal subunits to the start codon. However, it plays a role in many functions besides translation. It has been shown to form supramolecular complexes, catalyze biochemical reactions, and regulate gene expression (183, 184, 185). Bacterial riboswitches have been found to be important in controlling nucleic acid, vitamin, and purine metabolism (186). Bacterial expression can be regulated by small noncoding RNAs (185). RNA is involved in regulating gene expression in eukaryotes by siRNA and micro RNA silencing of chromosomes and binding to mRNA sequences to cause degradation or inhibition of protein synthesis (187).

RNA also plays a role in regulating protein synthesis. One example is RNA regulation of ferritin mRNA. Ferritin mRNA contains iron regulatory elements at the 5′ and 3′ ends which recruit proteins involved in regulating iron metabolism (190-193). The bovine growth hormone receptor has many 5′ UTR splice variants that have been shown to have varying degrees of translation (194).

Another form of RNA regulation is when structural barriers in the mRNA secondary structure prevent or enhance scanning of the 43S complex to the AUG start codon (188, 183, 189). mRNAs with highly structured 5′ UTRs often code for regulatory proteins such as ligand

receptors, DNA binding proteins, transcription factors, and growth factors (35,197). Studies that analyzed mRNA 5′ UTR structure were first performed by Kozak, and they showed that secondary structure near the 5′ end inhibited protein synthesis (170). Through *in vitro* work she determined that a -30kcal/mol hairpin inhibits translation when it is positioned within 12 bases of the 5′ cap (34). However, this same type of hairpin does not have an inhibitory effect when it is positioned 52 bases downstream of the cap (34). In her early studies using Cos7 cells, she found that a -30 kcal/mol hairpin did not inhibit translation, but a -50kcal/mol hairpin inhibited translation 85-95% (195). Recent studies by Tsien using advanced algorithms for determining hairpin thermodynamic stability have concluded that, in Cos7 cells, translation efficiency sharply decreases as the hairpin increases in stability from -25 to -35 kcal/mol (35). This lab also showed that a hairpin within the first 4 bases from the 5′ cap inhibits translation, but a hairpin at a +7 or +13 position stimulates translation in live cells (35). Studies in live cells showed that no hairpin was able to completely block translation. It was proposed that, during this type of severe inhibition, the complex might skip over the hairpin or the skipping event may occur by ribosomal shunting (35).

Additional work in yeast and Cos7 cells has revealed that hairpins with a higher GC content cause greater inhibition of translation, independent of their intrinsic stability (35, 196). It was hypothesized that structures with relatively weak thermodynamic stability still hinder translation if they contain high GC content. This idea was based on a model for scanning complex unwinding of mRNA secondary structure that involved the complex scanning in a progressive manner to locally unzip each base pair (35). Under this model it was predicted that if mRNA contains a high enough GC content in one area, then it might exceed the amount of energy available to the scanning complex for unwinding.

mRNA Turnover

mRNA turnover is one of the key factors that controls gene expression in the cell. The half lives of mRNAs can differ substantially. Some mRNAs have longer decay rates and remain in the cell for several cycles, while others have rates that are 100-fold shorter than a single generation cycle (198). Environmental cues can also control mRNA degradation rates and quickly convert previously unstable transcripts to stable constructs. 7-methylguanosine cap addition to the 5′ end and polyA tail incorporation into the 3′ end are two key RNA modifications. These modifications ensure transcript stability, enable proficient processing and export from the nucleus, and aid in protein synthesis (199). Alterations in normal mRNA turnover have been suggested to cause a variety of problems such as cancer, coronary disease, and chronic inflammatory issues (200). mRNA degradation is also vital during nonsense mediated decay for turnover of mRNAs encoded by mutant alleles. An important regulatory step in mammalian gene expression is the control of cytoplasmic mRNA half lives. Since Vhs regulates the rate of mRNA turnover, it plays a key role in the overall scheme of gene regulation in infected cells.

The primary mode of mRNA turnover begins with removal of the 3′ poly(A) tail. The majority of studies have been performed with yeast. In this model, the polyA tail is removed by the poly(A) binding protein (Pab)1-dependent Pan2/Pan3 (poly(A) nuclease) complex (201, 202, 203). Carbon catabolite repression 4 (Ccr4) and a Ccr4-associated factor (Caf1) have also been suggested to be important for mRNA deadenylation (203, 204). Following removal of the poly(A) tail, decapping enzyme *Dcp1* is stimulated and removes the 5′ cap with the help of several additional factors (205, 206). The remaining RNA transcript is then susceptible to 5→′3′ or 3′→5′ mediated cleavage. RNA is cleaved in the 5′→3′ direction by 5′ exonuclease *Xrn1* (207).

It is subject to 3′→5′ digestion by the exosome. In yeast, 5′→3′ exonuclease activity is substantially more rapid, and the overall disappearance of mRNA is believed to be attributed to this digestion (208-210). The deadenylation-dependent mRNA decay pathway is not as clearly understood for large multicellular organisms.

Poly(A) binding protein binding to the poly(A) tail helps protect the mRNA from degradation (213). PABP also binds the eIF4G scaffolding protein, a component of the eIF4F cap-binding complex (214). These interactions cause mRNA to circularize *in vitro*, permit translation, and are believed to protect the transcript from exposure to deadenylases and decapping enzymes (215). *in vitro* and *in vivo* studies have shown that the deadenylating nuclease PARN binds the 5′ cap to access the poly(A) tail for degradation (216). Furthermore, eIF4E and cap analog inhibit PARN activity because they serve as competitors for 5′ cap binding (216, 217). However, in the presence of cap analog, decapping activity is stimulated because eIF4E and PARN are blocked from binding the 5′ cap and translation initiation is inhibited (217,218). It is believed that, following degradation of the poly(A) tail, PARN dissociates from the transcript allowing binding of the decapping enzyme to the 5′ cap (199). Interestingly, mRNAs are destabilized when translation initiation is inhibited, but they are stabilized in the presence of translation elongation-inhibiting drugs like cycloheximide (211, 212).

The sequence within a transcript can impact how RNA is regulated. Certain sequences have been determined to promote or deter mRNA decay. One example is mRNA which contains an A + U rich element (ARE) in the 3′ UTR. Many mRNAs that contain an ARE encode growth factors, cytokines, or proto-oncogenes (200, 219). Several different types of ARE-containing mRNAs have been identified. These AREs appear to accelerate the rate of removal of the poly(A) tail, leading to rapid mRNA degradation (200). On the other hand, some mRNAs contain

sequences which allow stabilization in the cell. The 3′ end of α–globin mRNA contains a cytosine-rich region which promotes assembly of a stabilizing complex that inhibits mRNA decay (220, 221, 222). c-fos mRNA contains an ARE sequence in its 3′UTR and a major protein-coding –region determinant (mCRD) sequence in its 5′UTR (223). The mCRD promotes assembly of a complex in the transcript's coding region that leads to rapid destabilization (223). Interleukin-2 mRNA contains sequence elements at its 5′ and 3′ ends which have opposite functions. In the absence of T cell activation, the 3′ ARE allows rapid deadenylation and constant mRNA instability. However, once T cells are stimulated, the transcript is stabilized by interaction with nucleolin and YB-1 proteins at its 5′ UTR responsive element (225). This element recruits factors involved in the c-Jun amino-terminal kinase (JNK) signaling pathway (224).

In non-sense mediated decay, mRNA transcripts with premature stop codons are degraded. The premature stop codon isn't recognized until translation termination, and yeast studies reveal that the decay process does not involve deadenylation (226). Instead, mRNA is decapped by the same decapping enzymes used in the deadenylation-dependent decay.

CHAPTER 2

MATERIALS AND METHODS

Plasmids and DNA Isolation and Separation

pBK2

The pBK2 plasmid (8) was constructed by Bradley Karr, a previous member of the lab. It contains a *BglII*/*SmaI* 1,165 bp HSV-1 thymidine kinase fragment that was inserted into the pSP64polyA vector purchased from Promega (Madison, WI) at *BamHI*. The final construct contains an SP6 promoter upstream of a 5′ UTR that is 91 bases long and encodes all but the last 6 codons of the thymidine kinase sequence followed by a stretch of 30 dA:dT nucleotides. The vector confers ampicillin resistance. Prior to *in vitro* transcription, the plasmid was linearized with *EcoRI* and then added to an RNA synthesis reaction resulting in RNA template of 1244 bases. pBK2 plasmid was used for construction of all site-directed mutants and hairpin constructs.

pKOSamp

pKOSamp was constructed by David Everly, Jr., a previous member of the lab (32). It contains the *UL41* open reading frame of HSV-1 strain KOS downstream of a CMV and T7 promoter. The *HindII*/*XbaI* fragment of pKOS (31) was cloned into the corresponding sites of Invitrogen vector pCDNA1.1amp (San Diego, CA). The fragments contained 89 bp of viral DNA upstream of the *UL41* gene. The DNA was linearized with *XbaI*. *in vitro* transcription followed by *in vitro* translation resulted in a 58 kDa protein.

pcDNA1.1amp

pcDNA1.1amp was used for control samples during mock transfections to confirm that cells were transfected with equal amounts of DNA. It was purchased from Invitrogen (San Diego, CA) and previously propagated in TOP10F' *E.coli* competent cells by David Everly, Jr. It confers ampicillin resistance and eukaryotic origins from SV40 and polyoma virus. *in vitro* transcription is carried out with a T7 phage RNA polymerase promoter and the immediate early CMV promoter allows expression in cells. The vector also contains polyadenylation signals and a SV40 splice region.

p333amp

p333amp was previously created by David Everly, Jr. It contains the *UL41* open reading frame of HSV-2 strain 333 excised at *HindIII*/*XbaI* from p333 (31) and cloned into pcDNA1.1amp (San Diego, CA) at the corresponding positions (32). It contains a T7 and CMV immediate early promoter upstream of *UL41*. The DNA was linearized with *XbaI* followed by *in vitro* transcription and *in vitro* translation resulting in a 58 kDa protein.

pC53

The C53 bicistronic vector was kindly provided by Peter Sarnow (38, 80). It contains an upstream cistron which encodes renilla luciferase and a downstream cistron encoding firefly luciferase (Fig. 4). The intergenic region encodes EMCV RNA secondary structure with mutations making it a nonfunctional IRES (ΔEMCV) (26, 38, 80). The vector was created by cleaving pRL-SV40 vector from Promega (Madison, WI) with *BglII* and *XbaI* to yield a fragment

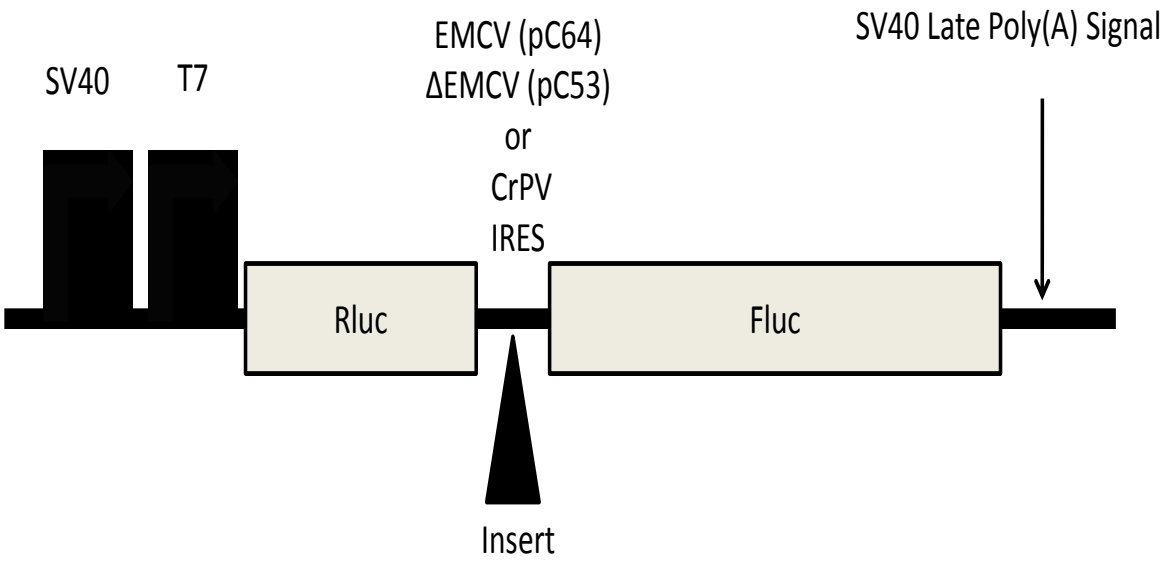

Figure 4.Cartoon Depiction of Bicistronic Construct

Figure 4 shows the bicistronic construct containing a functional EMCV IRES (pC64), nonfunctional EMCV IRES (pC53), or the cricket paralysis viral IRES (CrPV) in the intergenic region. SV40 and T7 promoters precede the first cistron, renilla luciferase (Rluc). The downstream cistron is firefly luciferase (Fluc), and it is followed by an SV40 late poly(A) signal.

containing the T7 and SV40 promoter upstream of renilla luciferase. This fragment was then inserted into the Promega pGL Basic Vector (Madison, WI) at *SmaI* following a Klenow reaction.

A nonfunctional EMCV IRES fragment of around 440 bases (26) was then added to the intergenic region of the construct at *EcoRI* (38, 80). The vector has ampicillin (amp) resistance and a late SV40 polyadenylation signal following the second cistron. For these studies C53 was linearized with *BamHI*, and *in vitro* transcription resulted in an RNA template of 3390 bases. The first cistron is located from bases 12-946 and the second cistron is located from bases 1474-3126 of the RNA template. The intergenic region is between bases 947-1473 of the RNA transcript.

pCrPV

The CrPV bicistronic vector was kindly provided by Peter Sarnow (38, 80). It contains an upstream cistron which encodes renilla luciferase and a downstream cistron encoding firefly luciferase (Fig. 4). The intergenic region encodes a CrPV functional IRES (38, 80). The vector was created by cleaving pRL-SV40 vector from Promega (Madison, WI) with *BglII* and *XbaI* to yield a fragment containing the T7 and SV40 promoter upstream of renilla luciferase. This fragment was then inserted into the Promega pGL Basic Vector (Madison, WI) at *SmaI* following a Klenow reaction. A functional CrPV IRES fragment of 189 bases was then added to the intergenic region and is located between bases 1474-1662 of the sequence (38, 80). The vector has ampicillin resistance and a late SV40 polyadenylation signal following the second cistron. For these studies CrPV was linearized with *BamHI*, and *in vitro* transcription resulted in an RNA template of 3594 bases. The first cistron is located from bases 12-947 and the second cistron is located from bases 1678-3330 of the RNA template. The intergenic region is between bases 948-1677 of the RNA transcript.

pC64

pC64 was kindly provided by Peter Sarnow (38, 80). It contains an upstream cistron which encodes renilla luciferase and a downstream cistron encoding firefly luciferase (Fig. 4). The intergenic region encodes a functional EMCV IRES (26, 38, 80). The vector was created by cleaving pRL-SV40 vector from Promega (Madison, WI) with *BglII* and *XbaI* to yield a fragment containing the T7 and SV40 promoter upstream of renilla luciferase. This fragment was then inserted into the Promega pGL Basic Vector (Madison, WI) at *SmaI* following a Klenow reaction. A functional EMCV IRES fragment of around 440 bases (26) was then added to the intergenic region of the construct at *EcoRI* (38, 80). The vector has ampicillin resistance and a late SV40 polyadenylation signal following the second cistron. For these studies pC64 was used solely for transient transfections.

pCITELUC

pCITE-4c(+) was purchased from Novagen (Madison, WI). The vector contains a pCITE region which encodes the EMCV IRES from EMCV strain pEC9 nucleotides 212-713 of the sequence (81). A T7 phage RNA polymerase promoter is located upstream of the IRES and a poly A recognition sequence is located from nucleotides 701-730 of the vector. For construction of the pCITELUC vector, renilla luciferase from the Promega vector pGEMLUC (Madison, WI) was cloned downstream of the EMCV IRES. Both vectors were first propagated in JM109 competent cells from Promega (Madison, WI) following the transformation protocol. Five colonies were picked and grown in LB media containing 100ug/ml ampicillin for 8 hours (hr.) at 37˚C, 300 revolutions per minute (rpm). After 8 hr., 50ul of the starter culture was added to 25 milliliters (ml) Luria-Bertani broth (LB) with 100ug/ml amp, and cultures grew overnight at

37˚C, 300rpm.

DNA was extracted using a Qiagen Midi Prep Kit (Germantown, MD) and 15 micrograms (ug) of DNA was double digested, first by incubating DNA with *XhoI* for 3 hr. at 37˚C followed by addition of *BamHI* and an additional 3 hour incubation at 37˚C with both enzymes at a concentration of 5 units (U)/ug DNA. The samples were then phenol/chloroform extracted and precipitated with 2.5 volumes 95% ethanol and 0.1 volume 3M sodium acetate, pH 5.2 overnight at -80˚C. Digestion of pCITE-4c(+) vector with *BamHI* and *XhoI* produced a 40 nucleotide (nt.) and 3661 nt. DNA fragment. Digestion of pGEMLUC with these enzymes resulted in DNA fragments of 3215 and 1716 nucleotides. The double digested DNA was then pelleted by spinning it at 13,000 rpm in a table top microcentrifuge at 4˚C for 20 minutes. The pellets were resuspended in 20ul 10mM Tris-Cl pH 7.5 + 1mM EDTA (TE buffer) pH 8.0 and stored until further use. 15ul of the sample was run on a 1% agarose 1X TAE gel with 0.5ug/ml ethidium bromide (EtBr) at 100 Volts (V) for 1.5 hours. The 3361 nt vector from pCITE-4c(+) and the 1716 nt. insert from pGEMLUC were excised and extracted using the Qiagen Gel Extraction Kit (Germantown, MD) and samples were eluted with 30ul elution buffer (EB).

13ul of the 1716 nt. renilla luciferase insert was combined with 1.85ul of the 3661 nt. pCITE-4c(+) vector in a T4 DNA ligase reaction with a final concentration of 1X T4 DNA ligaton buffer and 1U total T4 DNA ligase from Promega (Madison, WI). Samples incubated at room temperature for 30 minutes. 5ul of sample was used for transformation of 100ul JM109 competent cells following the Promega protocol (Madison, WI). 100ul, 1:10, and 1:100 dilutions were spread on LBamp plates, and colonies grew overnight at 37˚C.

8 colonies were picked and grown up in 4ml LBamp with 100ug/ml ampicillin for 8 hours at 37˚C, 300rpm. The starter cultures were then diluted as described previously and grown

up overnight. 900ul aliquots were stored in box LAS plasmids 1 with a final concentration of 10% sterile glycerol, and the samples were labeled pCITE4c(1-8)LUC. Pellets were harvested by centrifuging for 15 minutes at 6,000 relative centrifugal force (rcf). DNA was extracted using the Qiagen Midi Prep Kit (Germantown, MD) and pellets were resuspended in TE buffer pH 7.9.

Plasmids were tested for proper construction by double digestion of 2ug of sample with *BamHI* and *XhoI*. Samples were then run on a 1% agarose 1X TAE gel with 0.5ug/ml EtBr and a BioRad 1kb marker (Hercules, CA) to confirm a vector around 3.7kb and a 1.7kb insert. All plasmids except pCITE4c4LUC were constructed correctly.

DNA Isolation and Separation

Following plasmid construction, all vectors used for the *in vitro* transcription reaction were grown in starter cultures of 3ml LB containing 100ug/ml of amp for 8 hours at 37˚C and 300 rpm. 200ul was then added to 100ml of LBamp and grown up 12-16 hours followed by extraction with Qiagaen Midi Prep Kit (Germantown, MD) and resuspension in 100ul of H_2O or 10mM Tris-Cl pH 8.5 [elution buffer (EB)]. 10ug of DNA was used in a linearization reaction to ensure that transcription ended at the same location so that all starter RNA was the same length. 50U of restriction enzyme was added to the reaction for a final concentration of 5U/ug DNA. DNA samples incubated at 37°C for 4 hr. followed by precipitation with a 0.1 volumes of 3M sodium acetate pH 5.2 and 2.5 volumes of 95% ethanol for 1 hour at -80˚C. Samples were then spun in a microcentrifuge for 20 min. at 4˚C and resuspended in 20ul H_2O or EB.

in vitro Transcription and RNA Labeling

Internally-labeled mRNA

8.50ul of EcoRI-linearized pBK2 DNA was added to a Promega SP6 Riboprobe *in vitro* transcription reaction (Madison, WI) containing 50U Recombinant RNasin Nuclease Inhibitor, 2.85ul H_2O, 50uCi [α-^{32}P]GTP with a specific activity of 800 Ci/mmol, 40U SP6 RNA polymerase, a final concentration of 1X SP6 Transcription Optimized Buffer, 10mM DTT, 0.5mM ATP, 0.5mM UTP, 0.5mM CTP, 50uM GTP, and 0.5mM capping analog in a total volume of 50ul. The components incubated at 37˚C for 1 hr. 4U of RQ1 RNase-free DNase (1U/ul) was added to the system and samples incubated for 15 min. at 37˚C. RNA was then taken through two rounds of phenol/chloroform extraction at room temperature followed by precipitation with 2.5 volumes ice-cold Ethanol (EtOH) and 0.1 volumes 3M sodium acetate pH 5.2 at -80˚C overnight. mRNA was pelleted in a table top microcentrifuge for 20 minutes at 1300 rpm and 4˚C and resuspended in 20ul H_2O.

5′ Cap-labeled vs. 3′ PolyA Tail-labeled mRNA

6-9ul of *EcoRI* linearized pBK2 DNA was added to a Promega SP6 RiboMAX *in vitro* transcription kit (Madison, WI) containing 44ul H_20, 170U SP6 RNA polymerase, and a final concentration of 5mM of each dNTP and 1X SP6 Transcription Optimized Buffer in a total volume of 100ul. The reaction incubated at 37˚C for 3 hr. followed by addition of 4U RQ1 RNase-free DNase and an additional 15 min. incubation at 37˚C. The RNA was taken through 2 rounds of phenol/chloroform extraction and precipitated with 2.5 volumes of ice-cold 95% EtOH and 0.1 volume of 3M sodium acetate for at least 1 hr. at -80˚C. RNA was pelleted by spinning for 20 min. at 13,000 rpm and 4˚C. 20ug of pBK2 RNA was used in an unlabeled capping reaction, and

20ug was used in a labeled capping reaction using EPICENTRE's m7G Capping Kit (Madison, WI). For the experiment shown in Figures 14 and 15, 5.50ul of RNA was combined with 21.5ul H_2O and incubated for 8 min. at 65°C and then placed on ice. 40U ScriptGuard RNase Inhibitor, 20U ScriptCap Capping Enzyme, and a final concentration of 1X ScriptCap Capping Buffer, 1mM unlabeled GTP (for unlabeled cap sample) or 40uCi [α-^{32}P]GTP with a specific activity of 800Ci/mmol (for cap-labeled sample), and 0.1mM SAM were added to the tube. The samples were mixed and incubated at 37°C for 1 hr. The RNA was phenol/chloroform extracted and precipitated with 2.5 volumes ice-cold 95% EtOH and 0.1 volume 3M sodium acetate, pH 5.2 for at least 1hr. at -80°C.

The samples were resuspended in 9ul H_2O and used in an EPICENTRE poly(A) polymerase tailing reaction (Madison, WI). The sample with the labeled 5' cap received an unlabeled poly(A) tail, and the sample with the unlabeled 5'cap received a labeled poly(A) tail. The RNA was combined with 40U ScriptGuard RNase Inhibitor, 8U Poly(A) Polymerase, and 4ul cold 10mM ATP (for the RNA with a labeled 5' cap) or 10uCi [α-^{32}P]ATP with a specific activity of 3,000Ci/mmol + 3ul H_20 (for the RNA with an unlabeled 5' cap) in a total volume of 40ul. The reaction incubated at 37°C for 20 minutes. The samples were then precipitated with 2.5 volumes ice-cold 95% EtOH and 0.1 volume 3M sodium acetate, pH 5.2 for 1hr. at -80°C. RNA was pelleted at 13,000 rpm for 20 min. at 4°C and resuspended in 10ul H_2O. Samples were run on a 1.4% agarose 1X TBE gel containing 0.5ug/ml EtBr at 50 Volts for 3.5 hours. RNA bands were excised from the gel and purified with BioRad Freeze 'N Squeeze DNA gel extraction spin columns according to the protocol (Hercules, CA). RNA was precipitated using the procedure described previously, spun at 13,000 rpm and resuspended in 20ul H_2O.

Cap-labeled pBK2 mRNA Used in Titration Assay and Inhibition Studies with Cycloheximide, GMP-PNP, AMP-PNP, and Cap Analog

pBK2 RNA was synthesized with the Promega SP6 *in vitro* RiboMAX kit and extracted as described previously (Madison, WI). For these experiments, 50ug of RNA was used in a 5' cap-labeling reaction. It was first incubated with H_2O for 8 min. at 65˚C in order to unwind secondary structure. It was then combined with 80uCi of [α-^{32}P]GTP with a specific activity of 3000Ci/mmol, 40U ScriptCap Capping Enzyme, 100U of ScriptGuard RNase Inhibitor, and a final concentration of 0.1mM unlabeled GTP, 1X ScriptCap Capping Buffer, and 0.1mM SAM in a total volume of 100ul. Samples incubated at 37˚C for 1 hr. followed by phenol/chloroform extraction and precipitation with 2.5 volumes ice-cold EtOH and 0.10 volume 3M sodium acetate for at least 1 hr. at -80˚C. The RNA pellet was then spun at 13,000 rpm, dried, and resuspended in 20ul nuclease-free H_2O. This RNA was not gel-extracted prior to incorporation into the RRL system.

mRNA Used for Primer Extension Analysis

RNA was prepared by using 7-9ul linearized DNA in a Promega SP6 or T7 RiboMAX *in vitro* transcription reaction (depending on the construct), according to the protocol for synthesizing RNA without a cap analog (Madison, WI). Samples incubated at 37˚C for 2-4 hr. Following RNA synthesis, 4U of RQ1 RNase-free DNase was added to the system and tubes were incubated at 37˚C for 15 minutes. The RNA was taken through two rounds of phenol/chloroform extraction and then precipitated with 2.5 volumes ice-cold 95% EtOH and 0.1 volumes 3M sodium acetate pH 5.2 at -80˚C for at least 1 hour. RNA was pelleted for 20 min. at 13,000 rpm and 4˚C. Samples were resuspended in 20ul nuclease-free H_2O. 50ug samples were

used in an EPICENTRE m^7G capping reaction with unlabeled GTP according to the protocol (Madison, WI). Following the 1 hr. incubation at 37˚C, samples were precipitated with 2.5 volumes ice-cold 95% EtOH and 0.1 volumes 3M sodium acetate pH 5.2 for at least 1 hr. at -80˚C. Samples were then centrifuged for 20 min. at 13,000 rpm and 4˚C, and pellets were resuspended in 15ul nuclease-free H_2O. The RNA was then run on a 1.4% agarose 1X TBE gel containing 0.5ug/ml EtBr at 50V for 3.5 hours. RNA was extracted using BioRad Freeze 'N Squeeze tubes (Hercules, CA) followed by precipitation with 2.5 volumes ice-cold EtOH and 0.1 volumes 3M sodium acetate pH 5.2 for at least 1 hour at -80˚C. Samples were pelleted by centrifuging for 20 min. at 13,000 rpm and 4˚C. RNA was resuspended in 20ul nuclease-free H_2O.

in vitro Translation

Vhs Used for Internally-labeled RNA Substrates

6-9ul of pKOSamp *XbaI* linearized DNA was added to an *in vitro* T7 RiboMAX RNA synthesis reaction from Promega (Madison, WI) containing 23.06ul H_2O, 190U T7 RNA polymerase, a final concentration of 1X T7 Transcription Optimized Buffer, 1X DTT, 7.5mM ATP, 7.5mM UTP, 7.5mM CTP, 0.6mM GTP, and 3mM capping analog in a total volume of 100ul. The reaction incubated for 2-4 hrs. (for this experiment 2 hrs.) at 37˚C and then DNA was degraded by adding 5U RQ1 RNase-free DNase and incubating samples for 15 min. at 37˚C. RNA was taken through 2 rounds of phenol-chloroform extraction with equal volumes of solution followed by precipitation of RNA with of 2.5 volumes EtOH and 0.1 volume 3M sodium acetate pH 5.2 at -80˚C for at least 1 hour.

Unlabeled, capped pKOSamp mRNA was then pelleted by spinning in a table top centrifuge at 13,000 rpm for 20 min. at 4˚C, and the pellet was resuspended in 200ul EB. 2.3ug pKOSamp mRNA was used in an *in vitro* translation Promega Flexi RRL system (Madison, WI). One tube did not receive any pKOSamp RNA and served as the negative control where water replaced mRNA (RRL), and the other tube contained pKOSamp mRNA (Vhs). Both tubes contained 33ul RRL, 20uCi [^{35}S]methionine with a specific activity of 1200Ci/mmol, 40U RNasin, a final concentration of 20uM amino acid (-) methionine mix, 1mM magnesium acetate, 70mM KCl, and 2mM DTT in a final volume of 50ul. Prior to adding pKOSamp RNA, the RNA was heat denatured at 65˚C for 3 min. in order to unravel mRNA secondary structure. After all of the components were mixed, samples incubated at 30˚C for 1.5 hr. and were then placed on ice for rapid use or stored at -20˚C.

Vhs Assays with All Other mRNA (mRNA that was not internally labeled)

pKOSamp RNA was synthesized according to the methods described above. However, 14ug of mRNA was used for the *in vitro* translation reaction in the Flexi RRL system (Madison, WI) instead of the previously described 2.3ug.

Vhs Used to Test the Effect of Inhibitors on *in vitro* Translation

To test the effect of cycloheximide, GMP-PNP, and AMP-PNP on protein synthesis, normal Promega Flexi RRL *in vitro* translation reactions were cut in half (Madison,WI). Each tube contained 16.5ul RRL, 0.5ul 1mM amino acid minus methionine, [^{35}S]methionine as directed by the protocol, 1ul 25mM magnesium acetate, 0.70ul 2.5M KCl, 0.5ul 100mM DTT, and 20U RNasin. Different amounts of H_2O plus AMP-PNP, GMP-PNP, or cycloheximide were added

and samples incubated at 30˚C for 10 minutes. The different combinations of H_2O and analog/drug allowed various concentrations to be tested. After the incubation, 3.5-7.0ug of cap-unlabeled pBK2 or pKOSamp mRNA was added and samples incubated for 1.5 hr. at 30˚C. For positive controls, no drug/analog was added to the RRL system prior to addition of mRNA. For negative controls, mRNA was replaced with H_2O. The different concentrations tested were 0.1mM, 0.2mM, 0.5mM, 1mM, and 2mM non-hydrolyzable analogs and 50-100ug/ml cycloheximide.

Vhs Assay

Internally-labeled Substrate mRNA

30ul TE buffer pH 7.5 was added to Tube 1 for analysis of zero time point samples, 30ul of RRL lacking Vhs protein (RRL) from the *in vitro* translation reaction was added to Tube 2 to serve as the negative control, and 30ul of RRL containing Vhs protein (Vhs) was added to Tube 3 (Fig. 5). 5ul of capped, internally-labeled pBK2 mRNA was then added to each tube and 5ul aliquots were removed at the indicated time points and added to 245ul TE buffer pH 7.5 followed by mixing. This was to achieve a workable volume for accurate pipetting. The mixed sample was then added to 750ul TriZol which contained 15ug carrier tRNA, mixed, and incubated at room temperature for at least 5 minutes. 200ul chloroform was added to the tubes and then they were vigorously shaken for 15 seconds. The tubes incubated at RT for at least 2 minutes, and samples were spun in a table top microcentrifuge at 4˚C top speed for 15 minutes. The aqueous layer was transferred to a new tube, and samples were precipitated by addition of 500ul isopropanol to the new tube and incubation at RT for 10 minutes. The RNA was

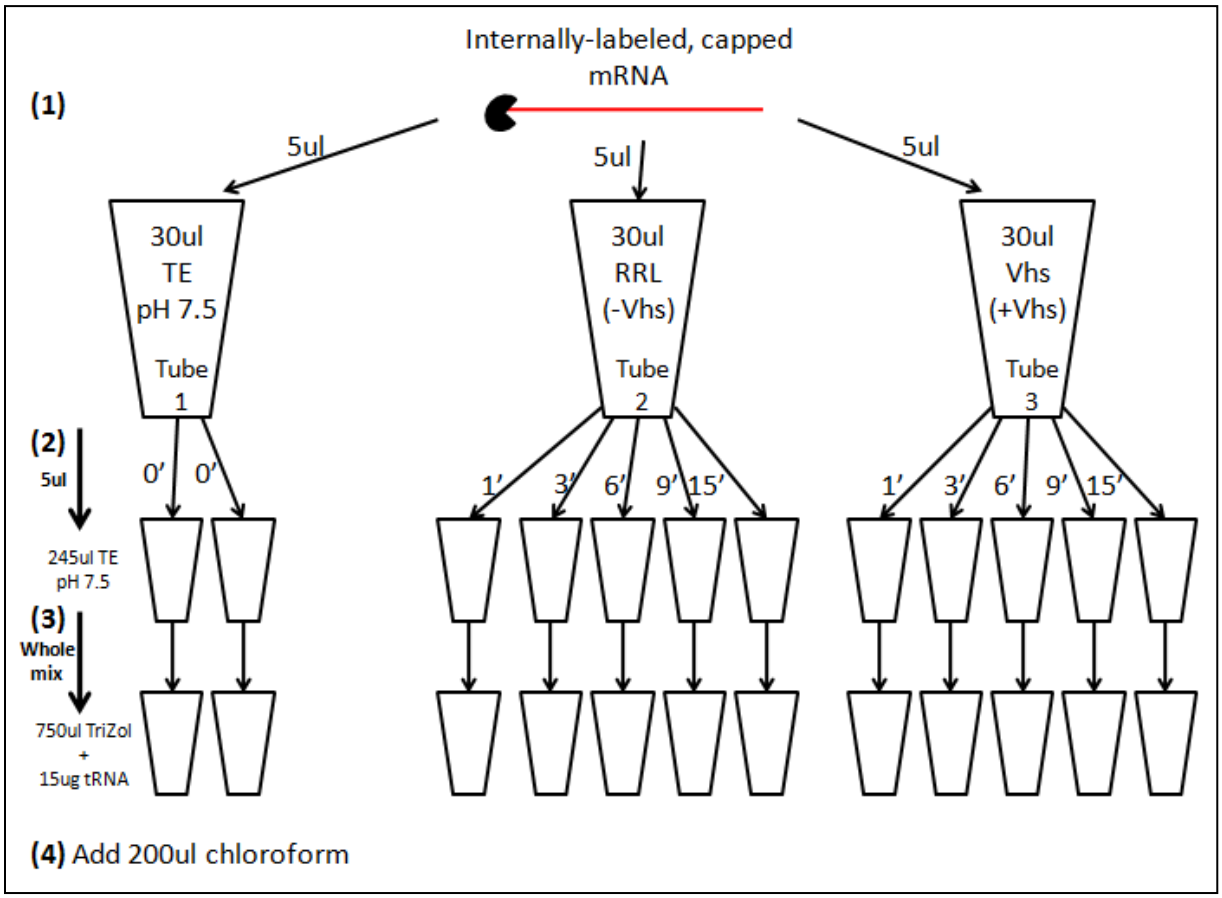

Figure 5.Vhs Assay Procedure with Internally-labeled mRNA Substrate

Figure 5 is a diagram of the Vhs assay procedure used for experiments that examined internally-labeled mRNA substrate. Step 1 shows the amount of substrate mRNA that was added to the zero time point (TE buffer pH 7.5), RRL lacking Vhs (RRL), or RRL containing Vhs (Vhs) system. Step 2 represents 5ul aliquot extractions at the indicated time points that were added to 245ul TE pH 7.5. Step 3 shows that the entire mixture was then added to 750ul Trizol containing 15ug of carrier tRNA, followed by addition of 200ul chloroform (listed in step 4).

centrifuged at 4˚C top speed for 10 minutes, and the pellet was air dried and resuspended in 10ul nuclease-free water. 5ul of samples was combined with 15ul Ambion NorthernMax formaldehyde load dye (Austin, TX) and samples were incubated at 65˚C for 15 minutes. They were then spun briefly, placed on ice for a few minutes, and loaded onto a 1.2% agarose 1XMOPS formaldehyde denaturing gel from Ambion's NorthernMAX Denaturing Gel Buffer (Austin, TX) and run at 50V for 3.5 hr. with recirculation of 1XMOPS buffer halfway through the run. The gel was then dried for 4 hr. at 80˚C and then placed under a phosphorimaging screen. The gel was then viewed by autoradiography using a Storm 840 Imager by GE Healthcare and GE ImageQuant 5.0 software (Waukesha, WI).

5'Cap-labeled vs. 3' Poly(A) Tail-labeled pBK2 mRNA

4.0ul of either 5' cap-labeled 3' polyA tail-unlabeled or 5' cap-unlabeled polyA tail-labeled pBK2 mRNA was added to (1) 12.60ul 10mM Tris-Cl pH 7.5 + 0.9ul H_2O (2) 12.60 RRL lacking Vhs (RRL) + 0.9ul H_2O, or (3) 12.60 RRL containing Vhs (Vhs) + 0.9ul H_2O (Fig. 6). The remaining procedure was carried out identical to the procedure described under Internally-labeled Substrate mRNA with the exception that mRNA was washed with 70% and 99.9% EtOH following precipitation and it was resuspended in 12ul nuclease-free H_2O. 5ul was used for analysis on a 1X MOPS gel and 5ul was used for analysis on a 7% polyacrylamide 8M urea 1X TBE sequencing gel. For analysis on the sequencing gel, the gel was cast for 45 min. and then preheated for 1.5 hrs. at 50W constant power. 5ul of the sample was then combined with 5ul of Ambion Gel Loading Buffer Dye II (Austin, TX) and tubes were heated to 90˚C for 10 min. Samples were then run on the preheated sequencing gel at a constant power of 50W for 1.5 hrs

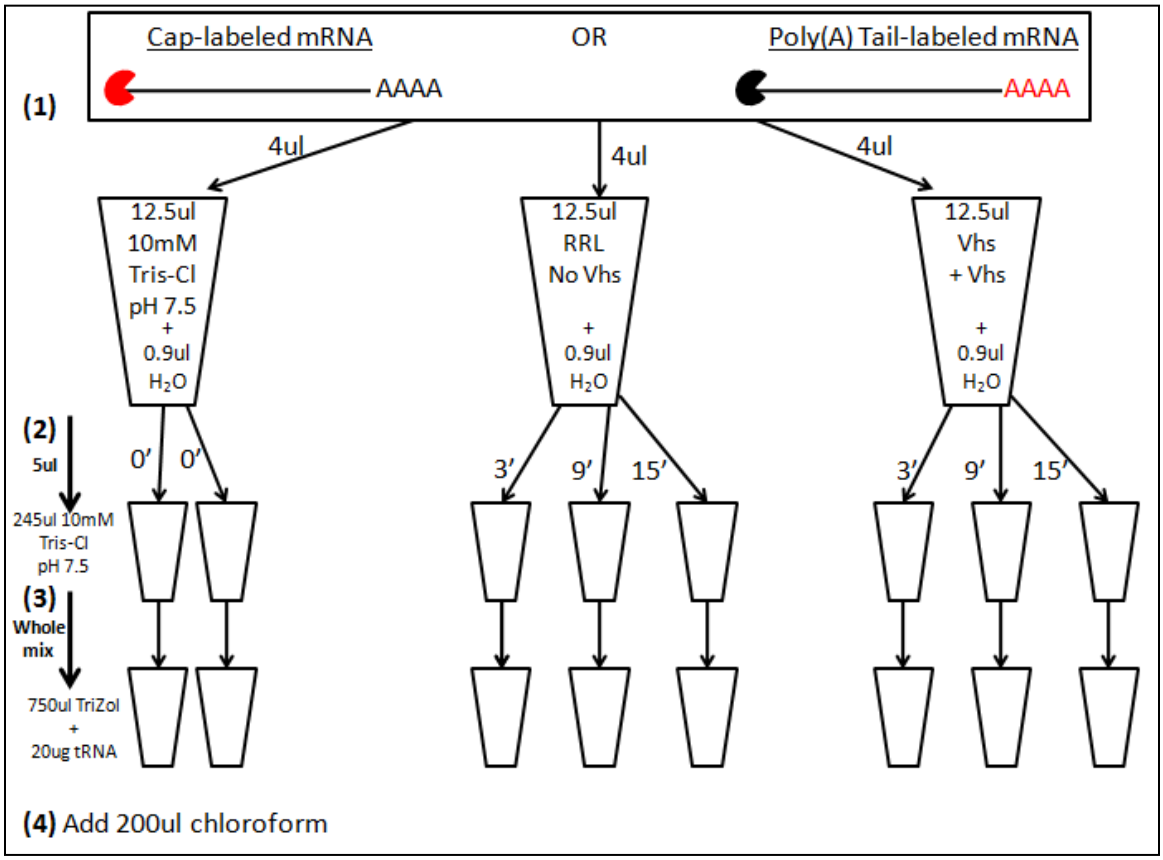

Figure 6.Vhs Assay Procedure for Cap-labeled or Poly(A) Tail-labeled mRNA

4ul of RNA substrate was incubated in 12.5ul 10mM Tris-Cl pH 7.5, 12.5ul RRL lacking Vhs, or RRL containing Vhs from left to right, respectively (1). 5ul aliquots were removed at the indicated time points and combined and mixed in 245ul 10mM Tris-Cl pH 7.5 (2). The entire mixture was then added to 750ul TriZol containing 20ug carrier tRNA and mixed (3). Following 5 minutes, 200ul of chloroform was added to each tube and samples were shaken vigorously followed by incubated for at least 2 minutes before centrifugation.

using a BioRad Sequi-Gen GT apparatus (Hercules, CA). The gel was transferred to Whatman 3MM filter paper, dried at 80˚C for 1 hr., and placed under a phosphorimaging screen for eventual analysis.

Vhs Titration

Following *in vitro* translation, RRL containing Vhs was diluted 2 fold with RRL lacking Vhs to yield 0.5X Vhs. 0.5X Vhs was then diluted 2 fold with RRL lacking Vhs to yield .25X Vhs. 12.60ul of the sample was used in a Vhs titration assay, and 12.60 ul of RRL without Vhs was used as a control. 3.4ul H_2O was added to each tube followed by addition of 2.5ul cap-labeled pBK2 mRNA. 5ul aliquots were removed from the system at 0, 3, 9, and 15 minute time points.

AMP-PNP

Six tubes were used in this study. Two tubes contained 12.60ul 10mM Tris-Cl pH 7.5 (Fig. 7). Two tubes contained 12.60ul RRL without Vhs (RRL), and two tubes contained 12.60ul RRL with Vhs (Vhs) (Fig. 7). One of the tubes in the group received 3.40ul H_2O and the other tube received 3.40ul of 9.44mM AMP-PNP from Sigma-Aldrich (St. Louis, MO) for a final concentration of 2mM AMP-PNP. After addition of H_2O or AMP-PNP, the tubes incubated at 30˚C for 12 min. followed by addition of 2.50ul pBK2 cap-labeled mRNA. 5ul aliquots were removed at 3, 9, and 15 minute time points from the RRL and Vhs samples and at 0 minutes from the 10mM Tris-Cl samples. The aliquots were added to 245ul 10mM Tris-Cl pH 7.5. The rest of the RNA extraction was performed as described previously. RNA did not undergo washes with 70% and 99.9% EtOH.

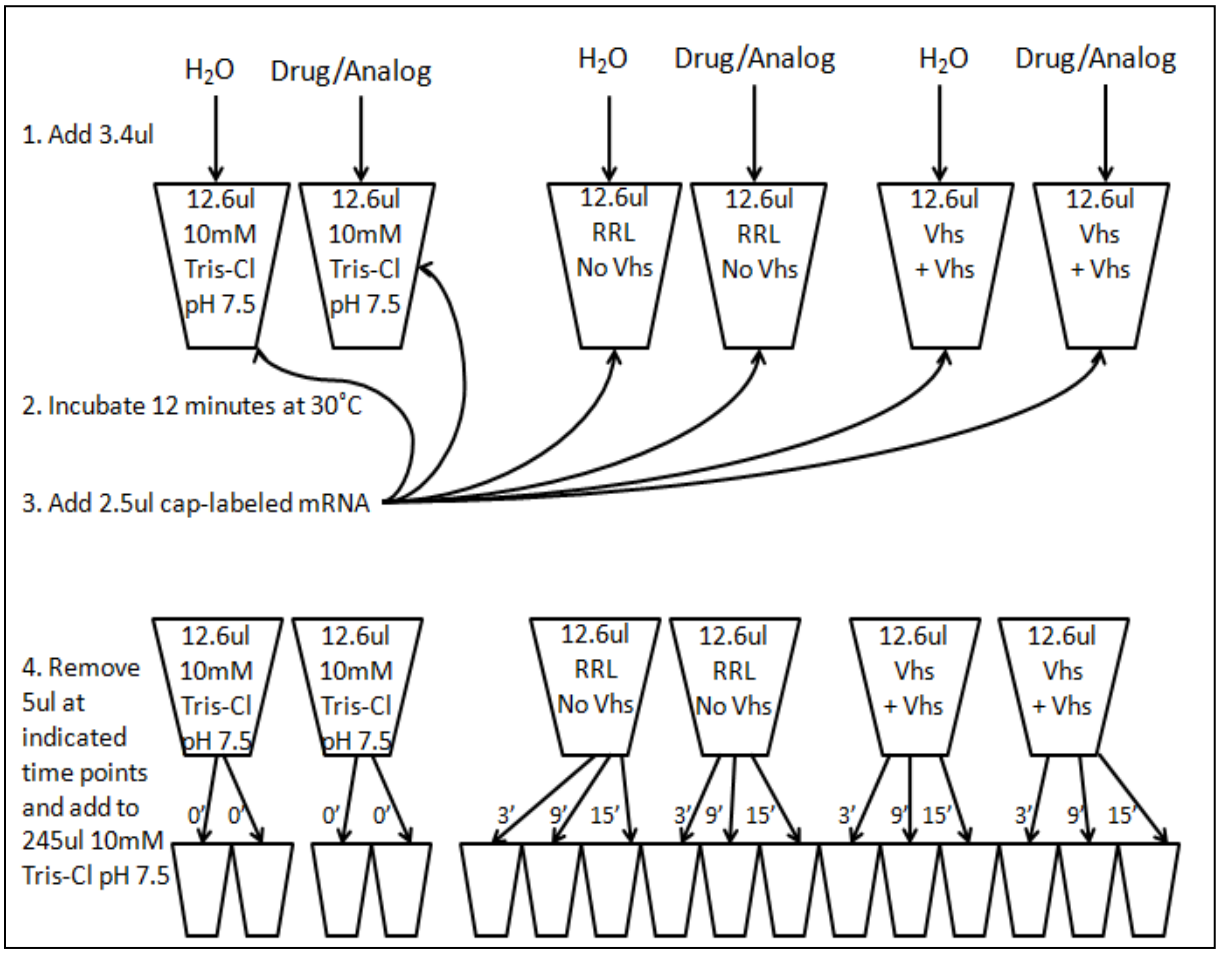

Figure 7.Vhs Assay Procedure from Inhibition Studies with Cap-labeled mRNA

3.4ul H_2O was added to three tubes containing 12.6ul of 10mM Tris-Cl pH 7.5, RRL without Vhs, or RRL with Vhs (1). 3.4ul of water + drug/analog was added to three other tubes with the same components (1). Samples were incubated for 12 minutes at 30˚C (2). 2.5ul Cap-labeled mRNA was added to samples (3) and aliquots were removed at the indicated time points and combined and mixed in 245ul 10mM Tris-Cl pH 7.5 (4). The entire mixture was then added to 750ul TriZol containing 14ug carrier tRNA and the remaining RNA extraction followed according to the protocol previously described.

For analysis of full length RNA, the pellets were resuspended in 5ul H_2O followed by addition of 15ul Ambion NorthernMAX formaldehyde load dye (Foster City, CA). Samples incubated for 15 min. at 65˚C and were then loaded onto a 1.4% agarose 1XMOPS denaturing gel and run at 50V for 3.5 hours. The gel was transferred to Whatman 3MM filter paper and dried for 4 hrs. at 80˚C.

For analysis of smaller RNA cut sites, pellets were resuspended in 10ul nuclease-free H_2O followed by addition of 10ul gel loading buffer dye II. Samples were heated at 95˚C for 5 min. and then loaded onto a 6% polyacrylamide 8M urea 1X TBE gel. They were run on a BioRad Protean II xi cell at 150V for 5.5 hours. The gel was then transferred to Whatman 3MM filter paper and dried for 3 hr. at 80˚C.

GMP-PNP

The reaction was performed identical to the AMP-PNP experiments except 1.60ul of 20mM GMP-PNP and 1.80ul nuclease-free H_2O were added to the tubes receiving GMP-PNP for a final concentration of 2mM GMP-PNP.

Cycloheximde

Experiments were performed identical to the AMP-PNP studies, except instead of AMP-PNP, cycloheximide was added to half of the tubes at a final concentration of 50ug/ml.

Cap analog

Experiments were performed identical to the AMP-PNP studies except AMP-PNP was replaced with Promega m^7G cap analog (Madison, WI). For 3mM inhibition studies, 1.20ul

40mM cap analog plus 2.40ul nuclease-free H_2O was added to half the tubes. For the 5mM cap analog studies, 2.0ul 40mM cap analog plus 1.60ul nuclease-free H_2O was added to half the samples.

Primer Extension Analysis

Vhs Assay

The Vhs assay was performed with identical amounts of Vhs and substrate mRNA as described in the Vhs assay protocol for the inhibition studies. The only difference was that the RNA used in these studies was gel extracted after the capping reaction. Following the Vhs assay, mRNA was washed with 70% and 95% EtOH, dried, and resuspended in 10-20ul nuclease-free H_2O (depending on the experiment). For each time point analyzed, 5ul of sample was used for primer extension analysis.

Primer labeling

10 picomoles (pmol) primer (Table 2) was combined with 30uCi [γ-^{32}P]ATP with a specific activity of 6,000 Ci/mmol, 10U T4 polynucleotide kinase, a final concentration of 1X T4 PNK buffer, and H_2O to a final volume of 10ul. Samples incubated at 37˚C for 10 min. and were then heated to 90˚C for 2 minutes to inactivate T4 PNK. Tubes were then centrifuged briefly in a microcentrifuge and water was added to a final concentration of 100fmol/ul. The primers used for primer extension analysis were ordered from IDT Technologies and are listed in Table 2 (Coralville, IA).

TABLE 2

PRIMERS USED FOR PRIMER EXTENSION ANALYSIS

Primer Description	**Sequence**
P 165 (pBK2)	5’-TCGGTTGCTATGGCCGCGAGAACGC-3’
P 235 (pBK2)	5’-CGTGGGCATTTTCTGCTCCAGGCGG-3’
P 325 (pBK2)	5’-GATATCGTCGCGCGAACCCAGGGCC-3’
EMCV (pCITELUC)	5’-TCATAGCCTTATGCAGTTGC-3’

RNA Melting and Reverse Transcription

5ul of RNA sample was combined with 1ul labeled primer plus 5ul AMV Primer Extension 2X buffer. The tubes were heated at 67˚C (or at a temperature near their T_m) for 20 min. and then incubated at RT for 10 minutes. 9ul of reverse transcription mix was added to each tube. Reverse transcription mix contains 5ul 2X AMV Primer Extension buffer, 1.4ul 40mM sodium pyrophosphate, 1.6ul nuclease-free H_2O, and 1U AMV reverse transcriptase. Samples incubated for 30 min. at 41-42˚C and then 20ul loading dye was added to each tube. Samples were heat denatured at 90˚C for 10 min. and loaded onto a pre-heated 7-8% polyacrylamide 8M urea 1X TBE gel. Samples were run at a constant power of 50W for 1.5 hr. on a BioRad Sequi-Gen GT apparatus (Hercules, CA). The gel was transferred to Whatman 3MM filter paper and dried for 1 hr. at 80˚C. The gel was then placed under a phosphorimaging screen and visualized through autoradiography.

RNA Circularization

Preparation of Circular pBK2 RNA

RNA was synthesized and extracted according to the procedure described above for the 5′ cap-labeled vs. 3′ poly(A) tail-labeled mRNA. 50ug RNA was then taken through a dephosphorylation reaction with 1X Dephosphorylation Buffer and 5U Calf Alkaline Intestine Phosphatase (CIAP) from the Ambion KinaseMAX kit (Foster City, CA). The final volume was 20ul. RNA incubated for 1hr. at 37˚C, and then 50ul of Phosphatase Removal Reagent (PRR) was added to the tube and samples incubated for 3 min. at RT with occasional flicking. Tubes were then centrifuged briefly for 15 seconds up to top speed, and the supernatant was carefully removed. The RNA was then precipitated by adding 2.5 volumes of ice-cold EtOH and 0.1

volumes 3M sodium acetate pH 5.2 for at least 1 hr. at -80˚C. The RNA was pelleted by centrifuging for 20 min. at 13,000rpm and 4˚C.

The pellet was resuspended in 16ul nuclease-free H_2O and used in a PNK kinase reaction to add a single monophosphate onto the 5′ end. 2ul 10X PNK Buffer, 1ul of unlabeled 10mM ATP, and 1ul PNK (10U/ul) were added to the tube and samples incubated for 1hr. at 37˚C. Tubes were then incubated for 2 min. at 90˚C to stop the reaction. 500mM Tris-Cl pH 7.5, 5mM EDTA, and 4.5M NaCl were then added to a final concentration of 10mM, 0.1mM, and 100mM, respectively. 10ug of pBK2 circle oligonucleotide (used 0.5ul of 20ug/ul solution) from IDT (Coralville, IA) was added to bind the 5′ and 3′ ends of the RNA (Table 3). This oligonucleotide was present in 6.5 molar excess compared to pBK2 mRNA. Samples were incubated at 90˚C for 5 min. followed by removal of the heat block to RT for a slow cool for 1.5 hrs. to anneal the oligonucleotide to RNA. 2ul of sample was set aside for eventual gel analysis. 4ul of T4 DNA ligase (1U/ul) and 8 ul 5X T4 DNA ligase buffer were added to the tube and the reaction incubated overnight at RT. Samples were then precipitated with 2.5 volumes ice-cold EtOH and 0.1 volumes 3M sodium acetate pH 5.2 for at least 1 hr. at -80˚C. The RNA was pelleted by centrifuging for 20 min. at 13,000 rpm and 4˚C. Samples were resuspended in 10ul H_2O. DNA loading dye was added to the samples and they were run on a 1.6% agarose 1X TBE gel containing 0.5ug/ml EtBr. Circular pBK2 was extracted and purified using BioRad Freeze ‘N Squeeze columns (Hercules, CA). Samples were resuspended in nuclease-free H_2O and the spectrophotometer was used to record concentrations.

TABLE 3

PRIMERS USED FOR CIRCULARIZING pBK2 AND EMCV RNA

Primer Description	**Sequence**
pBK2 Circularization	5’-TGCAGCCCAAGCTTGTATTCGGGCGTCGCAGATCGTCGGT-3’
pCITELUC (EMCV) Circularization	5’-TTTTTTTTTTTCAAATTTGTCCCGCTTAATTAAGGCCAAT-3’

Preparation of Linear mRNA

pBK2 RNA was synthesized and extracted according to the procedure described above for the 5′ cap-labeled vs. 3′ poly(A) tail-labeled mRNA. pCITELUC RNA was synthesized by adding 6-9ul *SpeI* linearized DNA to a Promega T7 RiboMAX *in vitro* transcription reaction (Madison, WI). The T7 reaction contained 20ul T7 5X Transcription Buffer, 7.50 of each 100mM dNTP, and 10ul T7 enzyme in a final volume of 100ul. The *in vitro* transcription reaction and RNA extraction followed the same guidelines as those previously described for RNA used for 5′ cap-labeled vs. 3′ poly(A) tail-labeled experiments. 50ug of RNA was then used in an EPICENTRE m^7G capping reaction (Madison, WI) with unlabeled GTP identical to the procedure described for mRNA used in the primer extension analysis experiment. RNA was then run on a 1.6% agarose 1X TBE gel containing 0.5ug/ml EtBr at 50V for 3.5 hours. The RNA fragment was excised and extracted from the gel with BioRad Freeze 'N Squeeze columns (Hercules, CA). Samples were resuspended in 20ul nuclease-free H_2O and the spectrophotometer was used to record concentrations.

Preparation of Circular EMCV RNA

7-9ul of *SpeI* linearized pCITELUC DNA was used in a Promega *in vitro* T7 RiboMAX RNA synthesis reaction (Madison, WI). However, in this reaction GMP was present in 10:1 abundance than GTP. 20ul of T7 5X Transcription Buffer, 7.5ul 100mM ATP, 7.5ul 100mM CTP, 7.5ul 100mM UTP, 6.75ul 100mM GMP, 0.75ul 100mM GTP, 33ul H_2O, and 10ul T7 enzyme mix were combined with the linearized DNA. Sample incubated at 37°C for 3.5 hours. Following the RNA synthesis reaction, 4U of RQ1 RNase-free DNase was added to sample, and tubes incubated at 37°C for 15 minutes. RNA was then phenol/chloroform extracted and precipitated

with 2.5 volumes ice-cold 95% EtOH and 0.1 volumes 3M sodium acetate pH 5.2 at -80˚C for at least 1 hour. RNA was pelleted by centrifuging for 20 min. at 13,000 rpm and 4˚C. Sample was resuspended in 13ul nuclease-free H_2O. Tris-Cl pH 7.5, EDTA, and NaCl were added to a final concentration of 10mM, 100mM, and 0.1mM, respectively. Next, 7ug of EMCV pCITELUC circular oligonucleotide was added (by adding 0.5ul of 14ug/ul stock) to the system so that it was present in an 8.42 fold higher molar ratio compared to RNA substrate. The primer was purchased from IDT (Coralville, IA). Sample was incubated at 90˚C for 10 minutes, and then the heat block was removed and placed at RT for a 1.5 hour slow cool to allow primer annealing. After cooling, T4 DNA Ligase Buffer was added to a final concentration of 1X. Lastly, T4 DNA ligase was added to a final concentration 100U/nanomole of RNA transcript and the ligation reaction incubated at RT overnight.

The next day, circular RNA precipitated with 2.5 volumes ice-cold 95% EtOH and 0.1 volumes 3M sodium acetate pH 5.2 at -80˚C for at least 1 hour. The RNA was spun down and gel extracted following the same procedure as described for pBK2 circular RNA.

Vhs Assay of Linear vs. Circular RNA

pBK2 Experiment

3.4ul (0.4ug) of linear or circular RNA was added to 12.60ul of 10mM Tris-Cl pH 7.5, RRL lacking Vhs, or RRL containing Vhs (Fig. 8). Samples incubated at 30˚C and 5ul aliquots were removed from the 10mM Tris-Cl sample immediately (0') and from the the RRL and Vhs samples at 3, 9, and 15 minutes. The aliquots were added to 245ul 10mM Tris-Cl pH 7.5 and mixed. The entire solution was then added to 750ul TriZol with 20ug carrier tRNA. The remaining RNA extraction was performed as described previously. RNA was washed with

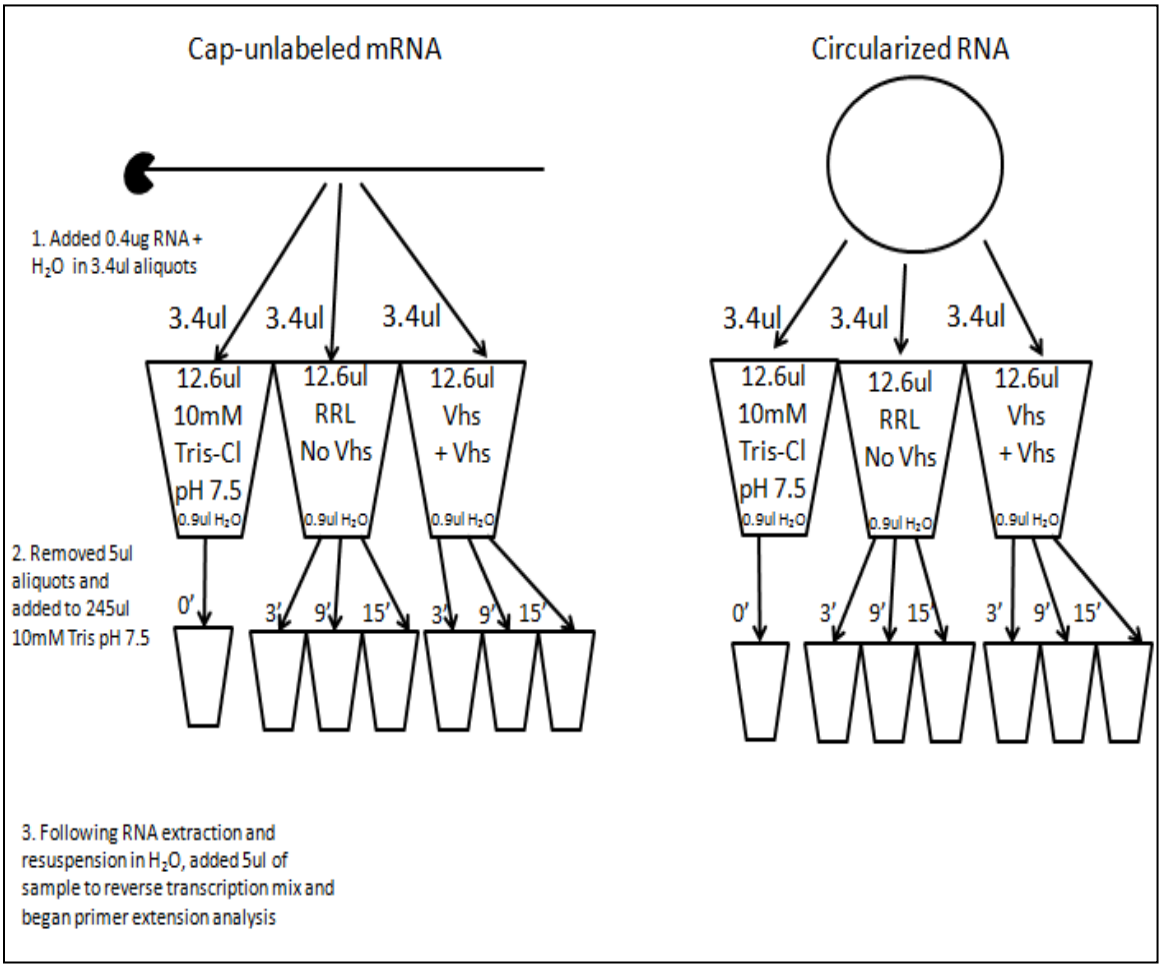

Figure 8.Vhs Assay Procedure for Analysis of Vhs Cleavage of Circular vs. Linear pBK2 RNA

0.40 ug linear or circular RNA was added to tubes containing 12.6ul of 10mM Tris-Cl pH 7.5, RRL without Vhs, or RRL with Vhs (1). 5ul aliquots were removed at the indicated time points and combined and mixed in 245ul 10mM Tris-Cl pH 7.5 (2). The RNA extraction was followed according to a previously described procedure. After RNA was resuspended, 5ul of sample was used for primer extension analysis.

70% and 99.9% EtOH and resuspended in 10ul nuclease-free H_2O. 5ul of sample was used for primer extension analysis.

EMCV Experiment

4.0ul (0.3ug) of linear or circular RNA was added to 8.40ul of 10mM Tris-Cl pH 7.5, RRL lacking Vhs, or RRL containing Vhs. Samples incubated at 30˚C, and 5ul aliquots were removed from the 10mM Tris-Cl sample immediately (0') and from the RRL samples at 3 and 15 minutes. The aliquots were added to 245ul 10mM Tris-Cl pH 7.5 and mixed. The entire solution was then added to 750ul TriZol with 20ug carrier tRNA. The remaining RNA extraction was performed as described previously. RNA was washed with 70% and 99.9% EtOH and resuspended in 5ul nuclease-free H_2O. The entire sample was used for primer extension analysis.

Site-directed Mutagenesis

The Stratagene Lightning Multi Site-directed Mutagenesis Kit was used to mutate pBK2 DNA (La Jolla, CA). All primers used for these studies were purchased from IDT Technologies (Coralville, IA). 50ng pBK2 DNA was combined with 100ng primer, 2.50ul 10X QuikChange Lightning Multi Reaction Buffer, 1ul dNTP mix, and 1ul QuikChange Lightning Multi Enzyme Blend in a final volume of 25ul. The primers used for mutagenesis are listed in Table 4. Sequence in red represents part of the AUG codon and sequence in blue represents bases within or surrounding the AUG codon that were mutated. The DNA was amplified by PCR according to the parameters listed in Table 5. Following PCR, samples were placed on ice for 2 minutes. 1ul *DpnI* was added in order to cleave the non-mutated methylated and hemimethylated DNA. Samples were mixed, briefly centrifuged, and incubated at 37˚C for 5 minutes. Figure 9 shows a

TABLE 4

PRIMERS USED FOR AUG MUTAGENESIS

Primer	**Sequence**
AUG1→CCC	5’-CCTTGTAGAAGCGCGTCCCGCTTCGTACCCCTGCC-3’
AUG1→AUG1--OPT	5’-GCGCCTTGTAGAAGCCACCATGGCTTCGTACCCC-3’
AUG2→CCC	5’-CGCCTGGAGCAGAAACCCCCCACGCTACTGCGG-3’
AUG2→AUA	5’-CGCCTGGAGCAGAAAATACCCACGCTACTGCGG-3’

TABLE 5

QUIKCHANGE LIGHTNING MUTAGENESIS PARAMETERS

Segment	**Cycles**	**Temperature**	**Time**
1	1	95˚C	2 minutes
2	30	95˚C 55˚C 65˚C	20 seconds 30 seconds 126 seconds
3	1	65˚C	5 minutes

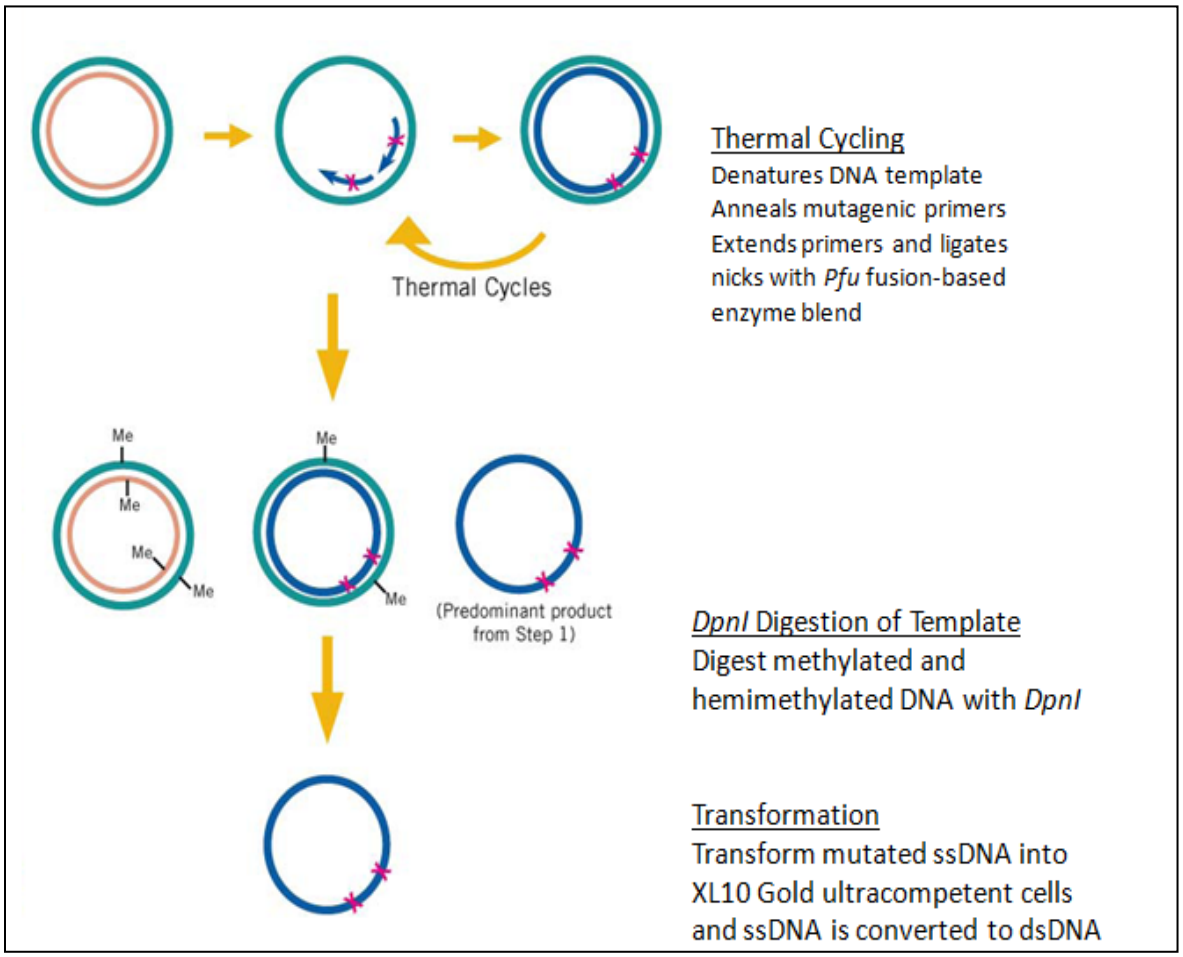

Figure 9.Procedure for Mutating AUG Codons

Figure 9 was obtained from the Stratagene protocol. Primer containing pBK2 sequence with mutations at or near the first or second AUG codon was used in these studies. During the PCR reaction, the primers bound to the antisense DNA strand, so DNA was synthesized to contain the proper mutations in the sense strand. DNA nicks were ligated with a *Pfu* fusion-based enzyme blend. Following PCR, *DpnI* was added to the system for cleavage of all methylated and hemimethylated DNA. Therefore, all non-mutated DNA was degraded, but DNA containing the mutation was spared. Lastly, XL10 Gold ultracompetent cells were transformed, and the single stranded DNA was converted to double stranded DNA *in vivo*.

diagram obtained from the Stratagene protocol that explains the mutagenesis procedure. The DNA was then propagated in Stratagene XL10-Gold ultracompetent cells according to the protocol, except that NZY^{+} broth was replaced with SOC media (La Jolla, CA). Colonies were picked and grown for 12-16 hours in 10ml LB cultures containing 100ug/ml amp. DNA was extracted using a Qiagen Mini Prep Kit (Germantown, MD). Mutations were confirmed through sequencing.

Construction of Hairpin and CAA Constructs

BamHI and *BglII* Restriction Enzyme Sites

Two primers were purchased from IDT Technologies (Coralville, IA) to mutate the pBK2 sequence to contain a *BamHI* restriction enzyme site upstream of the T7 promoter and a *BglII* restriction enzyme site downstream of the T7 promoter (Table 6). The *BamHI* site was located 27 bases upstream from the SP6 transcription start site, and the *BglII* site was located 58 bases downstream from the transcription start site and 26 nucleotides upstream from the first AUG. The mutations were created using Stratagene's QuikChange Lightning Multi Site-directed Mutagenesis Kit (La Jolla, CA). Both primers were added to one reaction. First, 1ul of 50ng/ul pBK2 DNA was combined with 2.50ul 10X QuikChange Reaction Buffer, 16.70ul nuclease-free H_2O, 1,80ul of 100ng/ul *BamHI* primer, 1ul of 100ng/ul *BglII* primer, 1ul dNTP mix, and 1ul QuikChange Lightning Multi Enzyme Blend. The *BamHI* primer was 25 nucleotides larger than *BglII*, therefore, an increased amount of *BamHI* was added to the reaction to obtain equal molar

TABLE 6

PRIMERS FOR CREATING *BAMHI* AND *BGLII* RESTRICTION ENZYME SITES

Primer	**Sequence**
BamHI Restriction Enzyme Site	5'-GCTACAATTAATACATAACCTTATGGATCCTACACATACGATTTAGGTGACACTA-3'
BglII Restriction Enzyme Site	5'-GGCGTGAAACTCCCGCAGATCTTCGGCCAG-3'

ratios. The components were mixed and then PCR amplified and propagated as described previously (Table 5, Fig.9)

10 colonies were picked from LBamp plates and grown in 10mL LB media with 100ug/ml ampicillin for 12-16 hr. at 37˚C and 300rpm. DNA was extracted using a Qiagen Mini Prep Kit (Germantown, MD) and resuspended in 50ul EB. The DNA was labeled pBK2 1-10 RE. Samples were then tested to confirm the *BamHI* or *BglII* restriction enzyme sites by separate restriction digests. Only 1 of the 10 colonies selected contained the two restriction enzyme sites, pBK2-4-RE. This construct was used for cloning of the hairpin and CAA constructs.

Cloning of IDT 98 Nucleotide Inserts

pIDTSMART-amp resistant vectors, which contained a 98 nucleotide sequence encoding a hairpin or CAA sequence within the multiple cloning site, were purchased from IDT Technologies (Coralville, IA). The 5' end of the sequence was flanked with a *BamHI* restriction enzyme site and the 3' end was flanked with *BglII*. The 98 base sequences are listed in Figure 10. Four constructs were ordered, the hairpin constructs were predicted to have a hairpin with a thermodynamic stability of -30kcal/mol (35). The CAA sequence has no predicted secondary structure (35). The sequence in green represents the bases that were mutated in the pBK2 sequence to yield a *BamHI* or *BglII* restriction enzyme site. The sequence in red represents the region that is transcribed in an *in vitro* SP6 reaction to make RNA, and the region in blue represents sequence that encodes a hairpin. The pIDTSMART-amp resistant vectors were

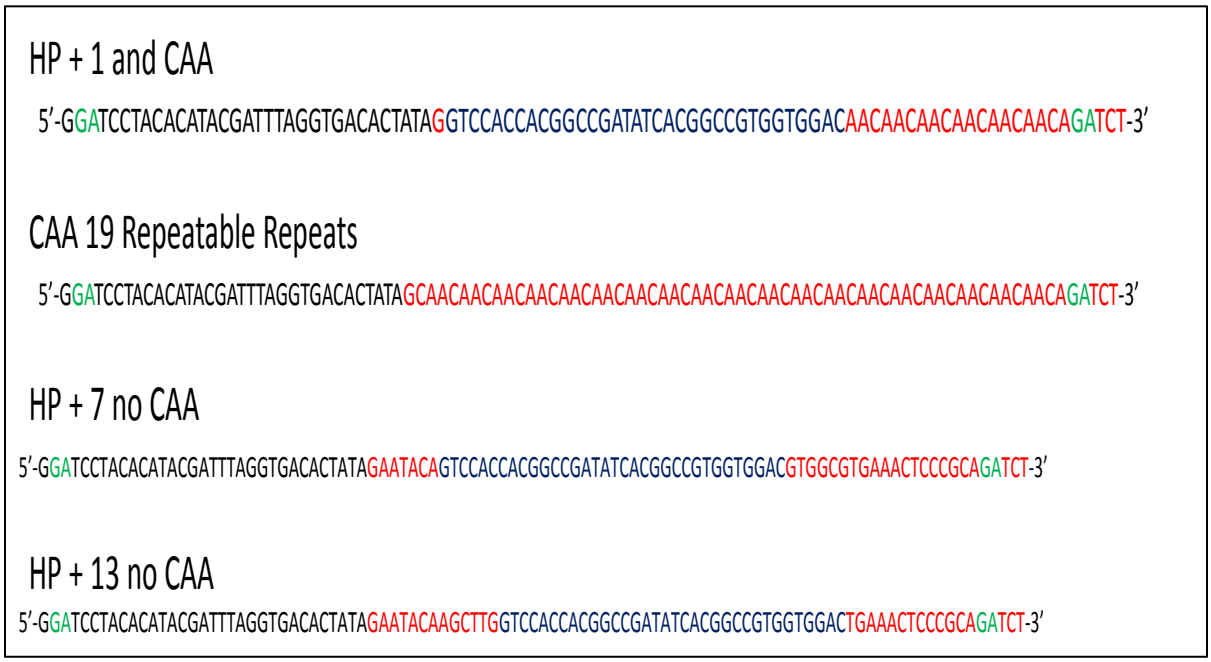

Figure 10.Nucleotide Sequence Constructed by IDT Technologies and Inserted into a pIDTSMART Mini Gene

The 5′ end of each sequence contains the BamHI restriction enzyme site and the3′ end contains BglII. Sequences were designed to contain a -30kcal/mol hairpin at a +1 shift from the 5′ cap followed be a CAA repeat, a CAA long stretch, a hairpin at a +7 shift from the 5′ cap, and a hairpin at a +13 shift from the 5′ cap from top to bottom, respectively.

propagated in HB101 competent cells, grown in LB media with 100ug/ml ampicillin, and extracted with Qiagen Mini Prep and Midi Prep Kits (Germantown, MD).

10ug of pIDTSMART and pBK2-4-RE DNA were used in a double digestion reaction with *BamHI* and *BglII*. Samples incubated at 37˚C for 3 hours. Samples were precipitated by adding 2.5 volumes ice-cold 95% EtOH and 0.1 volumes 3M sodium acetate pH 5.2 and freezing for at least 1 hr. at -80˚C. DNA was centrifuged for 20 min. at 13,000 rpm and 4˚C. The DNA was resuspended in 10ul nuclease-free H_2O and pIDTSMART DNA and pBK2-4-RE DNA were run on a 1.6% and 1.2% agarose, respectively, 1X TBE gel containing 0.5ug/ml EtBr. The large vector was excised from the pBK2-4-RE digested gel, and the small 93 base inserts were excised from the pIDTSMART vectors. The DNA was extracted from the gel using a Qiagen Gel Extraction Kit according to the protocol and samples were eluted in 50ul EB (Germantown, MD). The pIDTSMART insert and pBK2-4-RE vector were used in a ligation reaction with 6:1, 3:1, and 1:1 molar ratio ligations of insert to vector. 100ng of vector was used for the ligation reactions. Ligation reactions contained final volumes of 10ul with 400 cohesive end units of New England Biolabs T4 DNA ligase and a final concentration of 1X T4 DNA ligase buffer (Ispwich, MA). The reaction incubated at room temperature for 2 hours. 50ng of sample was used to transform Promega HB101 competent cells according to the protocol (Madison, WI). LBamp plates incubated at 37˚C overnight. Colonies were grown in LBamp as described previously, DNA was extracted using a Qiagen Mini Prep Kit, and the correct insertions were confirmed by restriction digests with *BamHI* and *BglII* (Germantown, MD). Since *BamHI* and *BglII* are ischizomers, if the pBK2 vector religated, then the plasmid could not be cleaved with the enzymes because ligation created novel restriction enzyme sites. The inserts were also confirmed through sequencing analysis.

RNA Synthesis and Radiolabeling

RNA was synthesized and extracted using the same protocol as previously described for 5′ cap-labeled vs. 3′ poly(A) tail-labeled RNA. For the +1 HP and 19 stretch of CAA repeats, 50ug RNA was incubated with 62.9ul nuclease-free H_2O at 65˚C for 8 minutes. 5ul (50uCi) of [α-^{32}P]GTP with a specific activity of 3,000Ci/mmol was combined with 5ul 3.33umol/L unlabeled GTP. Following incubation at 65˚C, the RNA was chilled on ice and 10ul 10X ScriptCap Buffer, 5ul 2mM SAM, 2.5ul RNase inhibitor, 8ul of the GTP mix, and 5ul ScriptCap Capping Enzyme were added to the RNA. For the +7HP and +13HP samples, the procedure was the same except that 23.30ul of [α-^{32}P]GTP with a specific activity of 3,000Ci/mmol was combined with 11.7ul of 3.33umol/L unlabeled GTP (but the same volume of GTP mix was used). The samples incubated at 37˚C for 1 hr. and were later phenol/chloroform extracted and precipitated for at least 1 hr. at -80˚C with 2.5 volumes ice-cold 95% EtOH and 0.1 volume 3M sodium acetate pH 5.2. The RNA was resuspended in 10ul and run on a 1.3% agarose 1X TBE gel containing 0.5ug/ml EtBr for 3.5 hours at 50V. RNA was excised and extracted with BioRad Freeze ‘N Squeeze tubes and then precipitated as described previously. Samples were resuspended in 20ul nuclease-free H_2O. The +1 HP and CAA RNA were incubated at 65˚C for 8 minutes and then cooled to RT for 1 hour in order to restore structure prior to the Vhs assay. The predicted RNA structures of the 4 constructs are shown in Figure 11.

Vhs Assay

1ul +1HP RNA + 3ul H_2O or 3ul CAA stretch RNA + 1ul H_2O was added to 8.40ul of either 10mM Tris-Cl pH 7.5, RRL without Vhs, or RRL with Vhs. The difference in amount of RNA added was determined by cpm measurements, and the amount added is estimated to be

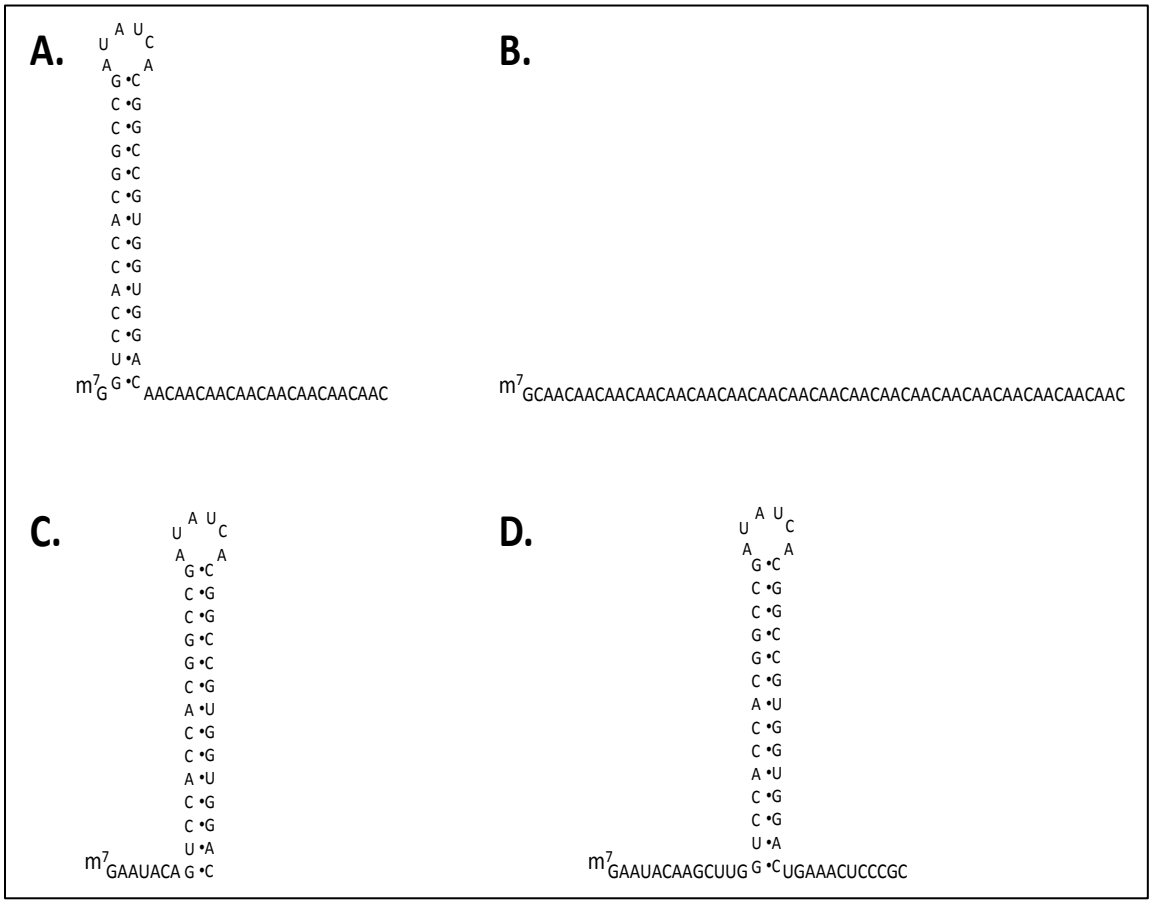

Figure 11.RNA Structures

Figure 11 shows the mRNA sequence of the first 59 bases of the 4 constructs containing either a hairpin or CAA stretch. HP+1 (A), CAA stretch (B), HP+7 (C), and HP+13 (D)

0.3ug. 5ul aliquots were removed immediately from the 10mM Tris solution (0 minutes) and at 3 and 15 minutes for the RRL samples. The remaining Vhs assay and RNA extractions were performed as described previously. RNA was run on a 7% polyacrylamide 8M urea 1X TBE gel. For the +7 and +13 HP samples, 2.80ul +7HP RNA +1.2ul H_2O or 4ul +13 HP RNA + 0ul H_2O was added to 8.40ul of either 10mM Tris-Cl pH 7.5, RRL without Vhs, or RRL with Vhs. The rest of the procedure was followed identical to the +1 HP and CAA stretch experiment.

Cells

Vero and HeLa cells were purchased from the American Type Culture Collection (Rockville, MD). They were grown in GIBCO essential medium (MEM) (Grand Island, NY) which contained antibiotics and 10% (vol/vol) calf serum (9).

Transient Transfections

Vero Cells

Vero cells were plated by splitting 1, 75cm^2 flask containing 1x10^7 cells/flask into 6, 60 x 15 mm dishes. 18 dishes were plated with 10ml MEM containing 10% CS. The cells grew for 48 hr. at 37˚C. After 45 hrs. of growth, the media was refreshed with 10ml MEM containing 10% CS. 4 hr. after the media was refreshed, cells were transfected with different combinations of 6ug of each plasmid (Fig. 12). Each type of dish contained 1 replicate. The procedure was performed according to the Promega Profection Transfection Kit protocol (Madison, WI). 16 hours after transfection, the media was refreshed with MEM 10% CS. Fourty-eight hours post transfection, the cells were washed two times with 1X PBS and then scraped in 400ul 1X Passive Lysis Buffer (PLB) from the Promega Dual Luciferase Reporter Assay System (Madison, WI).

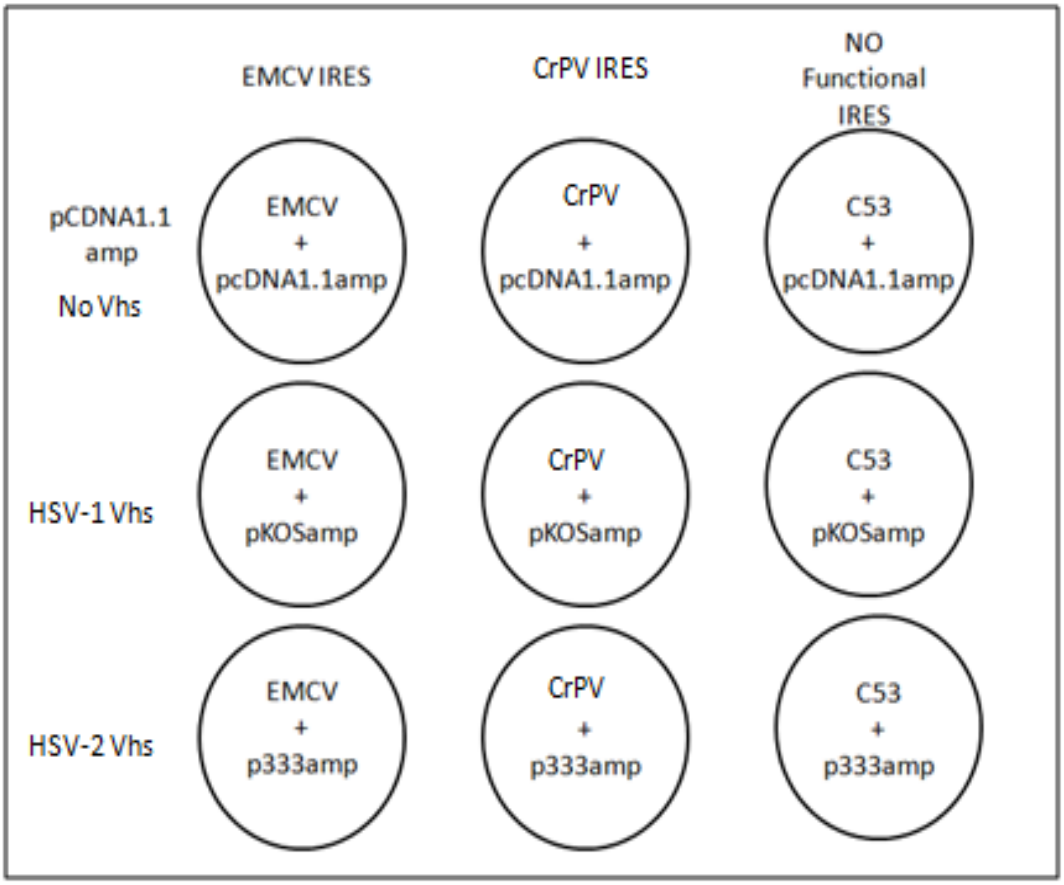

Figure 12.Outline of Plasmid Combinations

HeLa or Vero cells were transfected with 2 plasmids. 6ug of each plasmid was added to the cells. The plasmid combinations are listed above.

The replicate cell samples were pooled. Cells were mixed by pipette and taken through two rounds of freeze thaw in an EtOH/dry ice slurry. The lysate was cleared by centrifuging at top speed for 15 seconds. 20ul of sample was used to record renilla and firefly luciferase expression following the protocol described in the Dual Luciferase Reporter Assay Kit (Madison, WI).

HeLa Cells

HeLa cells were plated by splitting 1, 75cm^2 flask into 4, 60 x 15 mm dishes. 20 dishes were plated with 10ml MEM containing 10% CS, but only 18 dishes were used for the study. The cells grew at 37˚C for 24 hours, and then the media was refreshed with MEM 10% CS prior to transfection. Cells were transfected with 6ug of the same combinations of plasmid as previously described (Fig.12). The remaining procedure was performed identical to the Vero cell experiment.

RT PCR

HeLa cells were plated by splitting 1, 75cm^2 flask into 2, 100 x 20 mm dishes. Cells grew for 48 hours at 37˚C. Cells were then mock infected or infected with 20 PFU HSV-1 KOS in the presence of 5ug/ml Actinomycin D with MEM 1% CS. Cells were scraped at various time points by first washing two times with ice-cold 1X PBS followed by scraping cells into1ml 1X PBS. Cells were pelleted by centrifuging at top speed for 2 minutes at 4˚C. The pellets were resuspended in 238ul resuspension buffer containing a final concentration of 10mM Tris-Cl pH 7.5, 0.15M NaCl, and 1.5mM $MgCl_2$. Samples were inverted and vortexed briefly. Next, 12.5ul resuspension buffer + 10% NP40 was added and samples were placed on ice for 10 minutes. Nuclei were pelleted by centrifuging at top speed for 3 minutes at 4˚C. The supernatant was then transferred to new

tubes containing 750ul TriZol, and the solution was mixed and briefly vortexed. 200ul of chloroform was added and the sample was inverted and briefly vortexed. Samples were spun in the centrifuge at top speed for 5 minutes. The upper aqueous phase was transferred to a new tube, and 500ul isopropanol was added to precipitate RNA.

The sample was mixed and incubated at RT for 30 minutes. RNA was then pelleted by centrifuging at top speed for 10 minutes. The RNA was washed with 75% EtOH and resuspended in TE buffer pH 7.5. 50ul of RT Master Mix was then combined with 50ul of RNA with a concentration of 0.002-0.2ug/ul and RNA was reverse transcribed following the Applied Biosystems cDNA Archive Kit protocol (Foster City, CA). 10-100ng of cDNA plus RNase-free H_2O in a total of 9ul was combined with 1ul TaqMan Gene Expression Assay and 10ul TaqMan Universal PCR Master Mix (Foster City, CA). The experiment included 3 replicates. The plate was then added to a thermal cycler 7500 HT system for RT PCR analysis.

CHAPTER 3

RESULTS

The goal of this dissertation was to better understand the mechanism of Vhs cutting of messenger RNA (mRNA). Studies were designed to answer the following questions: (1) Does Vhs cleave mRNA encoding HSV-1 thymidine kinase at specific sites? (2) Are certain stages of translation initiation vital for Vhs cleavage of mRNA? (3) Does Vhs cut mRNAs that utilize a cap for translation initiation with equal efficiency as it cuts mRNAs that utilize an internal ribosome entry site? (4) How does Vhs cleave mRNAs that contain stable hairpins near the 5′ cap? The majority of these studies were performed using an *in vitro* Vhs assay system where Vhs protein was synthesized through *in vitro* transcription and translation followed by addition of RNA substrate (1).

The results reveal that Vhs cleaves thymidine kinase-encoding mRNA at specific sites near the 5′ cap. Blocking early events of translation initiation inhibits Vhs-induced mRNA degradation, while blocking later stages does not have a significant effect on Vhs activity. Additionally, Vhs is unable to cleave an mRNA that is normally translated by cap-dependent scanning if that mRNA is circularized to prevent it from initiating translation. Yet, Vhs retains the ability to specifically cut circularized RNA that does not use the traditional cap-dependent scanning mechanism. The later finding further supports the idea that a free 5′ end is important for Vhs degradation of scanned mRNAs. Furthermore, mutational studies indicate that Vhs may be associating with the scanning complex to reach some of its preferred cut sites. Inhibiting the scanning process by incorporating stable hairpins into the 5′ end of the RNA greatly reduces Vhs site-specific cutting. Interestingly, cutting at the 5′ end of mRNA is more efficient if the mRNA contains a sequence with no predicted secondary structure in the 5′ UTR.

Vhs Degradation of mRNA

Previous studies have shown that *in vitro* translated Vhs is the only viral protein required for RNase activity in a rabbit reticulocyte lysate system (1-5). In these assays antibodies against Vhs inhibit cleavage of mRNA (4). Additionally Vhs-1, a single point mutant where threonine is replaced by isoleucine at nucleotide 214, causes Vhs loss of function and is unable to cleave mRNA (4). During their investigation of RNA degradation, Smiley et al. showed that Vhs cleaves SRP-α mRNA at regions within the 5′ quadrant (5). This observation gives rise to a question, previously not addressed, of whether the 5′ cap scanning complex plays a significant role in Vhs cutting.

Vhs has been shown to associate with translation initiation factors and also have a preference for cleaving some mRNAs at specific sites near the 5′ end (5-8). These two findings support a model in which Vhs selectively cuts mRNA by associating with translation initiation factors. It is possible that, upon recruitment to the cap, Vhs maintains binding to these factors and travels with them in as a component of the scanning complex during translation initiation. Additional questions remain about the mechanism of Vhs cleavage, such as whether the initial processes of translation initiation are required for Vhs activity, and whether the AUG start codon has any importance.

Determining the Cut Sites in pBK2 mRNA

Vhs Cleavage of Internally-labeled, 5′ Cap-labeled, and 3′ Poly(A) Tail-labeled mRNA

To begin investigating the mechanism of Vhs cutting, an HSV-1 mRNA that encodes thymidine kinase (pBK2) was tested in a Vhs assay. pBK2 mRNA was selected for study because it undergoes the traditional cap-dependent scanning process during translation initiation and it

is degraded with half life rates comparable to cellular mRNAs in *vivo* (9). In the first study, mRNA substrate was internally labeled with [α-^{32}P]GTP during an *in vitro* transcription reaction. The mRNA was then added to a rabbit reticulocyte lysate *in vitro* translation system that either lacked or contained Vhs protein. Figure 13 shows typical results obtained from the *in vitro* translation reaction, prior to target mRNA addition, confirming that Vhs is only present when pKOSamp mRNA is added to the system. After mRNA substrate was combined with RRL, samples were removed at various time points followed by mRNA extraction and analysis via autoradiography (Fig. 14). There was a rapid disappearance of full length mRNA, accompanied by the appearance of one or more smaller sized fragments (Fig. 14). Vhs cleavage of pBK2 mRNA was not targeted to a region located in the middle of the transcript, because no distinct bands were detected. Instead, Vhs produced products just slightly smaller than full length. This indicated that the cleavage was originating from one of the ends of the mRNA (Fig. 14). Since the mRNA was internally labeled, it was not possible to determine from what end the cutting originated.

To further test this question, pBK2 RNA was synthesized in a large scale *in vitro* transcription reaction. Following transcription, the RNA was capped using an m^{7}G capping kit (EPICENTRE) containing vaccinia virus capping enzyme. During the capping process the RNA cap was either labeled with [α-^{32}P]GTP or given a cold cap with non-radioactive GTP. After the capping reaction, the mRNA with a labeled cap was added to a cold poly(A) tailing reaction, and the mRNA that received a cold cap was added to a hot polyA tailing reaction with [α-^{32}P]ATP. The mRNA substrates were then added to a Vhs assay and removed at the indicated time points (Fig. 15). Figure 15 shows a sharp disappearance of full length 5′ cap-labeled pBK2 mRNA at the 9 minute time point. This disappearance was not accompanied by the appearance of any large

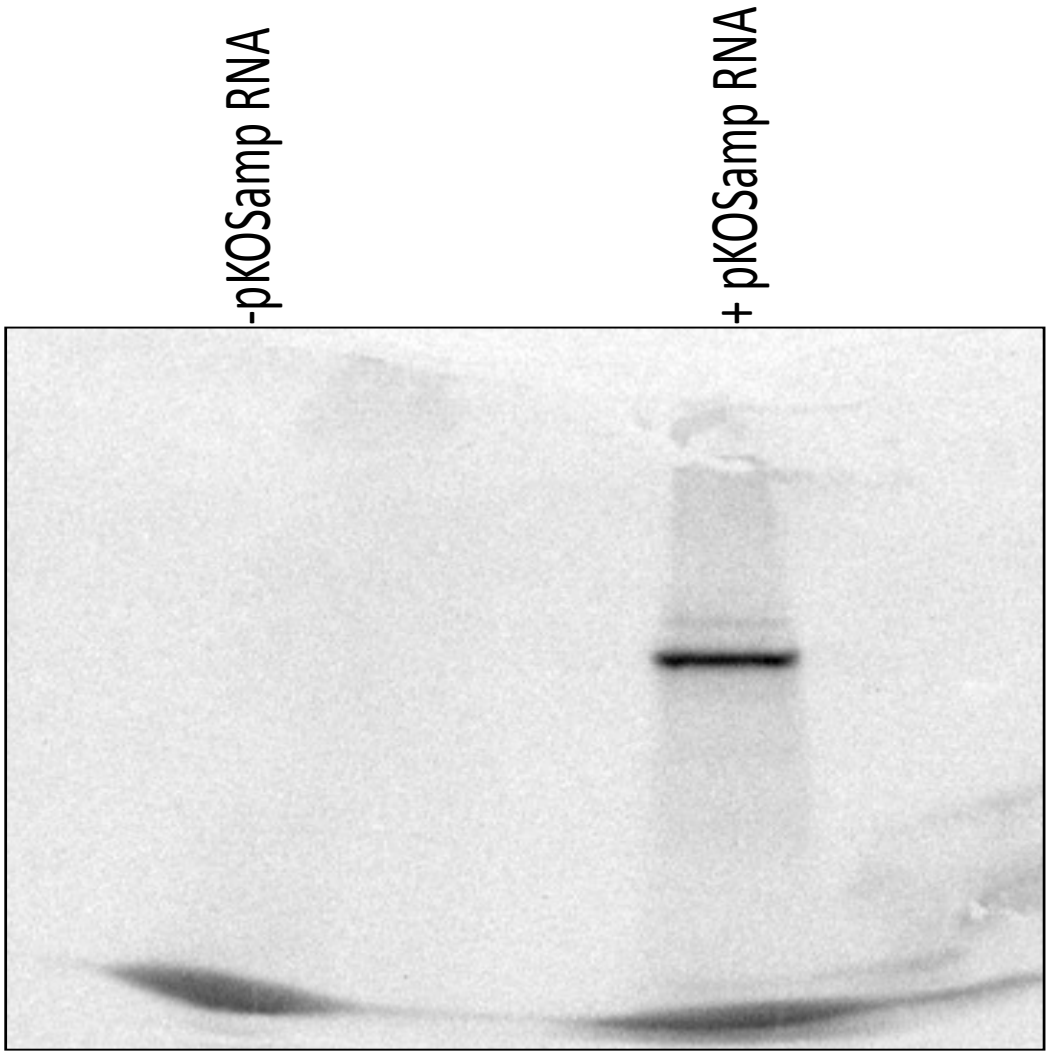

Figure 13.Sythesis of Vhs protein in a Rabbit Reticulocyte Lysate System

Figure 13 shows a SDS protein gel from an S-35 methionine-labeled *in vitro* translation reaction in a rabbit reticulocyte lysate system. –pKOSamp RNA represents a negative control where pKOSamp mRNA was not added to the system and instead was replaced with water. +pKOSamp RNA represents an *in vitro* translation reaction that contained pKOSamp mRNA (encodes Vhs). Samples incubated for 1.5 hours at 30˚C and where then run on an SDS-PAGE gel, dried, and viewed using autoradiography.

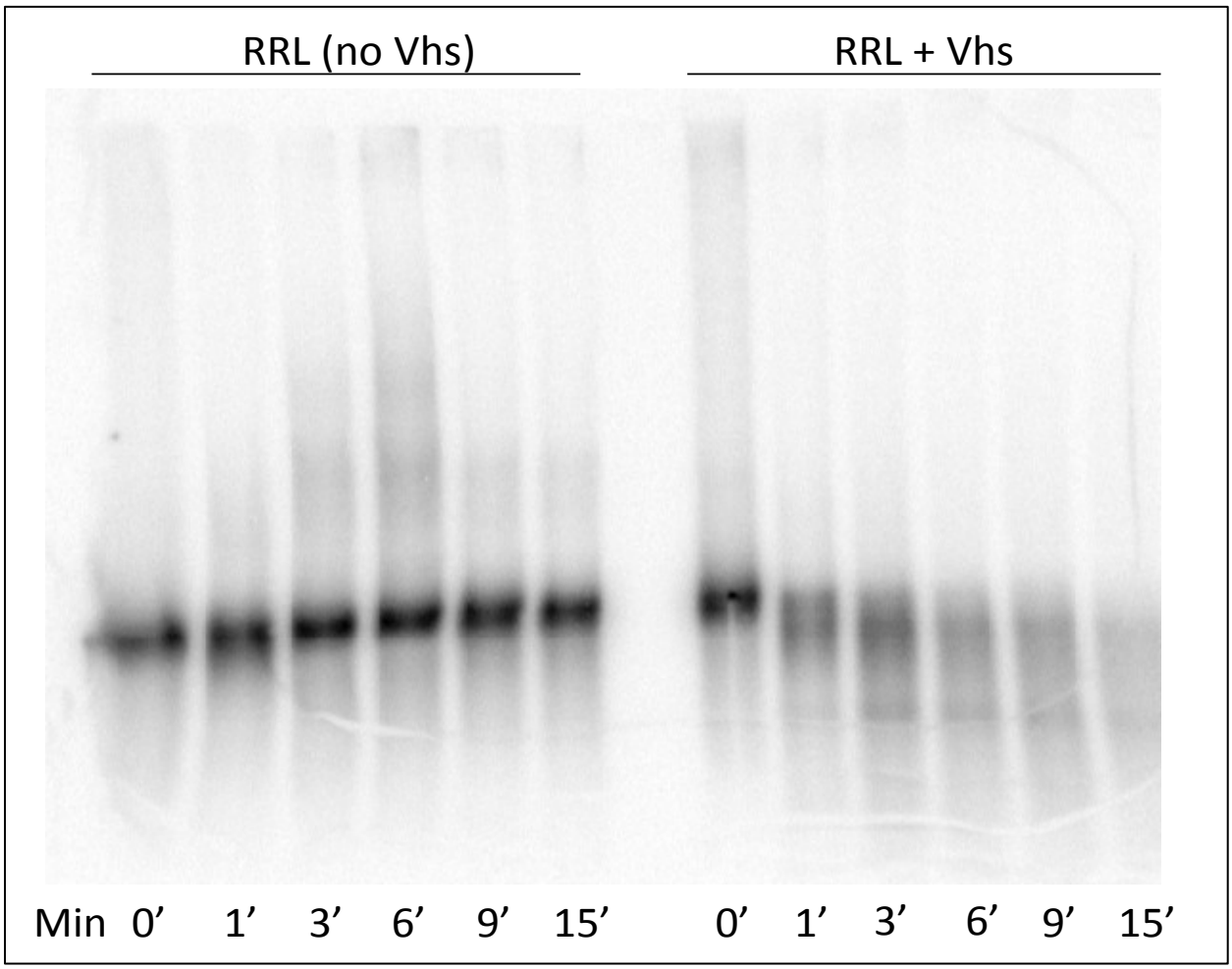

Figure 14.Vhs Degradation of Internally Labeled pBK2 mRNA

Figure 14 shows internally labeled pBK2 mRNA in the absence (RRL) or presence (RRL + Vhs) of *in vitro* translated Vhs protein. The mRNA was subjected to a time course assay with the minutes at which mRNA was removed listed above. RRL= rabbit reticulocyte lysate that lacked Vhs protein. Vhs=rabbit reticulocyte lysate that contained Vhs. Min=minutes mRNA incubated in rabbit reticulocyte lysate prior to removal.

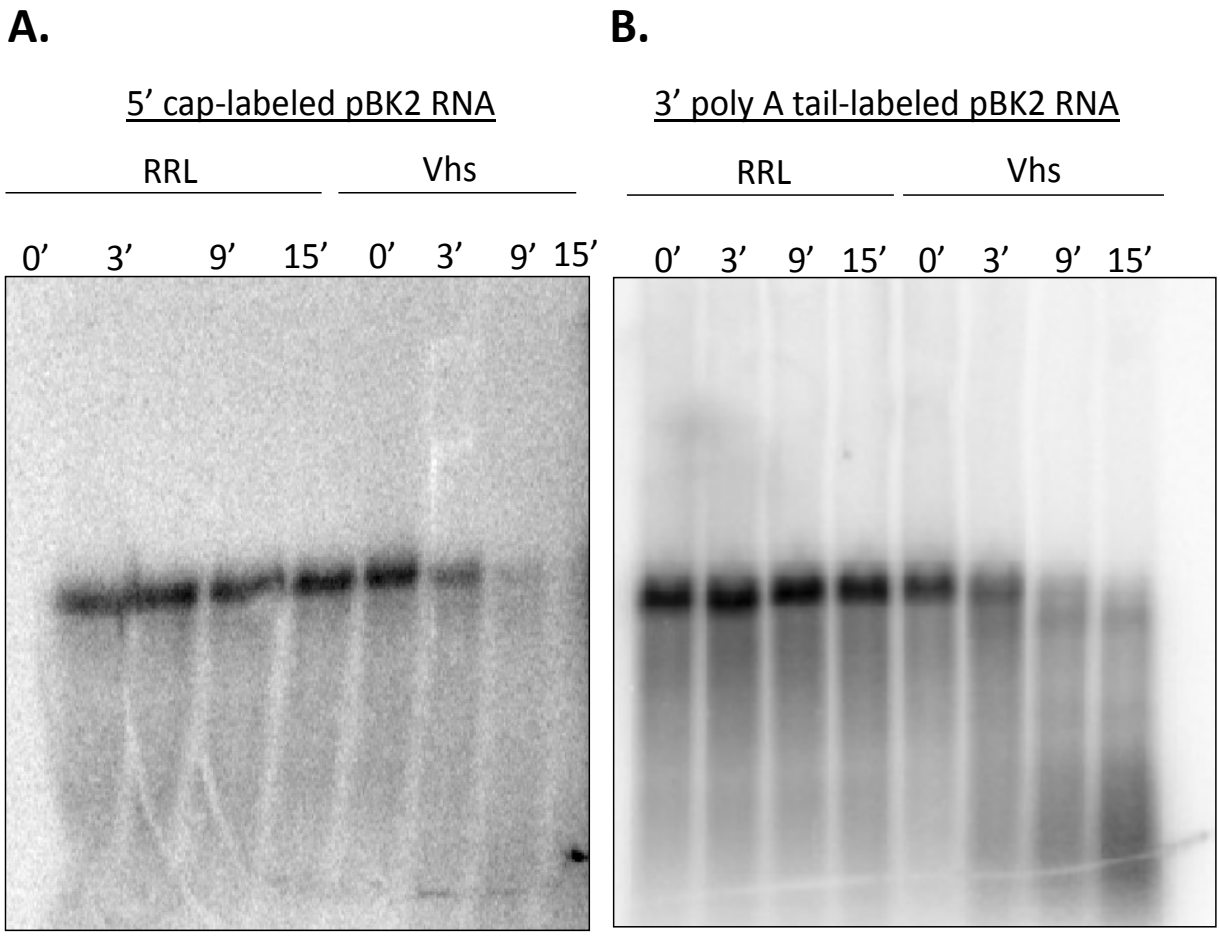

Figure 15.Vhs Degradation of Cap-labeled vs. Tail-labeled mRNA

Pictured above is pBK2 mRNA containing a 5′ labeled cap with a non-radioactive polyA tail (A) and pBK2 mRNA containing a 5′ non-radioactive cap with a 3′ labeled polyA tail (B). The gel was visualized by autoradiography representing total mRNA remaining after the Vhs assay. Lanes marked by RRL represent mRNA in the absence of Vhs and lanes marked by Vhs represent mRNA in the presence of Vhs (A and B). 0′, 3′, 9′, and 15′ represent minutes mRNA incubated in rabbit reticulocyte lysate before extraction. RRL=rabbit reticulocyte lysate lacking Vhs.Vhs=rabbit reticulocyte lysate containing Vhs.

fragments that were close in size to full length (Fig. 15). However, Vhs cleavage of 3′ poly(A) tail-labeled pBK2 mRNA resulted in appearance of a smear of products that were large enough to visualize on a 1.3% agarose 1XMOPS gel (Fig. 15 compare A and B). The results suggest that Vhs cleaves pBK2 mRNA at regions near the 5′ end, and produces cleavage products that are too small to be visualized by a 1.3% agarose gel. This result supports previous reports from studies using northern blot analysis to examine cells that were infected with wild type HSV-1 which showed that the 5′ end of pBK2 mRNA was preferentially cleaved (8).

In order to examine the cut sites more closely, mRNA was run on a 7% polyacrylamide 8M urea 1X TBE gel using a DNA sequencing apparatus. By analyzing cap-labeled mRNA with this method, it was easy to identify specific cut sites produced by Vhs. Vhs cut pBK2 mRNA at several prominent sites all within the first 300 bases from the 5′ end (Fig. 16). However, this same type of end-directed cutting was not identified when analyzing the 3′ poly(A) tail-labeled mRNA to examine the downstream products produced by cutting (Fig. 16). Instead, Vhs cut this mRNA to produce cleavage products that were slightly shorter than full length substrate and were retained at the top of the gel (Fig. 16). The results of the two gels indicate a method of Vhs degradation involving Vhs cleavage of pBK2 mRNA at sites near the 5′ end, leaving a trailing product of larger mRNA that is detectable through 3′ poly(A) tail labeling.

Vhs Titration

To further characterize Vhs activity, it was important to set up a Vhs assay with serial two fold dilutions of Vhs (in order to confirm that the nuclease activity was due to Vhs alone). Cap-labeled pBK2 mRNA was added to RRL samples that contained different concentrations of Vhs. These dilutions were obtained by using a sample that contained RRL with undiluted Vhs

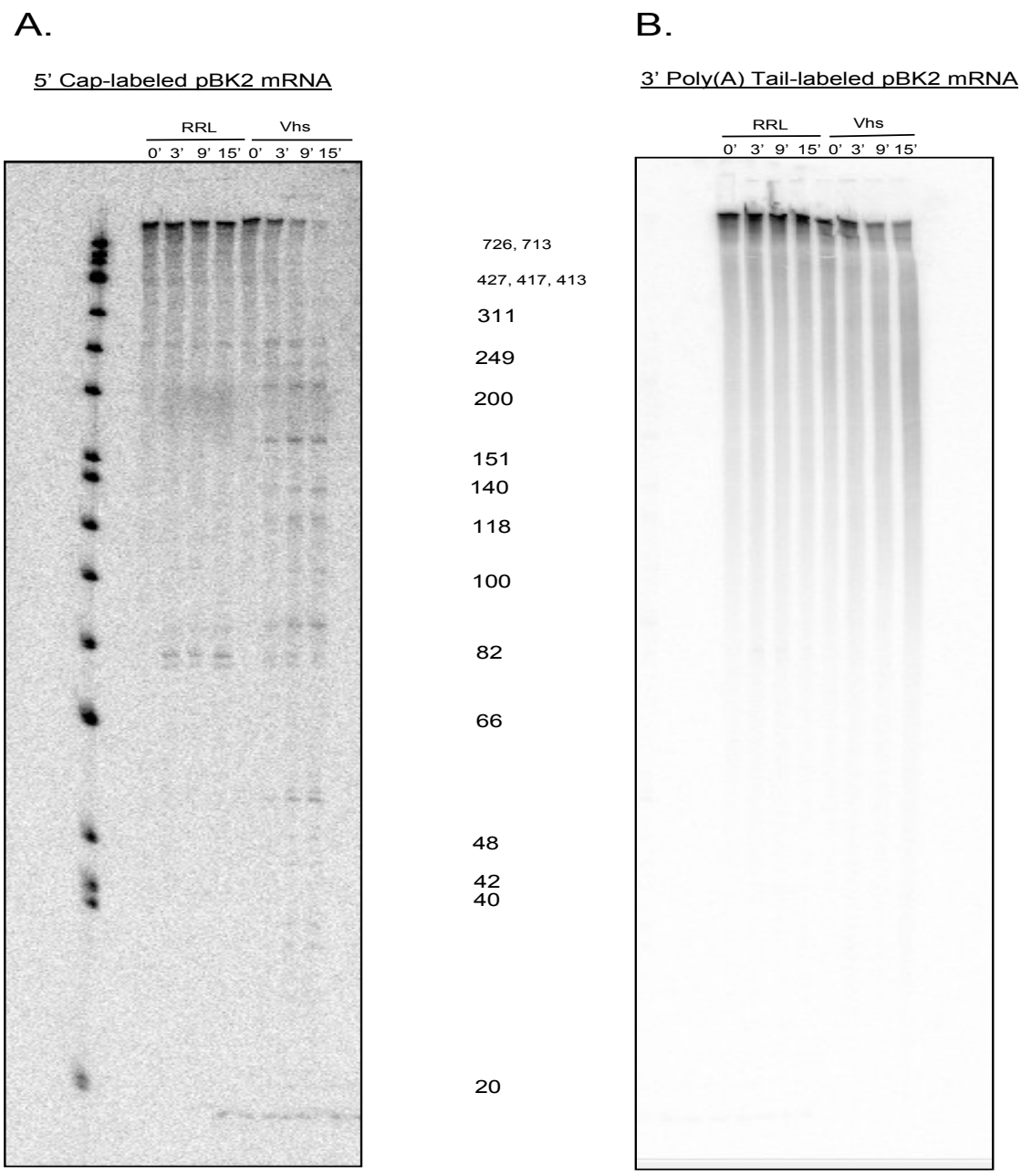

Figure 16.Analysis of Smaller pBK2 mRNA Cleavage Products

pBK2 substrate mRNA labeled at the 5′ end with a capping kit (A.) or at the 3′ end with a polyA tailing kit (B.) was added to a Vhs assay that either lacked (RRL) or contained (Vhs) Vhs protein. It was then removed at the indicated time points, extracted with TriZol, and run on a polyacrylamide sequencing gel. The mRNA was then visualized through autoradiography. Marker sizes are listed between the two gels. RRL=rabbit reticulocyte lysate lacking Vhs. Vhs=rabbit reticulocyte containing Vhs. M=ΦX174*Hinf1* markers.

protein (1X). After the *in vitro* translation reaction, the 1X sample was diluted in half with rabbit reticulocyte lysate that lacked Vhs to make the 0.5X sample. Lastly, the 0.5X sample of Vhs was diluted in half to make the 0.25X sample. The mRNA was added to the Vhs samples, extracted at various time points, and analyzed by autoradiography. RNA was degraded in a dose-dependent response where there was a correlation between the amount of Vhs protein in the system and the severity of mRNA cutting (Fig. 17). When analyzing the control samples which lacked Vhs, it was apparent that the system contained slight background RNase activity (Fig. 17). Yet, this background activity was minimal when compared to the mRNA degradation induced by Vhs (Fig. 17). Of particular note, for the most concentrated, undiluted sample of Vhs, complete mRNA degradation was achieved by the 9 minute time point.

Vhs Assay Using mRNA Substrate Labeled with a Higher Specific Activity

To enhance investigation of mRNA cut sites, two further experiments were performed involving (1) radioactive material with a higher specific activity or (2) an extended time point of mRNA and protein incubation. First, [α-^{32}P]GTP with a specific activity of 3,000 Ci/mmol was used in an *in vitro* m^{7}G capping reaction instead of the original 800 Ci/mmol. The rest of the Vhs assay was carried out identical to previous experiments. Figure 18 shows the results of the reaction using mRNA labeled with 3,000 Ci/mmol [α-^{32}P]GTP (Fig. 18B) compared to an older experiment with 800 Ci/mmol (Fig. 18A). Vhs produced 6 prominent cut sites all within the first 300 bases from the 5′ cap (Fig. 18) as well as several less prominent cut sites in the upstream region (Fig. 18B). The same cut sites that were identified when labeling mRNA with 800 Ci/mmol were also found when labeling with 3,000 Ci/mmol (Fig. 18). Using a hotter mRNA target, it was possible to detect bands that were otherwise faint when labeling with 800 Ci/mmol

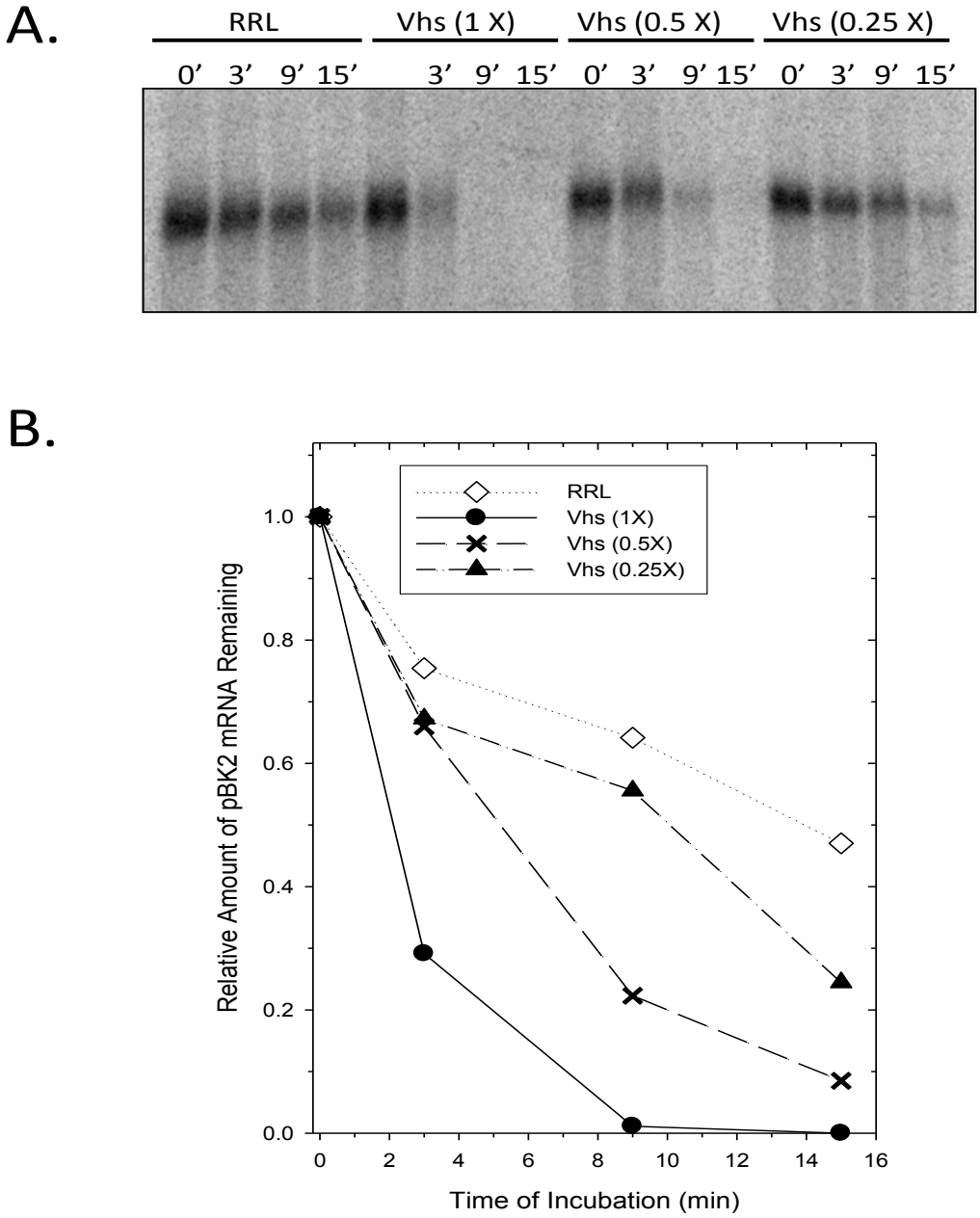

Figure 17.Degradation of pBK2 mRNA Using Serial Two Fold Dilutions of Vhs Protein

Cap-labeled pBK2 mRNA was added to rabbit reticulocyte lysate systems with serial two fold dilutions of Vhs protein or with reticulocyte lysate lacking Vhs protein. mRNA was then removed from the system at the indicated time points, extracted, and run on a full length 1.3% agarose 1XMOPS gel. It was further dried and analyzed through autoradiography, analyzing the remaining full length mRNA through volume reports (A). Scatter plot representation of amount of mRNA remaining after incubation of mRNA substrate with various concentrations of Vhs (B). RRL=rabbit reticulocyte lysate without Vhs protein, Vhs(1X)=rabbit reticulocyte lysate with undiluted Vhs protein, Vhs(.5X)=rabbit reticulocyte lysate with 2 fold dilution of Vhs(1X), Vhs(.25X)=rabbit reticulocyte lysate with 2 fold dilution of Vhs(.5X).

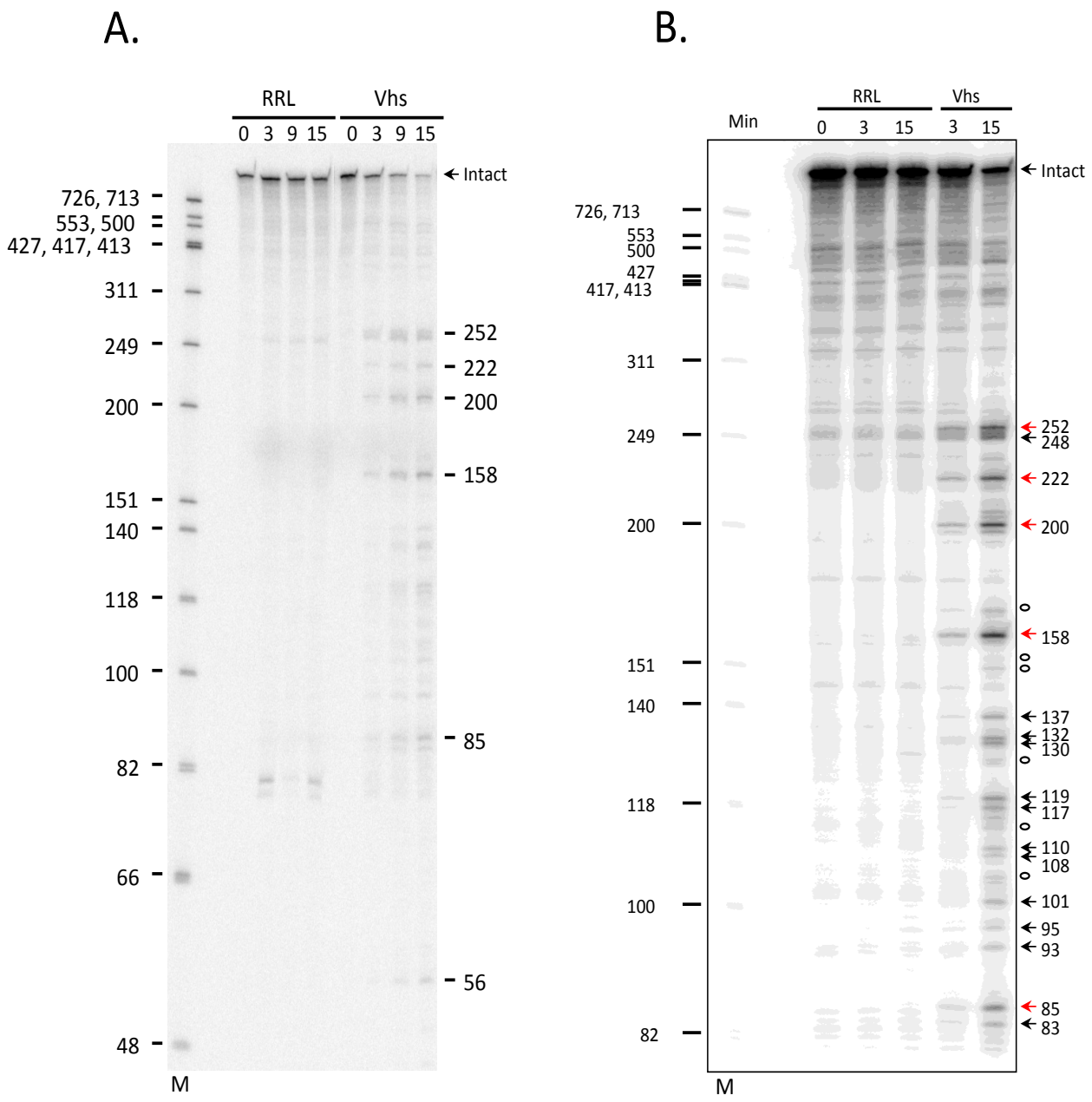

Figure 18. mRNA Cut Site Analysis After Using [α-^{32}P]GTP with 3,000 Ci/mmol

Pictured in Fig. 18 is 5' cap-labeled pBK2 mRNA following incubation with Vhs protein. RNA was either labeled with a specific activity of 800 Ci/mmol (A.) or 3,000 Ci/mmol (B.) in an *in vitro* cap-labeling reaction followed by purification and addition to a rabbit reticulocyte lysate lacking (RRL) or containing (Vhs) Vhs. mRNA was extracted at the indicated time points and analyzed by autoradiography. RRL=rabbit reticulocyte lysate without Vhs. Vhs=RRL containing Vhs. M=ΦX174*Hinf1* markers. Min.=amount of time in minutes mRNA incubated with rabbit reticulocyte lysate. Hash marks in A represent the most prominent cut sites identified. Red arrows in B represent the most prominent cut sites identified, black arrows represent cut sites identified, and hollow circles represent faint cut sites detected.

[α-^{32}P]GTP (Fig. 18B). Figure 19 shows the cut sites mapped to the pBK2 sequence.

Vhs Assay with Extended mRNA Incubation

To better understand the stability of the mRNA in the Vhs assay system after cleavage and whether Vhs cleaves mRNAs at different sites upon further time spent in the *in vitro* system, a Vhs assay was performed analyzing mRNA cleavage products at later time points following mRNA substrate addition to Vhs protein. In this experiment, cap-labeled mRNA substrate was incubated for 3, 15, 30, and 60 minutes in the presence or absence of Vhs protein followed by RNA extraction and analysis of the cleavage products through autoradiography. Interestingly, the pattern of Vhs cutting was the same over time, where it primarily produced mRNA fragments of the same size at the 30 and 60 minute time points as those at the 3 and 15 minute times (Fig. 20).

It appears that the RRL system did not contain a large amount of background nuclease activity, because the cleavage products that were produced early in the time course were not rapidly degraded by the 60 minute time point (Fig. 20). Vhs appeared to use the same mechanism for cleaving pBK2 mRNA at the beginning of the Vhs assay as it did upon further incubation in the RRL system, because with time several of the same RNA cleavage products were produced (Fig. 20). As incubation time increased, novel mRNA cleavage bands migrating between 30 and 50 bases were identified (Fig. 20). It is not clear how these cut sites were produced. They could be due to cutting of the initial products of Vhs cleavage a second time by either Vhs or a cellular enzyme. At this time it is also uncertain if Vhs produces a single cut on the mRNA template, or if it remains associated with the transcript for additional rounds of cleavage.

A. Cut Sites Detected Using [α-^{32}P]GTP with a Specific Activity of 800 Ci/mmol

B. Cut Sites Detected Using [α-^{32}P]GTP with a Specific Activity of 3,000 Ci/mmol

Figure 19.Mapping pBK2 mRNA Cut Sites with 5' Cap Labeling

The cut sites from the 5' cap-labeled experiments using with a specific activity of 800 Ci/mmol (A.) or 3,000 Ci/mmol (B.) are labeled in Figure 19. The boxes include the first 330 bases of the pBK2 mRNA sequence. Black arrows show the estimated location where cutting occurred. The bolder arrows depict the most prominent cut sites and the less intense arrows show the cut sites that were less abundant (B). The sequence marked in red highlights the first three AUG codons of the sequence.

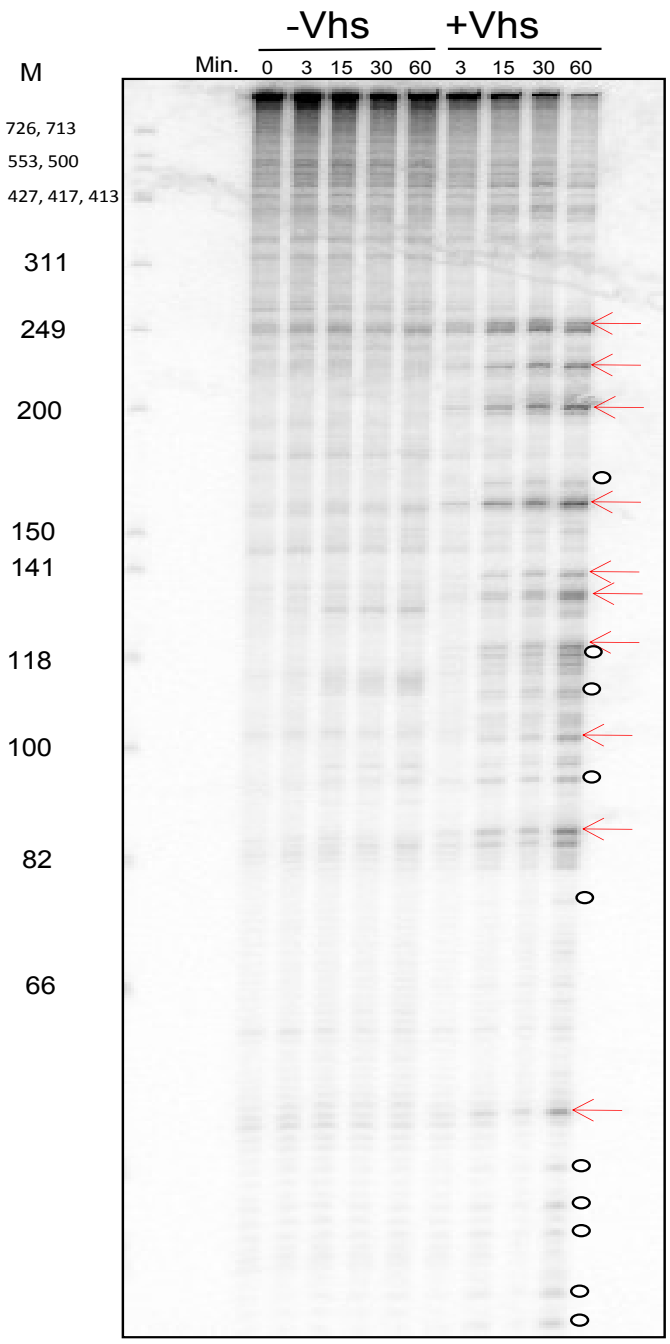

Figure 20.Vhs Assay with pBK2 mRNA Using Extended Time Points

Cap-labeled pBK2 mRNA was added to rabbit reticulocyte lysate lacking (RRL) or containing (+ Vhs) Vhs protein. Sample was then removed at the indicated time points followed by RNA extraction and analysis through autoradiography. The red arrows indicate the prominent cut sites produced by Vhs, and the hollow circles indicate the less abundant RNA cleavage products. M=ΦX174*Hinf1* markers. 0', 3', 15', 30', and 60' indicate minutes mRNA substrate incubated with Vhs prior to extraction.

Primer Extension Analysis

The previous study focused on using 5′ cap-labeled mRNA to identify the upstream products produced by Vhs cleavage. Another way to study nuclease activity is to examine the downstream products produced by cutting through primer extension analysis. In this study, pBK2 mRNA was capped in an m^7G capping reaction with unlabeled GTP. The mRNA was then added to a RRL system either lacking or containing Vhs. Samples were removed at various time points followed by RNA extraction. Lastly, mRNA was analyzed in a primer extension reaction using three radiolabeled primers that bound to different regions near the 5′ end. The primers used in this study were named P165, P235, and P325. Their names indicate the length of bases the primers would synthesize if they bound to the RNA and reverse transcribed all the way to the 5′ cap. Therefore, P165 means that, if the primer were to extend to the 5′end, then it would produce a product of 165 bases.

As is apparent from Figure 21, during the reverse transcription process reverse transcriptase stalls at many pause sites. The pause sites are likely due to mRNA structural barriers. Because of this, the only bands that are attributed to Vhs cutting are those identified solely in the 15 or 30 minute time point in the presence of Vhs. The cut sites identified are marked by red dots (Fig. 21A) or black arrows (Fig. 21B). The cut sites identified through primer extension are diagrammed in Figure 22. Primer extension analysis was a more sensitive method for determining RNA cut sites since, upon radiolabeling, the sample was directly added to a gel for analysis and did not undergo further washes. Longer incubation of Vhs with mRNA substrate resulted in additional cutting of mRNA (Fig. 22B). The prominent cut sites were

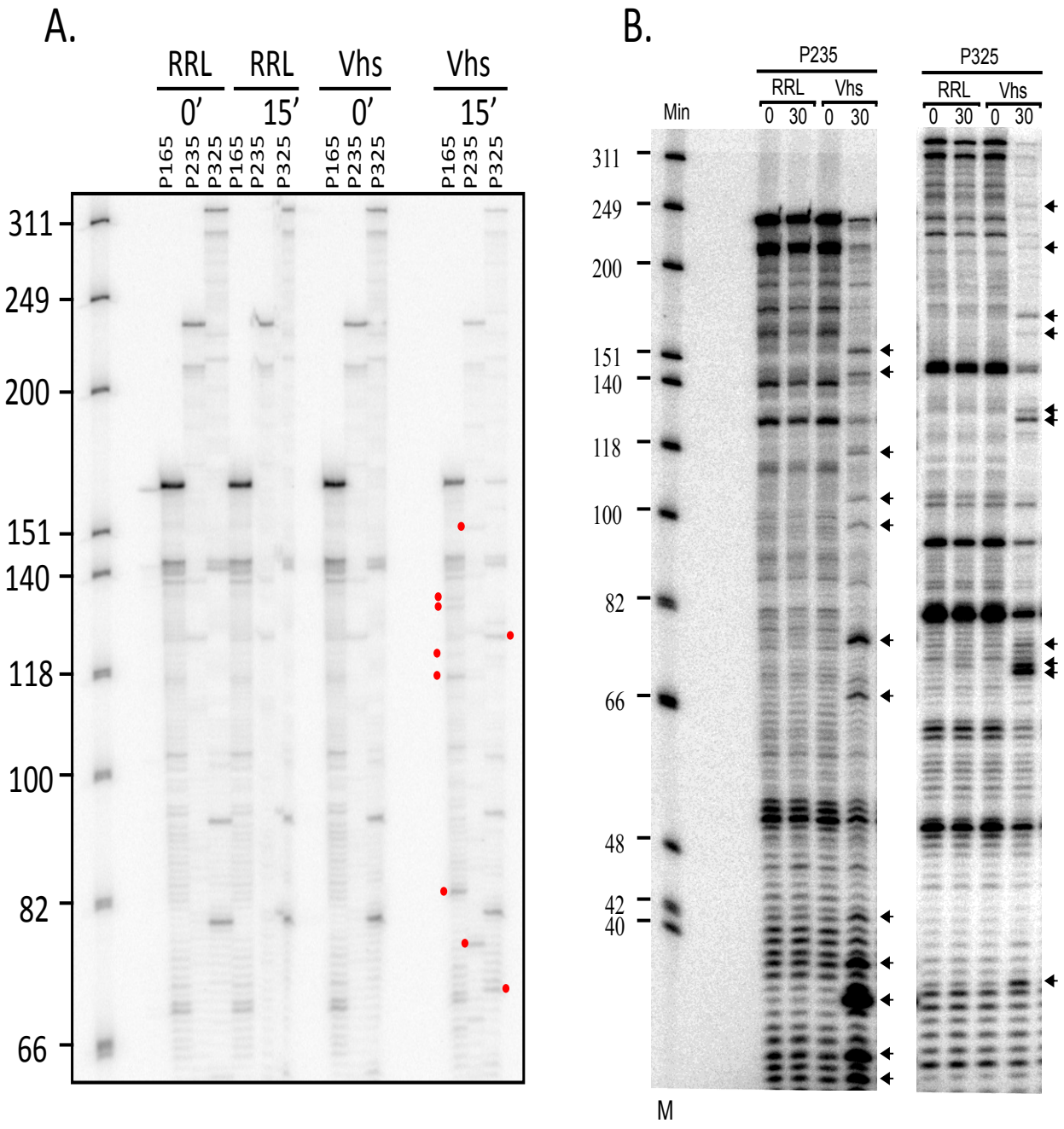

Figure 21.Primer Extension Analysis of pBK2 mRNA Cut Sites

Primer extension analysis of pBK2 mRNA at 15 (A.) and 30 (B.) minute time points. pBK2 mRNA was added to rabbit reticulocyte lysate in the absence (RRL) or presence (Vhs) of Vhs protein. Samples were removed at the indicated time points followed by RNA extraction and analysis through primer extension. P165, P235, and P325 are the primers that recognize different regions of the pBK2 mRNA sequence, and if they extend to the 5' cap during primer extension they produce a DNA band of 165; 235; or 325 bases, respectively. The red dots (A) and black arrows (B) mark bands caused by Vhs cutting. M=ΦX174 *Hinf1* markers.

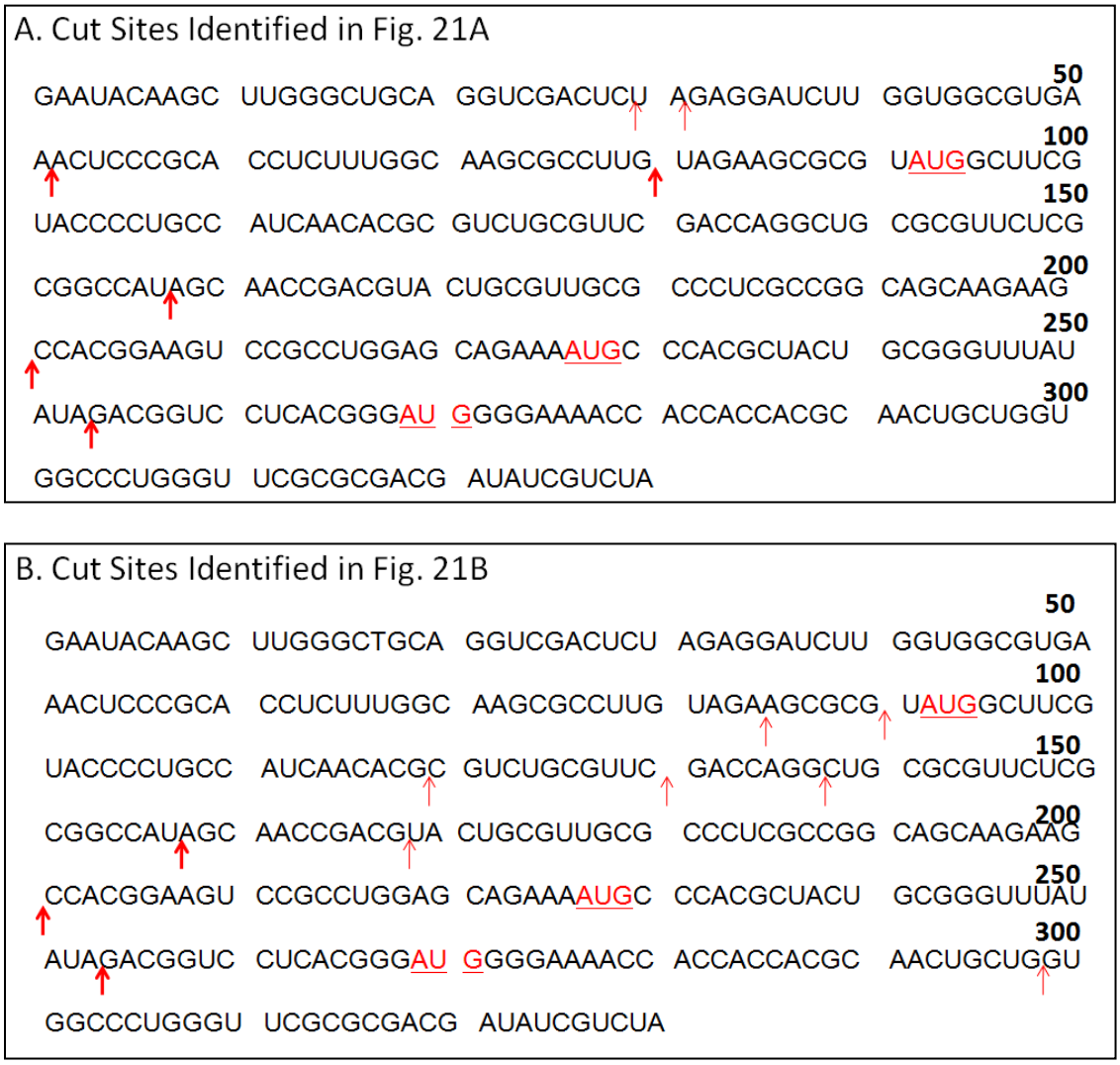

Figure 22.Mapping pBK2 mRNA Cut Sites Using Primer Extension Analysis

The cut sites identified from the primer extension experiments are labeled in the diagrams above. mRNA was incubated with Vhs for 15 (A) or 30 (B) minutes. The boxes include the first 330 bases of the pBK2 mRNA sequence. Red arrows show the estimated location of cutting. The bolder arrows depict the most prominent cut sites and the less intense arrows show the cut sites that were less abundant. The sequence marked in red highlights the first three AUG codons from the 5' end.

repeatedly detected through primer extension (Fig. 22). Figure 22B does not show a prominent cut site at bases 51 or 80 because primer 165 was not used in the experiment.

A summary of the prominent cut sites identified through both 5′ cap labeling and primer extension is pictured in Figure 23. The black arrows indicate the cut sites determined by 5′ cap labeling which represent the upstream cleavage products. The red arrows mark those found by primer extension analysis which identify the downstream products produced by cutting. Notably, most of the prominent cut sites established through the two methods line up or are very close to one another (Fig. 23).

These data support previous reports that Vhs is an endoribonuclease (2, 4, 5, 10, 11, 12, 13). Several of the cut sites are close to and slightly upstream from the first three AUG codons of the pBK2 sequence (Fig. 23). This finding suggests that Vhs may interact with the scanning complex upon association with the eIF4F cap-binding complex, and that its cut sites may be reached by piggybacking on the complex during scanning. Yet, under this mechanism for cutting, one would expect the cut sites to be limited to regions solely upstream or at the first AUG codon. This is because, upon reaching the start codon, the scanning complex stalls in a process that is followed by loss of initiation factors and recruitment of the large ribosomal subunit. In this case, Vhs would not be expected to cleave mRNA near regions of the second and third AUGs because scanning wouldn't progress to these areas. However, it's important to note that the first two AUGs are in a suboptimal context when compared to the Kozak consensus sequence, but the third AUG is in an optimal context (Fig. 23). In this case, one cannot rule out that the scanning complex may experience leaky scanning while reading the mRNA sequence during translation initiation. Previous work in the lab has shown that pBK2 produces three

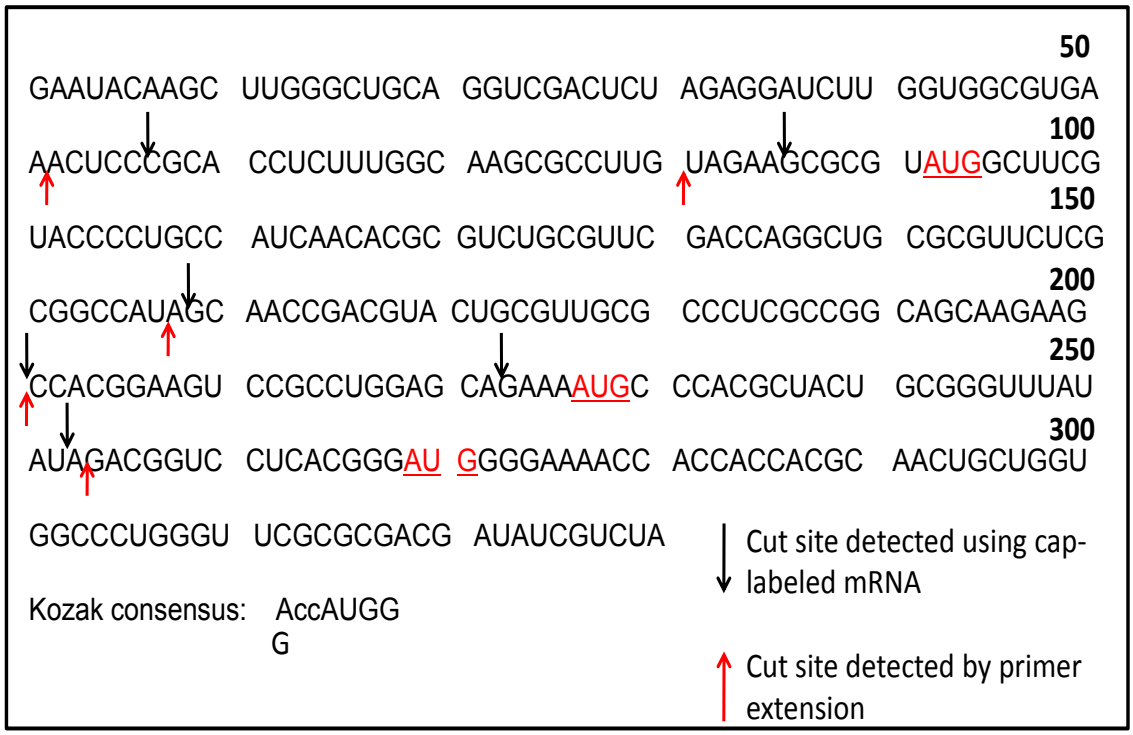

Figure 23.Summary of the Prominent Cut Sites Identified through 5' Cap-labeling and Primer Extension Analysis

Figure 23 shows a diagram of the prominent cuts sites identified through primer extension analysis and 5' cap-labeling of pBK2 mRNA. The black arrows show the cut sites found through 5' cap-labeling and the red arrows indicate those identified through primer extension analysis. The sequence in red highlights the first three AUGs of the pBK2 mRNA sequence. The Kozak consensus sequence is listed on the lower left corner, showing the optimal locations for purine residues surrounding the AUG codon. The first and second codons are in a suboptimal context compared to the Kozak consensus sequence, yet the third AUG is in an optimal context. The arrows mark the estimated cut site locations, and the slight differences in location could be due to uncertainties in size estimates between gels.

protein products in an *in vitro* RRL system, and these protein products correspond to initiating synthesis from the first three AUGs of the pBK2 mRNA sequence (Karr and Read, unpublished).

The Effect of Translation Initiation Inhibition on Vhs Cleavage

Cycloheximide Experiments

To test the importance of translation initiation for mRNA cleavage, inhibition studies were performed that blocked various stages of translation initiation. First, as a control, studies were designed to test the effect of cycloheximide on Vhs activity in a RRL system. Cycloheximide is an antibiotic produced by *Streptomyces griscus* which has been shown to block protein synthesis in yeast and mammalian cells (15-21). The antibiotic blocks protein synthesis by inhibiting peptide bond formation. In the presence of cycloheximide, translation initiation factors and the 40S ribosomal subunit still associate near the 5′ cap and scanning occurs to the AUG start codon. The large ribosomal subunit still binds to the 40S subunit, but no protein is made. Studies with HSV-1 infected cells in the presence of Actinomycin D have found that cycloheximide does not inhibit Vhs's ability to degrade mRNA (14).

In the present study, RRL containing or lacking Vhs was incubated with 50ug/ml cycloheximide or water for 12 minutes at 30˚C. Following the incubation, cap-labeled pBK2 mRNA was added to the system, and RNA was extracted at various time points followed by analysis on a 1.3% agarose 1X MOPS gel (Fig. 24). In the presence of cycloheximide, Vhs showed similar levels of mRNA degradation as the control which lacked cycloheximide (Fig. 24). This gel shows that protein synthesis is not required for Vhs degradation of mRNA. To study the effect of cycloheximide in more detail, an identical assay was performed and samples were run on a 7% polyacrylamide 8M urea 1X TBE gel to examine site-specific cleavage (Fig. 25).

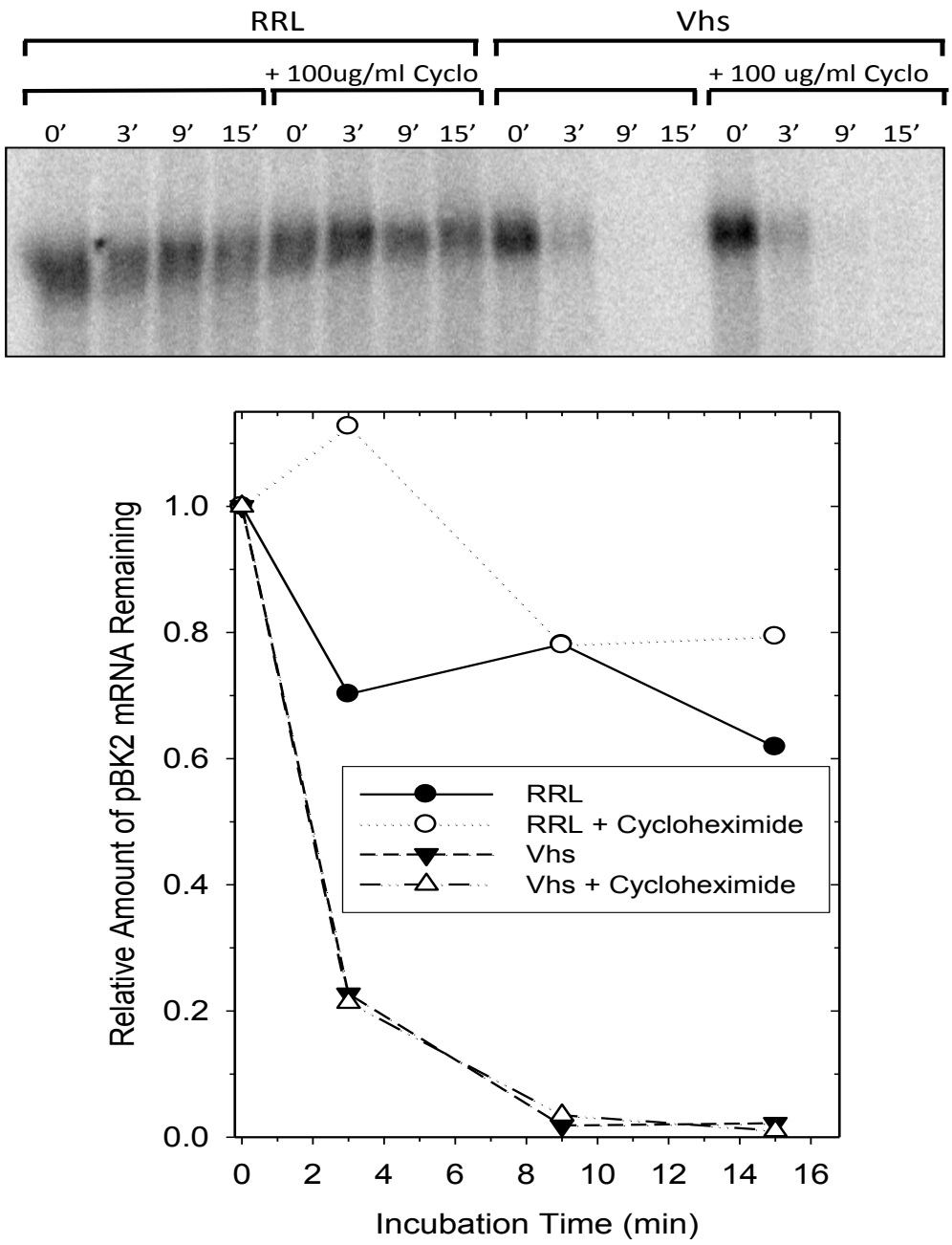

Figure 24.Vhs Degradation of pBK2 mRNA in the Presence of Cycloheximide

Rabbit reticulocyte lysate containing (Vhs) or lacking (RRL) Vhs protein was combined with water or cycloheximide (+Cyclo) to a final concentration of 50ug/ml. After a 12 minute incubation, cap-labeled pBK2 mRNA was added and samples were extracted at the indicated time points listed above. RNA was extracted and analyzed on a 1.3% agarose 1X MOPS gel through autoradiography. After exposure, the gel was scanned and relative amount of mRNA remaining was quantified using ImageQuant 5.0 software. RRL=rabbit reticulocyte lysate that lacks Vhs. Vhs=rabbit reticulocyte lysate that contains Vhs protein. Min=minutes mRNA incubated in rabbit reticulocyte lysate before removal. Cyclo=cycloheximide.

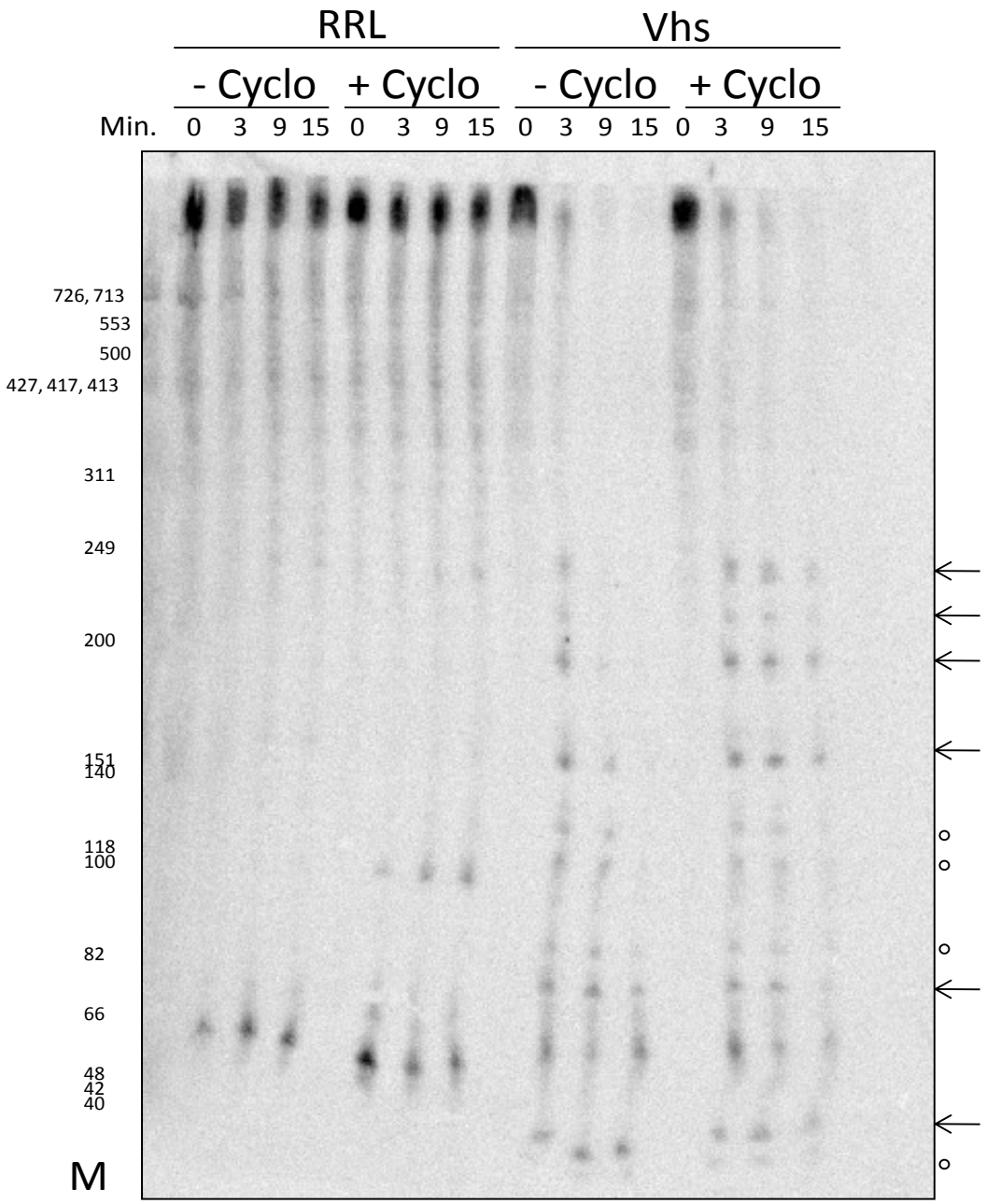

Figure 25.Vhs Site Specific Cleavage of pBK2 mRNA in the Presence of Cycloheximide

Cap-labeled pBK2 mRNA samples from the same experiment performed in Figure 24 were run on a 7% polyacrylamide 8M urea gel to examine Vhs site-specific cutting. –Cyclo represents sample that was incubated with water for 12 minutes prior to addition of pBK2 mRNA. +Cyclo represents sample that was incubated with 50ug/ml cycloheximide prior to mRNA addition. The black arrows mark the prominent cut sites identified due to Vhs cutting and the hollow circles indicate the less prominent cut sites determined. RRL=rabbit reticulocyte lysate without Vhs. Vhs=rabbit reticulocyte lysate containing Vhs. Min.=minutes pBK2 mRNA incubated in rabbit reticulocyte lysate before extraction. M=ΦX174*Hinf1* markers.

Cycloheximide did not inhibit Vhs's ability to specifically cleave pBK2 mRNA, because in its presence Vhs produced the exact same cutting pattern at 3 minutes of incubation (Fig. 25). It is possible that further cleavage of the primary mRNA degradation products is more rapid in the absence of cycloheximide (Fig. 25).

GMP-PNP Experiments

In the next study, GMP-PNP, a nonhydrolyzable analogue of GTP, was used to block an earlier stage of translation initiation. GMP-PNP hinders GTP hydrolysis, and this process is required for loss of translation initiation factors from the AUG start codon and recruitment of the large ribosomal subunit. However, GMP-PNP does not block assembly of the 48S complex (22, 23). Therefore, in the presence of GMP-PNP, initiation factors and the small ribosomal subunit are still recruited to the 5′ cap and the scanning complex is able to scan to the start codon. Yet, after scanning, translation initiation is inhibited and the 60S ribosomal subunit is not recruited to the mRNA template.

Rabbit reticulocyte lysate containing or lacking Vhs was incubated with water or 2mM GMP-PNP for 12 minutes at 30˚C followed by addition of cap-labeled pBK2 mRNA. All samples contained endogenous GTP that was present in the RRL system. Samples were then aliquotted at various time points followed by RNA extraction and analysis through autoradiography. Studies found that GMP-PNP had at most a modest inhibition on Vhs cutting of mRNA (Fig. 26). However, at the fifteen minute time point Vhs was able to degrade mRNA to comparable levels as mock in the presence of GMP-PNP (Fig. 26). Next, samples were run on a 7% polyacrylamide 8M urea 1X TBE gel to analyze Vhs site-specific cleavage in the presence of GMP- PNP (Fig. 27).

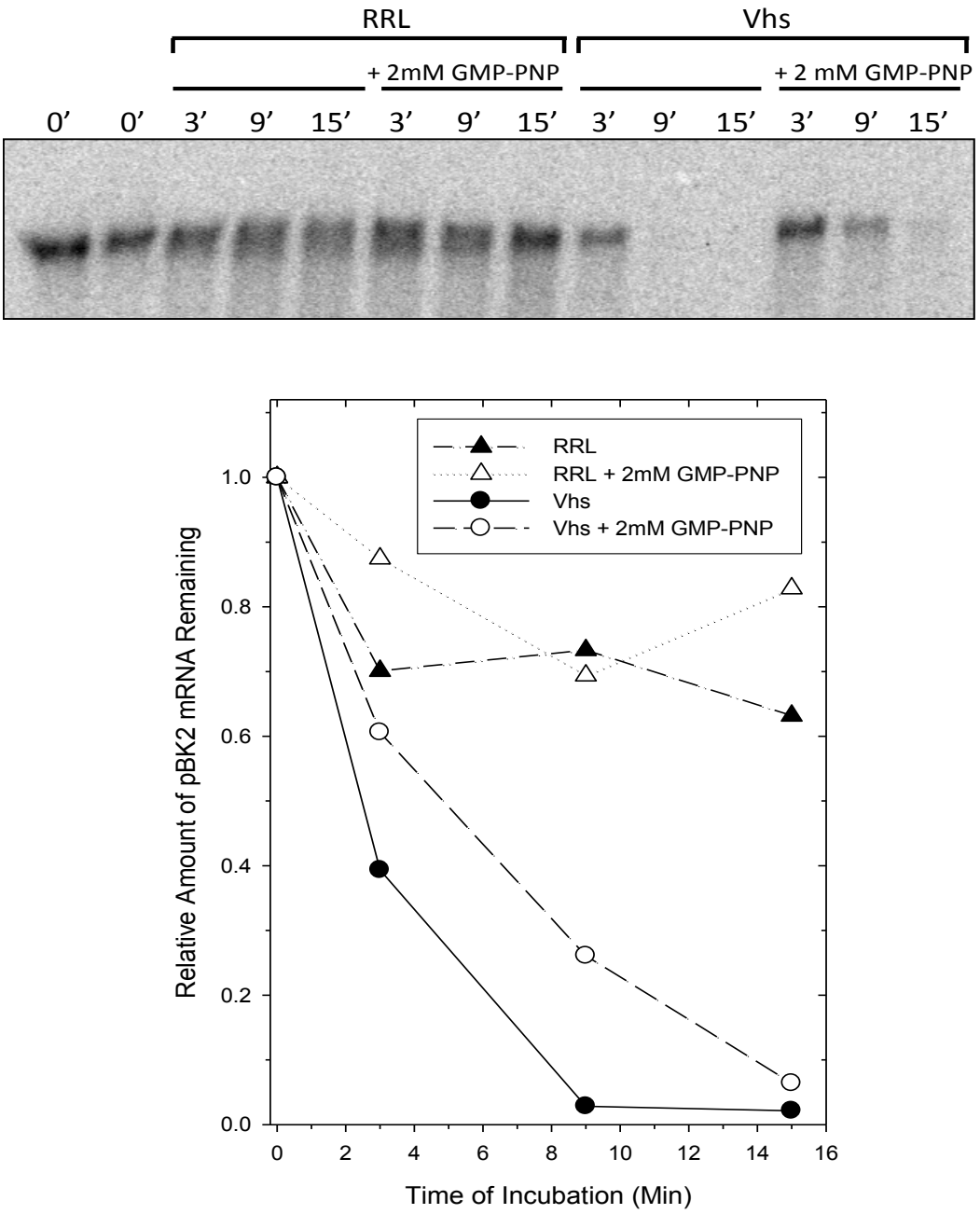

Figure 26.Vhs Degradation of pBK2 mRNA in the Presence of GMP-PNP

Rabbit reticulocyte lysate containing (Vhs) or lacking (RRL) Vhs protein was incubated with 2mM GMP-PNP (+GMP-PNP) or water for 12 minutes prior to addition of cap-labeled pBK2 mRNA. Samples were removed at the indicated time points followed by RNA extraction and analysis through autoradiography (top picture). Following scanning, mRNA levels were quantified using ImageQuant 5.0 software (bottom picture). RRL=rabbit reticulocyte lysate without Vhs. Vhs=rabbit reticulocyte lysate containing Vhs. Min=minutes that pBK2 mRNA incubated in rabbit reticulocyte lysate before extraction.

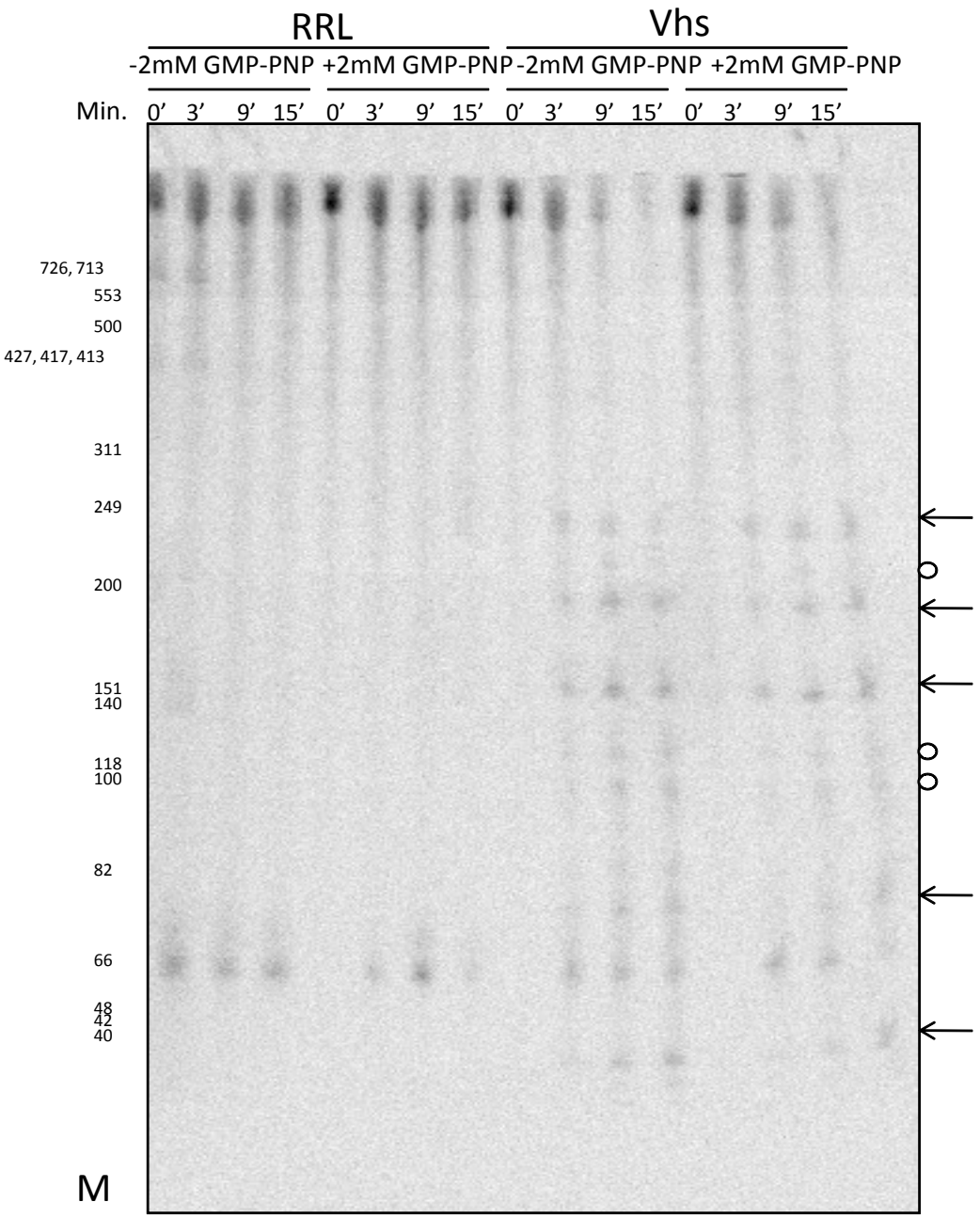

Figure 27.Vhs Site Specific Cleavage of pBK2 mRNA in the Presence of GMP-PNP

Prior to addition of cap-labeled pBK2 mRNA, rabbit reticulocyte lysate that contained (Vhs) or lacked (RRL) Vhs was incubated with 2mM GMP-PNP (+GMP-PNP) or water (-GMP-PNP) for 12 minutes at 30˚C. Cap-labeled pBK2 mRNA was then added and samples were removed at the indicated time points followed by RNA extraction. Samples were then run on a 7% polyacrylamide 8M urea 1X TBE gel and analyzed through autoradiography. The black arrows show the prominent cut sites detected and the hollow circles mark the less prominent cut sites. RRL=rabbit reticulocyte lysate that does not contain Vhs. Vhs=rabbit reticulocyte lysate that contains Vhs. Min.=minutes that mRNA incubated in the rabbit reticulocyte system before removal. M=ΦX174*Hinf1* markers.

Similar results were also obtained using a sequencing gel, where GMP-PNP did not hinder Vhs's ability to produce the same specific cut sites (Fig. 27).This indicates that recruitment of the large ribosomal subunit to the mRNA template is not vital for Vhs cleavage of mRNA.

AMP-PNP Experiments

To test whether an earlier stage of translation initiation was important for Vhs cleavage of mRNA, ATP hydrolysis was blocked by using the nonhydrolyzable analog of ATP, AMP-PNP. ATP is essential for RNA helicase activity of eIF4A and the eIF4F cap binding complex which helps unwind RNA secondary structure and make it accessible for binding of translation initiation factors and scanning to the start codon. AMP-PNP hinders 48S complex formation, and it has been reported to reduce binding of translation initiation factors to the 5' end (23, 60). The experiment was performed identically to the GMP-PNP experiment, except a final concentration of 2mM AMP-PNP or water was incubated with rabbit reticulocyte lysate instead of GMP-PNP. All samples contained an endogenous mixture of ATP which was present in the RRL system. AMP-PNP significantly inhibited Vhs cutting of pBK2 mRNA, where in its presence degradation levels were similar to control levels that lacked Vhs (Fig. 28). This result suggests that ATP hydrolysis for unwinding mRNA secondary structure and/or for recruitment of initiation factors and the small ribosomal subunit to the 5'cap is necessary for Vhs cleavage.

To further study the effect of AMP-PNP on Vhs degradation of mRNA, samples were run on a 7% polyacrylamide 8M urea 1X TBE gel (Fig. 29). The arrows identify the most prominent cleavage products and the hollow circles identify the less prominent sites (Fig. 29). Vhs was still able to produce some of the same specific cut sites in the presence of AMP-PNP (Fig. 29 black arrows). This is because, although AMP-PNP significantly inhibited cutting of total

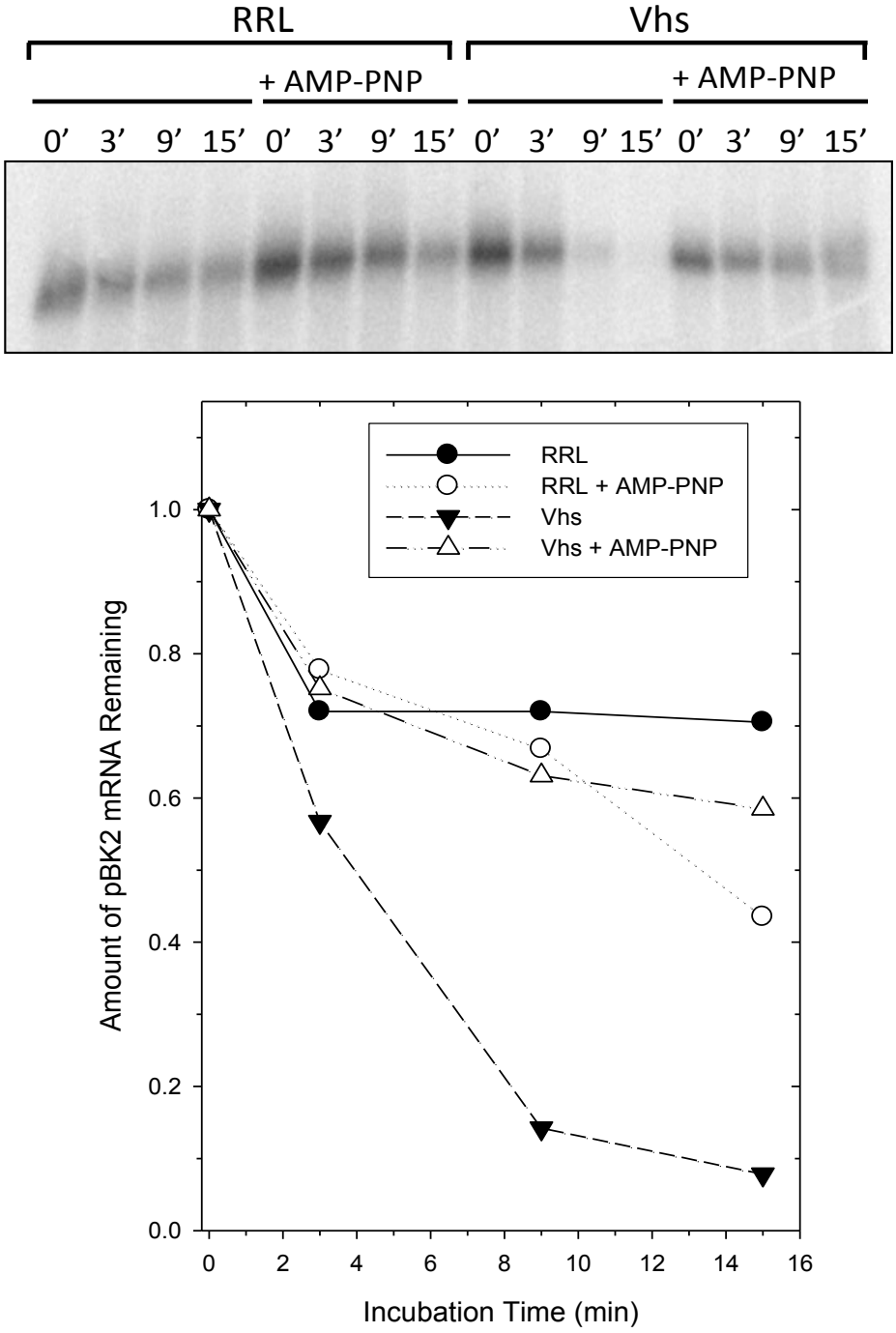

Figure 28.Vhs Degradation of pBK2 mRNA in the Presence of AMP-PNP

Rabbit reticulocyte lysate containing (Vhs) or lacking (RRL) Vhs protein was incubated with 2mM AMP-PNP (+AMP-PNP) or water for 12 minutes at 30˚C prior to addition of cap-labeled pBK2 mRNA. Samples were removed at the indicated time points followed by RNA extraction and autoradiography (top picture). Following scanning, mRNA was quantified with ImageQuant 5.0 software (bottom picture). RRL=rabbit reticulocyte lysate in the absence without Vhs. Vhs=rabbit reticulocyte lysate containing Vhs. Min.=minutes mRNA incubated in rabbit reticulocyte system before removal.

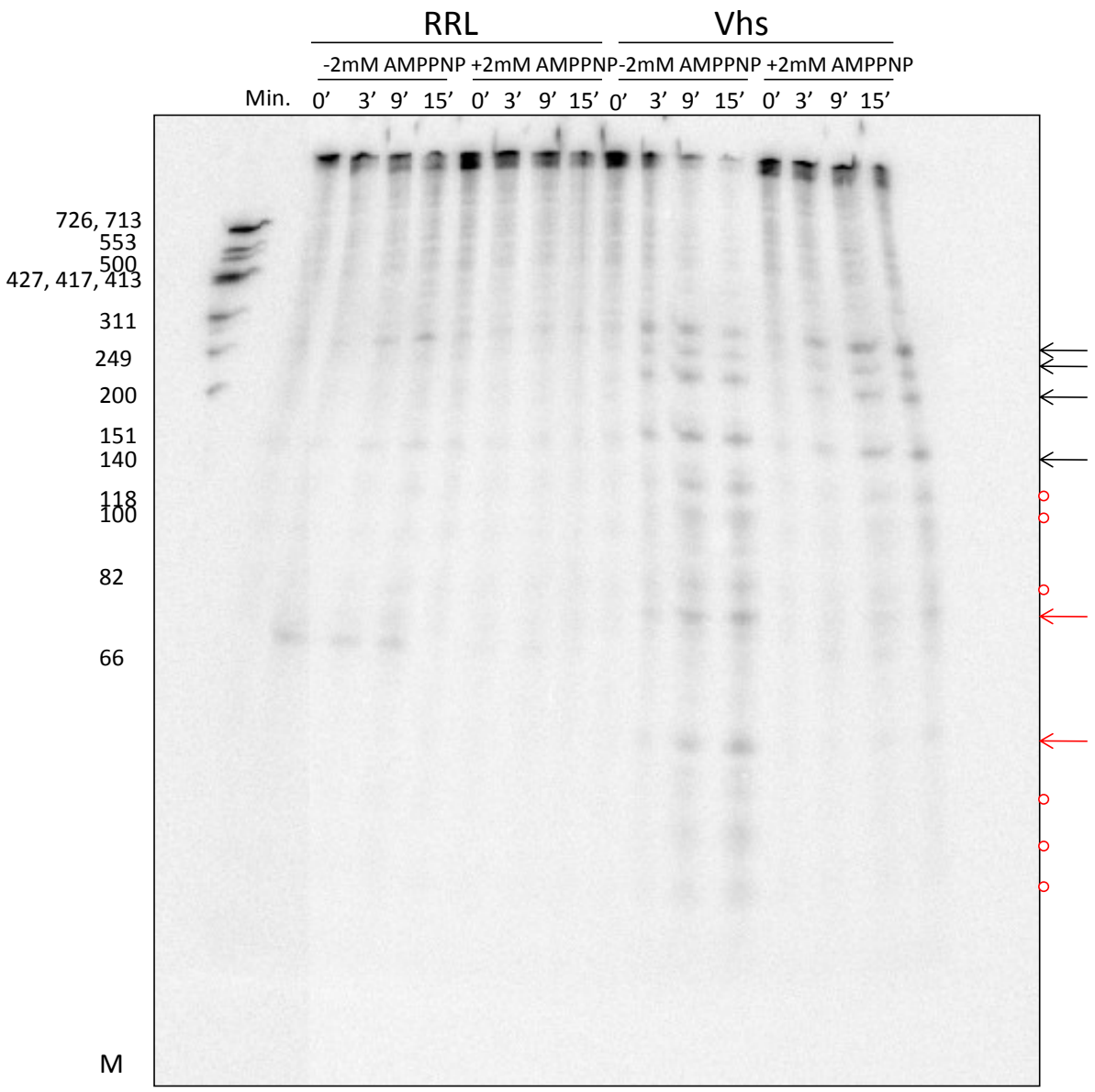

Figure 29.Vhs Site Specific Cutting of pBK2 mRNA in the Presence of AMP-PNP

Rabbit reticulocyte lysate containing (Vhs) or lacking (RRL) Vhs incubated with 2mM AMP-PNP (+AMP-PNP) or water for 12 minutes at 30˚C. Cap-labeled pBK2 mRNA was then added at to the system and samples incubated at 30˚C at the time points indicated above. Samples were then removed followed by RNA extraction. RNA was run on a 7% polyacrylamide 8M urea 1X TBE gel and analyzed by autoradiography. The black arrows represent prominent cut sites that were not hindered by addition of AMP-PNP. Red arrows and hollow circles mark the more prominent and less prominent cut sites that were inhibited by AMP-PNP, respectively. RRL=rabbit reticulocyte lysate that lacked Vhs. Vhs=rabbit reticulocyte lysate that contained Vhs. Min.=amount of minutes pBK2 mRNA incubated in rabbit reticulocyte lysate prior to extraction.

pBK2 mRNA, it didn't cause complete inhibition. However, AMP-PNP strongly inhibited specific cutting at regions in the first 150 bases of the mRNA sequence (Fig. 29, cut sites highlighted in red). Cycloheximide, GMP-PNP, and AMP-PNP were all tested in an *in vitro* translation reaction using S^{35} methionine to confirm their inhibition on translation (Fig. 30).

Cap Analog Experiments

Another way to study the importance of early stages of translation initiation is to use an m^7G cap analog to inhibit binding of initiation factors to the 5' cap of the mRNA template. In the next study, rabbit reticulocyte lysate was incubated with 3mM cap analog or water for 12 minutes at 30˚C followed by addition of cap-labeled pBK2 mRNA. Samples were incubated in RRL for various time points followed by RNA extraction. RNA was then run on a 1.3% agarose 1X MOPS gel and analyzed by autoradiography (Fig. 31). 3mM cap analog slightly inhibited Vhs cleavage of pBK2 mRNA (Fig. 31 compare the 9 and 15 min. time points of Vhs in the presence and absence of cap analog). To get a closer look at the inhibition, another Vhs assay was performed with 5mM cap analog and RNA samples were run on a 7% polyacrylamide 8M urea 1X TBE gel to look at the cap analog's effect on site-specific cleavage (Fig. 32).

Here, it is obvious that the cap analog inhibits Vhs cleavage of the first 80 nucleotides of pBK2 (Fig. 32 compare the 9 and 15 minute time points of Vhs in the presence and absence of cap analog). However, the inhibition was incomplete and Vhs was still able to cleave pBK2 mRNA at sites further downstream in the presence of cap analog (Fig. 32 Vhs + cap analog at 9 and 15 minutes). It's important to note that the cap analog has been reported to only have a 50% inhibition on translation in the rabbit reticulocyte system (25). It will be important to see if the

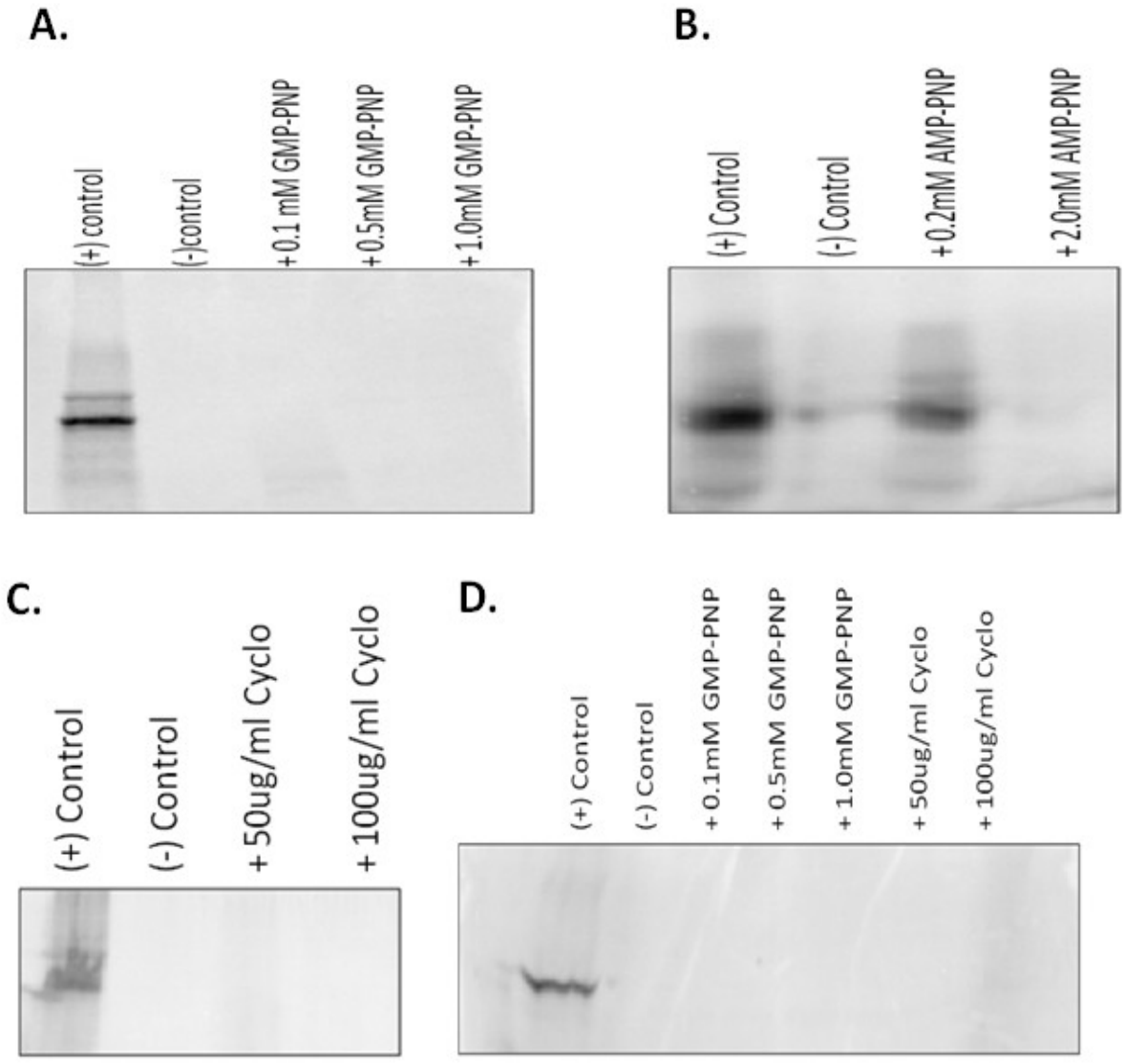

Figure 30.Cycloheximide, GMP-PNP, and AMP-PNP Inhibition on *in vitro* Translation

Various inhibitors were added to rabbit reticulocyte lysate that contained all of the components of an *in vitro* translation reaction except mRNA substrate. The sample incubated for 10 minutes at 30˚C followed by addition of unlabeled mRNA substrate. Protein was labeled with S^{35} methionine. The samples were run on an SDS PAGE gel followed by autoradiography for protein analysis. Reactions that contained pBK2 mRNA are shown in A-C and those that received pKOSamp mRNA (encodes Vhs) are shown in D. Cyclo=cycloheximide.

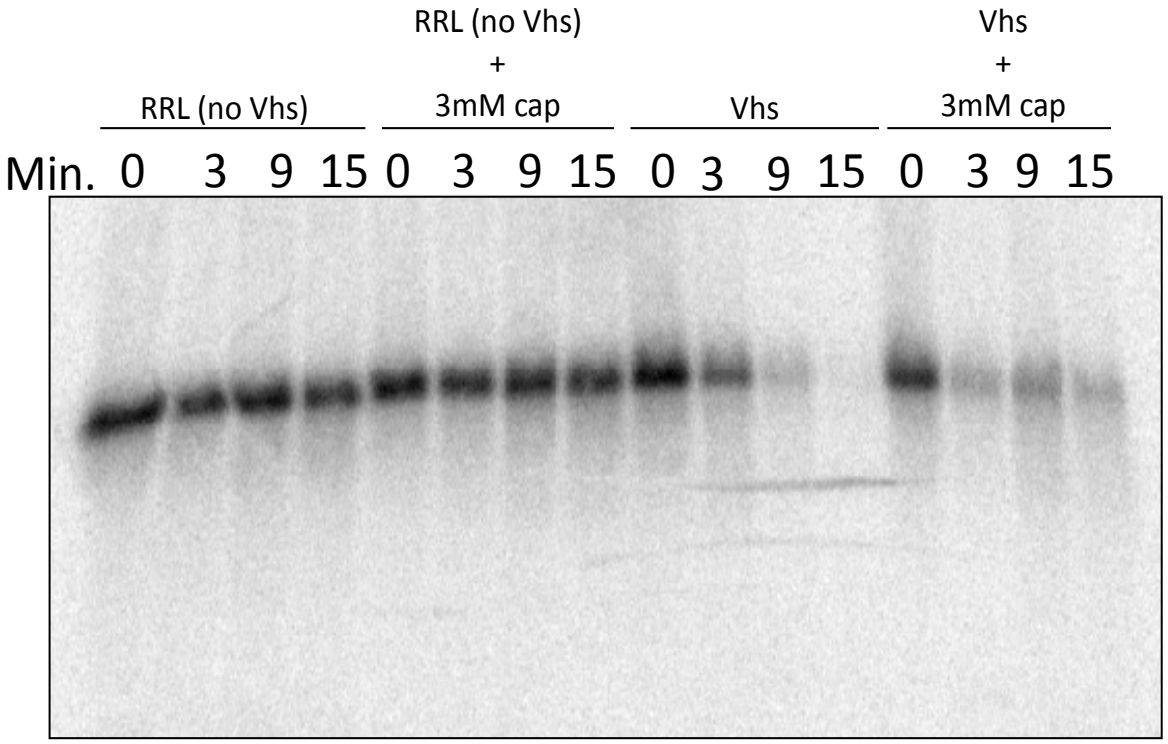

Figure 31.Vhs Degradation of pBK2 mRNA in the Presence of Cap Analog

Pictured in Figure 31 is cap-labeled pBK2 mRNA after addition of 3mM cap analog (+3mM cap) or water to the rabbit reticulocyte lysate system. Cap analog was incubated with rabbit reticulocyte lysate for 12 minutes at 30˚C prior to addition of mRNA. Samples were removed at the indicated time points followed by RNA extraction and analysis on a 1X MOPS 1.3% agarose gel. Min.=minutes that RNA incubated in rabbit reticulocyte prior to removal. RRL=rabbit reticulocyte lysate that does not contain Vhs. Vhs=rabbit reticulocyte lysate that contains Vhs.

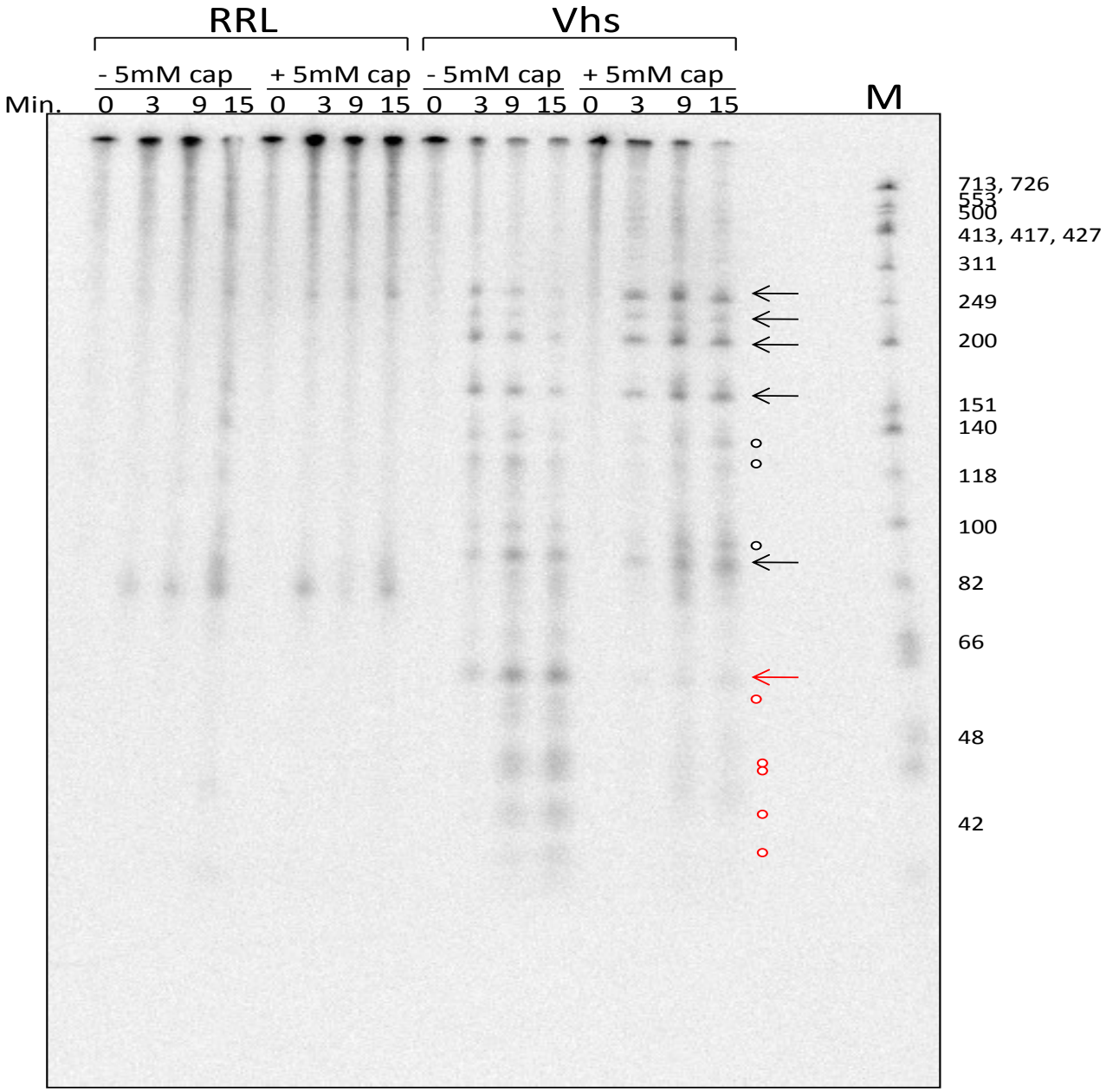

Figure 32.Vhs Site Specific Cutting of pBK2 mRNA in the Presence of Cap Analog

Figure 32 shows cap-labeled pBK2 mRNA from a Vhs assay that contained 5mM cap analog (+5mM cap) or water. Rabbit reticulocyte lysate containing (Vhs) or lacking (RRL) Vhs was incubated with cap analog to a final concentration of 5mM for 12 minutes at 30˚C. Cap-labeled pBK2 mRNA was then added to the system and samples were removed at the indicated time points followed by RNA extraction. RNA was then run on a 7% polyacrylamide 7M urea 1X TBE gel and analyzed by autoradiography. Min.=amount of time in minutes that mRNA incubated in rabbit reticulocyte system before removal. RRL=rabbit reticulocyte lysate that does not contain Vhs. Vhs=rabbit reticulocyte lysate containing Vhs. M=ΦX174 *Hinf1* markers. Arrows=prominent cut sites produced by Vhs. Hollow circles=less prominent cut sites produced by Vhs. Red symbols=cleavage products that are inhibited in the presence of cap analog.

downstream cut sites that are produced in the presence of cap analog *in vitro* are also produced *in vivo*.

Vhs Cutting of Circular RNAs

The next group of studies was designed to take advantage of previous knowledge about translation initiation of circular RNA. Sarnow and colleagues had demonstrated that RNA that undergoes cap-dependent scanning during translation initiation was not translated if it was circularized (26). This is because circularizing RNA will block recruitment of translation initiation factors to the 5′ end, hence, inhibiting translation initiation. However, the same article showed that circularizing an RNA which does not experience the traditional cap-dependent scanning mechanism for translation initiation but instead allows internal binding of translation initiation factors and the small ribosomal subunit will not hinder translation (26). Knowing that Vhs is an endonuclease, one might predict that it would have the ability to cleave circular RNA at the same sites as capped linear RNA. Yet, a considerable amount of data indicates that Vhs associates with cellular translation initiation factors that are necessary for cap-dependent scanning (6, 7, 13, 27, 28, Agarwal, D. et al. unpublished). Vhs association with eIF4H or eIF4AI/II appears to be vital for activity in infected HeLa cells (28, Agarwal et al. unpublished). These data combined with recent findings that Vhs prefers to cleave pBK2 mRNA at specific sites near the first three AUG codons indicate that Vhs may initially bind the mRNA template by associating with translation initiation factors that target to the 5′cap. If this is the case, then Vhs may reach its cut sites by piggy-backing on the scanning complex. If this is the mechanism Vhs uses for cleavage of RNA that experiences cap-dependent scanning, then Vhs would require a

free 5′ end to access the mRNA template and it wouldn't be able to cut this mRNA if it is in circular form.

pBK2 Circular RNA Experiment

In the current study pBK2 RNA was synthesized and taken through a dephosphorylation reaction (Fig. 33). Next, a single, non-radioactive monophosphate was added to the 5′ end using polynucleotide kinase (Fig. 33). The 5′ and 3′ ends were brought together with a complementary oligonucleotide, and T4 DNA ligase was used to seal the ends together (Fig. 33). RNA was then run on an agarose gel and the circular form was gel extracted and taken through a Vhs assay. As a positive control, linear capped pBK2 RNA was tested in the Vhs assay as a comparison. In order to identify specific cut sites of circular RNA, primer extension analysis was performed using radiolabeled primer P165 (described previously Fig. 21). DNA samples were then run on a 7% polyacrylamide 8M urea 1X TBE gel and analyzed by autoradiography (Fig. 34). Vhs was unable to cleave circularized pBK2 RNA at the same specific sites as capped linear, indicating that Vhs requires a free 5′ end to specifically cut an RNA that undergoes cap-dependent scanning for translation initiation (Fig. 34 compare Linear Vhs 15′ with Circular Vhs 15′). A faint band correlating to cleavage at base 80 is apparent in the Circular Vhs 15′ sample, but it is attributed to cutting of the small amount of linear RNA contamination which is present in the Circular RNA sample.

EMCV Circular Experiment

As a control for the previous study, it was desirable to test Vhs cleavage of circular RNA that did not use the typical cap-dependent scanning mechanism during translation initiation.

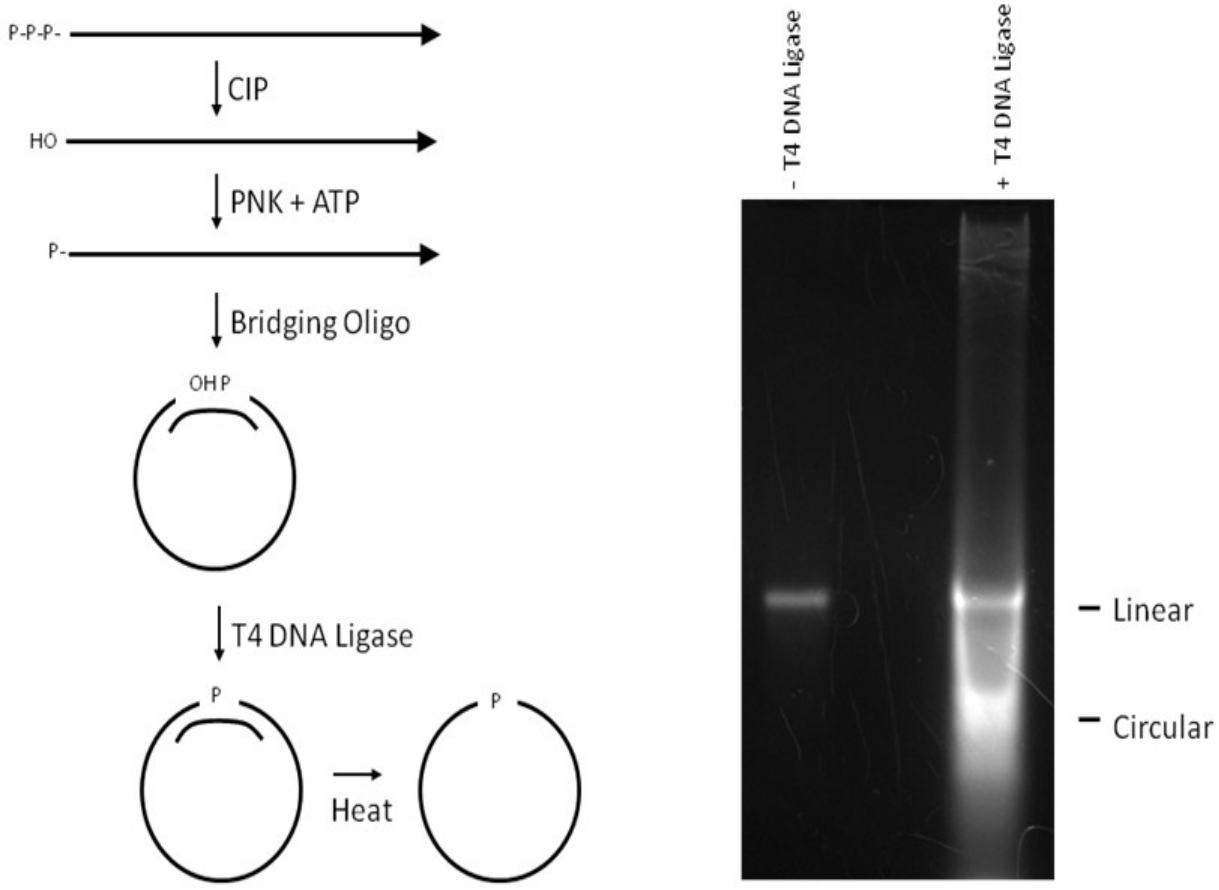

Figure 33.Circularization of pBK2 RNA

Pictured in Figure 33 is a diagram showing how pBK2 RNA was circularized (on left side). RNA was dephosphorylated with CIP followed by incorporation of a single monophosphate in a PNK reaction with unlabeled ATP. The 5’ and 3’ ends were brought together using a complementary bridging primer followed by a ligation reaction with T4 DNA ligase. The RNA was heated to remove the bridging oligonucleotide and run on an agarose gel to extract circular RNA (pictured on right). CIP=calf alkaline phosphatase. PNK=polynucleotide kinase.

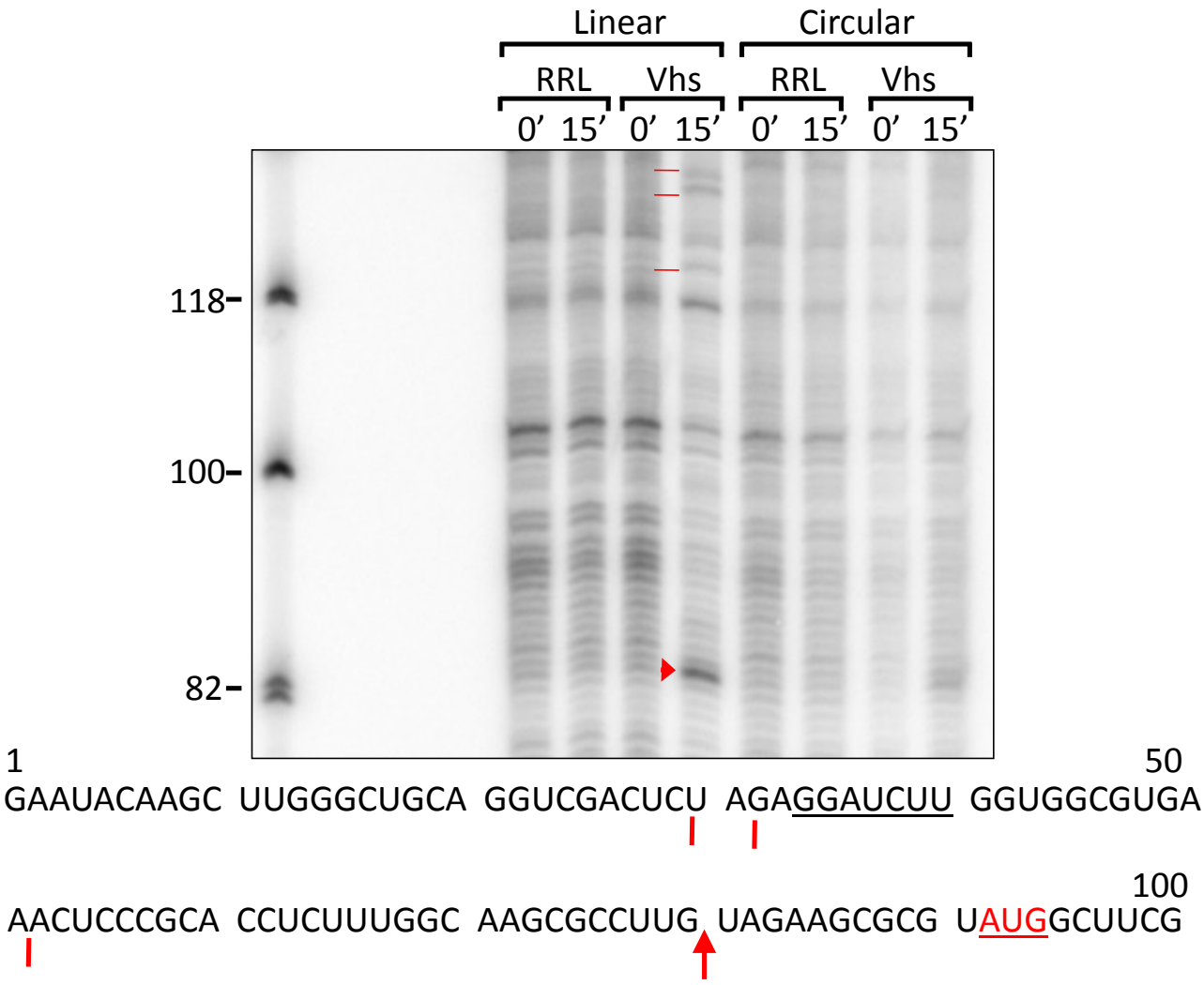

Figure 34.Primer Extension Analysis of Vhs Cleavage of Capped Linear pBK2 mRNA and Circular pBK2 RNA

Sequencing gel of DNA from primer extension analysis of RNA samples after Vhs assay with capped, linear (Linear) or circular (Circular) pBK2 RNA. Hash marks show the less prominent cut sites and arrows mark the prominent cut sites. Pictured below the gel is a diagram of the first 100 bases of the pBK2 sequence with the cut sites labeled in regards to the pBK2 sequence. RRL=rabbit reticulocyte lysate without Vhs. Vhs=rabbit reticulocyte that contains Vhs. Min.=amount of time in minutes that RNA incubated in rabbit reticulocyte lysate before removal. M.=ΦX174 *Hinf1* markers

Vhs has previously been shown to target cutting just downstream of the EMCV IRES (1-2). Additional studies have shown that a T214I Vhs point mutant, Vhs-1, (which is unable to bind eIF4H) is still able to target cutting downstream of the EMCV IRES (3). For the next study, it was desirable to test a previously studied mRNA that internally directed the recruitment of the small ribosomal subunit and various initiation factors. EMCV RNA was chosen for the following study because it had previously been studied in an RRL system.

First, to confirm that the system was set up properly, it was important to repeat the study previously performed by the Smiley lab to show that Vhs cuts EMCV at a specific region downstream of the IRES. Cap-labeled EMCV mRNA was incubated with RRL containing or lacking Vhs for various times followed by RNA extraction. The RNA was then run on a 1.3% agarose 1X MOPS gel and visualized by autoradiography (Fig. 35). Vhs targeting at a site downstream from the EMCV IRES was observed (Fig. 35). The EMCV RNA used for the study contained an IRES between bases 16-518 from the 5′ cap.

After Vhs targeting downstream of the EMCV IRES was confirmed, studies continued to test Vhs cleavage of circular EMCV RNA. EMCV RNA was synthesized using a T7 RiboMAX kit that contained GMP instead of GTP to add a single monophosphate to the 5′ end. After synthesis, the RNA was circularized using the same method as that described in Figure 33. Circular EMCV RNA was then gel extracted (Fig. 36B) and tested in a Vhs assay with linear cap-labeled EMCV as a comparison. Following the Vhs assay, RNA was analyzed by primer extension analysis using a primer that bound to bases 681-700 of the RNA sequence. After primer extension, the DNA was run on a 7% polyacrylamide 8M urea 1X TBE gel and visualized by autoradiography.

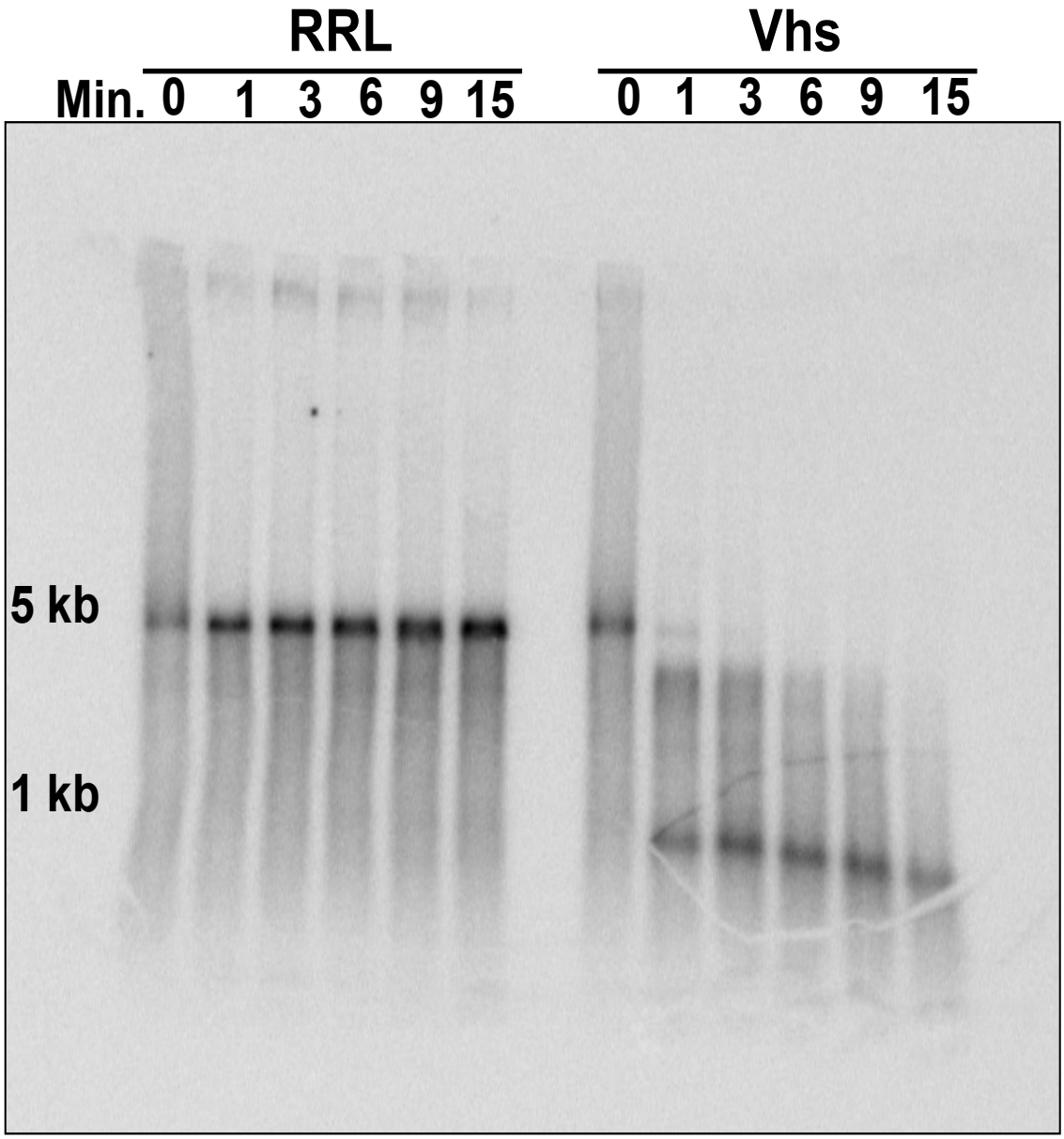

Figure 35.Vhs Site Specific Targeting Downstream of the EMCV IRES

Cap-labeled EMCV mRNA in the absence (RRL) or presence (Vhs) of Vhs protein. Min.=amount of time in minutes that mRNA incubated in rabbit reticulocyte lysate system prior to removal. RRL=rabbit reticulocyte lysate that contains Vhs. Vhs=rabbit reticulocyte lysate that lacks Vhs.

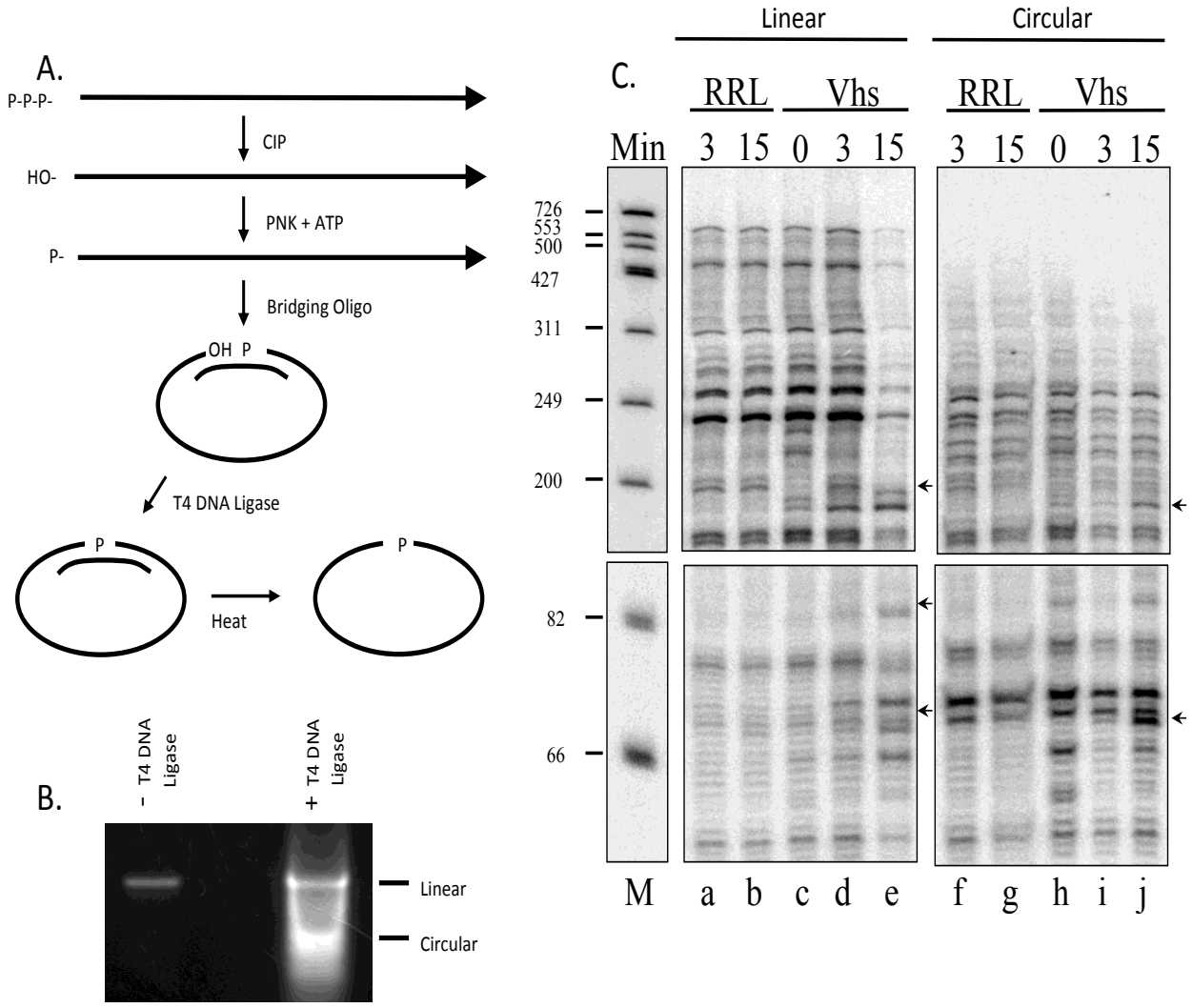

Figure 36.Primer Extension Analysis of Vhs Cleavage of EMCV RNA

Cartoon depiction of EMCV IRES structure showing location of initiation factor binding in regards to the AUG start codon (A). Agarose gel of circular vs. linear EMCV RNA (B). Sequencing gel of DNA samples from primer extension analysis of RNA from Vhs assays with capped linear RNA and circular EMCV RNA (C). Black arrows mark cut sites produced by Vhs. RRL=rabbit reticulocyte lysate that lacks Vhs. Vhs=rabbit reticulocyte lysate that contains Vhs. Min.=amount of time in minutes RNA was incubated with rabbit reticulocyte lysate prior to removal. M=ΦX174 *Hinf1* markers.

Vhs cleavage of capped, linear EMCV mRNA produced three prominent cut sites (Fig. 36C). Vhs was able to produce two of these specific cut sites when EMCV RNA was circularized, indicating that it does not require a free 5′ end in order to cleave an RNA that does not use cap-dependent scanning as a mechanism for translation initiation (Fig. 36C compare lane e with lane j). The primer used for cut site analysis bound to nucleotides 681-700 from the 5′ cap. So, for linear mRNA, when the primer extended to the 5′ cap during reverse transcription, it produced a DNA band of 700 bases (Fig. 36C a-e). However, for circularized RNA, primer extension did not create a run off band of 700 bases, and instead the primer extension stopped at random sites beyond 700 bases (Fig. 36C f-j top of gel). Figure 36 shows where the cut sites are located in regards to the EMCV sequence. Vhs specifically cleaved capped, linear EMCV mRNA near bases 510, 618, and 630. These regions were at the end of the IRES or just downstream from this region of high secondary structure (Fig. 37). The two reproducible cut sites produced in circular EMCV RNA were near bases 510 and 630 (Fig. 37).

Vhs Cleavage of pBK2 AUG Mutants

Mutating the First AUG to a Non-AUG

The previous experiments showed the importance of having a free 5′ end for Vhs site-specific cleavage of pBK2 RNA, an RNA that uses cap-dependent scanning during translation. To further test whether the scanning process might be involved in Vhs cleavage, studies were performed with pBK2 mutants which contained mutations in or surrounding the first AUG codon. In the first study the pBK2 sequence was mutated to change the first AUG codon to a non-AUG, CCC sequence. If Vhs is associating with translation initiation factors for recruitment to the 5′ end and accessing its cut sites by piggybacking on the scanning complex, a plausible

Figure 37.Diagram of EMCV Sequence Showing Vhs Cut Sites

Pictured in Figure 37 is the EMCV RNA substrate sequence from the Vhs assay in Figure 36. The three arrows show the cut sites produced by Vhs cutting of capped, linear RNA. The red arrows mark those that were obtained from Vhs cutting of circular EMCV RNA. The sequence marked in blue is the region that contains the EMCV IRES. The sequence highlighted in orange represents the first AUG after the EMCV IRES.

model is that its cut sites are determined by the amount of time that the complex spends in any one area of the RNA sequence. This amount of time could be affected by the degree of RNA secondary structure or the length of time the complex spends pausing to locate the start codon.

For this experiment it was hypothesized that mutating the first AUG to a non-AUG would hinder Vhs site specific cleavage near the area. Under this prediction the scanning complex would spend a shorter amount of time in the region when it lacked an AUG codon because it would no longer pause at the AUG to allow for removal of initiation factors and recruitment of the large ribosomal subunit. Cap-labeled wild type pBK2 and AUG1→CCC (pBK2 with a mutation in its first AUG to convert it to CCC) mRNA were examined in a Vhs assay. Following RNA extraction, samples were run on a 7% polyacrylamide 8M urea 1X TBE gel and viewed by autoradiography (Fig. 38A). From this study it was apparent that Vhs was not able to specifically cleave pBK2 mRNA just upstream from the original location of the first AUG start codon if the AUG was mutated to a CCC (Fig. 38A compare WT pBK2 Vhs and AUG1→CCC at 30 min.). The same result was found through primer extension analysis of unlabeled WT pBK2 and AUG1→CCC transcripts following a Vhs assay using primer 165 (Fig. 38B). This suggests that Vhs is associating with the scanning complex to reach some of its cleavage sites. It also suggests that, when the scanning complex pauses on the RNA template after locating the AUG start codon, it leads to a higher probability that Vhs will cut RNA in that area due to the longer amount of time spent in that region.

Mutating the Bases Surrounding the First AUG to Put it into an Optimal AUG Context

To continue testing the possibility that Vhs utilizes the scanning complex to reach some of its preferred cleavage sites, Vhs assays were performed using constructs where the

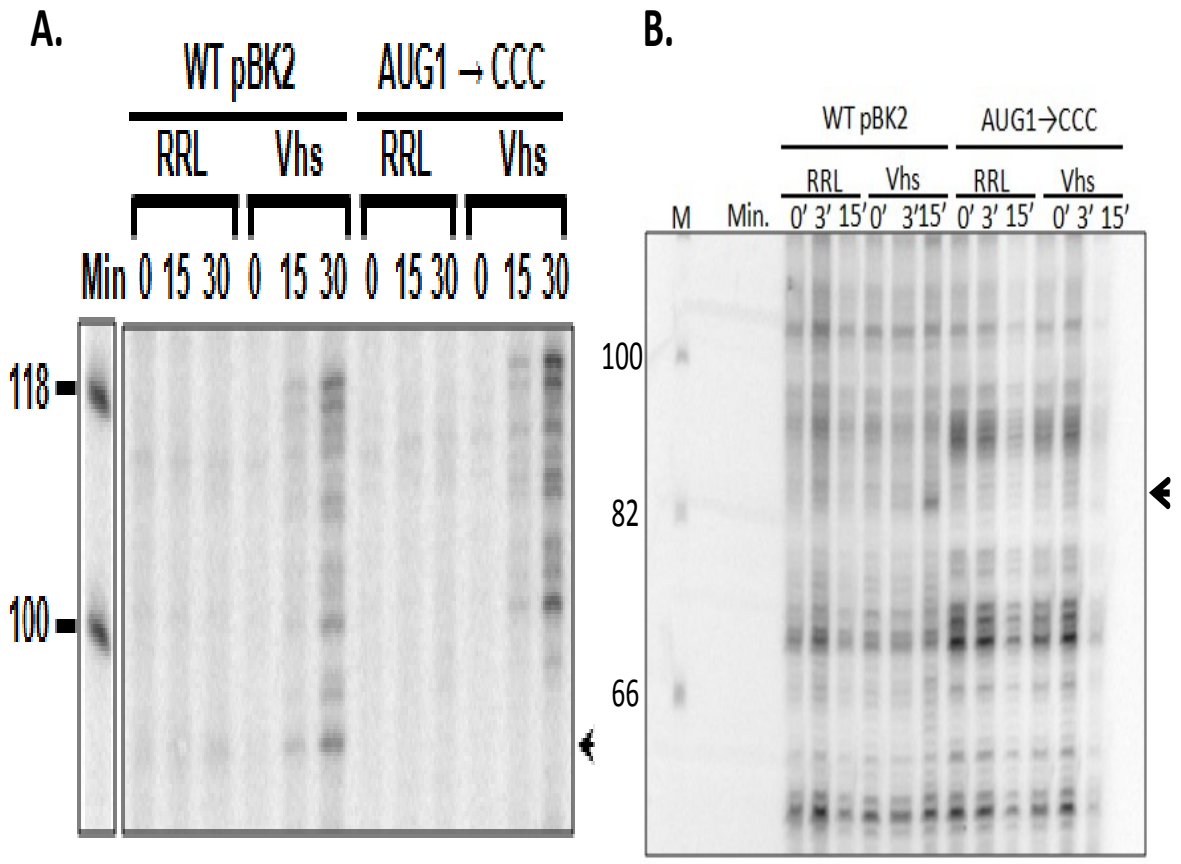

Figure 38.Vhs Cleavage of pBK2 mRNA with a Mutation in the First AUG Codon

Pictured in Figure 38 is a sequencing gel of cap-labeled RNA from a Vhs assay (A) or labeled DNA from primer extension following a Vhs assay (B). Rabbit reticulocyte lysate was incubated with wild type pBK2 mRNA (WT pBK2) or pBK2 mRNA with a mutation where the first AUG was replaced with CCC (AUG1→CCC). RNA was extracted at various time points, run on a 7% polyacrylamide 8M urea 1X TBE gel and visualized by autoradiography (A). For the gel in B, unlabeled WT pBK2 or AUG1→CCC RNA were taken through a Vhs assay followed by RNA extraction. The RNA was then used for primer extension analysis with primer 165, and the DNA was run on a sequencing gel. The arrow marks the cut site that was produced in wild type pBK2 mRNA but not AUG→CCC pBK2 mutant. RRL=rabbit reticulocyte lysate that does not contain Vhs. Vhs=rabbit reticulocyte lysate which contains Vhs. Min.=minutes RNA incubated with rabbit reticulocyte lysate prior to removal.

suboptimal context of the first AUG was converted to an optimal context. According to the Kozak consensus sequence, the region surrounding the AUG codon can have an impact on how strong the start codon is at initiating translation (29). An optimal start codon has a purine at positions -3 and +4 from the start codon, and within the purines adenine is preferntial at -3 and guanine at +4 (29). The strength of the start codon is also enhanced if cytosines are located at -4, -2, and -1 from the AUG (29).

The pBK2 sequence was mutated to convert bases surrounding the first AUG to create an optimal context that read CACCAUGG from -4 to +4 of the AUG, respectively (Fig. 39A). Cap-labeled wild type pBK2 and pBK2 mRNA with the optimal AUG mutations (AUG1-OPT) were studied in a Vhs assay, run on a 7% polyacrylamide 8M urea 1X TBE gel, and visualized by autoradiography (Fig. 39). Vhs showed enhanced cutting at regions upstream from the AUG codon when the regions surrounding AUG were mutated to make it an optimal start codon (Fig. 39). This indicates that Vhs has a higher probability of cleaving mRNA near its start codon if it is in an optimal context, supporting the idea that Vhs travels with the scanning complex during translation initiation to access some of its preferred cut sites.

Vhs cleavage of pBK2 mRNA with a single (Fig. 40A) or triple mutation (Fig. 40B) in the second AUG codon was also tested (Fig. 40). However, mutations in the second codon did not appear to hinder Vhs site specific cleavage (Fig. 40). The pBK2 mutants were tested in an *in vitro* translation reaction for their ability to make thymidine kinase (Fig. 41). This gel shows that the primary protein product produced corresponds to translation from the first AUG (Fig. 41). The second AUG does not appear to be vital for translation of pBK2 mRNA, and this seems to correlate with Vhs cleavage of pBK2 transcripts that have mutations in this codon.

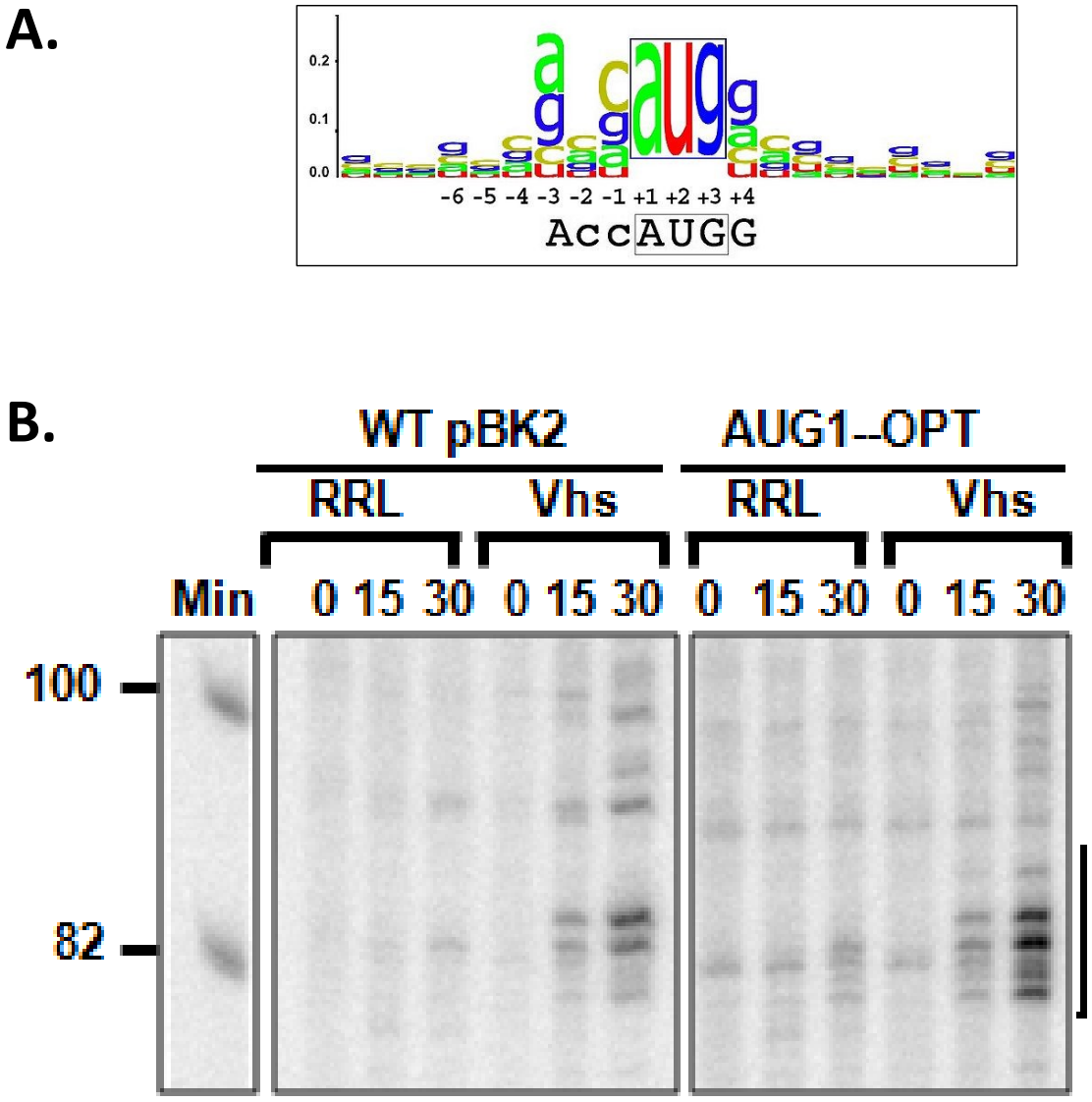

Figure 39.Vhs Cleavage of pBK2 mRNA with an Optimal Start Codon

Diagram of optimal bases surrounding the AUG start codon according to the Kozak consensus sequence (A). Sequencing gel of RNA from Vhs assay (B). Cap-labeled wild type pBK2 mRNA (WT pBK2) and mutated pBK2 mRNA with an optimal start codon (AUG1-OPT) were added to rabbit reticulocyte lysate and samples were removed at the indicated time points followed by RNA extraction. Samples were run on a 7% polyacrylamide 8M urea 1X TBE gel and visualized by autoradiography. The black hash mark shows a region with enhanced cutting. RRL=rabbit reticulocyte lysate lacking Vhs. Vhs=rabbit reticulocyte lysate that contains Vhs. Min.=amount of time in minutes that RNA incubated in the rabbit reticulocyte lysate system.

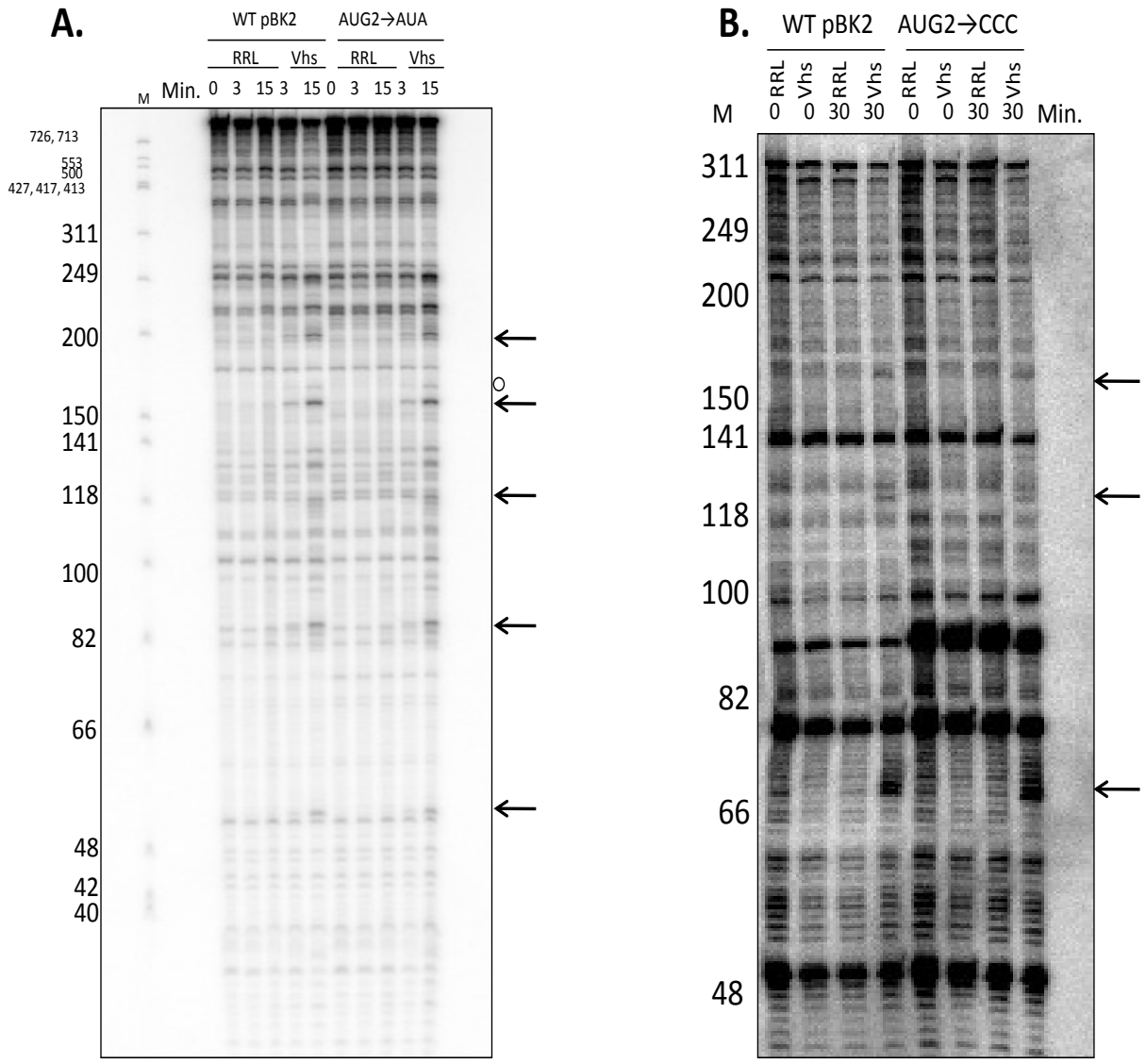

Figure 40.Vhs Degradation of pBK2 mRNA with a Mutation in the Second AUG Codon

Sequencing gel of cap-labeled WT pBK2 mRNA and pBK2 mRNA with a single point mutation in the AUG to convert it to AUA (A). Sequencing gel of primer extension analysis of unlabeled WT pBK2 mRNA and pBK2 mRNA with a mutation in the second codon to change it to CCC (AUG2→CCC) that were tested in a Vhs assay (B). Primer 325 was used during the reverse transcription. Arrows mark prominent cut sites identified and hollow circles mark less prominent cut sites. RRL=rabbit reticulocyte lysate that did not contain Vhs. Vhs=rabbit reticulocyte lysate that contained Vhs. Min.=amount of time in minutes that RNA incubated in rabbit reticulocyte system prior to removal.

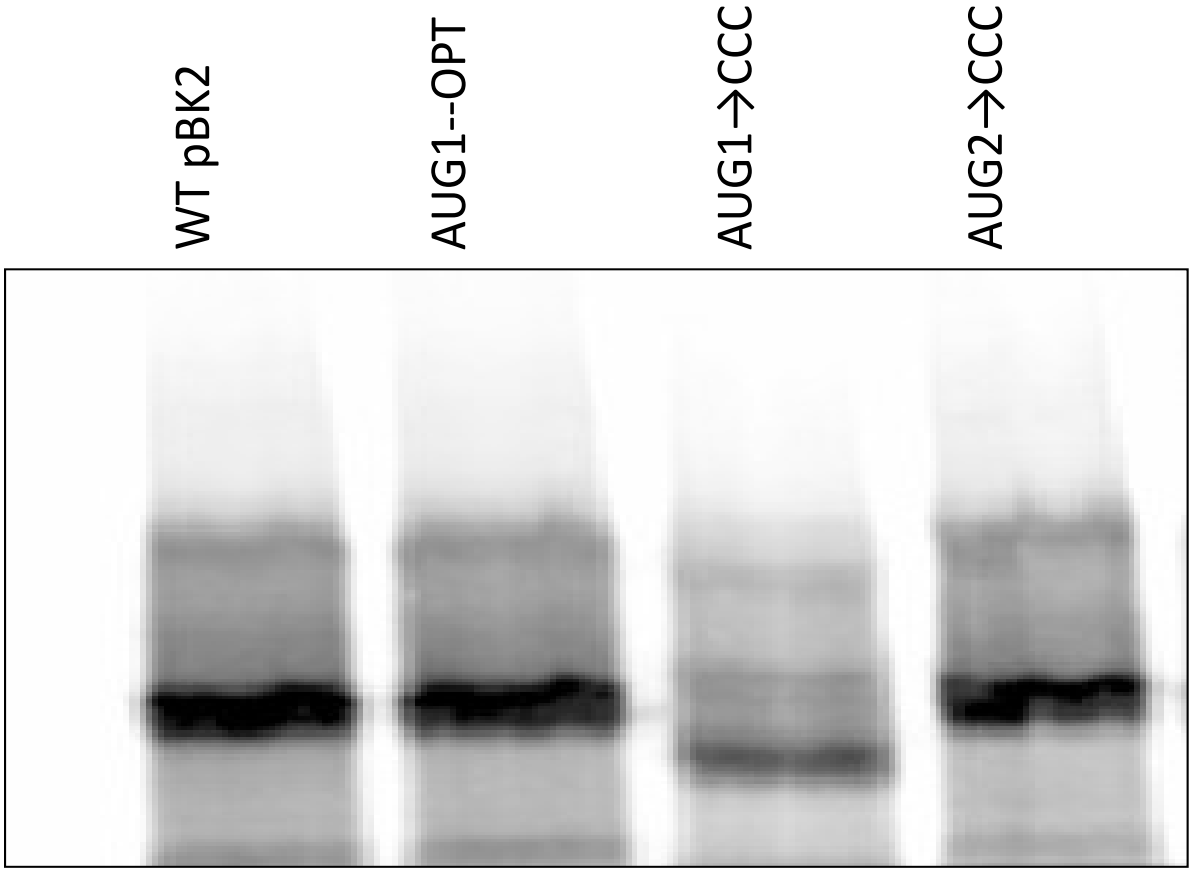

Figure 41.Protein Synthesis of pBK2 Mutants

Wild type pBK2, AUG1-OPT, AUG1→CCC, or AUG2→CCC mRNA were added to an *in vitro* translation reaction and protein was synthesized with S-35 labeled methionine. Samples were run on an SDS-PAGE gel, fixed, and visualized through autoradiography.

Vhs Cleavage of pBK2 RNA that Lacks a 5′ Cap

Previous studies showed that hindering initiation factor recruitment to the 5′ end (by circularizing RNA or the use of AMP-PNP or cap analog) inhibited Vhs cleavage. The next question to answer was if a 5′ cap was required for Vhs degradation of mRNA. Knowing the importance of initiation factor involvement in Vhs cleavage, it was predicted that a 5′ cap would also be vital for tying Vhs to the 5′ end. This is because the eIF4F complex binds the 5′ cap (specifically through eIF4E) during translation initiation and Vhs has previously been shown to associate with the eIF4F cap complex and eIF4A (7, 59).

To test this question, 5′ cap-labeled and 5′ end-labeled pBK2 mRNA were compared in a Vhs assay experiment (Fig. 42). pBK2 RNA was synthesized and either labeled in an m7G capping reaction or taken through a dephosphorylation reaction and labeled with a single monophosphate at the 5′ end. pBK2 RNA was then added to rabbit reticulocyte lysate containing or lacking Vhs protein and incubated for various times followed by extraction. Samples were then run on a 7% polyacrylamide 8M urea 1X TBE gel and visualized by autoradiography (Fig. 42). The results clearly indicated that Vhs is not able to cut pBK2 mRNA at specific sites near the 5′ end when the RNA lacks a cap (Fig. 42 compare A and B Vhs 15′). To make sure that the lack of specific cutting wasn't due to unequal amounts of labeled pBK2, 5′ end-labeled RNA was tested in an additional Vhs assay with comparable levels of radiolabeled mRNA (Fig. 42C).

HSV-2 Vhs Degradation of pBK2 mRNA

An *in vitro* Vhs assay had never been performed using Vhs from HSV-2. Within infected cells, HSV-2 Vhs is much more potent than HSV-1 Vhs. In cotransfection assays, cells need to be transfected with 40-fold less HSV-2 Vhs than HSV-1 Vhs to yield the same effect on gene

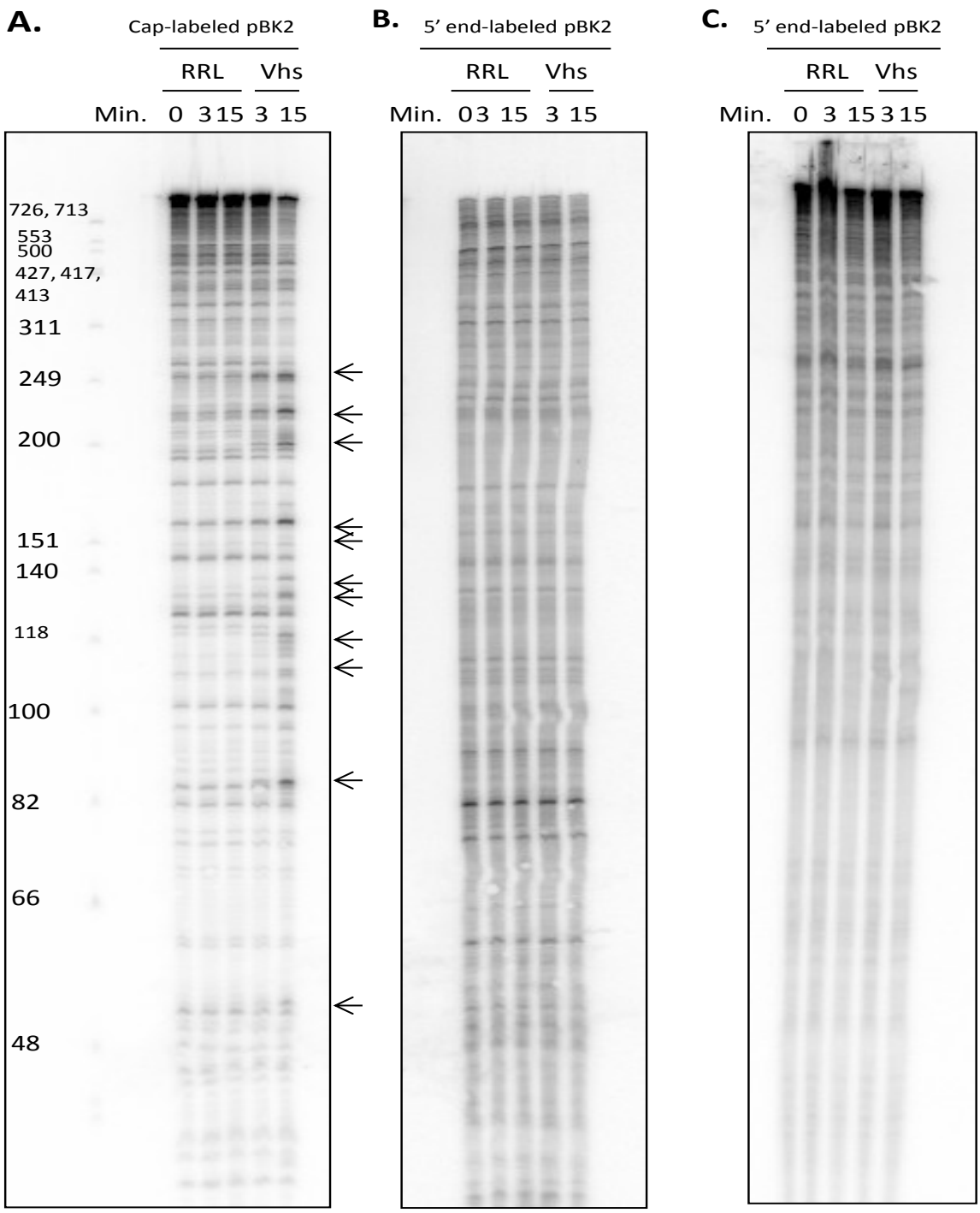

Figure 42.Vhs Degradation of Cap-labeled vs. 5' End-labeled pBK2 RNA

Vhs assay with cap-labeled (A) or 5' end-labeled (B and C) pBK2 mRNA. A and B are from the same experiment. RNA from gel C was used as a comparison for RNA loading samples comparable to A. Black arrows mark the cut sites produced by Vhs. RRL=rabbit reticulocyte lysate without Vhs. Vhs=rabbit reticulocyte lysate containing Vhs. Min=minutes RNA incubated with rabbit reticulocyte lysate prior to removal. M=ΦX174 *Hinf1* markers.

expression (31, 32). The Vhs protein of HSV-1 strain KOS and HSV-2 strain 333 show 87% sequence homology (31). To test whether the difference in mRNA cleavage could be replicated *in vitro*, Vhs from HSV-1 KOS and HSV-2 333 were compared in a Vhs assay using cap-labeled pBK2 as the substrate mRNA (Fig. 43). Interestingly, the two proteins produced the same cleavage products and cut pBK2 with close to the same efficiency (Fig. 43 compare +Vhs HSV-1 and +Vhs HSV-2 at the 15′ time point). If anything, HSV-1 Vhs may have been stronger at cleaving mRNA since more cleavage products appear at the HSV-1 Vhs 3′ time point (Fig. 43). The results indicate that additional factors, which are not present in the RRL system, are required for HSV-2 Vhs to achieve increased nuclease activity. It remains uncertain whether these are viral or cellular factors.

Vhs Cleavage of mRNAs Containing an IRES

As mentioned previously, Vhs specifically cleaves EMCV mRNA just downstream of its IRES. Since Vhs-1 retains the ability to cleave downstream of the EMCV IRES, it has been suggested that the cleavage event could be due to association with eIF4A. This is because the T214I mutant lacks the ability to bind eIF4H, but still associates with eIF4A and eIF4B. It was desirable to test if Vhs could specifically target downstream of an IRES that does not use the canonical factors for translation initiation. This would provide information about what factors might be required for cleavage.

The cricket paralysis virus contains an internal ribosome entry site that directly recruits the small ribosomal subunit by mimicking a pseudo tRNA-like structure in its IRES. In doing so, it does not require the canonical translation initiation factors or Met-tRNA$_{Met^i}$ because the CCU triplet of the IRES pseudoknot occupies the P site of the 40S small ribosomal subunit. The large

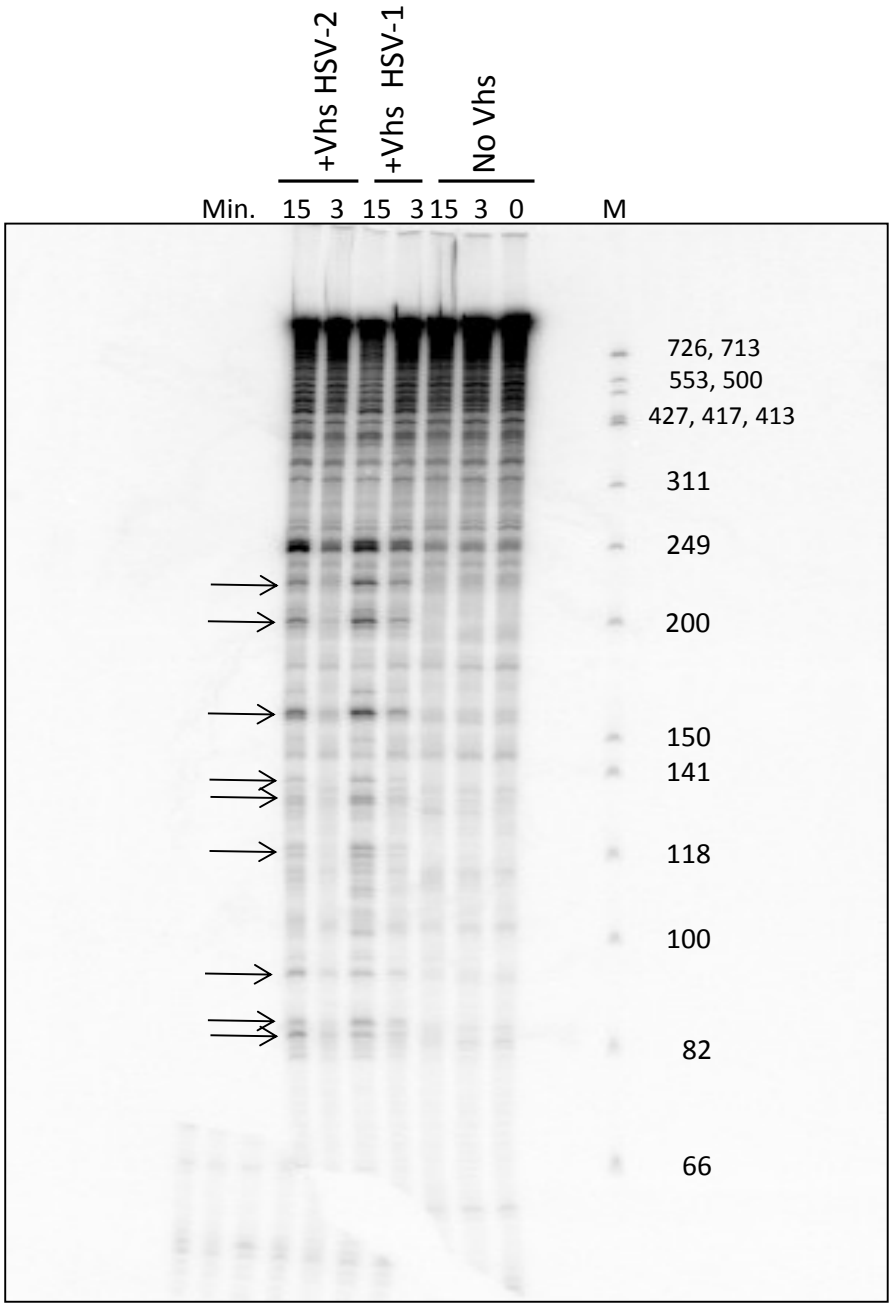

Figure 43.HSV-1 and HSV-2 Vhs Degradation of Cap-labeled pBK2 mRNA

Sequencing gel of cap-labeled pBK2 mRNA following a Vhs assay with HSV-1 and HSV-2 Vhs. The black arrows show the cut sites produced by Vhs cleavage. Min.=amount of time in minutes pBK2 mRNA incubated in rabbit reticulocyte lysate prior to removal. M=ΦX174 *Hinf1* markers.

ribosomal subunit is then directly recruited to form the 80S ribosome. Since substantial data indicate that Vhs association with translation initiation factors is vital for mRNA cleavage, it was hypothesized that Vhs would be less efficient at cleaving CrPV mRNA since that IRES does not use translation initiation factors for ribosomal recruitment during translation initiation.

For this study, EMCV and CrPV cap-labeled mRNA were tested in a Vhs assay followed by RNA extraction. The samples were then run on a 1.3% agarose 1X MOPS gel and visualized by autoradiography (Fig. 44). The effect of 2mM AMP-PNP was also tested in this experiment since ATP hydrolysis appears to be necessary for the eIF4A/eIF4G complex to induce conformational changes in the coding regions downstream of the IRES (33). These conformational changes make room for binding of the 40S ribosomal subunit during translation initiation of EMCV RNA (33). Vhs clearly cut downstream of the EMCV IRES and this site-specific cutting was reduced by the addition of AMP-PNP, a non hydrolyzable analog of ATP (Fig. 44A red arrow). However, this same type of site-specific cutting was not observed in CrPV mRNA, where no sharp cleavage product was produced (Fig. 44B). In order to better see the EMCV cleavage product inhibition in the presence of AMP-PNP, a lighter exposure was taken and is shown Figure 44C.

To analyze Vhs cleavage of CrPV and EMCV mRNA in further detail, the RNA samples were run on a 7% polyacrylamide 8M urea 1X TBE gel (Fig. 45 B and C). Vhs cleaved CrPV mRNA at nucleotides 36, 47, 102, 123, 129, 140, and 241 from the 5′ cap (Fig. 45B). The CrPV internal ribosome entry site is located between bases 1474-1662 of the transcript. Through analysis on a 1.3% agarose 1XMOPS gel and a sequencing gel, Vhs was not found to cleave CrPV near its IRES (Fig. 44B and 45B). Additionally, Vhs was able to produce the same cuts sites that were identified in the CrPV transcript in an mRNA construct (referred to as C53) that had

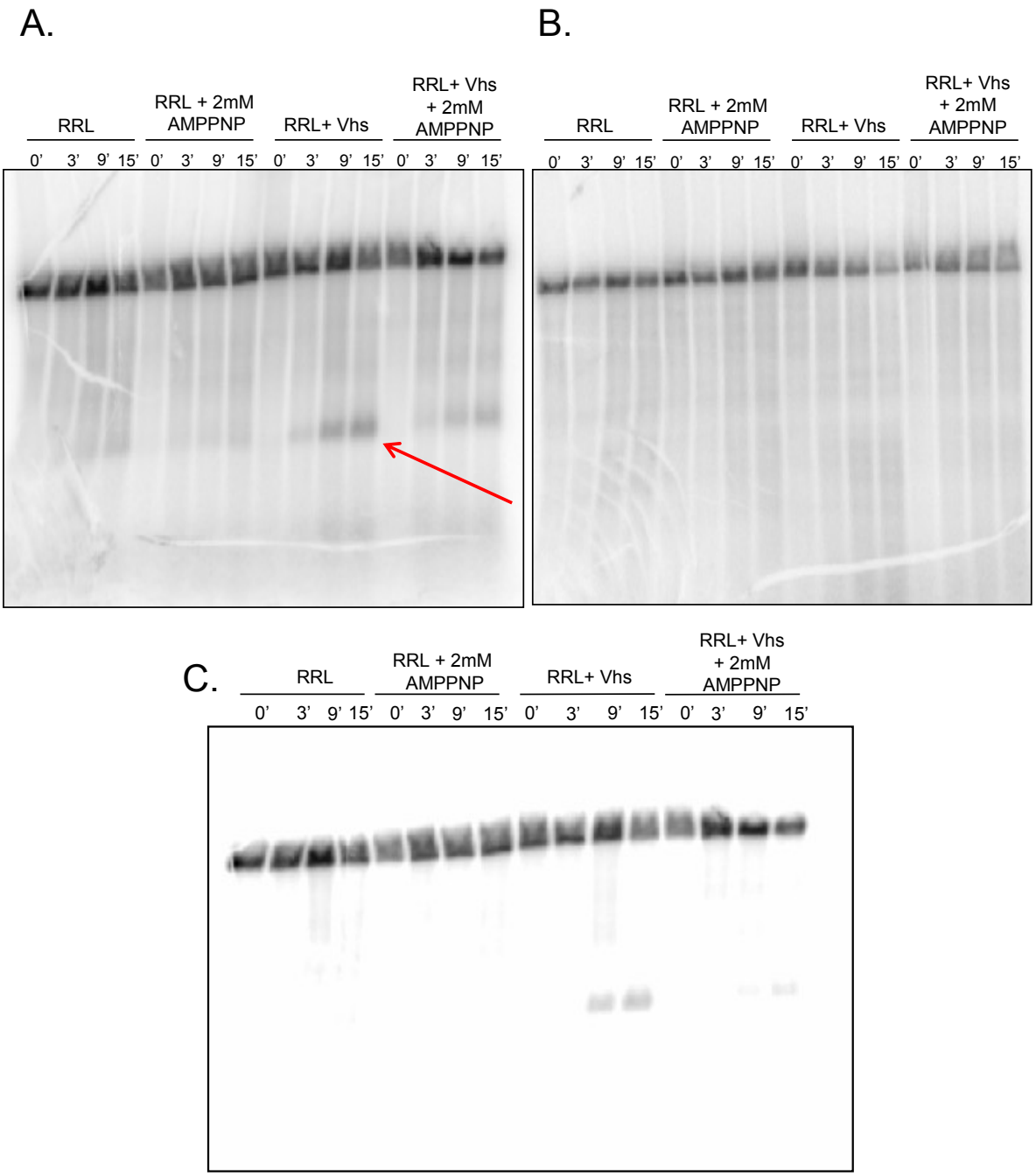

Figure 44.Vhs Site Specific Targeting of EMCV mRNA but not CrPV mRNA

Cap-labeled EMCV mRNA(A) and CrPV mRNA (B) following Vhs assay. Lighter exposure of A (C). Red arrow indicates specific cleavage product just downstream of the EMCV IRES. RRL=rabbit reticulocyte lysate that lacks Vhs. Vhs=rabbit reticulocyte lysate which contains Vhs.

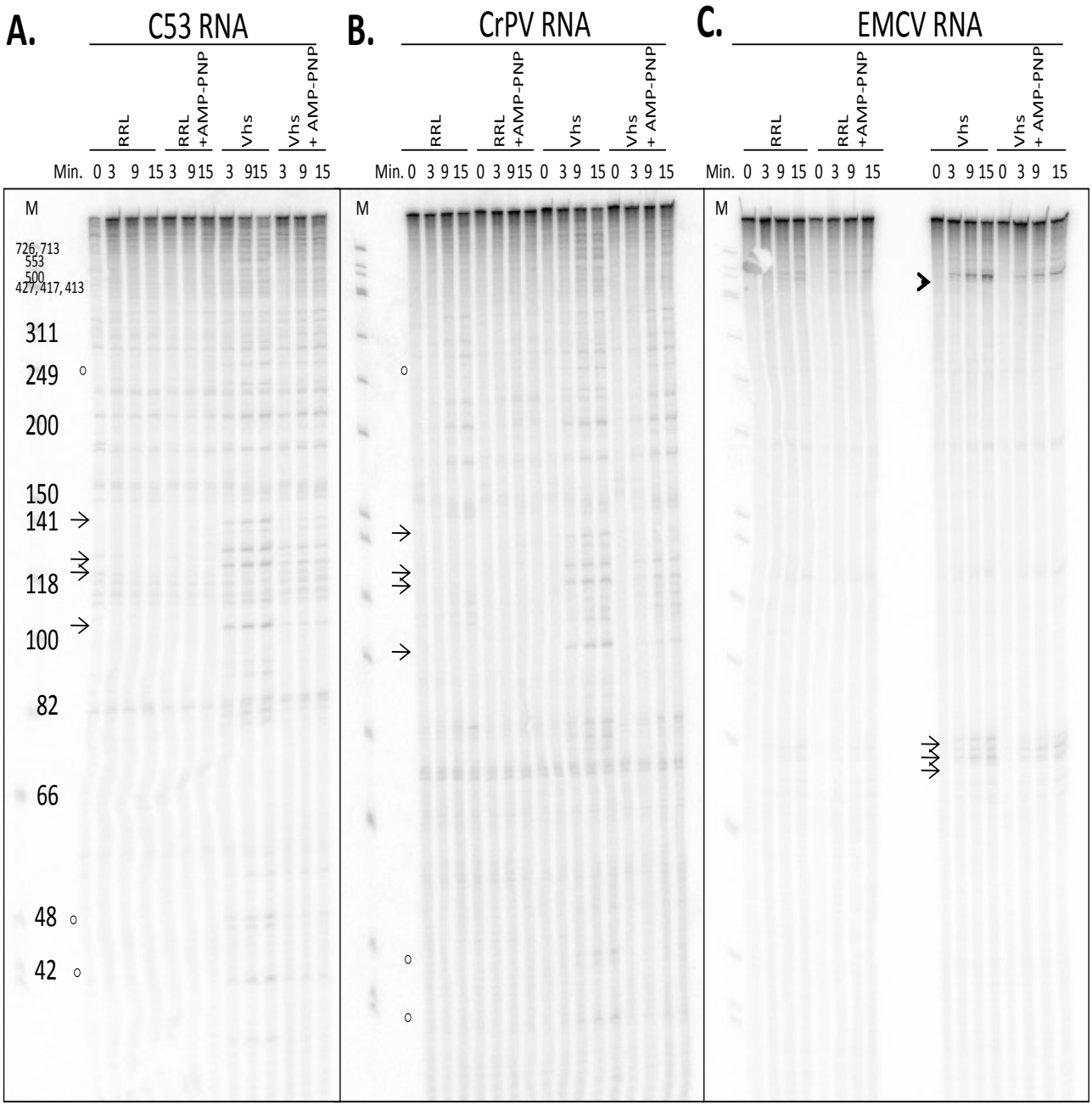

Figure 45.Site-specific Cleavage of CrPV and EMCV IRES-containing mRNA

Sequencing gels of cap-labeled CrPV (B) or EMCV (C) mRNA following a Vhs assay. The RNA tested in gel A (C53) contains sequence that is identical to the CrPV transcript, except that it lacks the CrPV internal ribosome entry site. RRL=rabbit reticulocyte lysate without Vhs. Vhs=rabbit reticulocyte lysate that contains Vhs. Arrowhead=very prominent cut site. Arrows=prominent cut site. Hollow circles=less prominent cut site.

identical sequence to the CrPV transcript with the exception that it lacked the CrPV IRES (Fig. 45A). Therefore, the addition of a CrPV IRES did not direct novel cutting (Fig. 45 compare A and B). Vhs cleaved EMCV RNA near base 550 from the 5′ cap, and it also produced less prominent cut sites near bases 78, 82, and 84 (Fig. 45C). The summary of the results from the sequencing gel further confirm that Vhs cut downstream of the EMCV IRES but not CrPV IRES (Fig. 45).

The Effect of Secondary Structure on Vhs Cleavage

Another way to test the role of cap-dependent scanning in Vhs cleavage is to test how Vhs cleaves mRNA that contains a stable hairpin near the 5′ end. *in vitro* studies have shown that hairpins with a thermal stability of -30kcal/mol that are located within the first 12 bases of the RNA cap have an inhibitory effect on translation initiation, most likely caused by blocking the cap-dependent scanning process (34). It was predicted that inhibiting the scanning process would also reduce Vhs site-specific cleavage of mRNA if Vhs association with the scanning complex is vital for cleavage.

Vhs Cleavage of pBK2 mRNA with a Hairpin One Base Downstream of the 5′ Cap

For the following study, the first 59 bases of the pBK2 transcript were replaced with a sequence containing a hairpin beginning one nucleotide downstream from the cap and extending through base 35 followed by a stretch of 8 CAA repeats (Fig. 46A). As a control, the first 59 bases of pBK2 were replaced with a stretch of 19 CAA repeats (Fig. 46B). The CAA sequence was chosen because it is predicted to have no secondary structure (35). The hairpin sequence used for this study was previously reported to have a thermal stability of -30 kcal/mol and inhibit protein synthesis in live cells when located within the first 4 bases downstream of the

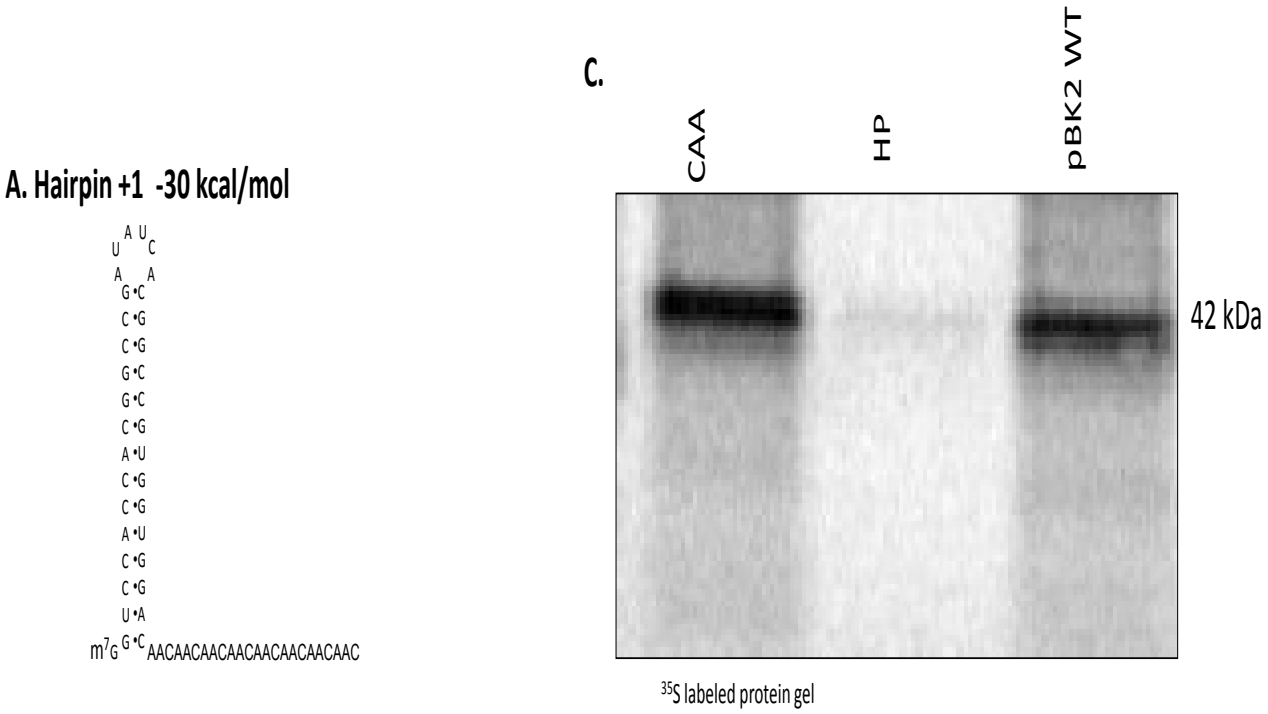

Figure 46.Diagram of Sequences Inserted into pBK2 and Protein Gel Analysis of Constructs

Model of the first 59 nucleotides of the pBK2 sequence which was replaced with sequence that encoded a -30kcal/mol hairpin 1 base downstream from the 5' cap in the first 35 bases of the transcript followed by a CAA stretch of 8 CAA repeats (A). Model of the first 59 nucleotides of the pBK2 sequence which was replaced with a stretch of 19 CAA repeats (B). S-35 methionine-labeled protein SDS-PAGE gel (C). The type of mRNA added to the *in vitro* translation system is listed above. Sample CAA contains RNA with a complete CAA stretch throughout the first 59 bases, sample HP+1 contains RNA that contains a hairpin 1 base downstream from the 5' cap in the first 35 bases of the pBK2 sequence, and sample pBK2 WT contains wild type pBK2 RNA which was not mutated.

5′ cap (35). The RNA constructs were synthesized by *in vitro* transcription in a large scale reaction and purified through gel extraction. During the RNA synthesis the transcripts received a 5′ cap. They were then tested in an *in vitro* translation reaction using S-35 labeled methionine (Fig. 46C). Insertion of a hairpin beginning one nucleotide downstream from 5′ cap inhibited protein synthesis while insertion of a CAA stretch did not have an effect on translation (Fig. 46C).

The RNAs were further tested in a Vhs assay. For this experiment the RNA was synthesized in a large scale reaction without a cap, labeled with [α-^{32}P]GTP in an m^{7}G capping reaction, and purified through gel extraction. The RNA was then added to rabbit reticulocyte lysates that contained or lacked Vhs, and samples were removed at various time points. RNA was then extracted and run on a 7% polyacrylamide 8M urea 1X TBE gel and visualized by autoradiography (Fig. 47B). Interestingly, the presence of a hairpin beginning one nucleotide from the 5′ cap greatly reduced Vhs site-specific cutting at regions further downstream (Fig. 47 compare A. pBK2 mRNA Vhs and B. HP +1 Vhs at 3 and 15 min.). However, Vhs still cleaved the mRNA and produced two prominent cut sites in the CAA region just downstream from the hairpin (Figure 47B). When analyzing Vhs cleavage of pBK2 mRNA with a stretch of 19 CAA repeats, it was found that Vhs cutting was selective for the first 65 bases from the 5′ end (Fig. 47B CAA_{19} Vhs 3 and 15 min.). Most of the cutting yielded a ladder of evenly spaced bands separated by approximately 3 nucleotides (Fig. 47B). It appears that Vhs cleaved the stretch of 19 CAA repeats after every C of the CAA sequence (Fig. 47B). This is consistent with previous reports that Vhs cleaves mRNA after C's and U's (10). These data suggest that Vhs prefers cleaving mRNA at regions of the transcript that have a low amount of secondary structure.

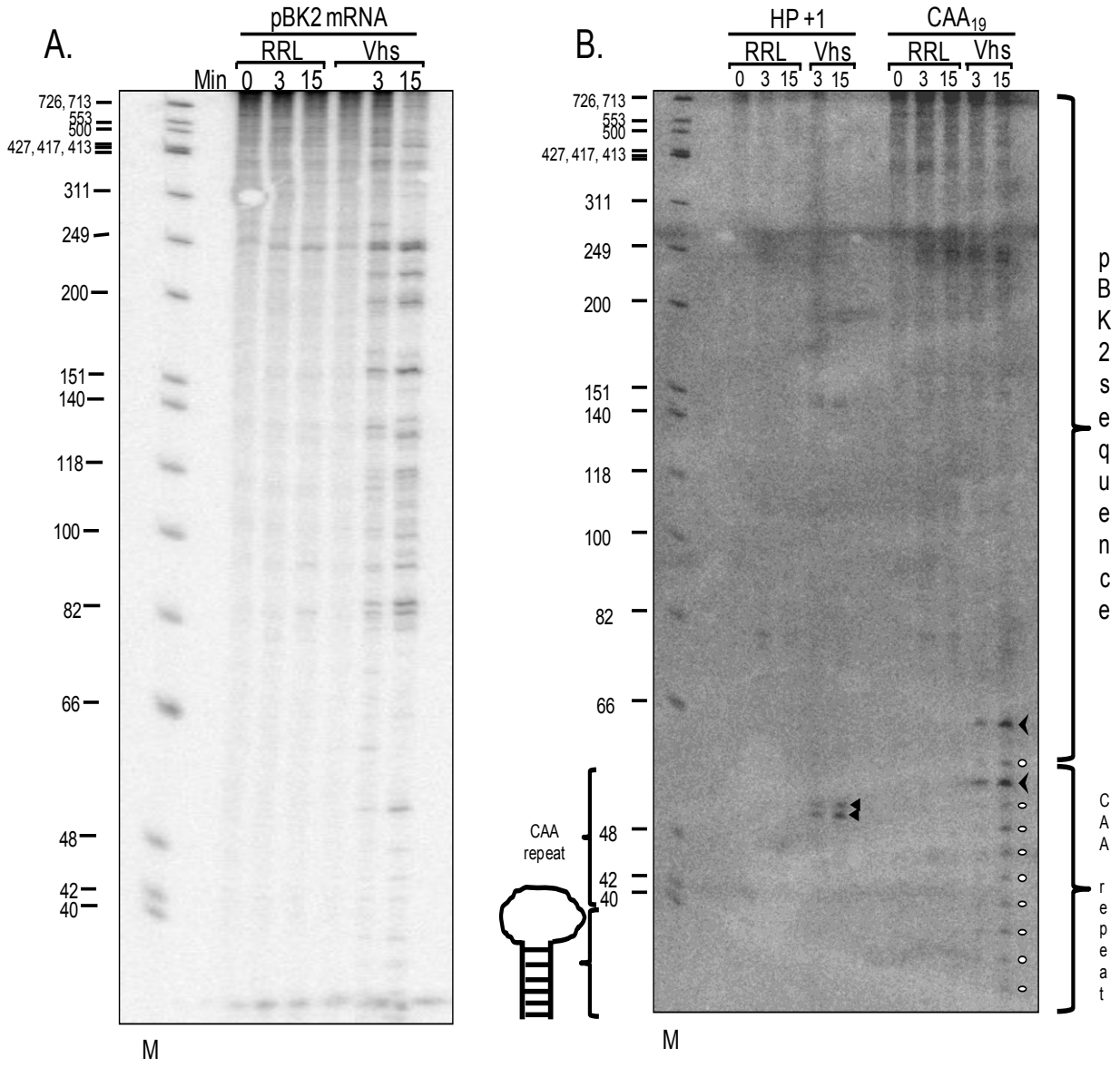

Figure 47.Vhs Cleavage of pBK2 mRNA with a Hairpin One Nucleotide Downstream from the 5' Cap or an mRNA with a CAA Stretch

Sequencing gels of cap-labeled WT (A) +1 HP (B) and CAA stretch (B) mRNA following a Vhs assay. The gel pictured in A is from Figure 17 and was placed in this figure as a comparison to show how Vhs cuts wild type pBK2 mRNA. The gel on the right shows Vhs cutting of pBK2 mRNA with replacements in the first 59 bases of the transcript. The RNA labeled HP+1 contains a hairpin structure positioned one base from the 5' cap that is 34 bases long followed by a 25 base stretch of CAA sequence. The RNA in labeled CAA_{19} contains a CAA stretch of 19 repeats in the first 59 bases of the transcript. Arrowheads mark the prominent cut sites produced by Vhs and white filled in circles indicate the less prominent cut sites. The diagrams to the left and right of the gel in B depict the location of the hairpin, CAA stretch, and pBK2 sequence. RRL=rabbit reticulocyte lysate that lacks Vhs. Vhs=rabbit reticulocyte lysate that contains Vhs.

Vhs Cleavage of pBK2 mRNA with a Hairpin 7 Bases or 13 Bases Downstream of the 5′ Cap

To continue testing the effect of secondary structure on Vhs cleavage, pBK2 transcripts were constructed to contain a hairpin beginning +7 or +13 nucleotides downstream from the 5′ cap. Part of the pBK2 sequence was replaced with the same -30 kcal/mol hairpin sequence used for studying a hairpin positioned one nucleotide from the 5′ cap. Bases 8-41 or 14-47 of the wild type pBK2 sequence were replaced with the 34 base hairpin for construction of HP + 7 and HP +13, respectively. The only difference with this hairpin experiment was that the regions surrounding the hairpin were restored with pBK2 sequence and did not contain CAA repeats. The cap-labeled constructs were then studied in a Vhs assay and analyzed using a DNA sequencing gel (Fig. 48B).

Vhs was unable to produce many of the same specific cut sites (as it did in WT pBK2 mRNA) when the mRNA contained a hairpin beginning +7 or +13 bases from the 5′ cap (Fig. 48B). Vhs cleaved +7 HP mRNA at prominent sites near bases 58 and 252 and at less prominent sites at bases 42, 158, 200, and 222. The novel cut sites produced in a +7 HP transcript were at positions 42 and 58 (Fig. 48B). It is particularly interesting how shifting the hairpin location from one base downstream of the 5′ cap to 7 bases downstream restored Vhs cleavage at sites further downstream near nucleotides 158, 200, 222, and 252 (compare Fig. 47B with Fig. 48B). Vhs cleavage appeared to shift from an original preference near nucleotide 55 to a novel preference for a site a little further downstream at 58 (Fig. 48B) Notably, the faint targeting at position 42 is positioned one base downstream of the hairpin construct (Fig. 48B).

The presence of a hairpin 13 nucleotides downstream from the 5′ cap appeared to hinder Vhs cleavage of the first 60 nucleotides of pBK2 mRNA (Fig. 48B). Vhs produced prominent cut sites at bases 61 and 252 and less prominent cut sites at bases 85, 93, 160, 200, and 222 (Fig. 48B).

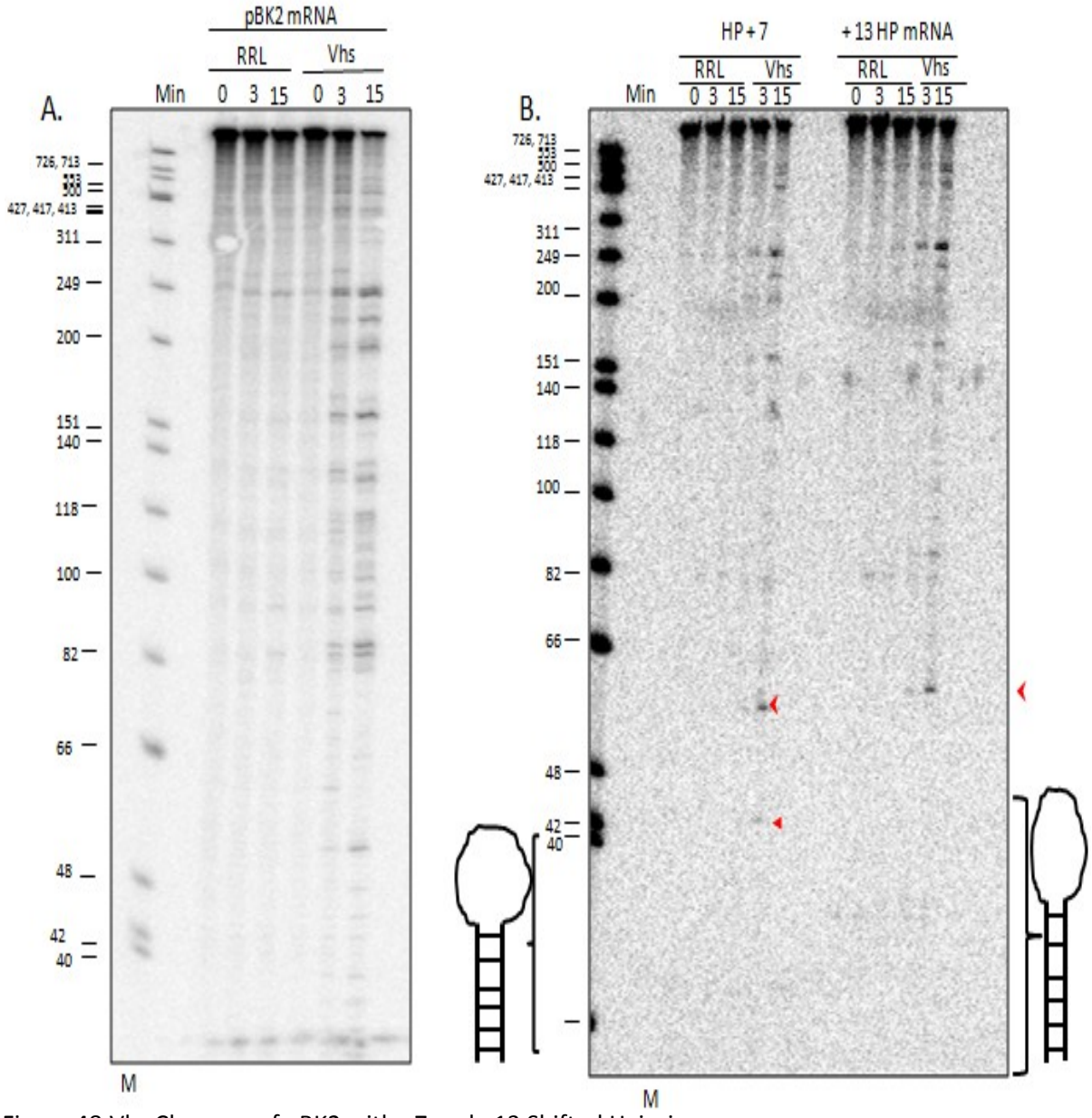

Figure 48.Vhs Cleavage of pBK2 with +7 and +13 Shifted Hairpins

Sequencing gels of cap-labeled WT (A), +7 HP (B), and +13 HP (B) mRNA following a Vhs assay. The gel pictured in A is from Figure 17 and was placed in this figure as a comparison to show how Vhs cuts wild type pBK2 mRNA. The gel in B shows Vhs cutting of pBK2 mRNA with hairpin shifts in the transcript. The RNA labeled by HP +7 is pBK2 mRNA that was replaced at bases 8-41 with a hairpin structure, which is positioned 7 bases downstream from the 5' cap and is 34 bases long. The RNA labeled HP + 13 contains pBK2 mRNA that was replaced at bases 14-47 with a hairpin structure that is positioned 13 bases downstream from the 5' cap. Red arrowheads mark the prominent cut sites produced by Vhs. The diagrams to the left and right of the gel in B depict the location of the hairpins in relation to the pBK2 sequence. RRL=rabbit reticulocyte lysate that lacks Vhs. Vhs=rabbit reticulocyte lysate that contains Vhs.

It is uncertain how the shift in hairpin location affects translation, because the +7 and +13 HP transcripts still need to be tested in an *in vitro* translation reaction. It is also unclear if the restoration of cutting to sites further downstream was due solely to a change in protein synthesis or due to the fact that the +7 and +13 HP constructs lacked a CAA repeat. The CAA unstructured sequence in the +1 HP construct could have been vital for targeting Vhs to regions near the cap leading to a decrease in preference for regions further downstream.

Vhs Cleavage of Cellular IRES-containing mRNAs

Many of the previous studies were designed to investigate the role of cap-dependent scanning in Vhs cleavage. In the next line of studies it was desirable to switch directions and ask if Vhs cleaved cellular mRNAs which use cap-independent methods for protein synthesis with equal efficiencies as cellular mRNAs that undergo cap-dependent scanning. Many mRNAs that are preferentially translated when translation efficiency is reduced, such as times of stress or during mitosis, have been found to contain internal ribosome entry sites (36, 37, 39). Several cellular mRNAs that contain IRESs encode proteins that are stimulated by stress, and some of these proteins are involved in serum response, inflammation, and angiogenesis (37, 38). Less information is available on cellular than viral IRESs and fewer generalizations can be made. Cellular IRESs do not require a high degree of secondary structure to be functional like viral IRES, and they can consist of short segments that are noncontiguous (39). It was unknown whether Vhs would be targeted to these RNAs with the same efficiency as mRNAs that undergo cap-dependent scanning since little is known about the requirements for translation of a cellular IRES.

To test this, HeLa cells were infected or mock infected with 20 PFU WT HSV-1 KOS in the presence of Actinomycin D. Cells were scraped at various time points followed by RNA extraction and real time PCR using probes specific for 4 cellular mRNAs that contain IRESs (Vimentin,Nap-1-like, Cyr61, and ODC) and one cellular mRNA that is translated by cap-dependent scanning (GAPDH). Figure 49 shows a column graph of relative mRNA levels after 5 hrs. mock infection or infection with wild type virus. The black bars represent mock infection levels normalized to a value of 1, and the blue bars show RNA levels in the presence of virus. Vhs degraded three for the IRES-containing mRNAs with equal efficiencies as it degraded GAPDH mRNA (Fig. 49 compare relative levels of GAPDH mRNA to other mRNAs). At the five hour time point, most RNAs that were infected were present in much lower abundance compared to RNAs that were infected with mock virus (Fig. 49). However, Cyr61 mRNA levels were 2 fold higher than mock levels at the 5 hour time point (Fig. 49).

The results were analyzed in a graph comparing mock and infected mRNA levels at 0 and 5 hour time points (Fig. 50). All mRNAs were degraded when infected with HSV-1. Cyr61 mRNA has a short half life in uninfected cells (Fig. 50). Cyr61 mRNA encodes the cysteine-rich angiogenic factor 61, an extracellular matrix-associating protein involved in stimulating cell migration, mediating cell adhesion, inducing angiogenesis, and regulating genes important for wound healing (40, 41, 42, 43, 44). Cyr61 gene expression is rapidly turned on and off in the cell, so it is, therefore, not surprising that Cyr61 mRNA has a short half-life in uninfected cells. However, it is surprising that Cyr61 mRNA is not as rapidly degraded in the presence of WT KOS (Fig. 50). It appears that HSV-1 infection stabilizes Cyr61 mRNA (Fig. 50).

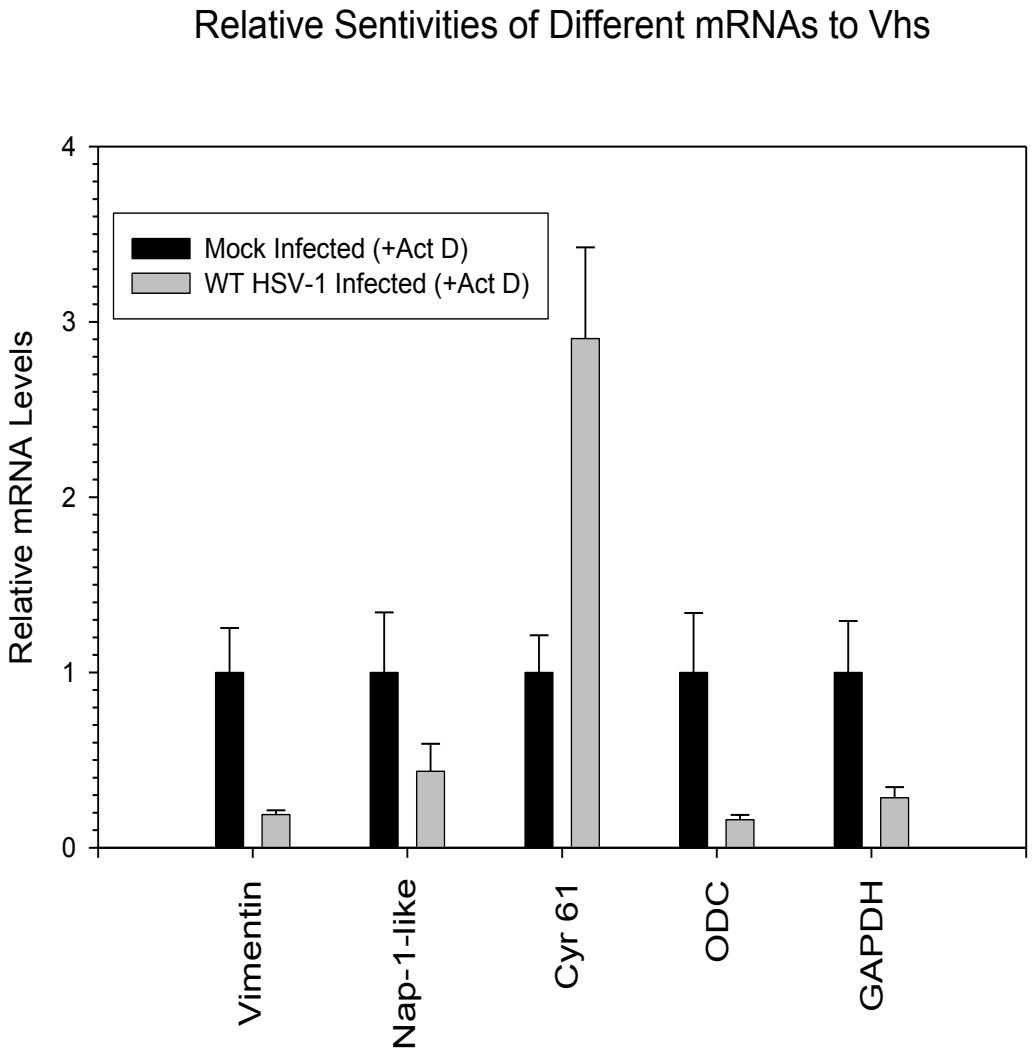

Figure 49.Vhs Cleavage of Cellular IRES-containing mRNAs

Column graph representation of relative mRNA levels after 5 hours infection or mock infection of HeLa cells with 20pfu WT KOS in the presence of Actinomycin D. Black bars represent relative mRNA levels after 5 hrs. mock infection. Light blue bars represent relative mRNA levels after 5 hrs. infection. Cyr61=cysteine-rich angiogenic factor. ODC=ornithine decarboxlyase. GAPDH=glyceraldehyde-3-phosphate dehydrogenase

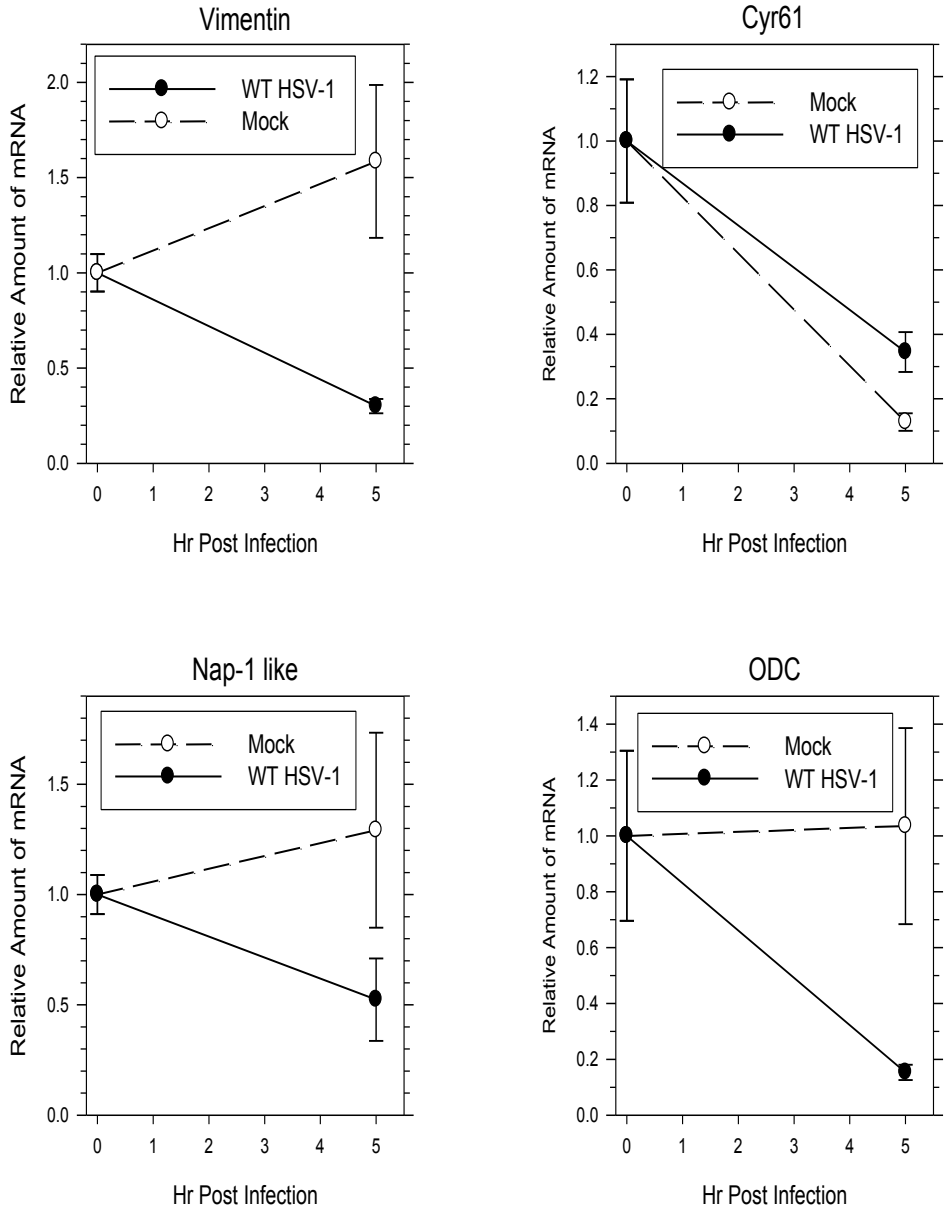

Figure 50.Relative Amount of mRNA Following Mock and HSV-1 Infection After 5 Hours

Graph representation of the relative amount of mRNA following infection or mock infection with WT KOS determined by Real Time PCR analysis. Dashed lines represent mRNA levels following mock infection and solid lines represent RNA levels following WT infection. The type of mRNA examined is listed above each graph.

The Effect of Vhs on Reporter Gene Expression

Vero Cell Experiment

Since the cellular factors required for translation from various cellular IRESs are unknown, it was desirable to test viral IRESs in an *in vivo* system. For this study, three bicistronic constructs were tested that contained renilla luciferase as the upstream codon and firefly luciferase as the downstream codon (Fig. 51A). The control construct, C53, did not contain an internal ribosome entry site between the two cistrons. The other two constructs contained either an EMCV IRES or a CrPV IRES in the intercistronic region (Fig. 51A). Measuring the ratio of the upstream cistron renilla luciferase (RLUC) to the downstream cistron firefly luciferase (FLUC) is a standard way of analyzing IRES activity. Vero cells were transfected with one of the three plasmids and the increase of translation of the downstream cistron in the presence of an IRES was confirmed (Fig. 51B). Studies were then performed transfecting Vero cells with one of the target plasmids plus either pKOSamp which encodes HSV-1 KOS Vhs, p333amp which encodes HSV-2 333 Vhs, or control plasmid that did not encode Vhs. Cells were harvested after 48 hours followed by analysis of protein expression using a Promega 20/20 GloMAX luminometer (Fig. 52). Control levels of renilla and firefly luciferase were normalized to a value of 1.

HSV-2 Vhs shut off RLUC and FLUC protein synthesis much more rapidly than HSV-1 Vhs (Fig. 52). Interestingly, HSV-2 Vhs turned down expression of C53 renilla luciferase more efficiently than the downstream cistron firefly luciferase, with an FLUC/RLUC ratio of 5.6 (Fig. 52). However, HSV-2 Vhs had on opposite effect on the protein expression of CrPV and EMCV protein, whose mRNA contained an IRES, where their FLUC/RLUC ratios were 0.61 and 0.46, respectively (Fig. 52). In the presence of HSV-1 Vhs, the CrPV and EMCV upstream cistrons

A.

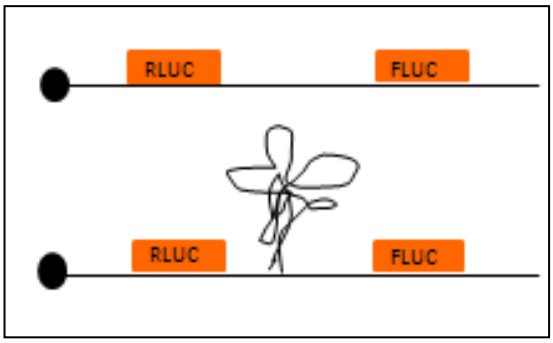

B.

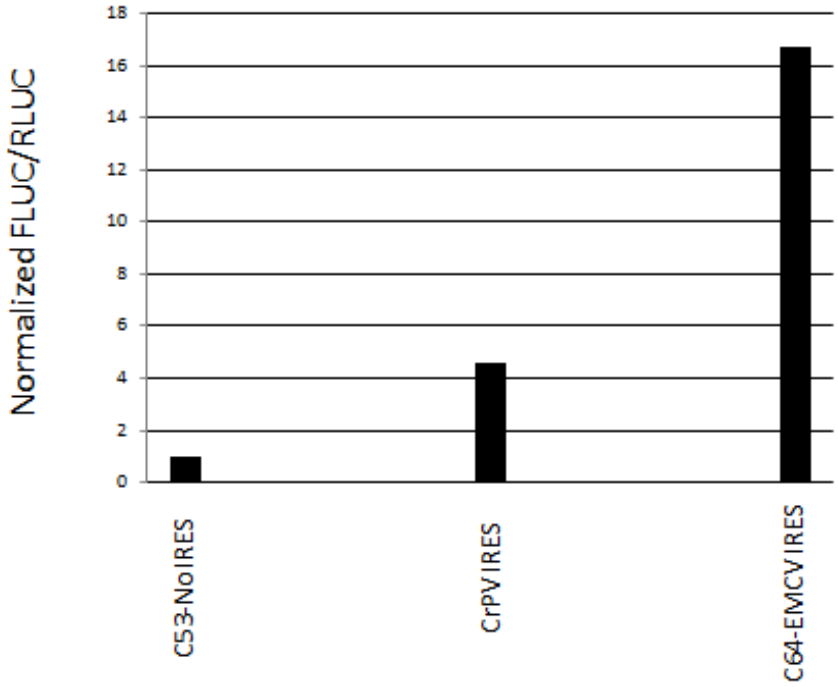

Figure 51.Insertion of an IRES Between Two Cistrons Increases Translation of the Downstream Cistron

Diagram of mRNA from a bicistronic construct that lacks (top) or contains (bottom) an IRES in between the two cistrons (A). The mRNA is pictured with a 5' cap and an upstream cistron containing renilla luciferase (RLUC) and a downstream cistron containing firefly luciferase (FLUC) (A). Graph results showing the increase of translation of the second cistron when an IRES is inserted into the intergenic region (B). C53=construct that did not contain an IRES. This was the control whose FLUC/RLUC ratio was normalized to 1. CrPV IRES=construct that contained the cricket paralysis virus IRES. C64-EMCV IRES=construct that contained the encephalomyocarditis virus IRES.

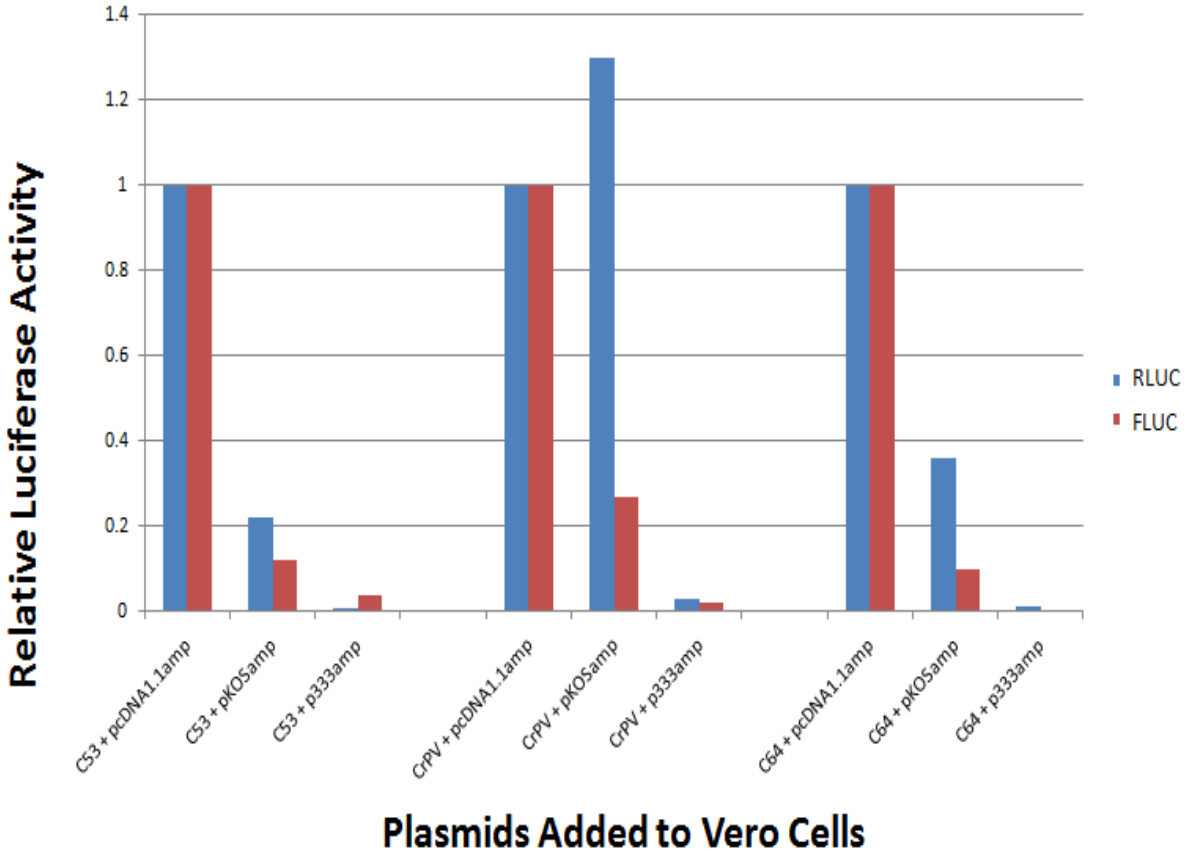

Figure 52.Protein Expression of Bicistronic Constructs in the Presence of HSV-1 or HSV-2 Vhs in Vero Cells

Vero cells were transfected with the plasmid combinations listed on the x-axis. Cells were harvested after 48 hours and protein levels were measured using a Promega 20/20 GloMAX luminometer. The control (pcDNA1.1amp) expression levels of renilla and firefly luciferase were normalized to 1. For the control samples, cells were transfected with DNA that did not encode Vhs. Protein levels in the presence of HSV-1 (pKOSamp) or HSV-2 (p333amp) Vhs were compared to control values using Excel. RLUC=renilla luciferase, the upstream codon. FLUC=firefly luciferase, the downstream codon.

were always expressed much higher than the downstream cistrons with RLUC/FLUC ratios of 4.81 and 3.60, respectively (Fig. 52). On the other hand, in the presence of HSV-1 Vhs, the C53 RLUC/FLUC ratio was 1.83 (Fig. 52). Notably, HSV-1 Vhs did not decrease expression of the CrPV upstream cistron, where the renilla luciferase level was 1.3 compared to the control (Fig. 52). Even though HSV-1 Vhs did not reduce expression of CrPV renilla luciferase, it still reduced expression of the downstream cistron to 27% (Fig. 52). HSV-1 Vhs had an effect of lowering the EMCV upstream and downstream cistrons to 36% and 10% (Fig. 52).

HeLa Cells

Previous studies by the Smiley lab, which analyzed Vhs at later times post infection, showed that Vhs's effect on translation varied between HeLa and Vero cell lines (254). To investigate whether this difference could be observed in shutoff of the bicistronic constructs, HeLa cells were additionally studied. Results showed that HSV-1 Vhs was not able to decrease expression of the C53 and CrPV cistrons (Fig. 53). The C53 renilla and firefly protein expression was 128% and 96% in the presence of HSV-1 Vhs, respectively (Fig. 53). In the presence of HSV-1 Vhs, the CrPV renilla and firefly protein expression was increased to 236% and 152%, respectively.

Conversely, for mRNAs containing the EMCV IRES (C64), HSV-1 Vhs caused a slight reduction in the levels of renilla and firefly luciferase protein expression, where their values were 73% and 76%, respectively (Fig. 53). HSV-2 Vhs was also not as efficient at protein shutoff of the bicistronic constructs in HeLa cell as it was in Vero cells (compare Fig. 52 with Fig. 53). HSV-2 Vhs was able to shut off expression of the upstream cistron much more efficiently than the downstream (Fig. 53). Specifically, it reduced C53, CrPV, and EMCV renilla luciferase to a

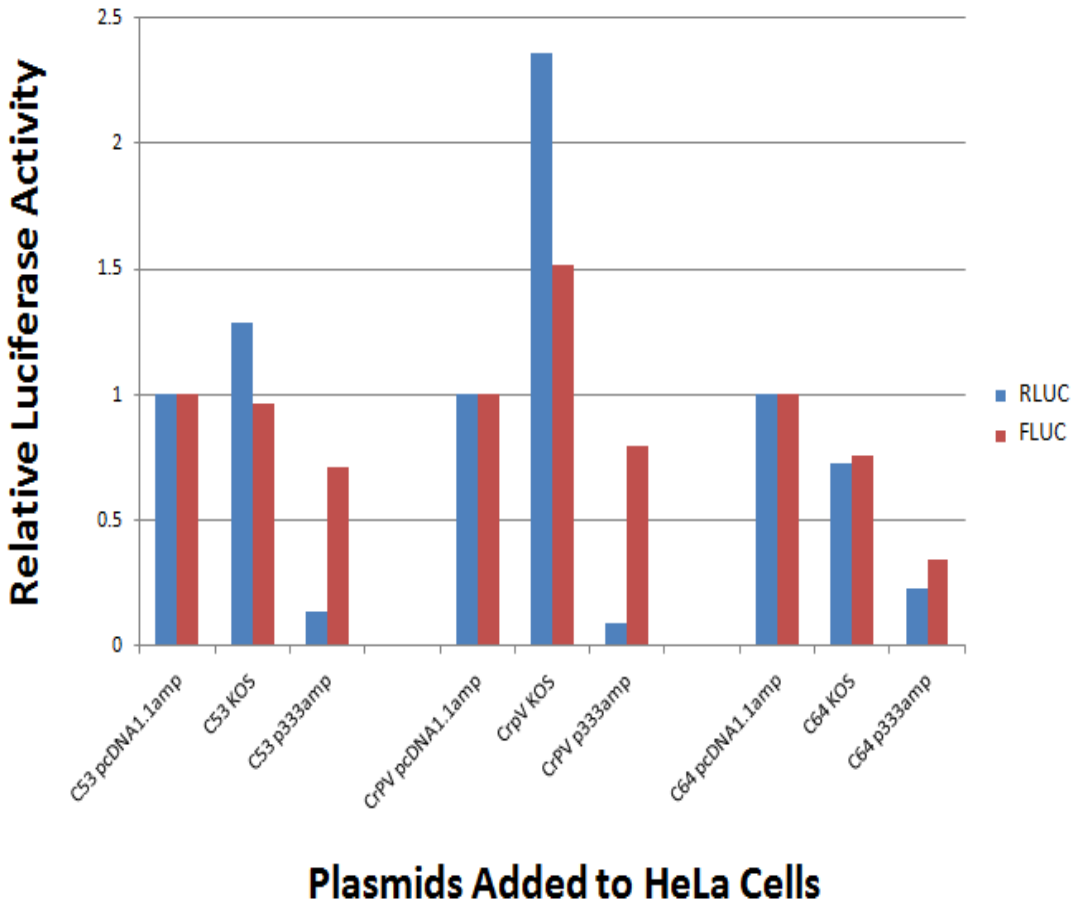

Figure 53.Protein Expression of Bicistronic Constructs in the Presence of HSV-1 or HSV-2 Vhs in HeLa Cells

HeLa cells were transfected with the plasmid combinations listed on the x-axis. Cells were harvested after 48 hours and protein levels were measured using a Promega 20/20 GloMAX luminometer. The control (pcDNA1.1amp) expression levels of renilla and firefly luciferase were normalized to 1. For the control samples, cells were transfected with DNA that did not encode Vhs. Protein levels in the presence of HSV-1 (pKOSamp) or HSV-2 (p333amp) Vhs were compared to control values using Excel. RLUC=renilla luciferase, the upstream codon. FLUC=firefly luciferase, the downstream codon.

final percentage of 13.90%, 9.40%, and 22.90%, respectively (Fig. 53). HSV-2 Vhs was not as potent at decreasing expression of the downstream cistron, where C53, CrPV, and EMCV levels were 71.40%, 79.50%, and 65.80%, respectively (Fig. 53). HSV-1 Vhs did not show a large difference in the expression levels of renilla and firefly luciferase. However, addition of HSV-2 Vhs led to larger variances between the upstream and downstream codons. The expression of the downstream cistron was much higher than the upstream for C53 and CrPV, resulting in FLUC/RLUC ratios of 5.10 and 8.50, respectively (Fig. 53). Current studies are directed at optimizing RNA analysis conditions to understand how the mRNA of these proteins gets cleaved by Vhs in both HeLa and Vero lines, in an effort to correlate RNA degradation with protein expression.

CHAPTER 4

DISCUSSION

Prior to this dissertation, the role of early events in translation initiation in Vhs mRNA cleavage had not been analyzed. Previous studies performed in cell culture had only tested the effect of blocking later stages in translation initiation by using cycloheximide to inhibit protein synthesis (14). Many mRNAs have previously been studied in the rabbit reticulocyte system, but they were primarily used to examine Vhs site-specific cleavage sites in an attempt to determine whether Vhs preferred cleaving after a particular nucleotide or if it recognized a sequence of bases. This dissertation addresses the following questions: (1) How does Vhs cleavage of pBK2 mRNA compare with its degradation of other mRNAs? (2) How is Vhs cleavage of mRNA affected by inhibitors of translation, mutations in and around the AUG start codon, and insertion of stable hairpins in the 5′ UTR? and (3) How do the data lead to a model of Vhs action?

Significance of Vhs Degradation of pBK2 mRNA

Studies in the RRL system found that Vhs cleaved pBK2 mRNA at 6 prominent sites, all within the first 300 bases from the 5′ cap (Fig. 18). Several of these sites were near or just upstream from the first three AUGs from the cap. Most of the cut sites were identified by both 5′ cap-labeling and primer extension analysis, further supporting the conclusion that Vhs is an endonuclease (Fig. 18 and Fig. 21). Thymidine kinase mRNA had not been tested previously in an *in vitro* RRL system, but its degradation had been studied by Northern blot analysis in HSV-1 infected Vero cells. (8). Results from these studies indicated that the 5′ end was cleaved more rapidly than the 3′ end, suggesting Vhs preferentially targets the 5′ cap (8). Vhs has been shown to degrade SRPα (the signal recognition particle receptor alpha) mRNA *in vitro* at specific sites

within the 5′ quadrant of the RNA from bases 200-700 (5). Additional studies by Smiley showed that secondary cleavage of the 3′ cleavage product that results from Vhs cutting of an mRNA with an EMCV IRES proceeds in a 5′ to 3′ direction (48). The endoribonucleolytic activity was concluded to be sequence nonspecific with a slight preference for cleaving between purines (5). The results from this dissertation and the previously mentioned experiments support a model where Vhs is targeted to the 5′ end of viral and many constitutively expressed cellular mRNAs.

However, Vhs has been reported to not cleave all mRNAs at the 5′ end (4). According to Zelus et al., Vhs cleaves globin γ mRNA at regions near the 3′ UTR, and in these studies Vhs appeared to cleave preferentially at AC and CU dinucleotides (4). It has been suggested that Vhs cleavage near regions at the 5′ cap is dependent on the type of mRNA studied (45-47). Where it was previously believed that all mRNAs had similar sensitivity to Vhs cleavage, more recent reports have suggested that Vhs degrades certain mRNAs with different efficiencies (9, 14, 45-47, 49, 50, 52-54). Roizman has shown that certain mRNAs, such as IEX-1, cox-2, IkB, and c-Fos, which contain AU-rich elements (AREs) and have very short half lives appear to be regulated differently upon infection (45-47). During infection these mRNAs are deadenylated and then cleaved just upstream of the AREs, leaving a stable 5′ product that remains in the cell for an extended time prior to degradation (45-47). Since the ARE is located in the 3′ UTR, these data support a model where Vhs is targeted to the 3′ end of the transcript. Vhs has been suggested to target the 3′ UTR of mRNAs containing AREs by binding the protein tristetraprolin (45, 50). This has been built around the findings that TPP protein levels are increased after infection with HSV-1 and TPP has been found to associate with Vhs in coimmunoprecipitation assays (45, 50). Tristetraprolin is a protein that has an important role in the degradation of some AU-rich mRNAs by facilitating their recruitment to the exosome (51, 56, 57).

At present, whether or not Vhs cleaves cellular stress-inducible IEX-1 mRNA at its 3′ UTR is controversial. Initial studies on HSV-1 regulation of ARE mRNAs suggested that these mRNAs were spared from cutting due to ICP27 binding at the ARE (58). Additional studies have implicated that the increase in intermediate IEX-1 mRNA products is not due to Vhs cleavage but is instead due to HSV-1 infection having an inhibitory effect on the normal turnover of ARE mRNAs (5).

pBK2 mRNA is most likely cleaved at regions near the 5′ end because it has two defining characteristics. (1) It is an mRNA that is translated by cap-dependent scanning and (2) It does not contain an AU-rich element or other sequence to direct Vhs to its 3′ UTR. Vhs has been shown to associate with translation initiation factors eIF4A, eIF4H, eIF4B, and the eIF4F cap binding complex (6, 7, 13, 27, 59). siRNA-mediated knockdown experiments have revealed that eIF4H and eIF4AI/II are both vital for Vhs degradation of housekeeping mRNAs, while eIF4B is not required (28, Agarwal et al. unpublished). Vhs association with these initiation factors may be what targets it to the 5′ cap of mRNA, which would provide a clear explanation for why Vhs is selective for degrading mRNA opposed to non-messenger RNA.

Analyzing cut site location can lead to predictions about how the scanning apparatus is composed. Currently, varying opinions exist about whether eIF4G, 4A, and 4H are located behind or in front of the 40 ribosomal subunit (reviewed in 73). Modeling by cryoelectron microscopy predicted that the factors were positioned behind the ribosome so that the ribosome would unwind mRNA secondary structure and the factors would serve to 'ratchet' mRNA through the binding channel using their helicase activity (74). However, an alternative model has proposed that eIF4G, 4A, and 4H are positioned in front of the 40S ribosomal subunit and are involved in unwinding mRNA secondary structure before it enters the mRNA binding

channel (75). Perfoming more detailed experiments on Vhs-induced cleavage of mRNA will aid in improving the current understanding of the orientation of the translation initiation scanning complex. This is because, if Vhs is found to remain associated with translation initiation factors during cutting, then implications can be made about where the factors are located in regards to other components that make up the scanning complex.

Prior to this dissertation, no previous associations had been made between Vhs cleavage sites and their proximity to AUG codons. It is uncertain if this mode of cutting is specific for pBK2 mRNA and whether additional factors were involved in Vhs cleavage near AUG codons such as a pBK2 mRNA secondary structure. If Vhs associates with cellular initiation factors and is recruited to the 5′ end, it may remain associated with components at the 5′ cap and travel with the scanning complex to reach its cut sites during translation initiation. In this model for Vhs cleavage, many factors could have a role in Vhs's probability of cleavage. It could be that Vhs has a higher probability of cleaving mRNA at regions of the transcript that are just upstream of mRNA with high degrees of secondary structure. Under this proposal, the scanning complex might pause for a longer period of time in order for eIF4A helicase unwinding of secondary structure. The increased time that the complex spends in that region may allow Vhs to have enhanced accessibility. Since the 5′ UTR of mRNA often contains a high amount of secondary structure, it may be more likely that Vhs cleavage will occur in these locations if it piggybacks on the scanning apparatus. The AUG start codon may be an additional factor involved in Vhs cleavage. Following this concept, if Vhs is scanning the mRNA transcript with the scanning complex, then pausing at the start codon may increase the likelihood of cutting.

Vhs cuts pBK2 mRNA at specific sites near the first three AUGs. This lab has previously shown that pBK2 mRNA undergoes leaky scanning during *in vitro* translation in a rabbit

reticulocyte lysate system (Karr et al., unpublished). If pBK2 mRNA experiences leaky scanning during *in vitro* translation in a RRL system, then it is possible that Vhs occasionally scans past the first or second AUG while associating with the scanning complex to locate some of its downstream cleavage sites. On the other hand, the mRNA secondary structure of pBK2 may bring sites that are further downstream in the primary sequence close to the 5′ cap. Alternatively, the cut sites near the second and third AUG could be produced by methods other than scanning in a currently undefined model. It is more likely that this is the case because pBK2 mutants with mutations in the second AUG did not affect Vhs cleavage of mRNA. It will be important to design future experiments directed at analyzing how Vhs cleaves a list of mRNAs that undergo cap-dependent scanning and to study whether the length of the 5′ UTR affects Vhs cleavage.

While analyzing the data from the experiments performed for this dissertation, a trend in Vhs cleavage after particular nucleotides was not noticed. It is important to point out that these studies were not performed with a sequencing marker, so exact cut site locations could not be determined. Instead, the cut sites identified are estimated to be within 5 bases of the stated position. Results did not indicate that Vhs preferably cut mRNA at a particular sequence. It is believed that Vhs cutting, at some cut sites, is influenced by factors that affect migration of the scanning complex along the mRNA transcript during translation initiation. In this regard, sequence is believed to still have a role in Vhs cleavage of mRNA because it determines mRNA secondary structure. The data from previous *in vitro* studies vary in regards to Vhs cut site preference. GST-purified Vhs was demonstrated to have substrate specificity similar to that of RNase A, where it preferred cleaving mRNA after C and U bases (10, 11). However, Zelus et al. have reported a preference for cleavage between AC and CU dinucleotides, and work by Smiley

has indicated that Vhs has a slight preference for cleaving between purines but an overall lax sequence specificity (4, 5).

Vhs Mechanism of Cleavage

Results obtained from mapping the cut sites of pBK2 mRNA led to studies directed at determining whether completion of certain stages of translation initiation is required for Vhs cleavage. Data from the first part of the dissertation suggest that Vhs cleavage may be tied to translation initiation since Vhs cleaves pBK2 mRNA at regions near the 5′ cap and some of these cut sites are near AUG codons. With previous knowledge that Vhs associates with translation initiation factors, it was believed that early events of translation initiation might be important for Vhs cleavage. The data indicated that protein synthesis was not required for Vhs cleavage of pBK2 mRNA in a RRL system, because mRNA degradation levels in the presence of cycloheximide were comparable to degradation levels in the absence of cycloheximide (Fig. 24 and 25). In studies using GMP-PNP to inhibit GTP hydrolysis, it was found that recruitment of the large ribosomal subunit was not vital for Vhs cleavage of mRNA, albeit blocking 60S ribosomal recruitment had a modest inhibition on Vhs RNase activity (Fig. 26 and 27). These findings were in accordance with previous reports in HeLa cells that revealed HSV-1-induced RNA cleavage activity separated with the postribosomal fraction (55). Moreover, the cycloheximide experiment supported previous studies by Frenkel which showed that inhibiting protein synthesis of HeLa cells infected with WT KOS did not hinder Vhs cleavage (14).

When AMP-PNP was added to reduce recruitment of translation initiation factors to the 5′ cap and hinder ATP hydrolysis, Vhs cleavage was inhibited (Fig. 28-29). AMP-PNP also inhibits scanning of the scanning complex to the start codon (23). When looking more closely at

mRNA cleavage, it was found that AMP-PNP inhibited cleavage of the first 150 bases from the 5′ cap (Fig. 29). This result was very interesting because it implied that the cut sites further downstream from the first 150 bases may have been achieved using an alternative pathway other than association with the scanning complex. However, the cutting may be due to the fact that AMP-PNP did not completely inhibit Vhs activity. It's possible that under these conditions Vhs was still able to bind some initiation factors (albeit to lesser extent) and associate with the 5′ cap but scanning may have been reduced. If this was the case, then perhaps the regions further downstream are actually close to the 5′ cap when the RNA is folded, which would explain why they are the most prominent cut sites in the presence of AMP-PNP. It's important to mention that the cleavage sites past the first 150 bases of the transcript are also the most prominent cut sites produced in the absence of AMP-PNP (Fig. 18 and data not shown from previous studies using lower concentrations of Vhs).

The nonhydrolyzable ATP analog AMP-PNP hinders translation initiation in two ways. It reduces recruitment of translation initiation factors to the 5′ cap, and it inhibits ATP hydrolysis to block scanning of the scanning complex to the AUG start codon. Therefore, it remains uncertain what events are vital for Vhs cleavage of mRNA. However, it is likely that both kinds of inhibition may be involved in Vhs activity. siRNA-mediated knockdown of eIF4AI and eIF4AII has shown that they are necessary for Vhs cleavage of GAPDH mRNA (Agarwal et al. unpublished). Current work in the lab using hippuristanol, a natural inhibitor of eIF4F and free eIF4A found in coral *Isis hippuris*, suggests that inhibiting eIF4A strongly inhibits Vhs cutting of mRNAs (61, Agarwal et al. unpublished). Results from this dissertation have indicated that mRNA secondary structure has a role in regulating Vhs cleavage (Fig. 47 and Fig. 48). Since ATP

hydrolysis is necessary for unwinding secondary structure to make it accessible for scanning during translation initiation, it is believed to be important in Vhs activity.

One way to determine the stage at which AMP-PNP has an inhibitory effect on Vhs activity is to study mRNA degradation in the presence of a *trans*-dominant R362Q eIF4A mutant. R362Q allows recruitment of the protein to the eIF4F cap binding complex, but it disrupts cycling of eIF4A through the eIF4F complex and inhibits eIF4F activity (62, 63). This mutant also inhibits eIF4F RNA helicase activity, so it prevents binding of the small ribosomal subunit (62). However, R362Q does not inhibit eIF4A/eIF4B helicase activity (62). Using a *trans*-dominant mutant would still allow recruitment of initiation factors to the 5′ cap, but it would inhibit later stages of translation initiation such as scanning. It would also be advantageous to perform similar tests using an mRNA containing the EMCV IRES to see how eIF4A inhibitors affect Vhs cleavage.

Studies testing the effect of a cap analog on Vhs site-specific cutting revealed that a free cap analog hindered Vhs cleavage at the first 80 bases from the pBK2 5′ cap (Fig. 32). The use of a cap analog does not completely inhibit translation in a RRL system because not all initiation factors can be sequestered from binding mRNA. It is interesting that in the presence of AMP-PNP Vhs cleavage at the first 150 bases of pBK2 is inhibited (Fig. 29), yet in the presence of cap analog cutting is only inhibited before the first 80 bases. It is possible that Vhs is able to cleave mRNA at regions further upstream in the presence of cap analog because RNA helicase activity hasn't been disrupted. The ratio between eIF4E and eIF4A in a RRL system has been determined to be 1:10 (62). Therefore, once eIF4E is sequestered from the system, there is still plenty of eIF4A that Vhs may associate with. It is uncertain if Vhs has the ability to associate with free eIF4A or if

it is only able to bind the eIF4F component. It is also unknown if binding free eIF4A would target Vhs to regions other than near the 5′ end.

The results from the cap analog and AMP-PNP experiments indicate that Vhs may use more than one method for accessing its mRNA cut sites. In this case cut sites in the first 150 bases of the sequence may be reached by traveling with the scanning complex, but cut sites further downstream may be accessed by alternative methods. The fact that pBK2 mRNA is cleaved at sites within the first 300 bases from the 5′ end and that a cap is required to achieve this cutting suggests that the 5′ cap is required for Vhs to gain access to the mRNA transcript. It is possible that Vhs binding to eIF4H and eIF4AI/II and loading onto the cap is required for Vhs cleavage of all mRNAs. After loading at the 5′ cap, Vhs may scan with the scanning complex to reach its cut sites or it may be directed to alternative sites by another mechanism (Fig. 54). Some of the time Vhs may be redirected to sites further downstream by a mechanism depending on the secondary structure of mRNA transcript or by the influence of additional protein factors that bind the mRNA transcript. It is not known whether Vhs cleavage of ARE-containing mRNAs requires a 5′ cap. It is possible that Vhs must first associate with translation initiation factors to target mRNA, and that Vhs then binds TPP and is redirected to the 3′ UTR to cleave the ARE.

Vhs appears to require a free 5′ end to access at least some of its cut sites. When pBK2 RNA was circularized, Vhs was unable to produce the same specific cut sites near the first AUG as it did in linear pBK2 RNA (Fig. 34). This suggests that recruitment of initiation factors to the 5′ end is important for Vhs cleavage, because initiation factors cannot bind RNA at the 5′ end when it is circularized. The fact that Vhs was able to specifically cleave circularized EMCV RNA further supported the idea that Vhs associates with components of the translational apparatus to cleave mRNA that undergoes cap-dependent scanning.

The experiments with mutant pBK2 mRNAs containing mutations in or near the first AUG shed light on Vhs association with the scanning complex. Unwinding of mRNA secondary structure in the 5′ UTR and traveling of the small ribosomal subunit along mRNA are the two connected processes of scanning. eIF1 and eIF1A are both required for this process, because they're believed to induce a conformation conducive for 43S scanning (64, 65). eIF4A, eIF4G, and eIF4B and ATP are also required for scanning, and the amount of ATP and eIF4A needed for this process correlates with the amount of secondary structure in the 5′ UTR (64, 66, 67).

Previous reports had never tested the effect of mutating AUG codons on Vhs cleavage. After observing that blocking early stages of translation initiation had an inhibitory effect on Vhs activity, it was predicted that mutating the AUG codon would also change Vhs site-specific cutting. Mutating the first AUG to a non-AUG sequence hindered Vhs site-specific cleavage in that area, however Vhs still cleaved mRNA at the same specific sites in other regions of the transcript (Fig. 38).

This was the first study to show that mutating sequences in substrate mRNA changes Vhs site-specific cleavage. The data are consistent with a model in which Vhs cutting near the start codon is due to Vhs association with the translation scanning apparatus, and that when the sequence is converted to a non-AUG, the complex scans past the area and Vhs is no longer able to cleave the mRNA in that region. Furthermore, mutating bases surrounding the AUG to make it an optimal AUG resulted in increased cleavage at regions upstream (Fig. 39). This outcome also correlates with Vhs usage of the scanning complex to reach its cut sites. However, it is unknown how these mutations change the secondary structure of the RNA. It is possible that mutating the sequence will change the secondary structure and that this might have an effect on

cleavage. The secondary structures of both sequences were analyzed using mFOLD, and they were predicted to have the same RNA configuration. Additionally, mutating the second AUG to a non-AUG did not affect Vhs's ability to produce the same site-specific cleavage products (Fig. 40). When comparing the protein products of the various RNA constructs, it is apparent that the predominant protein synthesized from wild type pBK2 mRNA corresponds to translation from the first AUG (Fig. 41). Therefore, mutating the second AUG did not hinder protein synthesis, and it seems probable that this is why Vhs site-specific cleavage was unaffected. This finding suggests that the cut sites near the second AUG are not due to leaky scanning, and instead Vhs may be using another mechanism to reach the cut sites further downstream. Mutating the first AUG to a non-AUG caused the scanning complex to scan past the region and initiate synthesis at the second AUG. It is believed that the cut sites at other locations were still produced because the sequence surrounding the first AUG was identical to wild type pBK2. The data indicate that Vhs travels with the scanning complex to reach at least some of its cut sites.

CrPV and EMCV RNA were studied to get a better idea of how Vhs targets mRNA. Earlier studies by the Smiley lab revealed that Vhs can cleave EMCV mRNA just downstream of its IRES and that the T214I point mutant retains this ability (1, 2, 3). Since Vhs-1 lacks the ability to associate with eIF4H, it seems that Vhs may be associating with another cellular initiation factor. It was previously shown that eIF4B is not vital for Vhs degradation of GAPDH mRNA in HeLa cells, so it was speculated that it also would not be essential for mRNA cleavage *in vitro* (28). So far, Vhs has been shown to associate with eIF4H, eIF4A, eIF4B, and the eIF4F cap binding complex (6, 7, 13, 27, 29). Consistent with the hypothesis that Vhs association with initiation factors targets it to mRNA, RRL, eIF4H, and eIF4B were shown to stimulate Vhs expressed in yeast *Saccharomyces cerevisiae* (12, 27). However, only addition of RRL restored

targeting downstream of an EMCV IRES, suggesting that an additional mammalian factor (other than eIF4B and eIF4H) was involved in targeting (27).

If Vhs targeting downstream of an IRES was due to association with a cellular translation factor, then a good candidate would be eIF4A. An indirect method for testing this was to study two viral IRESs that had different requirements for eIF4A. The EMCV IRES does not require cap-binding protein eIF4E, but it does require eIF2, eIF3, eIF4A and the central third of eIF4G for eIF4A binding (23, 70). No scanning is involved, and the large 60 S ribosomal subunit binds directly to the AUG located just 3′ of the IRES (68, 69). The CrPV IRES does not utilize eIF4A nor any initiation factors for protein synthesis, and instead the 40S ribosomal subunit binds to a pseudo-tRNA-like structure of the IRES (71). Vhs was able to target cleavage downstream of the EMCV IRES, but it was not able to specifically cleave downstream of the CrPV IRES (Fig. 44 and Fig. 45). This suggests that a factor involved in EMCV translation initiation plays a role in Vhs targeting to that IRES. It is still uncertain whether or not this factor is eIF4A, but future studies will investigate this by using eIF4A inhibitors.

The fact that AMP-PNP inhibited Vhs targeting downstream of the EMCV IRES makes it a strong possibility that eIF4A is involved in cutting. It was also observed that Vhs cut EMCV RNA at regions near the 5′ end (Fig. 45). These cut sites may be produced by Vhs cap-dependent scanning in the *in vitro* system. Vhs has been suggested to use cap-dependent and cap-independent methods for mRNA cleavage, and Vhs-1 has been speculated to only inhibit Vhs cap-dependent cleavage (28). It would be interesting to investigate whether the T214I point mutant is hindered from producing these 5′ cleavage products. The fact that Vhs cleaves at a specific location downstream of the EMCV IRES could be a result of the effect of a high amount of secondary structure in that RNA or it could be through the possible involvement of initiation

factors in targeting to the transcript. In this dissertation, results revealed that Vhs did not cut downstream of the CrPV IRES, suggesting that association with initiation factors may be what's driving Vhs cleavage downstream of the EMCV IRES.

In summary, the data point to a model for Vhs cleavage that involves utilizing components of the translation initiation apparatus to reach cuts sites within the first 150 bases of the sequence. Targeting to the 5′ end may be achieved by binding initiation factors that are recruited to the cap during protein synthesis (Fig. 54). The 5′ cap is vital for site-specific cleavage, indicating the importance of the cap in recruitment of Vhs to the 5′ end to produce cleavage products within the first 300 bases of the transcript. Later stages of translation initiation such as binding of the large ribosomal subunit and protein synthesis are not required for Vhs cleavage. A free 5′ end is necessary for Vhs to produce specific cut sites, suggesting that initiation factors are important for Vhs selectivity.

Our observations that mutations of AUG codons or their surrounding bases affect Vhs cutting support a model where Vhs piggybacks on the scanning complex to reach some of its cut sites (Fig. 54). However, Vhs appears to use an additional method for cleavage in the rabbit reticulocyte system, because it is still able to produce cut sites downstream of 150 bases in the presence of drugs that block early stages of translation initiation. It will be interesting to determine if Vhs cuts at these same sites *in vivo*. Possible alternative methods for Vhs cleavage may involve the mRNA secondary structure or proteins that bind the template and redirect Vhs to cut mRNA in a manner independent of the scanning process. It is still unclear how long Vhs remains associated with the mRNA transcript after cleavage. It has been suggested that Vhs may dissociate from mRNA after a single cut, and the remaining template may be degraded by cellular nucleases (4, 55, 72).

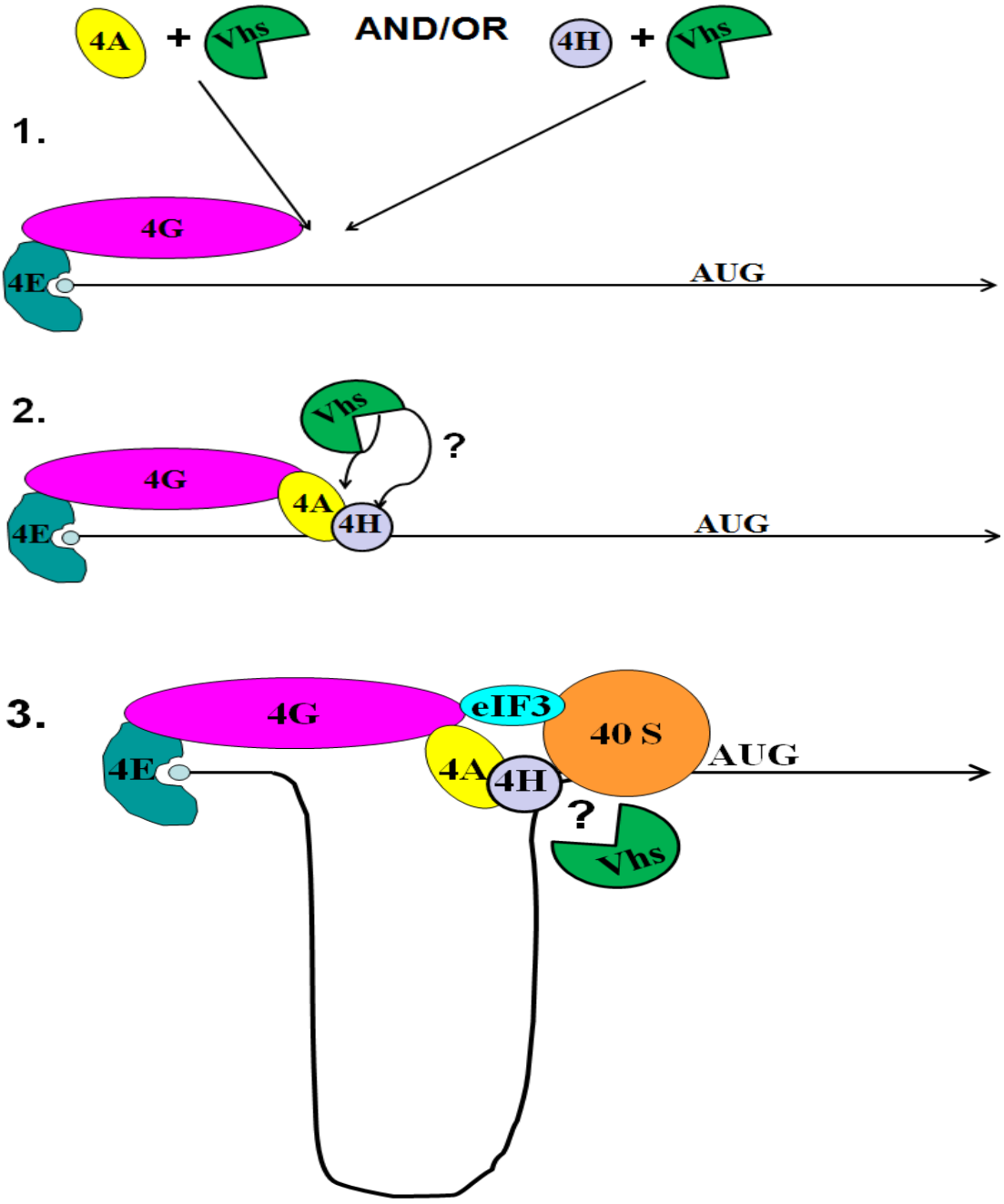

Figure 54.Model of Vhs Cleavage of mRNA

Figure 54 shows a cartoon model of how Vhs may reach its mRNA cut sites. In step one Vhs binds eukaryotic translation initiation factors eIF4AI/II and eIF4H. In step two this binding targets Vhs to the 5' end of the transcript. Part three shows that, once Vhs reaches the 5' cap, it cleaves mRNA by scanning with the scanning complex. Vhs also uses alternative mechanisms for reaching its cut sites. An alternative mechanism may involve mRNA secondary structure or structural proteins that bind the mRNA template.

Vhs Cleavage of mRNA Containing Hairpins

Hairpins located close to the 5′ cap have an inhibitory effect on cap-dependent scanning. Stable hairpins were studied as an alternative way to block early events in translation initiation. Placing a hairpin one nucleotide downstream from the 5′ cap inhibited synthesis of thymidine kinase, and it strongly reduced Vhs site-specific cleavage at regions further downstream (Fig. 47). From these results it appears that blocking the scanning process hinders Vhs's ability to travel along the mRNA transcript and access RNA cut sites. The mRNA construct contained a stretch of 8 CAA repeats following the hairpin, and this is where Vhs cleaved the mRNA (Fig. 47). It is possible that the CAA region is much closer to the 5′ cap than it appears since it follows right after the stem-loop hairpin which projects out from the cap. It could be that having a region with no predicted secondary structure increases the likelihood of Vhs cutting in that area. The control CAA sequence results support this idea because in the presence of a stretch of 19 CAA repeats one nucleotide downstream from the cap, Vhs produced a ladder of evenly spaced bands, where it appeared to cut the sequence after every C of the CAA stretch. This supports previous reports by Roizman that Vhs cleaves after C and U bases (10). Cleavage was strongest at the very end of the CAA stretch and at the very beginning of the pBK2 sequence. One possibility could be that the scanning complex travels through the CAA repeat region with ease but pauses for an extended amount of time once it reaches the pBK2 sequence which contains a higher degree of secondary structure.

Inserting a hairpin +7 or +13 bases downstream from the 5′cap restored Vhs cleavage at sites further downstream. It is still uncertain the effect of the +7 and +13 constructs on translation. It also is unclear whether cutting was restored to sites further downstream due to restoration of scanning or due to the absence of a CAA region at the 5′ end. Vhs did produce a

faint cut site immediately following the +7 hairpin construct. Similar results were obtained with the transcript that contained a hairpin one nucleotide downstream from the cap with a CAA repeat following the hairpin structure. However, Vhs did not specifically cleave the +13 construct after its hairpin. It's uncertain whether this is because the hairpin was at a greater distance from the 5′ cap. Previous reports from *in vitro* studies have shown that hairpins located in the first 12 bases from the 5′ cap have an inhibitory effect on translation, while a hairpin positioned 52 bases downstream from the cap did not (34). If this is the case, then perhaps it explains why Vhs targets downstream immediately after the +7 hairpin but not the +13 hairpin. If scanning is hindered in the +7 construct, then maybe Vhs docking at the 5′ cap keeps it in close proximity to the +7 hairpin, permitting cleavage. Current studies are testing the importance of the CAA unpredicted structure sequence in more depth.

Significance of Vhs Cleavage of Cyr61 mRNA

HSV-1 infection stabilized Cyr61 mRNA. In endothelial and fibroblast cells (in the absence of infection) Cyr61 mRNA levels are regulated very rapidly in the cell because this transcript is involved in survival, adhesion, ion-transport, cell division, and motility (40, 41, 42, 76, 77, 78). Its 3′ UTR contains an AU-rich element believed to be important for rapid mRNA turnover (78). It is speculated that Vhs stabilization of Cyr61 may be regulated by Vhs association with factors involved in ARE mRNA-mediated decay. Vhs was previously reported to stabilize the 5′ cleavage product of another ARE-containing cellular mRNA, IEX-1, through binding TPP (50, 79). TPP is involved in regulating the degradation of ARE-containing mRNAs (50, 56, 57, 79). It was found to first cleave IEX-1 at its ARE, followed by stabilization of the 5′ cleavage product (46, 47, 49). Therefore, it is suggested that Vhs may associate with TPP to

stabilize Cyr61 mRNA. It is possible that this mRNA may still be cleaved in its 3′ UTR, because, in my experiments, the probe used for Real Time PCR bound to a region upstream of the ARE. These findings support previous reports by Roizman that Vhs shows selectivity when degrading cellular mRNAs that contain an AU-rich element (46, 47, 49, 50, 79). If in fact Vhs does specifically cleave Cyr61 mRNA at its 3′ ARE, then this will have a large impact on cell signaling and show one more way that Vhs shuts off important pathways involved in biogenesis and cell longevity.

REFERENCES

1) **Saffran, H.A., M.M. Elgadi, and J.R. Smiley.** 2001. Herpes Simplex Virus Vhs Protein, p. 440-451. *In* J. N. Abelson and M.I. Simon (eds. in chief), Methods in Enzymology. Academic Press, California.
2) **Elgadi, M.M., and J.R. Smiley**. 1999. Picornavirus internal ribosome entry site elements target RNA cleavage events induced by the herpes simplex virus virion host shutoff protein. J.Virol. **73**: 9222-9231.
3) **Lu, P., H.A. Saffran, and J.R.Smiley**. 2001. The vhs1 mutant form of herpes simplex virus virion host shutoff protein retains significant internal ribosome entry site-directed RNA cleavage activity. J. Virol. **75**(2):1072-1076.
4) **Zelus, B.D., R.S.Stewart, and J. Ross**. 1996. The virion host shutoff protein of herpes simplex virus type 1: messenger ribonucleolytic activity *in vitro*. J. Virol.**70**: 2411-2419.
5) **Elgadi, M.M., C.E.Hayes, and J.R.Smiley**. 1999. The herpes simplex virus protein induces endoribonucleolytic cleavage of target RNAs in cell extracts. J. Virol. **73**: 7153-7164.
6) **Feng, P., D.N.Everly, and G.S.Read**. 2001. mRNA decay during herpesvirus infections: interactions between a putative viral nuclease and a cellular translation factor. J.Virol.**75**: 10272-10278.
7) **Feng, P., D.N.Everly, and G.S. Read**. 2005. mRNA decay during herpes simplex virus (HSV) infections: protein-protein interactions involving the HSV virion host shutoff protein and translation factors eIF4H and eIF4A. J.Virol.**79**: 9651-9664.
8) **Karr, B.M. and G.S. Read**. 1999. The virion host shutoff function of herpes simplex virus degrades the 5′ end of a target mRNA before the 3′ end. Virology. **264**(1): 195-204.
9) **Oroskar, A. A. and G.S. Read**. 1989. Control of mRNA stability by the virion host shutoff function of herpes simplex virus. Virology. **63**: 1897-1906.
10) **Taddeo, B**. **and B. Roizman.** 2006. The virion host shutoff protein (UL41) of herpes simplex virus 1 is an endoribonuclease with a substrate specificity similar to that of RNase A. J. Virol. **80:** 9341-9345.
11) **Taddeo, B., W. Zhang, and B. Roizman.** 2006. The U(L)41 protein of herpes simplex virus 1 degrades RNA by endonucleolytic cleavage in absence of other cellular or viral proteins. Proc. Natl. Acad. Sci. **103:**2827-2832.
12) **Lu, P., F. E. Jones, H. A. Saffran, and J. R. Smiley**. 2001. Herpes simplex virus virion host shutoff protein requires a mammalian factor for efficient *in vitro* endoribonuclease activity. J. Virol. **75:** 1172-1185.
13) **Everly, D.N., Jr., P. Feng, I.S. Mian, and G.S. Read.** 2002. mRNA degradation by the virion host shutoff (Vhs) protein of herpes simplex virus: genetic and biochemical evidence that Vhs is a nuclease. J. Virol. **75:** 8560-8571.

14) **Kwong, A.D., and N. Frenkel.** 1987. Herpes simplex virus-infected cells contain a function(s) that destabilizes both host and viral mRNAs. Proc.Natl.Acad.Sci. **84:** 1926-1930.
15) **Kerridge, D.** 1958. The effect of actidione and other antifungal agents on nucleic acid and protein synthesis in *Saccharomyces carlsbergensis*. J.Gen.Microbiol. **19:** 497-506.
16) **Young, C.W., P.F. Robinson and B. Sacktor.** 1963. Inhibition of the synthesis of protein in intact animals by acetoxycycloheximide and a metabolic derangement concomitant with this blockade. Biochem. Pharmacol. **12:** 855-865.
17) **Colombo, B., L. Felicetti and C. Baglioni.** 1965. Inhibition of protein synthesis by cycloheximide in rabbit reticulocytes. Biochem. Biophys. Res. Commun. **18:** 389-395.
18) **Colombo, B., L. Felicetti and C. Baglioni.** 1966. Inhibition of protein synthesis in reticulocytes by antibiotics. I. effects on polysomes. Biochim. Biophys. Acta. 119: 109-119.
19) **Trakatellis, A.C., M. Montjar and A.E. Axelrod.** 1965. Turnover of messenger ribonucleic acid and protein biosynthesis in the mouse mammary adenocarcinoma H2712. Biochemistry. **4:** 1678-1686.
20) **Korner, A.** 1966. Effect of cycloheximide on protein biosynthesis in rat liver. Biochem. J. **101:** 627-631.
21) **Godchaux, W., S.D. Adamson, and E. Herbert**. 1967. Effects of cycloheximide on polyribosome function in reitculocytes. J. Mol. Biol. **27:** 57-72.
22) **W.C. Merrick.** 1992. Mechanism and regulation of eukaryotic protein synthesis. Microbiol. Rev. **56:** 291-315.
23) **Pestova, T.V., C.U.T. Hellen and I.N. Shatsky.** 1996. Canonical eukaryotic initiation factors determine initiation of translation by internal ribosomal entry. J. Virol. **16:** 6859-6869.
24) **Hsu, W., H.A. Saffran, and J.R. Smiley.** 2005. Herpes simplex virus infection stabilizes cellular IEX-1 mRNA. J. Virol. **79:** 4090-4098.
25) **Merrick W.C. and D. Barth-Baus.** 2007. Use of reticulocyte lysates for mechanistic studies of eukaryotic translation initiation. Methods in Enzymology. **429:** 1-21.
26) **Chen, C. and P. Sarnow.** 1995. Initiation of protein synthesis by the eukaryotic translational apparatus on circular RNAs. Science. **268:** 415-417.
27) **Doepker, R.C., W.L. Hsu, H.A. Saffran, and J.R. Smiley.** 2004. Herpes simplex virus virion host shutoff protein is stimulated by eIF4B and eIF4H. J. Virol. **78:** 4684-4699.
28) **Sarma, N., D. Agarwal, L.A. Shiflett, and G.S. Read**. 2008. Small interfering RNAs that deplete the cellular translation factor eIF4H impede mRNA degradation by the virion host shutoff protein of herpes simplex virus. J. Virol. **82:** 6600-6609.
29) **Kozak, M.** 1987. An analysis of 5′-noncoding sequences from 699 vertebrate messenger RNAs. Nucleic Acids Res. **15:** 8125-8148.

30) **Hill, T., R. Sinden, and J. Sadler.** 1983. Herpes simplex virus types 1 and 2 induce shutoff of host protein synthesis by different mechanisms in friend erythroleukemia cells. J. Virol. **45:** 241-250.
31) **Everly, D. N., and G. S. Read.** 1997. Mutational analysis of the virion host shutoff gene (UL41) of herpes simplex virus (HSV): characterization of HSV types 1 (HSV-1)/HSV-2 chimeras. J. Virol. **71:** 7157-7166.
32) **Everly, D. N., and G. S. Read.** 1999. Site-directed mutagenesis of the virion host shutoff gene (UL41) of herpes simplex virus (HSV): analysis of functional differences between HSV type 1 (HSV-1) and HSV-2 alleles. J. Virol. **73:** 9117-9129.
33) **Kolupaeva, V.G., I.B. Lomakin, T.V. Pestova, and C.U.T. Hellen.** 2003. Eukaryotic initiation factors 4G and 4A mediate conformational changes downstream of the initiation codon of the encephalomyocarditis virus internal ribosomal entry site. J. Virol. **23:** 687-698.
34) **Kozak, M.** 1989. Circumstances and mechanisms of inhibition of translation by secondary structure in eukaryotic mRNAs. Mol. Cell. Biol. **9:** 5134-5142.
35) **Babendure, J.R., J.L. Babendure, J.H. Ding, and R.Y. Tsien. 2006**. Control of mammalian translation by mRNA structure near caps. RNA. **12:** 851-61.
36) **Qin, X. and P. Sarnow.** 2004. Preferential translation of internal ribosome entry site-containing mRNAs during the mitotic cycle in mammalian cells. J. Biol. Chem. **279:** 13721-13728.
37) **Johannes, G. and P. Sarnow.** 1998. Cap-independent polysomal association of natural mRNAs encoding c-myc, BiP, and eIF4G conferred by internal ribosome entry sites. RNA. **4:** 1500-1513.
38) **Johannes, G., M.S. Carter, M.B. Eisen, P.O. Brown, and P. Sarnow**. 1999. Identification of eukaryotic mRNAs that are translated at reduced cap binding complex eIF4F concentrations using a cDNA microarray. Proc. Natl. Acad. Sci. **96:** 13118-13123.
39) **Hellen, C.U.T. and P. Sarnow.** 2001. Internal ribosome entry sites in eukaryotic mRNA molecules. Genes Dev. **15:** 1593-1612.
40) **Kireeva, M.L., F-E. Mo, G.P. Yang, and L.F. Lau**. 1996. Cyr61, product of a growth factor-inducible immediate-early gene, promotes cell proliferation, migration and adhesion. Mol. Cell Biol. **16:** 1326-1334.
41) **Kireeva, M.L., B.V. Latinkic, T.V. Kolesnikova, C-C Chen, GP. Yang, A.S. Abler, and L.F. Lau.** 1997. Cyr61 and Fisp12 are both signaliing cell adhesion molecules: comparison of activities, metabolism, and localization during development. Exp. Cell Res. **233:** 63-77.
42) **Grzeszkiewicz, T.M., D.J. Kirschling, N. Chen, and L.F. Lau.** 2001. CYR61 stimulates human skin fibroblasts migration through integrin alpha vbeta 5 and enhances mitogenesis through integrin alpha vbeta 3, independent of its carboxy-terminal domain. J. Biol. Chem. **276:** 21943-21950.

43) **Babic, A.M., M.L. Kireeva, T.V. Kolesnikova, and L.F. Lau.** 1998. CYR61, product of a growth factor-inducible immediate-early gene, promotes angiogenesis and tumor growth. Proc. Natl. Acad. Sci. USA. **95:** 6355-6360.
44) **Chen, C-C., F-E. Mo, and L.F. Lau.** 2001. The angiogenic inducer Cyr61 induces a genetic program for wound healing in human skin fibroblasts. J. Biol. Chem. **276:** 47329-47337.
45) **Escalatine, A., B. Taddeo, L. Evans, and B. Roizman.** 2004. The herpes simplex virus 1 UL41 gene-dependent destabilization of cellular RNAs is selective and may be sequence-specific. Proc.Natl.Acad.Sci. U.S.A. **101:** 3603-3608.
46) **Esclatine, A., B. Taddeo, and B. Roizman.** 2004. The UL41 protein of herpes simplex virus mediates selective stabilization or degradation of cellular mRNAs. Proc. Natl. Acad. Sci. U.S.A. **101:** 18165-18170.
47) **Taddeo, B., A. Esclatine, and Bl. Roizman.** 2004. Post-transcriptional processing of cellular RNAs in herpes simplex virus-infected cells. Biochem. Soc.Trans. **32:** 697-701.
48) **Perez-Parada, J., H.A.Saffran, and J.R. Smiley.** 2004. RNA degradation induced by the herpes simplex virus vhs protein proceeds 5′ to 3′ in vitro. J. Virol. **78:** 13391-13394.
49) **Taddeo, B., A. Esclatine, W. Zhang, and B. Roizman.** 2003. The stress-inducible immediate-early responsive gene IEX-1 is activated in cells infected with herpes simplex virus 1, but several viral mechanisms, including 3′ degradation of its RNA, preclude expression of the gene. J. Virol. **77:** 6178-6187.
50) **Esclatine, A., B. Taddeo, and B. Roizman.** 2004. Herpes simplex virus 1 induces cytoplasmic accumulation of TIA-1/TIAR and both synthesis and cytoplasmic accumulation of tristetraprolin, two cellular proteins that bind and destabilize AU-rich RNAs. J. Virol. **78:** 8582-8592.
51) **Blackshear, P.J.** 2002. Tristetraprolin and other CCCH tandem zinc-finger proteins in the regulation of mRNA turnover. Biochem. Soc. Trans. **30:** 945-952.
52) **Oroskar, A.A., and G.S.Read.** 1987. A mutant of herpes simplex virus type 1 exhibits increased stability of immediate early (alpha) mRNAs. J. Virol. **61:** 604-606.
53) **Krikorian, C.R. and G.S. Read.** 1991. In vitro mRNA degradation system to study the virion host shutoff function of herpes simplex virus. J.Virol. **65:** 112-122.
54) **Schek, N., and S.L. Bachenheimer**. 1985. Degradation of cellular mRNAs induced by a virion-associated factor during herpes simplex virus infection of Vero cells. J. Virol. **55:** 601-610.
55) **Sorenson, C.M., P.A. Hart, and J. Ross**. 1991. Analysis of herpes simplex virus-induced mRNA destabilizing activity using an *in vitro* mRNA decay system. Nucleic Acid Res. **19:** 4459-4465.
56) **Chen, C.Y., R. Gherzi, S.E. Ong, E. L. Chan, R. Raijmakers, G.J. Pruijn, G. Stoecklin, C. Moroni, M. Mann, and M. Karin.** 2001. AU-binding proteins recruit the exosome to degrade ARE-containing mRNAs. Cell **107:** 451-464.

57) **Lykke-Andersen, J. and E. Wagner.** 2005. Recruitment and activation of mRNA decay enzymes by two ARE-mediated decay activation domains in the proteins TTP and BRF-1. Genes Dev. **19:** 351-361.
58) **Brown, C.R., M.S. Nakamura, J.D. Mosca, G.S. Hayward, S.E. Straus, and L. P. Perera.** 1995. Herpes simplex virus *trans*-regulatory protein ICP27 stabilizes and binds to 3′ ends of labile mRNA. J. Virol. **69:** 7187-7195.
59) **Page, H. and G.S. Read.** 2010. The virion host shutoff endonuclease (UL41) of herpes simplex virus interacts with the cellular cap-binding complex eIF4F. J. Virol. **84:** 6886-6890.
60) **Colon-Ramos, D.A., C.L. Shenvi, D.H. Weitzel, E.C. Gan, R. Matts, J. Cate, and S. Kornbluth.** 2006. Direct ribosomal binding by a cellular inhibitor of translation. Nat. Struct. Mol. Biol. **13:** 103-111.
61) **Bordeleau, M., J. Matthews, J. M. Wojnar, L. Lindqvist, O. Novac, E. Jankowsky, N. Sonenberg, P. Northcote, P. Teesdale-Spittle, and J. Pelletier.** 2005. Stimulation of mammalian translation initiation factor eIF4A activity by a small molecule inhibitor of eukaryotic translation. Proc. Natl. Acad. Sci. **102:** 10460-10465.
62) **Pause, A., N. Methot, Y. Svitkin, W.C. Merrick, and N. Sonenberg.** 1994. Dominant negative mutants of mammalian translation initiation factor eIF-4A define a critical role for eIF-4F in cap-dependent and cap-independent initiation of translation. EMBO J. **13:** 1205-1215.
63) **Pause, A. and N. Sonenberg.** 1992. Mutational analysis of a DEAD box RNA helicase: the mammalian translation initiation factor eIF-4A. EMBO J. **11:** 2643-2654.
64) **Pestova, T. and V. Kolupaeva.** 2002. The roles of individual eukaryotic translation initiation factors in ribosomal scanning and initiation codon selection. Genes and Dev. **16:** 2906-2922.
65) **Passmore, L.A.** 2007. The eukaryotic translation initiation factors eIF1 and eIF1A induce an open conformation of the 40S ribosome. Mol. Cell. **26:** 41-50.
66) **R.J. Jackson**. 1991. The ATP requirement for initiation of eukaryotic translation varies according to the mRNA species. Eur. J. Biochem. **200:** 285-294.
67) **Svitkin, Y. A. Pause, A. Haghighat, S. Pyronnet, G. Witherell, G.J. Belsham, and N. Sonenberg.** 2001. The requirement for eukaryotic initiation factor 4A (eIF4A) in translation is in direct proportion to the degree of mRNA 5′ secondary structure. RNA. **7:** 382-394.
68) **Kaminski, A., M.T. Howell, and R. J. Jackson.** 1990. Initiation of encephalomyocarditis virus RNA translation: the authentic initiation site is not selected by a scanning mechanism. EMBO J. **9:** 3753-3759.

69) **Pilipenko, E.V., A.P. Gmyl, S.V. Maslova, G.A. Belov, A.N. Sinyakov, M. Huang, T.D.K Brown, and V. I. Agol.** 1994. Starting window, a distinct element in the cap-independent internal initiation of translation on picornaviral RNA. J. Mol. Biol. **241:** 398-414.

70) **Pestova, T.V., I.N. Shatsky, and C.U.T. Hellen.** 1996. Functional dissection of eukaryotic initiation factor 4F: the 4A subunit and the central domain of the 4G subunit are sufficient to mediate internal entry of 43S preinitiation complexes. Mol. Cell. Biol. **16:** 6870-6878.

71) **Wilson, J.E., T.V. Pestova, C.U.T. Hellen, and P. Sarnow.** 2000. Initiation of protein synthesis from the A site of the ribosome. Cell. **102:** 511-520.

72) **Pak, A.S., D.N. Everly, K. Knight, and GS. Read.** 1995. The virion host shutoff protein of herpes simplex virus inhibits reporter gene expression in the absence of other final gene products. Virology. **211:** 491-506.

73) **Jackson, R.J., C.U.T. Hellen, and T.V. Pestova.** 2010. The mechanism of eukaryotic translation initiation and principles of its regulation. Nat. Rev. Mol. Biol. **10:** 113-127.

74) **Siridechadilok, B., C.S. Fraser, R.J. Hall, J.A. Doudna, and E. Nogales.** 2005. Structural roles for human translation factor eIF3 in initiation of protein synthesis. Science**. 310:** 1513-1515.

75) **Marintchev, A., K.A. Edmonds, B. Marintcheva, E. Hendrickson, M. Oberer, C. Suzuki, B. Herdy, N. Sonenberg, and G. Wagner**. 2009. Topology and regulation of the human eIF4A/4G4H helicase complex in translation initiation. Cell. **136:** 447-460.

76) **Grzeskiewicz, T.M., V. Lindner, N. Chen, S.C. Lam, and L.F. Lau**. 2002. The angiogenic factor cysteine-rich 61 (CYR 61, CCN1) supports vascular smooth muscle cell adhesion and stimulates chemotaxis through integrin alpha(6)beta(1) and cell surface heparin sulfate proteoglycans. Endocrinology. **143:** 1441-1450.

77) **Lin, M.T., C.C. Chang, S.T. Chen, H.L. Chang, J.L Su, Y.P. Chau, and M.L. Kuo.** 2004. Cyr61 expression confers resistance to apoptosis in breast cancer MCF-7 cells by a mechanism of NF-kappaB-dependent XIAP up-regulation. J. Biol. Chem. **279:** 24015-24023.

78) **O'Brien, T. P., G. P. Yang, L. Sanders, and L. F. Lau.** 1990. Expression of cyr61, a growth factor-inducible immediate-early gene. Mol. Cell. Biol. **10:** 3569-3577.

79) **Taddeo, B., W. Zhang, and B. Roizman.** 2010. Role of herpes simplex virus ICP27 in the degradation of mRNA by virion host shutoff RNase. J. Virol. **84:** 10182-10190.

80) **Wilson, J.E., M.J. Powell, S.E.Hoover, and P. Sarnow.** 2000. Naturally occurring discistronic cricket paralysis virus RNA is regulated by two internal ribosome entry sites. Mol. Cell. Biol. **20:** 4990-4999.

81) **Martin, L.R., Z.C. Neal, M.S. McBride, and A.C. Palmenberg.** 2000. Mengovirus and encephalomyocarditis virus poly (C) tract lengths can affect virus growth in murine cell culture. J. Virol. **74:** 3074-3081.

82) **Cunningham, A.L. and D.E. Dwyer.** 2004. The pathogenesis underlying the interaction of HIV and herpes simplex virus after co-infection. J. HIV Ther. **9:** 9-13.
83) **Roizman, B. and A. E. Sears.** 1996. Herpes simplex viruses and their replication. In Fields Virology, Fields B.N., D.M. Knipe, and P.M. Howley (eds). Lippincott-Raven: Philadelphia 2231-2295.
84) **Nicola, A.V., J. Hou, E. O. Major, and S.E. Straus.** 2005. Herpes simplex virus type 1 enters human epidermal keratinocytes, but not neurons, via a pH-dependent endocytic pathway. J. Virol. **79:** 7609-7616.
85) **Antinone, S.E. and G.A. Smith.** 2010. Retrograde axon transport of herpes simplex virus and pseudorabies virus: a live-cell comparative analysis. J. Virol. **84:** 5675-5679.
86) **Smith, G.A., L. Pomeranz, S.P. Gross, and L.W. Enquist.** 2004. Local modulation of plus-end transport targets herpesvirus entry and egress in sensory axons. Proc. Natl. Acad. Sci. U.S.A. **101:** 16034-16039.
87) **Lycke, E., B. Hamark, M. Johansson, A. Krotochwil, J. Lycke, and B. Svennerholm.** 1988. Herpes simplex virus infection of the human sensory neuron. An electron microscopy study. Arch. Virol. **101:** 87-104.
88) **Lycke, E., K. Kristensson, B. Svennerholm, A. Vahlne, and R. Ziegler.** 1984. Uptake and transport of herpes simplex virus in neurites of rat dorsal root ganglia cells in culture. J. Gen. Virol. **65**(Pt 1): 55-64.
89) **Luxton, G.W., S. Haverlock, K.E. Coller, S.E. Antinone, A. Pincetic, and G.A. Smith.** 2005. Targeting of herpesvirus capsid transport in axons is coupled to association with specific sets of tegument proteins. Proc. Natl. Acad. Sci. U.S.A. **102:** 5832-5837.
90) **Dohner, K. and B. Sodeik.** 2005. The role of the cytoskeleton during viral infection. Curr. Top. Microbiol. Immunol. **285:** 67-108.
91) **Garner, J.A.** 2003. Herpes simplex virion entry into and intracellular transport within mammalian cells. Adv. Drug Deliv. Rev. **55:** 1497-1513.
92) **Smith, G.A. and L.W. Enquist. 2002**. Break ins and break outs: viral interactions with the cytoskeleton of mammalian cells. Annu. Rev. Cell Dev. Biol. **18:** 135-161.
93) **Dohner, K., C.H. Nagel, and B. Sodeik.** 2005. Viral stop-and-go along microtubules: taking a ride with dynein and kinesins. Trends Microbiol. **13:** 320-327.
94) **Radtke, K., K. Dohner, and B. Sodeik.** 2006. Viral interactions with the cytoskeleton: a hitchhiker's guide to the cell. Cell Microbiol. **8:** 387-400.
95) **Diefenbach, R.J., M. Miranda-Saksena, M.W. Douglas, and A.L. Cunningham.** 2008. Transport and egress of herpes simplex virus in neurons. Rev. Med. Virol. **18:** 35-51.
96) **Mettenleiter, T.C.** 2004. Budding events in herpesvirus morphogenesis. Virus Res. **106:** 167-180.
97) **P.G. Spear.** 2004. Herpes simplex virus: receptors and ligands for cell entry. Cell. Microbiol. **6:** 401-410.

98) **Akhtar, J. and D. Shukla.** 2009. Viral entry mechanisms: cellular and viral mediators of herpes simplex virus entry. **276:** 7228-7236.
99) **Laquerre, S. R. Argnani, D.B.Anderson, S. Zucchini, R. Manservigi, and J.C. Glorioso.** 1998. Heparan sulfate proteoglycan binding by herpes simplex virus type 1 glycoproteins B and C, which differ in their contributions to virus attachment, penetration, and cell-to-cell spread. J. Virol. **72:** 6119-6130.
100) **Herold, B. C., R. J. Visalli, N. Susmarksi, C.R. Brandt, and P.G. Spear.** 1994. Glycoprotein C-independent binding of herpes simplex virus to cells requires cell surface heparan sulphate and glycoprotein B. J. Gen. Virol. **75:** 1211-1222.
101) **Herold, B.C., D. WuDunn, N. Soltys, and P.G. Spear.** 1991. Glycoprotein C of herpes simplex virus type 1 plays a principal role in the adsorption of virus to cells and in infectivity. J. Virol. **65:** 1090-1098.
102) **Campadelli-Fiume, G., M. Amasio, E. Avitabile, A. Cerretani, C. Forghieri, T. Gianni, and L. Menotti.** 2007. The multipartite system that mediates entry of herpes simplex virus into the cell. Rev. Med. Virol**. 17:** 313-326.
103) **P.G. Spear.** 1993. Entry of alphaherpesviruses into cells. Sem. Virol. **4:** 167-180.
104) **Spear, P.G., R.J. Eisenberg, and G.H. Cohen.** 2000. Three classes of cell surface receptors for alphaherpesvirus entry. Virology**. 275:** 1-8.
105) **Clement, C., V. Tiwari, P.M. Scanlan, T. Valyi-Nagy, B.Y. Yue, and D. Shukla.** 2006. A novel role for phagocytosis-like uptake in herpes simplex virus entry. J. Cell. Biol. **174:** 1009-1021.
106) **Heldwein, E.E., H. Lou, F.C. Bender, G.H. Cohen, R.J. Eisenberg, and S.C. Harrison.** 2006. Crystal structure of glycoprotein B from herpes simplex virus 1. Science. **313:** 217-220.
107) **Shieh, M.T., D. WuDunn, R.I. Montgomery, J.D. Esko, and P.G. Spear.** 1992. Cell surface receptors for herpes simplex virus are heparan sulfate proteoglycans. J. Cell Biol. **116:** 1273-1281.
108) **WuDunn, D. and P.G. Spear**. 1989. Initial interaction of herpes simplex virus with cells is binding to heparan sulfate. J. Virol. **63:** 52-58.
109) **Roizman, B., D.M. Knipe, and R.J. Whitley.** 2007. Herpes simplex viruses. In Fields Virology, Knipe D.M. and P.M. Howley (eds.) Lippincott-Raven: Philadelphia. 2501-2576.
110) **Knipe, D.M., W. Batterson, C. Nosal, B. Roizman, and A. Buchan.** 1981. Molecular genetics of herpes simplex virus. VI. Characterization of a temperature sensitive mutant defective in the expression of all early viral sensitive mutant defective in the expression of all early viral gene products. J. Virol. **38:** 539-547.
111) **Batterson, W., D. Furlong, and B. Roizman.** 1983. Molecular genetics of herpes simplex virus. VIII. Further characterization of a temperature-sensitive mutant defective in release of viral DNA and in other stages of the viral reproductive cycle. J. Virol. **45:** 397-407.

112) **Crouse, H.V., L.L. Coriell, H. Blank, and T.F. Scott.** 1950. Cytochemical studies on the intranuclear inclusion of herpes simplex. J. Immunol. **65:** 119-128.

113) **Quinlan, M.P., L. B. Chen, and D.M. Knipe. 1985**. The intranuclear location of a herpes simplex virus DNA-binding protein is determined by the status of viral DNA replication. Cell. **36:** 857-868.

114) **Monier, K. J. C. Armas, S. Etteldorf, P. Ghazal, and K.F. Sullivan**. 2000. Annexation of the interchromosomal space during viral infection. Nat. Cell Biol. **2:** 661-665.

115) **Morgan, C., M. Holden, and E. P. Jones.** 1959. Electron microscopic observations on the development of herpes simplex virus. J. Exp. Med.**110:** 643-656.

116) **Schwartz, J. and B. Roizman.** 1969. Similarities and differences in the development of laboratory strains and freshly isolated strains of herpes simplex virus in HEp-2cells: electron microscopy. J. Virol. **4:** 879-889.

117) **Simpson-Holley, M., R.C. Colgrove, G. Nalepa, J.W. Harper, and D.M. Knipe.** 2005. Identification and functional evaluation of cellular and viral factors involved in the alteration of nuclear architecture during herpes simplex virus 1 infection. J. Virol. **79:** 12840-12851.

118) **Maul, G.G., H.H. Guldner, and J.G. Spivack.** 1993. Modification of discrete nuclear domains induced by herpes simplex virus type 1 immediate early gene 1 product (ICP0). J. Gen. Virol. **74:** 2679-2690.

119) **Alvine, J. C., W.L. Steinhart, and C.W. Hill.** 1974. Transcription of herpes simplex type 1 DNA in nuclei isolated from infected Hep-2 and KB cells. Virology. **60:** 302-307.

120) **Costanzo, F., G. Campadelli-Fiume, L. Foa-Tomasi, and E. Cassai.** 1977. Evidence that herpes simplex virus DNA is transcribed by cellular RNA polymerase B. J. Virol. **21:** 996-1001.

121) **Honess, R.W. and D.H. Watson.** 1974. Herpes simplex virus-specific polypeptides studied by polyacrylamide gel electrophoresis of immune precipitates. J. Gen. Virol. **22:** 171-185.

122) **Honess, R.W. and B. Roizman.** 1974. Regulation of herpesvirus macromolecular synthesis. I. Cascade regulation of the synthesis of three groups of viral proteins. J. Virol. **14:** 8-19.

123) **Fenwick, M., L. Morse, and B. Roizman.** 1979. Anatomy of herpes simplex virus DNA: apparent clustering of functions effecting rapid inhibition of host DNA and protein synthesis. J. Virol. **29:** 825-827.

124) **Fenwick, M.L. and M.J. Walker.** 1978. Suppression of the synthesis of cellular macromolecules by herpes simplex virus. J. Gen. Virol. **41:** 37-51.

125) **Hill, T.M., J.R. Sadler, and J.L. Betz.** 1985. Virion component of herpes simplex virus type 1 KOS interferes with early shutoff of host protein synthesis. J. Virol. **56:** 312-316.

126) **Nishioka, Y. and S. Silverstein.** 1978. Alteration of the protein synthetic apparatus of Friend erythroleukemia cells infected with vesicular stomatitis or herpes simplex virus. J. Virol. **25:** 422-425.

127) **Nishioka, Y. and S. Silverstein.** 1978. Requirement of protein synthesis for the degradation of host mRNA in Friend erythroleukemia cells infected with herpes simplex virus type 1. J. Virol. **27:** 619-627.

128) **Oroskar, A.A. and G.S. Read.** 1987. A mutant of herpes simplex virus type 1 exhibits increased stability of immediate-early (alpha) mRNAs. J. Virol. **61:** 604-606.

129) **Read, G.S. and N. Frenkel.** 1983. Herpes simplex virus mutants defective in the virion-associated shutoff of host polypeptide synthesis and exhibiting abnormal synthesis of alpha (immediate early) viral polypeptides. J. Virol. **46:** 498-512.

130) **Strom, T. and N. Frenkel.** 1987. Effects of herpes simplex virus on mRNA stability. J. Virol. **61:** 2198-2207.

131) **Sydiskis, R.J. and B. Roizman.** 1966. Polysomes and protein synthesis in cells infected with a DNA virus. Science. **153:** 76-78.

132) **Sydiskis, R.J. and B. Roizman.** 1967. The disaggregation of host polyribosomes in productive and abortive infection with herpes simplex virus. Virology. **32:** 678-686.

133) **Herrera, F.J. and S.J. Triezenberg.** 2004. VP16-dependent association of chromatin-modifying coactivators and underrepresentation of histones at immediate-early gene promoters during herpes simplex virus infection. J. Virol. **78:** 9689-9696.

134) **Kent, J.R., P.Y. Zeng, D. Atanasiu, J. Gardner, N.W. Fraser, and S.L. Berger**. 2004. During lytic infection herpes simplex virus type 1 is associated with histones bearing modifications that correlate with active transcription. J. Virol. **78:** 10178-10186.

135) **Mackem, S. and B. Roizman.** 1980. Regulation of herpesvirus macromolecular synthesis: transcription-initiation sites and domains of alpha genes. Proc. Natl. Acad. Sci. U.S.A. **77:** 7122-7126.

136) **Mackem, S. and B. Roizman.** 1982. Structural features of the herpes simplex virus alpha gene 4, 0, and 27 promoter-regulatory sequences which confer alpha regulation on chimeric thymidine kinase genes. J. Virol. **44:** 939-949.

137) **Mears, W.E. and S.A. Rice.** 1998. The herpes simplex virus immediate-early protein ICP27 shuttle between nucleus and cytoplasm. Virology**. 242:** 128-137.

138) **Phelan, A. and J.B. Clements.** 1997. Herpes simplex virus type 1 immediate early protein IE63 shuttles between nuclear compartments and the cytoplasm. J. Gen. Virol. **78:** 3327-3331.

139) **R.M. Sandri-Goldin**. 1998. ICP27 mediates HSV RNA export by shuttling through a leucine-rich nuclear export signal and binding viral intronless RNAs through an RGG motif. Genes Dev. **12:** 868-879.

140) **Soliman, T.M., R.M. Sandri-Goldin, and S.J. Silverstein.** 1997. Shuttling of the herpes simplex virus type 1 regulatory protein ICP27 between the nucleus and cytoplasm mediates the expression of late proteins. J. Virol. **71:** 9188-9197.

141) **Soliman, T.M. and S.J. Silverstein.** 2000. Identification of an export control sequence and a requirement for the KH domains in ICP27 from herpes simplex virus type 1. J. Virol. **74:** 7600-7609.

142) **Chen, I.H., K.S. Sciabica, and R.M. Sandri-Goldin.** 2002. ICP27 interacts with the RNA export factor Aly/REF to direct herpes simplex virus type 1 intronless mRNAs to the TAP export pathway. J. Virol. **76:** 12877-12889.

143) **Hardy, W.R. and R.M. Sandri-Goldin.** 1994. Herpes simplex virus inhibits host cell splicing, and regulatory protein ICP27 is required for this effect. J. Virol. **68:** 7790-7799.

144) **Bryant, H.E., S.E. Wadd, A.I. Lamond, S.J. Silverstein, and J.B. Clements.** 2001. Herpes simplex virus IE63 (ICP27) protein interacts with spliceosome-associated protein 145 and inhibits splicing prior to the first catalytic step. J. Virol. **75:** 4376-4385.

145) **Sciabica, K.S., Q.J. Dai, and R.M. Sandri-Goldin.** 2003. ICP27 interacts with SRPK1 to mediate HSV splicing inhibition by altering SR protein phosphorylation. EMBO J. **22:** 1608-1619.

146) **S.C. Inglis.** 1982. Inhibition of host protein synthesis and degradation of cellular mRNAs during infection by influenza an herpes simplex virus. Mol. Cell Biol. **2:** 1644-1648.

147) **Kwong, A.D., J.A. Kruper, and N. Frenkel.** 1988. Herpes simplex virus virion host shutoff function. J. Virol. **62:** 912-921.

148) **Kwong, A.D. and N. Frenkel.** 1989. The herpes simplex virus virion host shutoff function. J. Virol. **63:** 4834-4839.

149) **Doherty, A. J., L.C. Serpell, and C.P. Ponting.** 1996. The helix-hairpin-helix DNA-binding motif: a structural basis for non-sequence-specific recognition of DNA**.** Nucleic Acids Res. **24:** 2488-2497.

150) **M.R. Lieber.** 1997. The FEN-1 family of structure-specific nucleases in eukaryotic DNA replication, recombination and repair. Bioessays. **19:** 233-240.

151) **Read, G.S., B.M. Karr, and K. Knight.** 1993. Isolation of a herpes simplex virus type 1 mutant with a deletion in the virion host shutoff gene and identification of multiple forms of the vhs (UL41) polypeptide. J. Virol. **67:** 7149-7160.

152) **Becker, Y., E. Tavor, Y. Asher, C. Berkowiltz, and M. Moyal.** 1993. Effect of herpes simplex virus type-1 UL41 gene on the stability of mRNA from the cellular genes: beta-actin, fibronectin, glucose transporter-1, and docking protein, and on virus intraperiotoneal pathogenicity of mewborn mice. Virus Genes**. 7:** 133-143.

153) **Leib, D.A., T.E. Harrison, K.M. Laslo, M.A. Machalek, N.J. Moorman, and H.W. Virgin.** 1999. Interferons regulate the phenotype of wild-type and mutant herpes simplex viruses *in vivo*. J. Exp. Med. **189:** 663-672.

154) **Smith, T.J., C.E. Ackland-Berglund, and D.A.Leib.** 2000. Herpes Simplex virus virion host shutoff (Vhs) activity alters periocular disease in mice. J. Virol. **74:** 3598-3604.

155) **Strelow, L., T. Smith, and D.A. Leib.** 1997. The virion host shutoff function of herpes simplex virus type 1 plays a role in corneal invasion and functions independently of the cell cycle. Virology. **231:** 28-34.

156) **Strelow, L. I. and D.A. Leib.** 1995. Role of the virion host shutoff (Vhs) of herpes simplex virus type 1 in latency and pathogenesis. J. Virol. **69:** 6779-6786.

157) **Strelow, L.I., and D.A. Leib.** 1996. Analysis of conserved domains of UL41 of herpes simplex virus type 1 in virion host shutoff and pathogenesis. J. Virol. **70:** 5665-5667.

158) **Smibert, C. A., D.C. Johnson, and J.R. Smiley.** 1992. Identification and characterization of the virion-induced host shutoff product of herpes simplex virus gene UL41. J. Gen. Virol. **73:** 46-470.

159) **Lorsch, J.R. and D. Herschlag.** 1998. The DEAD box protein eIF4A. 1. A minimal kinetic and thermodynamic framework reveals coupled binding of RNA and nucleotide. Biochem. **37:** 2180-2193.

160) **Lorsch, J.R. and D. Herschlag.** 1998. The DEAD box protein eIF4A. 2. A cycle of nucleotide and RNA-dependent conformational changes. Biochem. **37:** 2194-2206.

161) **Abramson, R.D., T.E. Dever, T.G. Lawson, B.K. Ray, R.E. Thach, and W.C. Merrick.** 1987. The ATP-dependent interaction of eukaryotic initiation factors with mRNA. J. Biol. Chem. **262:** 3826-3832.

162) **Ray, B.K., T.G. Lawson, J.C. Kramer, M.H. Cladaras, J.A. Grifo, R.D. Abramson, W.C. Merrick, and R.E. Thach.** 1985. ATP-dependent unwinding of messenger RNA structure by eukaryotic initiation factors. J. Biol. Chem. **260:** 7651-7658.

163) **Benne, R. and J.W.B. Hershey.** 1979. The activity of eukaryotic initiation factor eIF-2 in ternary complex formation with GTP and Met-tRNA.J. Biol. Chem. **253:** 3078-3087.

164) **Methot, N., A. Pause, J.W. Hershey, and N. Sonenberg.** 1994. The translation initiation factor eIF-4B contains an RNA-binding region that is distinct and independent from its ribonucleoprotein consensus sequence. Mol. Cell Biol. **14:** 2307-2316.

165) **von der Haar, T., J.D. Gross, G. Wagner, and J.E. McCarthy.** 2004. The mRNA cap-binding protein eIF4E in post-transcriptional gene expression. Nat. Struct. Mol. Biol. **11:** 503-511.

166) **Gross, J.D., N.J. Moerke, T. von der Haar, A.A. Lugovskoy, A.B. Sachs, J.E. McCarthy, and G. Wagner.** 2003. Ribosome loading onto the mRNA cap is driven by conformation coupling between eIF4G and eIF4E. Cell. **115:** 739-750.

167) **Volpon, L., M.J. Osborne, I. Topisirovic, N. Siddiqui, and K.L. Borden.** 2006. Cap-free structure of eIF4E suggests a basis for conformation regulation by its ligands. EMBO J. **25:** 5138-5149.

168) **Rogers, G.W. Jr., N.J. Richter, W.F. Lima, and W.C. Merrick.** 2001. Modulation of the helicase activity of eIF4A by eIF4B, eIF4H, and eIF4F. J. Biol. Chem. **276:** 30914-20922.

169)

170) **M. Kozak.** 1991. Structural features in eukaryotic mRNAs that modulate the initiation of translation. J. Biol. Chem. **266:** 19867-19870.

171) **Pestova, T.V., S.I. Borukhov, and C.U.T. Hellen.** 1998. Eukaryotic ribosomes require initiation factors 1 and 1A to locate initiation codons. Nature. **394:** 854-859.

172) **Pisarev, A. V., V.G. Kolupaeva, V.P. Pisareva, W.C. Merrick, C.U. Hellen, and T.V. Pestova.** 2006. Specific functional interactions of nucleotides at key -3 and +4 positions flanking the initiation codon with components of the mammalian 48S translation initiation complex. Genes Dev. **20:** 624-636.

173) **Unbehaun, A., S.I. Borukhov, C.U.T. Hellen, and T.V. Pestova.** 2004. Release of initiation factors from 48S complexes during ribosomal subunit joining and the link between establishment of codon-anticodon basepairing and hydrolysis of eIF2-bound GTP. Genes Dev. **18:** 3078-3093.

174) **Lomakin, I.B., V.G. Kolupaeva, A. Marintchev, G. Wagner, and T.V. Pestova.** 2003. Position of eukaryotic initiation factor eIF1 on the 40S ribosomal subunit determined by directed hydroxyl radical probing. Genes Dev. **17:** 2786-2797.

175) **Altire, M.A., D. Maag, and J.R. Lorsch.** 2005. P_i release from eIF2, not GTP hydrolysis, is the step controlled by start-site selection during eukaryotic translation initiation. Mol. Cell. **20:** 251-262.

176) **Olsen, D.S., E.M. Savner, A. Mathew, F. Zhang, T. Krishnamoorthy, L. Phan, and A.G. Hinnebusch.** 2003. Domains of eIF1A that mediate binding to eIF2, eIF3, and eIF5B and promote ternary complex recruitment in vivo. EMBO J. **22:** 193-204.

177) **Marintchev, A., V.G. Kolupaeva, T.V. Pestova, and G. Wagner.** 2003. Mapping the binding interface between human eukaryotic initiation factors 1A and 5B: a new interaction between old partners. Proc. Natl Acad. Sci. USA. **100:** 1535-1540.

178) **Acker, M.G, B.S. Shin, T.E. Dever, and J.R. Lorsch.** 2006. Interaction between eukaryotic initiation factors 1A and 5B is required for efficient ribosomal subunit joining. J. Biol. Chem. **281:** 8469-8475.

179) **Acker, M.G., B.S. Shin, J.S. Nanda, A.K. Saini, T.E. Dever, and J.R. Lorsch.** 2009. Kinetic analysis of late steps of eukaryotic translation initiation. J. Mol. Biol. **385:** 491-506.

180) **de Breyne, S., Y. Yu, A. Unbehaun, T.V. Pestova, and C.U.T. Hellen.** 2009. Direct functional interaction of initiation factor eIF4G with type 1 internal ribosomal entry sites. Proc. Natl. Acad. Sci. USA. **106:** 9197-9202.

181) **Pestova, T.V., I.N. Shatsky, S.P. Fletcher, R.J. Jackson, and C.U.T. Hellen.** 1998. A prokaryotic-like mode of cytoplasmic eukaryotic ribosome binding to the initiation codon during internal translation initiation of hepatitis C and classical swine fever virus RNAs. Gene Dev. **12:** 6-83.

182) **Schuler, M.** et al. 2006. Structure of the ribosome-bound cricket paralysis virus IRES RNA. Nature Struct. Mol. Biol. **13:**1092-1096.

183) **Sonenberg, N., J.W.B. Hershey, and M.B. Mathews.** 2000. Translational control of gene expression. Cold Spring Harbor Laboratory Press, Cold Spring Harbor, New York. 503-527.

184) **Gesteland, R.F. T.R. Cech, and J.F. Atkins.** 1999. The RNA world: The nature of modern RNA suggests a prebiotic RNA. Cold Spring Harbor Laboratory Press, New York.

185) **Brantl, S.** 2002. Antisense-RNA regulation and RNA interference. Biochim. Biophys. Acta. **1575:** 15-25.

186) **Nudler, E. and A.S. Mironov.** 2004. The riboswitch control of bacterial metabolism. Trends Biochem. Sci. **29:** 11-17.

187) **Westhof, E. and W. Filipowicz.** 2005. From RNAi to epigenomes: How RNA rules the world. Chembiochem. **6:** 441-443.

188) **J.E. McCarthy.** 1998. Posttranscriptional control of gene expression in yeast. Microbiol. Mol. Biol. Rev. **62:** 1492-1553.

189) **Gebauer, F. and M.W. Hentze.** 2004. Molecular mechanisms of translational control. Nat. Rev. Mol. Cell Biol. **5:** 827-835.

190) **Hentze, M.W., S.W. Caughman, T.A. Rouault, J.G. Barriocanal, A. Dancis, J.B. Harford, and R.D. Klausner.** 1987. Identification of the iron-responsive element for the translational regulation of human ferritin mRNA. Science. **238:** 1570-1573.

191) **Rouault, T.A., M.WW. Hentze, S.W. Caughman, J.B. Harford, and R.D. Klausner.** 1988. Binding of a cytosolic protein to the iron-responsive element of human ferritin messenger RNA. Science. **241:** 1207-1210.

192) **Goosen, B., and M.W. Hentze.** 1992. Position is the critical determinant for function of iron-responsive elements as translational regulators. Mol. Cell. Biol. **12:** 1959-1966.

193) **R.S. Eisenstein.** 2000. Iron regulatory proteins and the molecular control of mammalian iron metabolism. Annu. Rev. Nutr. **20:** 627-662.

194) **Jiang, H. and M.C. Lucy.** 2001. Variants of the 5′-untranslated region of the bovine growth hormone receptor mRNA: Isolation, expression and effects on translational efficiency. Gene. **265:** 45-53.

195) **M. Kozak.** 1986. Influences of mRNA secondary structure on initiation by eukaryotic ribosomes. Proc. Natl. Acad. Sci. **83:** 2850-2854.

196) **Vega Laso, M.R., D. Zhu, F. Sagliocco, A.J. Brown, M.F. Tuite, and J.E. McCarthy.** 1993. Inhibition of translational initiation in the yeast *Saccharomyces cerevisiae* as a function of the stability and position of hairpin structures in the mRNA leader. J. Biol. Chem. **268:** 6453-6462.

197) **M. Kozak.** 1991. An analysis of vertebrate mRNA sequences: intimations of translational control. J. Cell Biol. **115:** 887-903.

198) **Herrick, D., R. Parker, and A. Jacobson.** 1990. Identification and comparison of stable and unstable mRNAs in *Saccharomyces cerevisiae*. Mol. Cell. Biol. **10:** 2269-2284.

199) **Wilusz, C.J., M. Wormington, and S.W. Peltz.** 2001. The cap-to-tail guide to mRNA turnover. Nat. Rev. Mol. Cell Biol. **2:** 237-246.

200) **Chen, C.Y., and A.B. Shyu.** 1995. AU-rich elements: characterization and importance in mRNA degradation. Trends Biochem. Sci. **20:** 465-470.

201) **Brown, C.E., and A.B. Sachs.** 1998. Poly(A) tail length control in *Saccharomyces cerevisiae* occurs by message-specific deadenylation. Mol. Cell. Biol. **18:** 6548-6559.

202) **Boeck, R., S. Tarun, Jr., M. Rieger, J.A. Deardorff, S. Muller-Auer, and A.B. Sachs.** 1996. The yeast Pan2 protein is required for poly(A)-binding protein-stimulated poly(A)-nuclease activity. J. Biol. Chem**. 271:** 432-438.

203) **Tucker, M., M.A. Valencia-Sanchez, R.R. Staples, J. Chen, C.L. Denis, and R. Parker.** 2001.The transcription factor associated Ccr4 and Caf1 proteins are components of the major cytoplasmic mRNA deadenylase *in Saccharomyces cerevisiae*. Cell. **104:** 377-386.

204) **Chang, M., D. French-Cornay, H.Y. Fan, H. Klein, C.L. Denis, and J.A. Jaehning.** 1999. A complex containing RNA polymerase II, Paf1p, Cdc73p, Hpr1p, and Ccr4p plays a role in protein kinase C signaling. Mol. Cell. Biol. **19:** 1056-1067.

205) **LaGrandeur, T.E. and R. Parker.** 1998. Isolation and characterization of Dcp1p, the yeast mRNA decapping enzyme. EMBO J. **17:** 1487-1496.

206) **Beelman, C.A., A. Stevens, G. Caponigro, T.E. LaGrandeur, L. Hatfield, D.M. Fortner, and R. Parker.** 1996. An essential component of the decapping enzyme required for normal rates of mRNA turnover. Nature. **382:** 642-646.

207) **Hsu, C.L. and A. Stevens.** 1993. Yeast cells lacking 5′→3′ exoribonuclease 1 contain mRNA species that are poly(A) deficient and partially lack the 5′ cap structure. Mol. Cell. Biol. **13:** 4826-4835.

208) **Muhlrad, D., C.J. Decker, and R. Parker.** 1994. Deadenylation of the unstable mRNA encoded by the yeast MFA2 gene leads to decapping followed by 5′→3′ digestion of the transcript. Genes Dev. **8:** 855-866.

209) **Muhlrad, D., C.J. Decker, and R. Parker.** 1995. Turnover mechanisms of the stable yeast PGK1 mRNA. Mol. and Cell. Biol. **15:** 2145-2156.

210) **Beelman, C.A. and R. Parker.** 1995. Degradation of mRNA in eukaryotes. Cell. **81:** 179-183.

211) **Schwartz, D.C. and R. Parker.** 1999. Mutations in translation initiation factors lead to increased rates of deadenylation and decapping of mRNAs in *Saccharomyces cerevisiae*. Mol. Cell. Biol. **19:** 5247-5256.

212) **Beelman, C.A. and R. Parker.** 1994. Differential effects of translational inhibition in cis and in trans on the decay of unstable yeast MFA2 mRNA. J. Biol. Chem. **269:** 9687-9692.

213) **Bernstein, P. S., W. Peltz, and J. Ross.** 1989. The poly(A)-poly(A)-binding protein complex is a major determinant of mRNA stability in vitro. Mol. Cell. Biol. **9:** 659-670.

214) **Gingras, A.C., B. Raught, and N. Sonenberg.** 1999. eIF4 initiation factors: effectors of mRNA recruitment to ribosomes and regulators of translation. Annu. Rev. Biochem. **68:** 913-963.

215) **Wells, S.E., P.E. Hillner, R.D. Vale, and A.B. Sachs.** 1998. Circularization of mRNA by eukaryotic translation initiation factors. Mol. Cell. **2:** 135-140.

216) **Dehlin, E. M. Wormington, C.G. Korner, and E. Wahle.** 2000. Cap-dependent deadenylatin of mRNA. EMBO J. **19:** 1079-1086.

217) **Gao, M., D.T. Fritz, L.P. Ford, and J. Wilusz.** 2000. Interaction between a poly(A)-specific ribonuclease and the 5′ cap influences mRNA deadenylation rates *in vitro*. Mol. Cell. **5:** 479-488.

218) **Gao, M, C.J. Wilusz, S.W. Peltz, and J. Wilusz. 2001.** A novel mRNA decapping activity in HeLa cytoplasmic extracts is regulated by AU-rich elements. EMBO J. **20:** 1134-1143.

219) **Bakheet, T. M. Frevel, B.R. Williams, W. Greer, and K.S. Khabar.** 2001. ARED:human AU-rich element-containing mRNA database reveals an unexpectedly diverse functional repertoire of encoded proteins. Nucleic Acids Res. **29:** 246-254.

220) **Wang, X., M. Kiledjian, I.M. Weiss, and S.A. Liebhaber.** 1995. Detection and characterization of a 3′ untranslated region ribonucleoprotein complex associated with human α–globin mRNA stability. Mol. Cell. Biol. **15:** 1769-1777.

221) **Wang, Z. and M. Kiledjian.** 2000. The poly(A)-binding protein and an mRNA stability protein jointly regulate an endoribonuclease activity. Mol. Cell. Biol. **20:** 6334-6341.

222) **Wang, Z., N. Day, P. Trifillis, and M. Kiledjian.** 1999. An mRNA stability complex functions with poly(A)-binding protein to stabilize mRNA *in vitro*. Mol. Cell. Biol. **19:** 4552-4560.

223) **Veyrune, J.L., S. Carillo, A. Vie, and J.M. Blanchard.** 1995. c-fos mRNA instability determinants present within both the coding and the 3′ non coding region link the degradation of this mRNA to its translation. Oncogene. **11:** 2127-2134.

224) **Chen, C.Y., F. Gatto-Konczak, Z. Wu, and M. Karin.** 1998. Stabilization of interleukin-2 mRNA by the c-Jun NH2-terminal kinase pathway. Science. **280:** 1945-1949.

225) **Chen, C. Y., R. Gherzi, J.S. Andersen, G. Gaietta, K. Jurchott, H.D. Royer, M. Mann, and M. Karin.** 2000. Nucleolin and YB-1 are required for JNK-mediated interleukin-2 mRNA stabilization during T-cell activation. Genes Dev. **14:** 1236-1248.

226) **Muhlrad, D. and R. Parker.** 1994. Premature translational termination triggers mRNA decapping. Nature. **370:** 578-581.

227) **Sciortino, M.T., M. Suzuki, B Taddeo, and B. Roizman.** 2001. RNAs extracted from herpes simplex virus 1 virions: apparent selectivity of viral but not cellular RNAs packaged in virions. J. Virol. **75:** 8105-8116.

228) **Smibert, C.A., B. Popova, P. Xiao, J.P. Capone, and J.R. Smiley.** 1994. Herpes simplex virus VP16 forms a complex with the virion host shutoff protein vhs. J. Virol. **68:** 2339-2346.

229) **Lam, Q., C.A. Smibert, K.E. Koop, C. Lavery, J.P. Capone, S.P. Weinheimer, and J.R. Smiley.** 1996. Herpes simplex virus VP16 rescues viral mRNA from destruction by the virion host shutoff function. EMBO J. **15:** 2575-2581.

230) **Knez, J., P.T. Bilan, and J. P. Capone.** 2003. A single amino acid substitution in herpes simplex virus type 1 VP16 inhibits binding to the virion host shutoff protein and is incompatible with virus growth. J. Virol. **77:** 2892-2902.

231) **Taddeo B., M.T. Sciortino, W. Zhang, and B. Roizman.** 2007. Interaction of herpes simplex virus RNase with VP16 and VP22 is required for the accumulation of the protein but not for accumulation of mRNA. Proc. Natl. Acad. Sci. **104:** 12163-12168.

232) **Elliott, G. and P. O'Hare.** 1999. Intercellular trafficking of VP22-GFP fusion proteins. Gene Ther. **6:** 149-151.

233) **Aints, A., M.S. Dilber, and C.I. Smith.** 1999. Intercellular spread of GFP-VP22. J. Gene Med. **1:** 275-279.

234) **Sciortino, M.T., B. Taddeo, A.P. Poon, A. Mastino, and B. Roizman.** 2002. Of the three tegument proteins that package mRNA in herpes simplex virions, one (VP22) transports the mRNA to uninfected cells for expression prior to viral infection. Proc. Natl. Acad. Sci. USA. **99:** 8318-8323.

235) **Samady, L., E. Costigliola, L. MacCormac, Y. McGrath, S. Cleverley, C.E. Lilley, J. Smith, D.S. Latchman, B. Chain, and R.S. Coffin.** 2003. Deletion of the virion host shutoff protein (vhs) from herpes simplex virus (HSV) relieves the viral block to dendritic cell activation: potential of vhs$^-$ HSV vectors for dendritic cell-mediated immunotherapy. J. Virol. **77:** 3768-3776.

236) **Suzutani, T., M. Nagamine, T. Shibake, M. Ogasawara, I. Yoshida, T. Daikoku, Y. Nishiyama, and M. Azuma.** 2000. The role of the UL41 gene of herpes simplex virus type 1 in evasion of non-specific host defense mechanisms during primary infection. J. Gen. Virol. **81:** 1763-1771.

237) **Tigges, M.A., S. Leng, D.C. Johnson, and R.L. Burke.** 1996. Human herpes simplex virus (HSV)-specific CD8+ CTL clones recognize HSV-2 infected fibroblasts after treatment with IFN-gamma or when virion host shutoff functions are disabled. J. Immunol. **156:** 3901-3910.

238) **J.R. Smiley.** 2004. Herpes simplex virus virion host shutoff protein: immune evasion mediated by a viral RNase? J. Virol. **78:** 1063-1068.

239) **Smith, T.J., L.A. Morrison, and D.A. Leib.** 2002. Pathogenesis of herpes simplex virus type 2 virion host shutoff (vhs) mutants. J. Virol. **76:** 2054-2061.

240) **Duerst, R.J. and L.A. Morrison.** 2004. Herpes simplex virus 2 virion host shutoff protein interferes with type I interferon production and responsiveness. Virology. **322:** 158-167.

241) **Geiss, B.J., T.J. Smith, D.A. Leib, and L.A. Morrison.** 2000. Disruption of virion host shutoff activity improves the immunogenicity and protective capacity of the replication-incompetent herpes simplex virus type 1 vaccine strain. J. Virol. **74:** 11137-11144.

242) **Keadle, T.L., K.A. Laycock, J.L. Morris, D.A. Leib, L.A. Morrison, J.S. Pepose, and P.M. Stuart.** 2002. Therapeutic vaccination with vhs(-) herpes simplex virus reduced the severity of recurrent herpetic stromal keratitis in mice. J. Gen. Virol. **83:** 2361-2365.

243) **Walker, J., K.A. Laycock, J.S. Pepose, and D.A. Leib.** 1998. Postexposure vaccination with a virion host shutoff defective mutant reduces UV-B radiation-induced ocular herpes simplex virus shedding in mice. Vaccine.**16:** 6-8.

244) **Walker, J. and D.A. Leib.** 1998. Protection from primary infection and establishment of latency by vaccination with a herpes simplex virus type 1 recombinant deficient in the virion host shutoff (vhs) function. Vaccine. **16:** 1-5.

245) **Davison, A.J. and J.E. Scott.** 1986. The complete DNA sequence of varicella-zoster virus. J.Gen. Virol. **67:** 1759-1816.

246) **Berthomme, H., B. Jacquemont, and A. Epstein.** 1993. The pseudorabies virus host-shutoff homolog gene: nucleotide sequence and comparison with alphaherpesvirus protein counterparts. Virology. **193:** 1028-1032.

247) **Feng, X., Y.G. Thompson, J. B. Lewis, and G. B. Caughman.** 1996. Expression and function of the equine herpesvirus 1 virion-associated host shutoff homolog. J. Virol. **70:** 8710-8718.

248) **Telford, E.A.R., M.S. Watson, K. McBride, and A.J. Davison.** 1992. The DNA sequence of equine herpesvirus-1. Virology. **189:** 304-316.

249) **Everett, R. D., and M.L. Fenwick.** 1990. Comparative DNA sequence analysis of the host shutoff genes of different strains of herpes simplex virus: type 2 strain HG52 encodes a truncated UL41 product. J. Gen. Virol. **71:** 1387-1390.

250) **Jones, F.E., C.A. Smibert, and J.R. Smiley.** 1995. Mutational analysis of the herpes simplex virus virion host shutoff protein: evidence that Vhs functions in the absence of other viral proteins. J. Virol **69:** 4863-4871.

251) **Ceska, T.A. and J. R. Sayers.** 1998. Structure-specific DNA cleavage by 5′ nucleases. Trends Biochem. Sci. **23:** 331-336.

252) **Harrington, J. J. and M.R. Lieber**. 1994. Functional domains within FEN-1 and RAD2 define a family of structure-specific endonucleases: implications for excision repair. Genes Dev. **8:** 1344-1355.

253) **Szankasi, P. and G.R. Smith.** 1995. A role for exonuclease I from *S. pombe* in mutation avoidance and mismatch corrections. Science. **267:** 1166-1169.

254) **Saffran, H.A., G.S. Read, and J.R. Smiley.** 2010. Evidence for translational regulation by the herpes simplex virus virion host shutoff protein. J.Virol. **84:** 6041-6049.

VITA

Lora Ann Shiflett was born May 26th, 1984 in Des Moines, IA. She graduated from Colfax-Mingo High School in Colfax, Iowa in 2002. In May 2005, Lora graduated from Iowa State University in Ames, Iowa. She received a Bachelor of Science in Biology and a Minor in Spanish. In the fall of 2005 Lora began graduate school at the University of Missouri-Kansas City in Kansas City, Missouri where she received a Master's degree in Cell and Molecular Biology in the winter of 2007.